Copyright Warning & Restrictions

The copyright law of the United States (Title 17, United States Code) governs the making of photocopies or other reproductions of copyrighted material.

Under certain conditions specified in the law, libraries and archives are authorized to furnish a photocopy or other reproduction. One of these specified conditions is that the photocopy or reproduction is not to be "used for any purpose other than private study, scholarship, or research." If a, user makes a request for, or later uses, a photocopy or reproduction for purposes in excess of "fair use" that user may be liable for copyright infringement,

This institution reserves the right to refuse to accept a copying order if, in its judgment, fulfillment of the order would involve violation of copyright law.

Please Note: The author retains the copyright while the New Jersey Institute of Technology reserves the right to distribute this thesis or dissertation

Printing note: If you do not wish to print this page, then select "Pages from: first page # to: last page #" on the print dialog screen

ABSTRACT

UTILIZATION OF PROCESSED FLY ASH IN MORTAR

by
Walairat Bumrongjaroen

Grinding process is introduced to provide fine particles of coal fly ash that enhances the strength gain of cement mortars. It is discovered that grinding can make all the studied fly ashes more suitable for concrete use at higher replacement value than previously anticipated even when the effect of high carbon content is considered

In this study, new mechanisms for strength gain of fly ash mortars are proposed. They are dispersion and nucleation, which are results from the presence of fly ash in the cement mortar. These effects are shown to enhance the hydration of cement. The pozzolanic action of fly ash contributes strength at a later stage. Pozzolanic activity of fly ash is shown to increase with fineness of the ground fly ash.

Several types of fly ashes, wet bottom, dry bottom and low NO_x fly ashes are chosen as representative of the waste products of existing and the new burner technology. They were ground to different particle size distributions. Tests were conducted to determine the physical properties of these fly ashes and their performance in cement mortars. Optimum ranges of the grinding process were explored along with particle size analysis, chemical composition, mineralogy, and morphological aspects of raw and ground fly ash.

In order to see whether these processed fly ashes can be used at high percentages in cementitious products, the performance of mortars made from these fly ashes is examined. The strength contribution of fly ash in cement mortars through dispersion, nucleation, and pozzolanic action were investigated and found to perform equally or better than normal cement mortars as early as seven days. Furthermore, the study on the properties of mortars made of high-carbon ground fly ash from low NO_x furnace also showed similar strength enhancement. The major conclusion of this study is that grinding is a suitable mean to increase utilization of fly ash as cement replacement. The processing technique has economically been demonstrated to yield quality fly ash for use in concrete, thus reducing the amount of fly ash that needs to be disposed of in landfills.

UTILIZATION OF PROCESSED FLY ASH IN MORTAR

by
Walairat Bumrongjaroen

A Dissertation
Submitted to the Faculty of
New Jersey Institute of Technology
in Partial Fulfillment of the Requirements for the Degree of
Doctor of Philosophy

Department of Civil and Environmental Engineering

May 1999

APPROVAL PAGE

UTILIZATION OF PROCESSED FLY ASH IN MORTAR

Walairat Bumrongjaroen

Dr. Methi Wecharatana, Dissertation Advisor Professor of Civil and Environmental Engineering, NJIT	Date
Dr. C.T. Thomas Hsu, Committee Member Professor of Civil and Environmental Engineering, NJIT	Date
Dr. Dorairaja Raghu, Committee Member Professor of Civil and Environmental Engineering, NJIT	Date
Dr. Namunu J. Meegoda, Committee Member Associate Professor of Civil and Environmental Engineering, NJIT	Date
Mr. William Librizzi, Committee Member Director, Technology Application, HSMRC	Date

BIOGRAPHICAL SKETCH

Author: Walairat Bumrongjaroen

Degree: Doctor of Philosophy in Environmental Engineering

Date: May 1999

Undergraduate and Graduate Education:

- Doctor of Philosophy in Environmental Engineering,
  New Jersey Institute of Technology, Newark, NJ, 1999
- Master in Environmental Engineering,
  New Jersey Institute of Technology, Newark, NJ, 1994
- Bachelor in Environmental Engineering
  Chulalongkorn University, Thailand, 1990

Major: Civil Engineering

Presentations and Publications:

Methi Wecharatana, Walairat Bumrongjaroen, and Manaskorn Rachakornkij, 1998, "Characteristics of Processed Fly Ash for Concrete," *Sixth CANMET/ ACI International Conference on Fly Ash, Silica Fume, Slag and Natural Pozzolans in Concrete*, Bangkok, Thailand, May 31- June 5, pp. 1-15.

To my beloved father and mother

ACKNOWLEDGEMENT

I would like to take this opportunity to thank my advisor, Professor Methi Wecharatana, for his guidance, encouragement and valuable suggestions throughout the course of this thesis work. I am also grateful to Professor Peter Lederman and Professor John W. Liskowitz for their helpful discussion. I would also like to express my gratitude to my committee members, Professor C.T. Thomas Hsu, Professor Dorairaja Raghu, Professor Namunu Meegoda and Prof. William Librizzi for their constructive evaluation of this dissertation.

I am indeed appreciated Mr. Allyn Luke, assistant to the Chairman for Laboratories, Department of Civil and Environmental Engineering, for his excellent technical assistance in the experiment and persistent courtesy in editing my English. Dr. Chai Jaturapitakkul deserves a very special credit for his assistance and guidance throughout my MS studies here. The special thank must be given to Mr. Wiwat Kamolpornwijit for his suggestion and supervision in XRD and XRF system.

I would also like to acknowledge the contributions of the following people: Dr. Sudhi Mukherajee, Ms. Jane Wu, Mr. Chandrakant Patel, Mr. Clint Blockways, Mr. Manaskorn Rachakornkij, Mr. Pusit Lertwatanarak and Ms. Wonsiri Punurai. I also thank to all Thai students at NJIT to keep me joyful throughout my life studies here.

Last but not least, special gratitude to my parents and brothers, who have been a constant source of encouragement and support throughout my life.

TABLE OF CONTENTS

Chapter **Page**

Chapter **Page**

Chapter **Page**

Chapter **Page**

LIST OF TABLES

Table **Page**

Table **Page**

LIST OF FIGURES

Figure **Page**

Figure **Page**

Figure **Page**

Figure **Page**

Figure **Page**

Figure **Page**

Figure **Page**

Figure **Page**

CHAPTER 1

INTRODUCTION

562 million tons of coal fly ashes throughout the world were produced in 1989. Of this amount only 25 million tons were used as portland cement replacement in concrete, only 5% of the total coal ash generated. Other applications were as low-value road base material and fills. The remainder had to be disposed of as solid waste in landfills. Disposal of fly ash in this manner is not only wasteful it is costly because of the lack of landfill space and stringent environmental policy. The beneficial use of fly ash in concrete is the preferable option for safe and economical utilization of millions tons of fly ash. There is a critical need to fine new methods for using fly ash for its highest and best use.

Even though the beneficial use of fly ash in concrete has been known for many decades, it is still not yet fully utilized. The major obstacles to further use of fly ash are the large variation in physical and chemical properties, the high amounts of carbon and sulfur and the delayed setting and low early strength of fly ash concrete. According to ASTM C618, fly ash, which varies considerably in its properties, can be divided into two categories, fly ash meeting the physical and chemical standards as a pozzolan, and those not meeting that standard. Malhotra (1996) reported that at least 70% of total fly ash is generally suitable for use as a cement replacement in concrete but still only small amounts have been used. Moreover, its use as cement replacement is restricted to 20% of the cementitious mass. Because fly ash improves concrete workability, lowers the heat of hydration, increases the ultimate strength and improves the durability of concrete, many

researchers are studying the methods to increase utilization of fly ash as cementitious material. For example, studies by Malhotra (1995) have shown that concrete with up to 60% cement replacement passed ASTM C618 producing high strength and more durable concrete.

In recent years, the generation of salable fly ash is decreasing as an indirect result of controlling nitrogen oxides (NO_x) to meet the emissions standards of the 1990 Clean Air Act amendments. The consequence of this law has been to increase the amount of unburned coal in fly ash by reducing excess air in combustion zone therefore reducing the temperature in the boiler. The high volume of carbon in fly ash makes it unsuitable for use as cement replacement in concrete because the carbon tends to absorb organic compounds that are the key ingredients of many concrete admixtures like Air Entraining Agent (AEA) thereby lowering the durability of concrete (Hornain, 1992). Current studies focusing on how reducing amount of carbon in fly ash are the Electrostatic Separation method proposed by Tondu and Thompson (1996) and the Thermal method proposed by Suprenant (1992).

Jaturapitakkul (1995) showed that fine particles could be used as cement replacement without penalty. Unfortunately the separation technique he utilized only recovered 50% at best. Low NO_x fly ash has only 20% in this critical particle size range. It was wondered whether grinding of fly ash so all of it was in this critical particle range would produce the same effect.

In this study, we will show how to process fly ash to provide a consistent quality fly ash that is suitable for concrete applications. Several types of fly ashes, wet bottom, dry bottom and low NO_x fly ashes are chosen as representative of the waste products of

existing and up-and coming burner technology. They will be ground to different particle size distributions. Tests will be conducted to determine the physical properties and the behavior and performance of these ground fly ashes in mortars. In order to see whether these processed fly ashes can be used at high percentages in cementitious products, the performance of mortars made from these fly ashes will be examined. The strength contribution of fly ash through dispersion, nucleation, and pozzolanic action will be investigated. Furthermore, this study will evaluate the properties of mortars made of high-carbon ground fly ash from low NO_x furnace. The major conclusion of this study is that grinding is a suitable way to make all the fly ash useful as cement replacement. The processing technique is expected to improve the quality of fly ashes permitting the increased use of fly ash in concrete, thus reducing the amount of fly ash needing disposal in landfills.

This study seeks to accomplish one of the major objectives of environmental science. That is, to recycle waste materials into useful products and to create an asset out of a liability. This study will show that virtually any coal fly ash can be processed to produce a product that not only could eliminate, it will not eliminate but it can at least measurably reduce, a significant worldwide waste stream. Coal fly ash that is mostly destined for landfill can be processed, through grinding, into a beneficial cement component. The processed fly ash not only is removed from the waste stream but it can be used to impart highly desirable qualities to concrete.

CHAPTER 2

LITERATURE SURVEY

2.1 Fly Ash Formation

Fly ash is a by-product from the combustion of pulverized coal in electricity power plants. It is removed from the combustion gases by means of electrostatic precipitators. Characteristics of fly ash vary due to the combustion conditions. The combustion furnaces that are commonly used in most power plants are wet bottom, dry bottom, and low-NO_x furnace. The main difference between these three furnaces is the temperature in the combustion chamber. The wet bottom furnace is designed to have the burning temperature above the fusion temperature of the coal ash. The fly ash formed within this temperature range is glassy and spherical. This type of furnace is phasing out from industry since it tends to generate high emission of NO_x. The dry bottom furnace is designed to have flame below the ash fusion but it still produces NO_x. The low NO_x furnace is introduced to control the emission of NO_x by lowering the temperature in the combustion chamber. This furnace will gradually replace other types of furnaces. Other conditions that influence the characteristic of fly ashes are coal properties, combustion condition, and collection processes.

2.2 Chemical Composition and Mineralogy of Fly Ash

Generally, the chemical composition of fly ash shows a wide diversity, but the major chemicals of fly ash are SiO_2 (25-60%), Al_2O_3 (10-30%) and Fe_2O_3 (5-25%). Figure 2.1

shows the position of fly ash with a low calcium content in the ternary diagram SiO_2-Al_2O_3- CaO.

These fly ashes can be classified into two groups as class C and class F according to ASTM C-618. Class C fly ash, originated from lignitic coal, vastly has CaO content higher than 10% and the sum of SiO_2, Al_2O_3, MgO is more than 50%. Class F fly ash is originated from anthracite or bituminous coal. It consists of less than 10% CaO and the sum of the major oxides is more than 70%. The fly ash generated recently tends to have lower value of SiO_2 and higher carbon content.

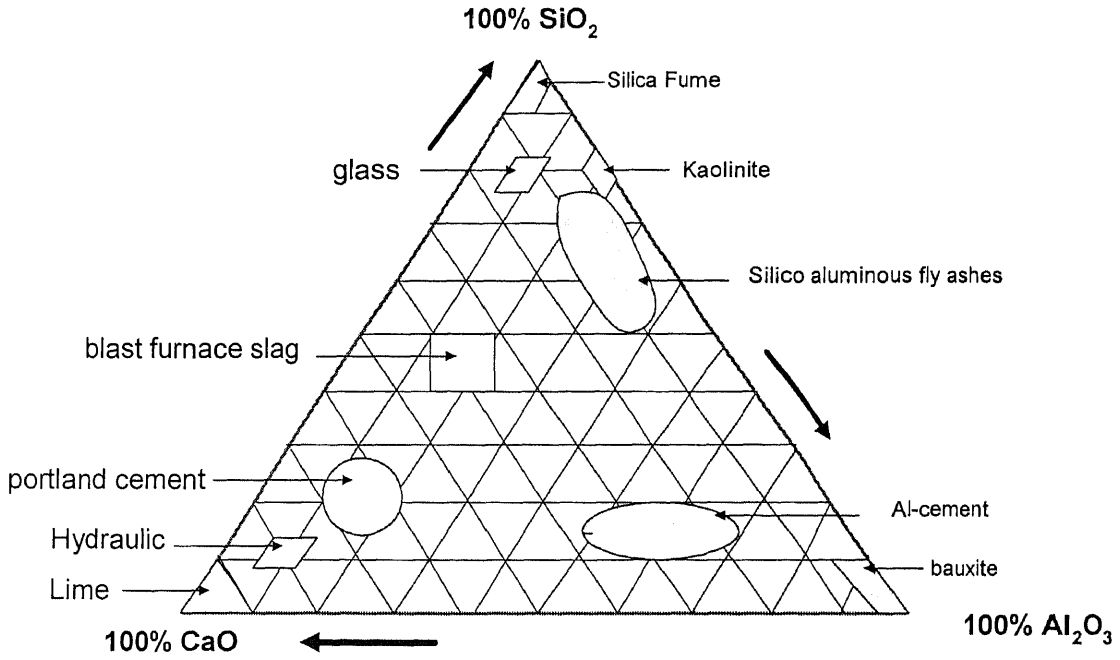

Figure 2.1 Survey of Products Containing SiO_2, Al_2O_3, and CaO (Fraay, 1989)

In early studies, many researchers have sought to correlate the chemical composition of fly ash with the properties of fly ash mortar or concrete. However, it has

been concluded that the chemical composition does not have a major contribution to the properties of fly ash concrete (Mantz, 1986).

Unlike portland cement, there is no direct relationship between the chemical and the mineralogy of fly ash. Thus mineralogy of fly ash has to be examined along with its chemical compositions. The phases of mineral exist in the fly ashes are governed by the impurities of original coals and combustion temperature (Hubbard and Dhir, 1985).

The mineralogy of fly ash also depends on combustion methods. The boiler operating at high temperature tends to have a large amount of crystalline phase. Thus the dry bottom fly ash has higher content of crystalline phase than that of the wet bottom ash. This also results in lower pozzolanic activity of the dry bottom fly ash than that of the wet bottom fly ash comparing at the same particle size. The examples of crystalline phase are quartz, mullite, hematite, magnetite, and free lime.

The mineral of fly ash can be separated into four groups; glass phase, crystalline phase, secondary constituents, and trace elements (Minnick, 1979). The glass phase is composed of silicate-aluminate glass, which renders the pozzolanic action of fly ash. The crystalline phases in fly ash particles are Mullite (24-34%); Quartz (2.8-8.5%); Hematite (Fe_2O_3), (1.1-2.7%); Magnetite (Fe_3O_4), (0.8-2.6%); Diopside (Ca, Mg_2)(Si_2O_6); Wollastonite (CaO. SiO_2) and some incompletely combusted clay minerals (Van Roode and Douglass, 1987). The crytalline phases are found mostly in fly ash particle size between 5 and 60 microns and scarcely found in particle smaller than 5 microns. Mullite has a needle crystal structure and normally does not present with glass phase. The secondary constituents are unburned coal, free lime (CaO), periclase (MgO) and some metal salts (Na_2SO_4, Ca, K_2O). They are attached to the fly ash particle, which is in

crystalline phase. Trace elements in fly ash are formed at the latest chamber path. They condense and deposit on the fly ash particle as the temperature in the combustion zone decreases as of the temperature gradient. At the same last zone, the fine fly ash is also produced, thus, the trace element tends to precipitate on the fine fly ash surface. From literature, the trace elements are solidified within fly ash concrete and the leaching rate of trace elements are less than that when it is not encapsulated in concrete.

Generally, the fly ash particle has an electrical double layer. The difference between the double layer is measured as zeta potential. The high workability of fly ash cement paste is due to the difference in zeta potential between fly ash and cement. This difference also has an effect on the chemisorption of calcium ion on the fly ash surface (Nagataki, 1984).

2.3 Particle Morphology and Size Distribution

Fly ash particles are heterogeneous in nature. It can exist as round particle, angular particle, cenosphere, plerosphere, broken pieces of coarser particles, or fused particles. Most of particles, which are formed at temperature over 1600-1700 °C, are spherical in shape and has size in the range of 1-50 microns. The fly ash from wet bottom boiler falls in to this category because it is operated in this temperature range. Since the temperature in dry bottom boiler is lower than that range, its fly ash has irregular particles beside spherical particles. The amount of irregular fly ashes increases in the low NO_x fly ash because it is produced under much lower temperature in order to reduce NO_x

The particle size distribution plays an important role in the rate of chemical reactivity in mortar or concrete. Thus it is essential to determine the complete size

distribution. With modern technology, using laser or other available techniques, it is possible to obtain a size distribution of powder down to 1 micron or less. This size distribution is expressed as the mass retained in each size band and the diameters of the bands.

Particle size is analyzed by utilizing the phenomenon of light scattering from the particle. The particle size of sample can be categorized into two regimes: particles with diameter smaller than wavelength and particles with diameter comparable or larger diameter than wavelength. Each regime uses different equation to calculate the particle size.

Mie theory is used for analyzing particles with the comparable in size or large relative to the wavelength of incident light (>0.3μm). The scattered light is the resultant of light waves originating from various parts of the particles. The near forward-scattered light is measured so as to reduce the refractive index effects.

Mastersizer applies the Mie theory to measure the particle size. The laser beam projects through a stream of particle. The scattered light from particles are collected by lens and projected on to multi-element detector and obscuration detector. The intensity and direction of light scattered by the particles are measured by multi-element detector and then analyzed by a computer, which calculates the size distribution of the sample.

The advantage of this technique is that it can measure particles in the range from 0.1 to 2000 microns. Sample can be measured in either dry or wet state. The amount of sample used in particle analysis is very small comparing to that required by sieve analysis and other methods. The deagglomeration procedure is applied in order to obtain the true size of each particle. It also gives high resolution in size below100 microns.

2.4 Fineness of Fly Ash

Fly ash particles are typically spherical, ranging from 1 to 150 microns in diameter (Berry and Malholtra, 1980). The large particle may be a result of the conglomeration of small spheres, colliding in a viscous stage. The particle size of fly ash depends on the type of coal, the grinding efficiency of coal, the combustion regime, the combustion temperature, volume of air forced into the oven and method of precipitation (Santhanam, 1981). Low In the new low NO_x furnace produces high amount of unburned coal in the gas stream due to its operation at low temperature. Therefore the fly ash received from low NO_x furnace tends to have coarser particle than the other furnace because unburned coal combines with fly ash. The size of fly ash is also influenced by the method of precipitation. The precipitator normally consists of four filters with different opening size. The first filter has the largest opening pore and the last filter has the smallest opening size. The fly ash particles removed by the first filter are coarser than those from the latter.

It is well known that the fineness of fly ash influences the properties of concrete, and there seems to be general agreement among researchers that the pozzolanic activity of fly ash are directly related to the amount of fine particles. Several authors, including Cabrera (1980), Cornelissen (1992), Hughes (1989), Monzo (1995), Nakamura (1992), Ravina (1980), Ranganath (1995), Slanicka (1991), Tazawa(1992), and Ukita (1992), studied the influence of fly ash fineness upon the concrete strength. Each researcher used different method of assessing the fineness of fly ash in his study.

Among the parameters that are used to represent fineness are the specific surface area, the weight retained on 45 microns-sieve (No.325), and the particle size distribution.

Fly ash can be classified in terms of its specific surface as measured by air permeability as well as Blaine's method. The air permeability method is usually used to measure the specific surface of cement and is based on the flow of dry air through a uniformly packed bed of particles. The bed of particles offers resistance to the flow of air, which is used to estimate the specific surface. This method of measurement is limited to the powder with uniform shape. Since the chemical reaction of fly ash depends largely on its surface area, this method has been used vastly when the chemical reaction of fly ash or the effect of this reaction is of interest.

Many researchers considered the specific surface as one of the principal parameters that define the rate of pozzolanic activity of fly ash. Ravina (1980) evaluated the sieve analysis and specific surface methods for determining fineness of fly ash. He found a linear relationship between the specific surface and pozzolanic activity index while the relation with the size retained on 45 microns sieve was linear only in a limited range. Ranganath (1995) also used the specific surface as a fineness parameter of fly ash. He found the correlation between combined parameter of fineness and silica content. The effect of fineness is dominant at early age, which is more of the physical mechanism such as dispersion of cement particles or micro-filler effect. Similar results have been reported by Harris, Thompson, and Murphy (1987). They found that the fineness and water requirement correlate with pozzolanic activity.

Since the specific surface directly governs the pozzolanic activity, which is the key contribution to concrete strength, it is considered to correlate with the development of mechanical strength. Nakamura (1992) measured the fineness of fly ash by its surface area and reported the high early strength and densified microstructure of fine fly ash

concrete. Tazawa (1992) examined the utilization of ultra-fine fly ash having as high specific area as 200,000 cm^2/g. He concluded that the compressive strength of mortar with ultra-fine fly ash is higher than normal control mortar. Slanicka (1991) observed the effect of surface area on the properties of concrete by using fly ash with different fineness. The chemical composition and mineralogy of those fly ashes used were fixed. He concluded that the fly ash with higher surface area tends to perform better than the one with lower surface area. This is because the finer fly ashes have more area for hydration and pozzolanic reaction to occur.

However Ravina (1980) considered this method is considered as a misleading technique. This is because the unburned coal particles are porous and hence increase the surface area significantly. This internal area of coal may or may not affect the pozzolanic activity depending on the reactivity of unburned coal. Nevertheless this area cannot be accounted for other physical mechanism such as packing effect and defloculation. In the mean time, in order to avoid the error from this method, it should not be used if high amount of unburned coal particles present.

The weight residue on a 45 microns-sieve (percentage retained) is specified as a value to represent the fineness of fly ash by ASTM C-618. The weight of fly ash be retained on a 45 microns sieve is not more than 34 % by weight. Lane (1991) suggested that this method is a more consistent indicator than the surface area. Berry et al (1989) also used these criteria to define the beneficiated fly ash. He found that this beneficiated fly ash improves pozzolanic activity, reduces water demand, and reduces alkali-aggregate reactivity. He concluded that this benefit is a result of larger surface area of small particles. The surface area of particles less than 10 microns is more than four times that

of raw fly ash. However the residue on the 45 microns sieve is a limited application since it considers only particles coarser than or finer than 45 microns (Hughes, 1989). It does not consider the size distribution of fly ash.

The particle size distribution (PSD) can be considered as a more extensive sieve analysis than the 45 microns sieve residue. Unlike the latter method which only two fractions are reported, the PSD method shows the volumetric percentage of fly ash in several small size ranges. Therefore it is a more thorough mean to study the influence of the each size fraction on properties of fly ash concrete. Recently this method is used widely since it can reveals the physical effect such as packing effect, filling effect and other functions of fly ash that can be only studied through the use of PSD. Moreover, the surface area which is a major factor of pozzolanic effect can be calculated from the PSD if most particle is spherical.

Although the measurement technique is highly accuracy but the classifying process has not been well developed so as to obtain the fly ash with the same size range. Therefore the effect of each single particle has not been revealed. So far, many researchers obtain single value from PSD such as grading modulus, mean diameter or maximum size and use this value as the fineness in their investigation

Grading Modulus is the surface area of spheres of the same size as the actual particles. The grading modulus is given by

$$G = \frac{6(1/D_1 - 1/D_2)}{\log_n(D_2/D_1)}$$

Consider a single grain size of diameter D. The size distribution between successive sieves is assumed to vary linearly to a log scale and D1 and D2 are the diameters of the

smallest and the largest size particles of the group. The shape factor can be introduced if necessary. The grading modulus of fly ash can be determined by multiplying the percentage retained within each band. The sum of these products divided by 100 yields G.

Hughes (1989) investigated all above three methods. From his result, neither the specific surface nor the amount of residue on 45 microns sieve represents the size distribution of fly ash. However, the grading modulus shows a good correlation with the workability of fly ash concrete. His result sound reasoning because the workability depends on the size of particle. But the fly ashes, which have the same specific surface, may or may not have the same PSD. Hugh also suggested that this grading modulus could be a good indication of the potential strength of fly ash concrete

Cornelissen (1992) studied the effect of fly ash grading modulus on mortar properties. He found that the higher grading moduli or finer fly ash used in mortar or concrete correlate well with mortar and concrete properties such as the strength and efficiency factors. Similar result has been observed by Jaturapitakkul (1992). He fractionated fly ashes into different fractions and calculated the fineness modulus of fractionated fly ashes. He found that the lower the fineness modulus of fly ash, the higher the compressive strength. In addition, he also investigated the three methods. He concluded that the fineness modulus gives more consistent results on compressive strength of concrete than the Blain fineness and the residue on 45 microns sieve.

Another group of researchers studied the performance of finer particle of fly ashes by using the range of particle size of fly ash as fineness. Ukita et al. (1992) classified fly ashes by air separation method to have the maximum particle diameters of about 20

microns, 10 microns, and 5 microns, respectively. In his research, it showed that the use of classified fly ash can reduce water requirement, improve workability, enhance strength and water tightness in concrete. His result showed that the as the percentage of finer particle ranging from diameters of 1 to 20 microns increases, the strength development of concrete that it cooperating is higher. Jaturapitakkul (1992) successfully sorted fly ashes to fraction, size <5 microns, <10 microns, <15 microns, <20 microns, < 30 microns and <150 microns. His result showed that the concrete made of finer fly ashes exhibits the higher strength than the coarser one. It passes the conventional cement at early age as 14 days for concrete made of 15% finest fly ash. His results disagree with that of Ukita (1992) that the higher percentage of fine fly ash used decreases the strength of concrete. Giergiczny and Werynska (1989) also examined the properties of fly ashes from several ranges. He used grinding process to grind fly ashes into different fraction; 0-20 microns, 20-40 microns, 40-60 microns, and > 60 microns. They found that the fly ash that has particle smaller than 20 microns offers the highest strength of mortar. There is a need to carry out an investigation to obtain an optimum percentage for each type of fly ash and its percentage that provide strength development at least comparable to conventional concrete.

However, some researchers can achieve the better performance of fine fly ashes only at later age. The test done by Raask and Bhaskar (1975) showed that up to 7 days the strength was not affected by the fineness. The effect can be seen after 28 days. Ukita (1992) found that it took 90 days before the strength of fine fly ashes concrete reaches that of plain concrete. The low early strength of fine fly ashes in their tests can be because the fly ash is not reactive enough or their particles are not fine enough. Attempts

have been made to find the proper fineness that accelerates the early strength of fly ash concrete and improve the overall performance of concrete. Butler and Mearing (1986) suggested that the 10 microns be the cutoff point between reactive and non-reactive particles but he did not carry out experiment to test his hypothesis. Monzo (1995) and his team also found that the enhancement of compressive strength is related mainly with content of fly ash particles smaller than 10 microns. The fly ash, which has higher amount of particles in this range, gave positive effects on compressive strength and flexural strength of mortar. It should be noted that both groups studied only one type of fly ash, this cut size may not be applied to other types of fly ashes.

It can be seen that the different criteria are applied to define the fineness of fly ash. They are directly or indirectly explain the surface area. Each researcher relates the fineness to the pozzolanic activity, which directly governs the strength. However, no definite qualitative examination on this matter has been reported. Also, the fineness of fly ash may provide strength through other functions such as deflocculation and nucleation, which has not been evaluated yet. The more thorough study on the function of fineness is needed so as to provide the mean to obtain the cut size for processing each type of fly ash.

2.5 Fly Ash as Cementitious Material

The use of fly ash as cement material was introduced as early as 1937. It was stated that the addition of fly ash improved the workability and compressive strength of concrete. Since then the use of fly ash have been studied by many researchers. One of the motives

in long-term studies is to make use the solid waste, which generated in enormous amounts each year.

Besides the improved workability and compressive strength, fly ash is found reduced water demand, reduced segregation, reduced permeability, increased plasticity, lowered heat hydration, and increased setting time (ACI 226, 1987). Some researches suggested that these improvements are results of increased packing density of the solid material (Hobbs, 1980), increase paste volume (Banfill, 1982), and a dispersion of cement flocs (Yamazaki, 1979). It also reduces the bleeding process in concrete, hence improves the bond between aggregate and matrix (Dhir, Hubbard, 1982). During the hydration process, fly ash accelerates the C_3S reaction by retarding the C_3A reaction (Cabrera, Plowman, 1980). After the fly ash becomes reactive which may take some times, there is a continuing contribution to strength through the production of cementitious material by pozzolanic reaction from fly ash.

However there exists the problem of using fly ash in concrete such as inconsistent quality of fly ash, delaying setting time, and have lower early strength of concrete. The quality assurance of fly ash is not consistent which varies due to the types of coal, type of furnace, and combustion condition. Based on type of coal, fly ash can be distinguished into two groups as class C and class F. Class C is a fly ash originating from lignitic coal and class F fly ash originating from anthracite or bituminous coal. Class C fly ash has higher lime content than class F fly ash. Therefore it can be used in much higher proportions than class F fly ash for concrete (Naik, Ramme, 1989). Even the same type of coal but obtained from different sources could have variation in chemical compounds. The type of furnace is also has an influence on quality of fly ash. In the market, there are

dry bottom furnace, wet bottom furnace, fluidized bed furnace, and low-NO_x furnace. Fly ashes generated from different furnaces differ in both chemical composition and fineness. The present study will attempt to examine the key characteristics of fly ash that governs the properties of fly ash concrete.

A major impediment to increase utilization of fly ash in concrete is its low early strength than those of normal concrete. This deficiency has been reported for many years (Ravidrarajah and Tam, 1989). However, in recent years, studies have been done to resolve this drawback. Maholtra and Painter (1989) reported high early strength, high later strength and satisfactory freeze-thaw resistance of concrete incorporating with high volume of class F fly ash (55%). However, their mix proportion contains high amount of superplasticizer, which may be the source that contributes strength at early age. If this is a case, the high cost of superplasticizer does not encourage the practice of their mix. Instead of proportioning the mix, some researchers modified the fly ash characteristics. Study by Ranganath (1995) showed that the early-age strength correlated better with fineness of fly ash than the soluble silica content. Tazawa (1992) and his team studied the properties of mortar incorporating ultra-fine fly ash, which has surface area 529,000 cm^2/g. They found that at 7 days the compressive strength of mortar with fine fly ash almost surpasses that of cement mortar. It appears that its rate of strength development is larger than that of mortar with silica fume. Ukita and his team (1992) used the classified fly ash having the maximum diameter of about 10 microns in their concrete. They reported the concrete has slightly lower strength only until 7 days of age, after that the concrete containing this fly ash is higher than normal concrete. However their mix also

contains the high amount of superplasticizer. The strength of that concrete may be enhanced by admixture.

2.6 Early Stage of Hydration Process

This stage occurs immediately after mixing and continues until the cement grain is fully hydrated. It composes of two mechanisms occurring simultaneously: hydration and nucleation. The chemical reaction of fly ash in concrete is only significant after a month. During that period its effect can be considered rather as a physical effect on hydration process such as nucleation, chemisorption and dispersion. In the hydration process, the product, i.e. CSH gel and $Ca(OH)_2$, precipitate grow on the surface of cement grain. The cement grain becomes bigger when this process undergoes. As stated by Power (1947) the fully hydrated cement grain will have size 2.4 time the original size. In nucleation process, the hydrates dissolving from cement grain will precipitate on fly ash surface. Fly ash acts as an inert material and nucleus for hydration compounds ($Ca(OH)_2$, CSH gel) to on (Butler and Mearing, 1986; Fraay, 1989). It is expected that the hydration product growing from cement grains and from fly ash particles connect together and this bond contributes strength to the matrix.

In normal cement paste, the grains tend to flocculate and leave the large pore between flocs. The cement grains initially adjoin by Coulomb attraction or Wander Wale force. The interconnection of hydration product will appear close to this contact area. These two phenomena will strengthen the bonds of matrix. Therefore, its early strength is high regardless of its high porosity. Unlike normal cement, the fly ash cement paste has smaller pores because of dispersion of cement and the existing of fly ashes in the pores.

However, from Jaturapitakul's result the strength at early age of fly ash paste is low. This may be because the binding material has not connected completely or the amount of hydration product is not sufficient to bind them. Gopalan (1993) proposed that the strength contribution of fly ash at early age is attributed from this nucleation mechanism.

However, opinions differ, other found that this phenomenon retards the cement hydration because of the chemisorption of calcium ion on the fly ash surface. The calcium ions in solution react with aluminum compound of fly ash forming AFt-phase on the surface of fly ash (Fajun, 1985). Likov (1997) found that even the above reaction exists, there is no difference in amount of the hydration product in the plain and fly ash containing pastes. But when more reactive material such as silica fume was used, the longer retardation of the hydration process occurred. This is because the silica fume binds all calcium ions in the solution. In this study the nucleation and chemisorption of hydration products by ground fly ash with various fineness was investigated.

It was also reported that fly Ash also help dispersing cement particles. When mixed with water the cement particles tend to flocculate and form large grain, which unreacted cement particle is covered with hydrated one. As a result, not all the cement particles undergo the hydration process. When fly ash is introduced in cement mortar, it disperses the cement flocs into smaller grains which is result in more hydrated cement or higher compressive strength (Yamazaki, 1979). In contrast, Yuan (1982) proposed that the fly ash particles are adsorbed on the cement grain but the dispersion of the cement particles and higher amount of hydrated cements still occur. The dispersion of cement by ground fly ash was also observed in this study.

2.7 Pozzolanic Activity of Fly Ash

Fly ash has a chemical effect in cement mortar and concrete which is called pozzolanic activity. It reacts with alkali to form compounds possessing cementitious properties. This process is a much slower process than cement hydration, which begins at the mixing period (Diamond, 1981).

The first step of pozzolanic action of fly ash is the breaking down and dissolution of the glassy phase of fly ash. In caustic environment, glassy phase of fly ash is depolymerized by OH^- of alkaline in the pore solution of concrete (Plowman, 1984). The alumina-silicates glass breaks down to molecular unit and dissolve to the pore solution. Calcium ion in the pore water combines with these compounds and form calcium-alumina-silicate-hydrates and calcium-aluminate-hydrates as the reaction expressed below:

$$SiO_2 + 2Na^+ \text{ (or } K^+) + 2OH^- \rightarrow Na_2(K_2)SiO_3H_2O$$

$$Ca^{2+} + SiO_2 + H_2O \rightarrow xCaO.ySiO_2.ZH_2O$$

$$Ca^{2+} + Al_2O_3 + H_2O \rightarrow xCaO.yAl_2O_3.zH_2O$$

$$Ca^{2+} + SiO_2/Al_2O_3 + H_2O \rightarrow xCaO.yAl_2O_3.zSiO_2.wH_2O$$

$$Ca^{2+} + SO4^{2-} + Al_2O_3 + H_2O \rightarrow xCaO.yAl_2O_3.zCaSO_4.wH_2O$$

Since the solubility of CSH is very low (5.5×10^{-49}) so these reaction products precipitate immediately near or on the surface of fly ash (James, 1986). The formation depends on the pH of pore solution and the distance that the parent ions diffuse to. This precipitated product becomes a dense layer over the fly ash and hinders the succeeding

pozzolanic reaction. After this point, the rate of pozzolanic action is much slower because the compounds participating the process must diffuse in and out from this layer. (Uchikawa, 1980).

The pozzolanic activity of fly ash in concrete is dependent on fly ash characteristics and its environment. The characteristics that affect this reaction are the reactivity of glass phase, the quantity of glass and the fineness of fly ash. The external factors are the pH of pore solution or OH^- ion, and the Ca^{2+} content. The dissolution of glass is due to the attack of OH^- ion on the surface of fly ash. The oxygen bond of glass is weakened and releases the silicon atom to the solution as silicate ion. The dissolution rate of fly ash is related to the reactivity of fly ash itself and OH^- content in pore solution. Since the amorphous phase or glassy phase tends to dissolve easier than the crystalline phase, fly ash with high percentage of amorphous tends to be more reactive than the one with lessen percentage of amorphous phase (Jun-Yuan, Scheetz, and Roy, 1984). The glassy phase of fly ash depends on the combustion condition and type of boiler. Therefore, the fly ash obtained from different sources such ash dry bottom boilers or wet bottom boiler fly ash tends to perform differently. In this study, the mineralogy of fly ash, which controls the solubility of glassy phase, will be investigated.

The dissolution of glass is also depended on the OH^- concentration per unit surface of silica, and its stability Urhan (1987). If high pH presents, as in the case of high concentration of OH^- per unit area, the glass will dissolve more. Fraay (1989) also shows that solubility of glass is dependent on the alkalinity of the pore water. He monitored the OH^-, Si^{2+}, and Ca^{2+} concentration of cement and fly ash paste. His results showed that at the beginning of cement hydration, the pH of pore water was usually about 12 but after

about one week the pH increased to a certain level that fly ash can dissolve Si^{2+}. He concluded that the well-known incubation period before the start of pozzolanic action is the results of low alkalinity of pore solution and prevention by precipitation of reaction product. Deliac (1989) stated that the solubility of silica can be increased by increasing the fineness of glass because more contact area of glass for OH^- to attack. Water cement is also an important factor with regard to pozzolanic activity. The pH of pore solution decreases when high water cement ratio is used due to the dilution effect.

The availability of calcium hydroxide (CH) is one of the factors affecting the pozzolanic reaction rate since it is the main compound in pozzolanic reaction. It is known that replacing cement with high amount of class F fly ash results in lower amount of calcium hydroxide in the paste. In addition the CH content decreases at later age. This is because the high alkaline in pore solution decreases the CH solubility (Fraay, 1989). By the time the pozzolanic reaction of fly ash starts, the CH in pore solution is low. As stated by Brunauer and Greenberg (1960), the C-S-H formed by pozzolanic reaction has lower C/S molar ratios, which may be due to more of Si^{2+} and Al^{3+} available from fly ash while the amount of Ca^{2+} is low. The amount of CH can be increased by decreasing the percentage of fly ash in the mix. The evidence of the unavailability of calcium can be seen from the strength of these two mixes that the strength of 50% fly ash mortar is less than 25% fly ash mortar at 180 days (Jaturapitakkul, 1992). Jaturapitakkul (1992) reported the effect of unavailability of lime at early age. He stated that the slow rate of strength development of fly ash concrete at early age is due to the unavailability of $Ca(OH)_2$. His result shows that the fly ash concrete with additional lime can accelerate the strength at 1 day. However, the faster rate of strength gain may be a result of the

hydration process between additional lime and cement. Fraay (1989) reported that the high concentration of calcium ion was observed in the pore solution of mortar with 20% replacement. Thus, the unavailability of CH at early age is likely to affect the hydration process not pozzolanic process since the fly ash has not dissolved yet. At early age, the addition of CH is more likely to increase the rate of cement hydration. Since fly ash remains in glassy phase at this stage, as such, pozzolanic reaction has not yet taken place at this point.

Apart from chemical influence, fineness is one of the principal parameters, which define the rate of pozzolanic activity. Berube (1995) conducted a test to study the effect of particle size distribution on the effectiveness of fly ash in suppressing expansion. He found that pozzolanic activity of fly ash depend largely on their size, the finer the particle size, the higher the pozzolanic activity, regardless of the process used to increase the fineness. Ravina (1980) measured the fineness in term of specific surface and size distribution. He found a linear relationship between fineness of fly ash and pozzolanic activity. Raask and Bhaskar (1975) determined the pozzolanic activity as the rate of dissolution of silica from fly ash particle in hydrofluoric acid. They found that the improvement of pozzolanic activity of fly ash is related to the increase of surface area, which can be done by grinding. The activity index is proportional to the square of the surface area of ash as followed the diffusion law. He also noted that this assumption could be applied only to fly ash of low carbon because the carbon residue, which has a large surface area, has no pozzolanic activity. In this study, the surface area of fly ash will be increased through grinding process.

Several methods have been used to measure pozzolanic activity of fly ash. It can be distinguished into two categories: chemical and mechanical. The examples of chemical tests are measuring the dissolving rate of glass in alkaline solution, or measuring the lime consumption of fly ash, which reacted with cement paste. From literature, there are many methods developed to measure the dissolving rate of glass in fly ash. The Blair method uses the HCl and NaOH solutions to dissolve the glass and determines the amount of compounds for pozzolanic action (Watt and Thorne, 1966). It should be noted that their solution is much stronger than the pore solution of fly ash cement paste with has $Ca(OH)_2$. Hence, the amount of dissolving compounds may be higher than it is in the real environment. In the Lea method which was also proposed by Watt and Thorne (1966), lime is used as the solution but it measures the change of conductivity of lime solution which may pose error with the presence of nonreacting compound dissolving in the solution. The Jambour method (Raask, 1975) applied the same principle as the Lea method except that it uses the HF solution. Another indirect method is measuring the weight of residue of fly ash in NaOH solution boiling for 2.5 minutes.

For direct method, the amount of free lime in fly ash cement paste is determined after some period of time. This can be done chemically, gravimetrically, or by using the XRD technique. Recently the XRD technique has been used by many researchers to examine the formation of hydration and pozzolanic products in fly ash cement paste at different ages. Tokyay and Hubbard (1992) investigated the relationships between the mineralogical phase in fly ash and the hydration and pozzolanic reaction. They were able

to indicate whether the fly ash is autopozzolanic or pozzolanic by observing the reaction products.

The mechanical test involves comparing the compressive strength of fly ash cement paste and normal cement paste at the age of 28 days. This method is called pozzolanic index (P.I.), which is the method suggested by ASTM. It is based on the assumption that the strength gain is a result of pozzolanic activity of fly ash. It should be noted that apart from pozzolanic activity fly ash might have physical functions that contribute the strength to the matrix. Therefore using this P.I. may not be a good indicator for pozzolanic activity of fly ash.

Many issues on the pozzolanic activity of fly ash have not yet investigated. There are the issue of the pozzolanic activity of new high carbon fly ash and the unburnt coal in fly ash and the means to accelerate the rate of this reaction. . The pozzolanic activity can be enhanced by increasing the three factors stated.

2.8 Grinding Process

The attritor is a mill containing internally agitated media. It has been generally referred to as a "stirred ball mill." The attritor's shaft and arms agitate the media into an expanded condition in which the media is in a random state of internal porosity. In this expanded condition, the media and particles are free to move and collide and impinge upon each other. This irregular movement is caused by the movement of the arms through the grinding media. A large number of small grinding media are agitated by a pin-shaped impeller in a cylindrical vessel. Three types of forces are generated: impact

action on media with other media, rotation force on the media, and tumbling force as media fall into the void.

The grinding process can be operated in either batch or continuous processing application. The batch grinding is employed when the prime consideration is the finest particle size possible and the tightest particle size distribution is necessary, and larger quantities are of lesser concern. The continuous grinding is chosen when the large production quantity is required, or when the material has a tendency to cake. Constantly moving material through the media bed prevents material build-up against the tank wall. However, the continuous process requires a stable condition be maintained inside the mill at all times. The retention time in the mill of both processes has to be long enough to reduce the particles to the size desired.

The efficiency of size reduction is a function of material to media ratio, grinding media, grinding time, rotation speed and the properties of material. A proper portion of material-to-media must be obtained. If the ratio of material-to-media is too high, the velocity and impact force of the media will be reduced and inefficient particle size reduction will result. On the other hand, if the ratio of material-to-media is too low, the media will impact against itself causing wear of the media. When the material and media ratios are optimized, efficient particle size reduction results.

The efficiency of grinding process depends not only on the material-to-media but also on the power input. The power input of attritor is used for agitating the media to achieve grinding and is not used for rotating or vibrating the heavy tank in addition to the media. Thus, the rotation speed of the attritor directly governs the efficiency of grinding process.

Previous studies on mineral systems have indicated that stirred ball milling may be a promising method for producing micronized material. It has been reported that mills having capacities greater than 20 tons/hour were used to grind coal to a median size of 6 μm. In this study, the optimum operating conditions have been determined to obtain the desired size of fly ash which is reported to give high strength to concrete is a median size below 10 μm.

One of the major concerns of using grinding method to process fly ash is the wearing off of the media. If happens, it raises the costs of processing fly ash hence making it undesirable to utilize. If the grinding condition such as revolution and grinding time is higher than optimum condition, the media wears off and adds contaminants to fly ash. This objective of this study is to obtain the optimum grinding condition to grind fly ash to have desired size range and fewer amounts of contaminants from media. The ratio of media to fly ash will be variable parameter for each grinding condition. The batch grinding is employed

2.9 Unburned Coal in Fly Ash

Bubbling Fluidized Bed Separator: Levy (1996) and his colleague propose the bubbling fluidized bed separator to reduce carbon percentage of fly ash. This method uses the combination of gravitational separation and acoustic system. Particles, which have low density, drift to the top of the bed by the air and the high-density particles stay in the lower level. The carbon distributes along the depth of the bed from high amount at the top and low amount at the bottom. However fly ash tends to agglomerate together and yield big particle which makes it difficult to fluidize. This research group applies high

intensity of acoustic field to disrupt the interparticle forces between these particles, permitting active bubbling of fine fly ash. To retrieve only the coarse portion that has high percentage of carbon, fly ash was sieved with 325-mesh fraction. This sieving also avoid the mixing of fine fly ash which has density close to carbon with carbon. In their study, 50% of LOI can be removed with a 65% ash recovery within the cost of $2/ton. The removal rate can be enhanced by increasing the intensity of acoustic system and lowering the ash recovery.

The electrostatic separation is proposed by Stencel and his team (1996) to reduce carbon from fly ash. This technique is based on the difference of polarity between fly ash and carbon. When particle collides with each other or wall, their polarity change which depends on difference between the surface work function of the colliding components. The particle that has low work function will give up electron to the particle that has high work function. When fly ash containing carbon passes through the charger, it becomes negative because it interacts with Cu surface while the carbon, which has low work function, becomes positive. When they are subjected to high voltage electrical field, negative particles are attracted to positive plate and positive particles are attracted to negative plate, which can be easily removed. The fly ash that used in their research are separated into three ranges: full size, > 75 μm, and <75 μm. Their result shows that in order to reduce 50% of carbon, the recovery rate of full range fly ash is 55-60%, that of coarse fly ash (>75 μm) is 45-55%, and that of fine fly ash (< 75 μm) is 80-95%. The treatment cost is $3/ton.

Suprenant (1992) applies the LOI test by ASTM to remove carbon from fly ash but in larger scale. Fly ash is preheated and dragged to ignition chamber, which has

temperature 750 °C. The high heat burns the carbon containing in fly ash. At the treated fly ash is then allowed to cool down in a water-cooled screw auger. At a power cost of 50 cent per ton, the unit can reduce LOI from 2.3% to 0.2% and from 6% to 1%. They claim that the heating costs for high LOI fly ash is lower because the carbon generates heat. The chemical and physical analyses have been performed on fly ash sample before and after processing. Their result shows that there is no change in other chemical or physical properties of fly ash.

The effects of carbon on fly ash concrete are known to include discoloration, poor air entrainment behavior, more water requirement, and low compressive strength. Unburned carbon in fly ash can make it unsuitable to use because it interferes with the action of air entraining agent (AEA) which is used to stabilize air bubbles in concrete. These compounds have a dual hydrophillic and hydrophillic nature. AEA stabilizes air bubbles by collecting at the air-water interface with their hydrophobic end protruding into the bubble surface and their hydrophillic end oriented into the aqueous phase and adsorbed on the surface of cement or fly ash particles (Freeman, 1997). Freeman (1997) found that hydrophobic end of AEA is attached on carbon surface area consisting of the external surface of carbonaceous particle and some internal surfaces of larger pores. This results in rendering them unavailable for attachment to air bubbles and this low-entrained-air concrete will have less resistance to freezing and thawing cycles.

Generally loss on ignition is the accepted means for monitoring fly ash carbon content. However many studies has demonstrated the inadequacy of LOI as an indicator of fly ash's air entraining performance. Their results showed that fly ash performance with air entraining agent varied significantly regardless of similar LOI value. LOI test is

not sufficient to indicate the interaction between AEA and fly ash because it does not specify the form and sorptive properties of carbon. Many researches has been done to investigate the measures that suitable to indicate this property.

Freeman (1997) studied the adsorptive behavior of carbon in fly ash by using modified foam index test to characterize the interaction between AEA and different carbon material (fly ash carbon, pelletized carbon, activated carbon, and coal). The rank order of their activities suggests an adsorption process occuring on non-microporous carbon surface. Their results show that the AEA/carbon interactions are time dependent and the degree of interaction correlates with the surface area of carbon. If the size distribution of carbon decreases, the area for affixing AEA increases. So far no technique can measure this area accurately. The Nitrogen BET surface area is not adequate because it includes microporosity that is not effective in AEA sorption.

Gao (1996) and his teams used carbon black as a model for soot, which they found it existing in fly ash. They concluded that the degree of interaction between AEA and carbon black increases with the decreasing of particle diameter or with the increasing of measured nitrogen surface area. Their results also showed that AEA adsorption is governed by the amount of hydrophobic carbonaceous surface area.

Another indirect methods for measuring the adsorptive behavior of fly ash have been proposed. Hill (1997) examined the performance of AEA and fly ash by applying thermal analysis and petrographic examination. He found that carbon in fly ash is composed of different forms. One type has the same properties as the original coal. The other types are particles that have melted, devolatilized, swelled and resolidified which is called "coke". This type is subdivided into two forms. The isotropic coke is disordered

in microscopic scale whereas anisotropic coke has more developed alignment of the molecules. The adsorptive carbons are generally isotropic. The hydrophobic end of AEA affixes to these areas resulting in shortage of AEA for attachment to air bubbles. Fly ash containing a large portion of isotropic coke has a greater adsorptive capacity than fly ash containing a high proportion of anionic coke. However used the optical method to count the number of isotropic and anisotropic coke. His results showed that the higher demand for AEA related to the presence of a higher proportion of isotropic to anisotropic carbon in fly ash. The liquid and vapor phase adsorption analysis suggested that the surface chemistry characteristics of the isotropic carbon resulted in a higher adsorptive capacity for polar compounds such as AEA.

In this study the adsorptive behavior of ground fly ash will be investigated. Since carbon in ground fly ash is also ground to small size. Its distribution is expected to decrease which may affect the adsorptive capacity to AEA. This study will be focused on characterization of ground fly ash, which has the same amount of loss on ignition. The BET specific are of all samples will be determined.

Previous researcher found that fly ash which has high amount of carbon has lower strength than fly ash with low carbon. It is known that the compressive strength of mortar depended mostly on particle size distribution of fly ash. Therefore carbon in fly ash which is usually big can reduce the strength significantly. This study used the ground fly ash which the carbon is ground to small size. The compressive strength of this ground fly ash is determined. The result will show the effect of the size of carbon.

The effect of residual carbon content in fly ash on the hardened cement paste properties was investigated by Hornain (1992). Fly ashes with three percentages of

residual carbon were used: 5, 7, and 12%. The order of fineness is the fly ash with 12, 7 and 5%. Their results show that strength of fly ash with 12% is not different from that with 7 and 5% and is lower than that of the normal cement specimens. The strength of these fly ashes mortars increase with time. They conclude that the high carbon content did not have any detrimental influence on the concrete mixture. Since fly ash with 12% is finer than 5% so it might be this fineness that contributes high strength to the mix and covers the effect of carbon in fly ash. In order to investigate the effect of carbon on strength, the fly ashes that used should have the same fineness.

CHAPTER 3

OBJECTIVES OF THE DISSERTATION

In this study, attempts have been made to process fly ash to ensure consistent quality and suitability for mortar application. To achieve this, it is essential to determine the properties of ground fly ash, which affect the strength of mortar. Among these important characteristics are particle size distribution, mineralogical composition, and chemical composition. The performance of fly ash mortar and the contribution of fly ash to the properties of mortar were investigated. Three major types of fly ashes, wet bottom, dry bottom, and low NO_x fly ashes were used to study the potential application and applicability of this proposed processing technology. Furthermore, this study evaluated the properties of mortars made of high-carbon ground fly ash. The processing technique is expected to improve the quality of fly ashes, to increase the usage of fly ash in concrete and to reduce the amounts of fly ash disposed off to the landfills. The experimental work is divided into five parts as follow:

3.1 Study the Grinding Mechanism on Fly Ash Fineness

The objective of this section is to modify the fineness of fly ash by using grinding technique. Raw feed fly ashes were ground to three different particle size distributions. To obtain the desired fineness of fly ash, one needs to understand the parameters governing the grinding mechanisms. The concerned parameters include the type of fly ash, the grinding time, and the fly ash to media ratio. The characteristic of fly ash

observed is its particle size distribution. These ground fly ashes were used throughout the program.

3.2 Study the Properties of Ground Fly Ash

In order to evaluate the effects of fly ash on the performance of its mortar, the characteristics of each fly ash have to be thoroughly understood. The key characteristic of fly ash, which affects the properties of fly ash mortar, is its particle size distribution. The raw fly ashes from different sources were ground into three different size distributions to study their effects on the strength of mortar. Since other characteristics of ground fly ashes may have influences as well, ground fly ashes were analyzed for their chemical composition, mineralogy, morphology, loss on ignition, as well as particle size distribution.

3.3 Study the Effect of Fly Ash on the Hydration of Fly Ash Paste

The study will investigate the effect of fly ash on the cement hydration process in fly ash paste. The pastes were made from raw and ground fly ash of different particle size distribution. Cement hydration in fly ash pastes was monitored during its early and late stages by observing the hydration products. Since fly ash does not react in early stages, its influence on mortar strength would seem to be some physical mechanisms imparted by the fly ash. The results show the effect of particle size on the hydration process at early age. At later age, where pozzolanic contribution of fly ash begins, fly ash reacts with calcium hydroxide in mortar, reducing the amount of lime, calcium hydroxide in the paste. Therefore, decreasing lime content would indicate pozzolanic activity occurring in

fly ash paste. This observation, utilization of lime by fly ash to produce pozzolanic material reducing the concentration of lime in the cement paste will help us to evaluate the role of particle size on the pozzolanic action of fly ash paste.

3.4 Study the Properties of Ground Fly Ash Mortar

Fly ash mortars were made using ground fly ashes of different particle sizes distribution. The compressive strengths of fly ash mortars were examined and compared. The strengths of these fly ash mortars were correlated to the particle size distributions of ground fly ashes. The result will help us to understand the effect of particle size of fly ash on the strength of mortar. The influence of the amount of cement replaced by ground fly ash was also examined. This was done by comparing the strength development of fly ash mortars at different percent replacement of ground fly ash. The optimum mix proportion of fly ash mortar for each fineness was determined. The optimum mix is defined as the highest amount of fly ash with strength of the matrix surpassing that of the control mortar at 28 days. The development of morphology and pore structure in each ground and unground fly ash mortars were monitored at selected curing ages using Environmental Scanning Electron Microscope (ESEM). The result should provide the optimum quantity for each size of ground fly ash to maintain the strength of fly ash mortar.

3.5 Study the Effect of Carbon in Fly Ash on Fresh and Hardened Mortar

The objective of this test is to investigate the effect of unburned coal on the properties of fly ash mortar. The low NO_x fly ash, which has high carbon, was used as a cement

replacement. The carbon in fly ash was varied by using thermal process and STI process. After the carbon removal process, the physical and chemical properties of each fly ash were determined. They were then ground to have the same particle size distribution. The ground and unground modified fly ash mortars were tested for air entraining absorption to see the difference in adsorptive capacity between ground and unground fly ashes. This behavior was measured by the consumption of air entraining admixture (AEA) by fly ash. The effect of residual carbon content in ground and unground fly ashes on the strength of mortar was investigated. Mortars were prepared with 25% and 35% of ground and unground fly ash. The result should confirm that the grinding method would be an effective mean to process undesired high carbon fly ash into beneficial fly ash.

CHAPTER 4

MATERIALS AND EXPERIMENTAL PROGRAMS

4.1 Experimental Program

In this chapter, the experimental programs for studying the influence of selected parameters on the compressive strength of ground fly ash mortars were conducted. The particle size distributions and mineralogy of fly ash is among the main parameters to be studied. The grinding process was used to process fly ash into different size distribution. The effect of fly ash on the compressive strength of mortar was carried out using different percentage of fly ash and different types of fly ashes. The study also includes the investigation on how fly ash contributes strength to the matrix by examining the microstructure, the pore size distribution, and the hydration process of fly ash mortar. In addition, the effects of carbon in ground fly ash on the properties of fresh and hardened mortar were also investigated.

Fly ashes used in this study were collected from four different power plants in the northeastern region of the U.S. Each power plant operates with different combustion process. The fly ashes that used in this program are designated as H, M, B, and GPU.

The standard ASTM 2"x2"x2" cube specimens were used for studying the compressive strengths of mortar. The test was performed on an MTS closed-loop servo-controlled hydraulic testing machine. Details of the test programs are described as follows:

4.2 Materials

Materials used in this study consist of Portland cement type-I, river sand, fly ash, and water.

Cement-A standard Portland cement type I

Sand-A siliceous sand passing through sieve No.4 (opening size 4.75 mm) was used for casting mortar

Fly Ash-Four types of fly ashes were used: fly ash from wet bottom furnace (MO), dry bottom furnace (BO, BOT, HO), and low NO_x burner (GPU1O, GPU2O).

Wet bottom and dry bottom ashes were selected to study the influence of boiler type and its combustion condition. The low NO_x fly ash was chosen to investigate the effect of unburned coal on properties of fly ash mortar. These fly ashes were ground into different particle sizes. The ground fly ashes were cast and tested for the strength on fly ash-cement mortar.

Water-Tap water was used throughout the experimental program.

4.3 Test Programs

4.3.1 Grinding Process

The objective of this study is to obtain the grinding condition that yields the desired particle size range with optimum energy and lower contamination. Two test programs were performed: selecting the media that poses lower contamination to ground fly ash and determining the suitable ratio of media to material and grinding time that can yield the required size distribution.

The raw fly ashes were ground into different particle size using the Attritor HSA-10 as shown in Figure 4.1. Since the present of iron contaminating from grinding media may alter the properties of ground fly ash mortar, the grinding media that gives the least iron contaminant to fly ash was selected. Two types of media were tested in comparison, zirconium beads and carbon steel media. The trace element of ground fly ash using these two media was analyzed by XRF.

After selecting the media type, three different fly ashes were ground into different size by varying different controlled parameters. The key factors in this test are material to media ratio (2.5:1, 2:1, and 1:2), and grinding time (1, 3, 5, 10, 20, and 30 min). At least three grinding times were used for each fly ash. The parameters, which are held constant, are type and size of grinding media (zirconium bead of 2.5-mm diameter), volume of media (2 liters), and stirring speed (1000 RPM). During each intermission a small amount of sample was taken out to determine the particle size distribution by optical method. The PSD from different grinding was plotted in the same graph, hence tracking the PSD of fly ash in the process. They were used in studying the relation of particle size of fly ash and strength development of fly ash mortar. Figure 4.2 shows the diagram of the grinding process.

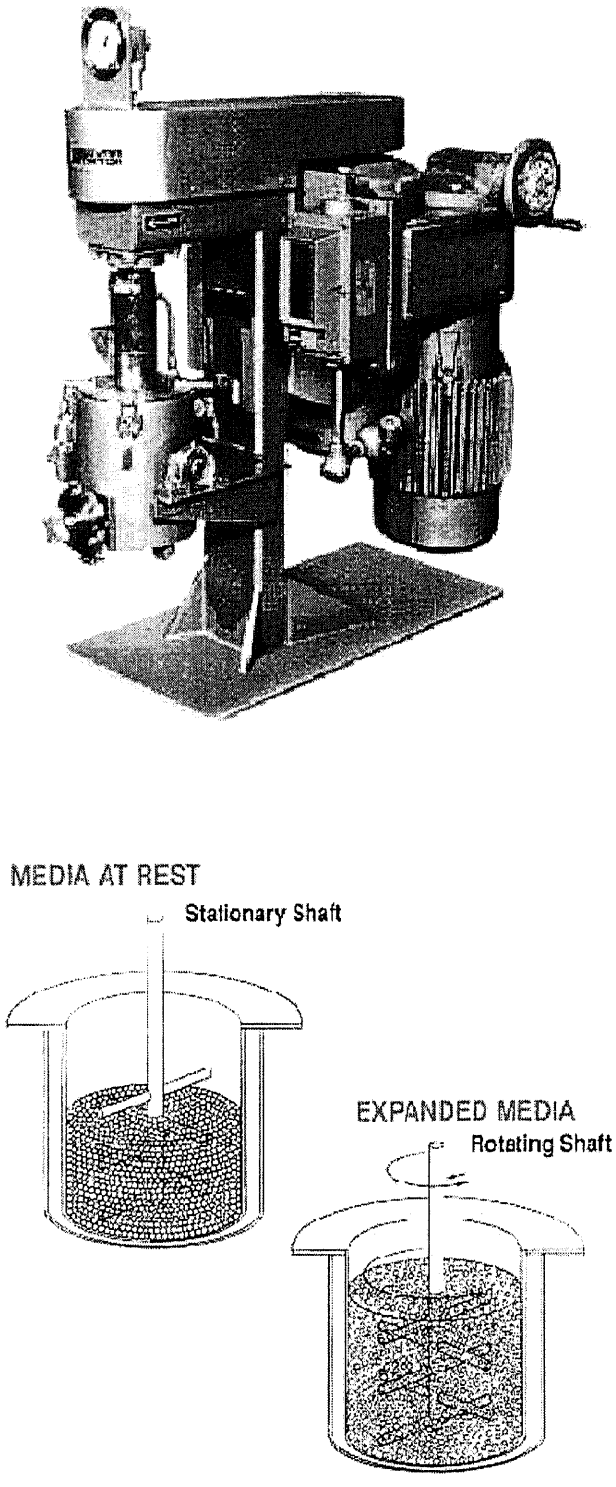

Figure 4.1 Attitor: (a) Lab-Scale Attritor Model HAS-1, (b) Rotating Shaft and Arms Agitating the Media during Grinding Process

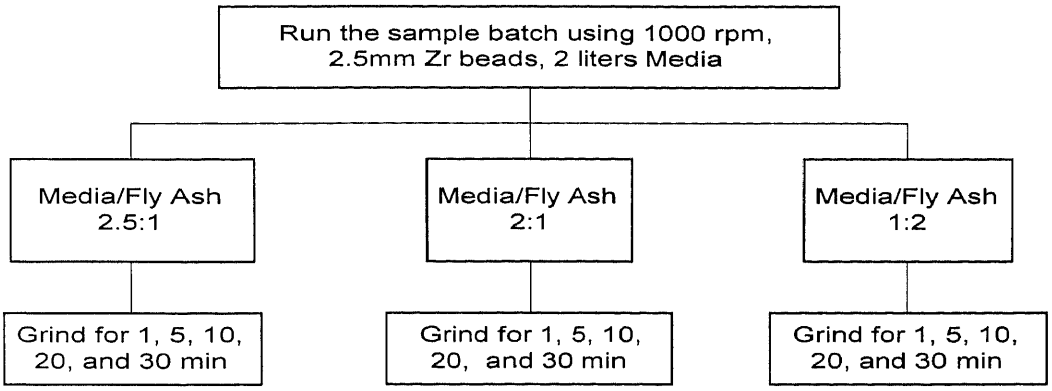

Figure 4.2 Experiment Diagram of Grinding Process

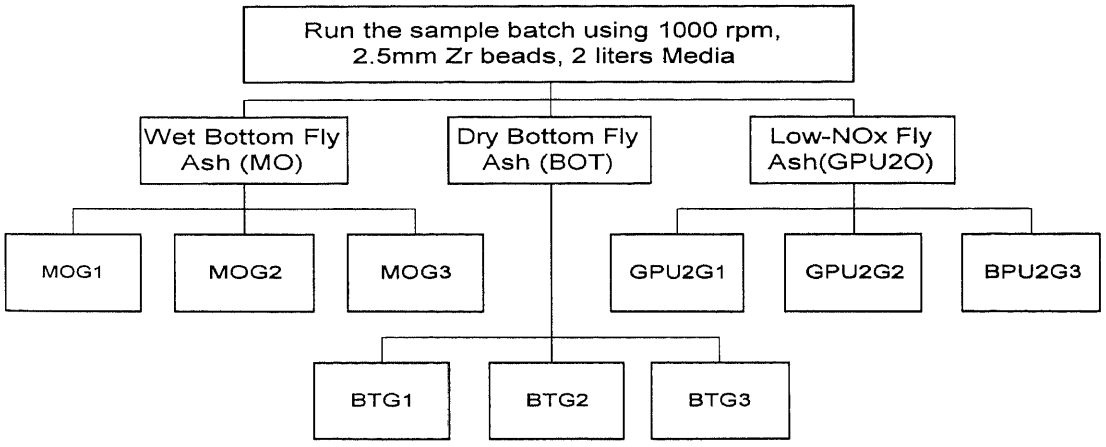

Figure 4.3 Experiment Diagram of Grinding Fly Ashes into Different Size Ranges

To prepare fly ash for the study on the effect of carbon on strength development of fly ash mortar, low and high carbon fly ash were ground to the same size distribution, which is below 10 microns. To achieve the proper grinding condition, trial run was done for each fly ash until matching PSD is obtained.

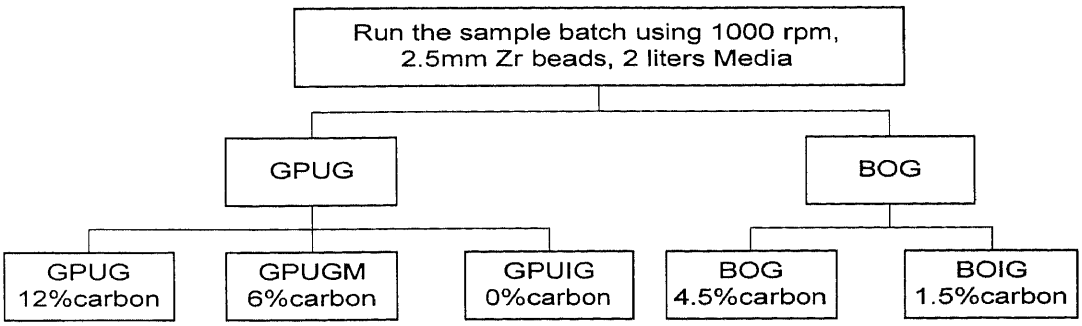

Figure 4.4 Experiment Diagram of Grinding Fly Ashes with Different Carbon Content

4.3.2 Carbon Removal Process

Carbon in fly ash is removed by burning fly ash at 750 °C for 3 hours. Fly ash from low NO_x burner is used in this test since it has high percentage of carbon. BO fly ash was treated by using the STI process and was performed by STI Company.

4.3.3 Bulk Chemical Composition

Bulk chemical compositions of ground fly ashes were determined by X-Ray Fluorescence. All fly ash samples were ground to have particle size of smaller than 50 microns. This is to reduce the error from particle size effect and segregation. The sample type is loose powder. The quantitative program that used for analyzing the sample is Semi Quantitative program (Semi Q).

4.3.4 Mineralogy of Fly Ash

The mineralogical study of the fly ash was analyzed by X-ray diffraction (XRD). Phillips PW 1050 diffractometer with CuKα radiation at generator setting of 40 kV and 50 mA

was used. Before XRD measurements the sample was ground by ceramic mortar for 10 minutes to obtain homogeneity of the grain size below 50 microns and they were then filled into specimen holder by backpacking for XRD analyses. The XRD scans were run at 0.05° steps, and with a 4 seconds per step. Phases were identified by reference to the ICDD Minerals Powder Diffraction files by means of PCD 4.0f software. The percentage of glassy phase of each ground fly ash was determined. The peak area of the graph between energy and 2-theta is defined as amount of crystalline phase in fly ash. The glassy phase is defined as a hump in the graph, which is the area under the base line of peak and above the background curve. These areas can be obtained by using PCD 4.0f software.

4.3.5 Morphology and Chemical Analysis of Surface of Fly Ash

The micrograph of each fly ash was taken by environmental scanning electron microscope equipped with an Energy Dispersive X-ray (EDX) attachment (Kevex 8000 model) with 20 kV accelerating voltage. Particle counting is conducted by using Mirage program. The element analysis of the surface of raw fly ash was examined by using Energy Dispersive Spectophotometer. Each sample will be taken at different magnifications and different location in order to obtain the representative image. The energy of electron was keep constant at 20 kV. The data from this test is used to identify the major element on each particle.

4.3.6 Particle Size Distribution of Fly Ash

The particle sizes of fly ash were determined by Microtrac SR150, a laser based particle sizer. The media that used for circulating fly ash is deionized water. To avoid clogging in circulating system, 99% isopropyl alcohol is used to run cement. 20 mg of fly ash was mixed with 60 ml of water and 10 ml of dispersing agent (Titron X). The mixture was placed in sonicator for 10 minute to disperse the cluster of fine particle before adding into the circulating media. The parameters, which are used to run the size measurement, are particle refractive index (1.81), shape of fly ash (irregular), fluid refractive index (1.33), and particle transparency (transparent). Each run takes 30 second. The average of three runs was used.

Four batches of fly ash are used to measure the particle size in this study. They are Mercer91, Mercer95, Hudson91 and Hudson95. Each batch is classified into different categories by weight.

Mercer91: M13F91, M14F91, M15F91, M16F91, M17F91, M18F91, M18C91, MO91

Mercer95: M8F95, M9F95, M12F95, MO95, MOG95, M8CG195, M8CG295

Hudson91: H3F91, H5F91, H6F91, H7F91, H10F91, H11F91, H1C91, HO91

Hudson95: H7F95, H8F95, H7C95, H8C95

Step Involved in Particle Size Analysis

1) Study the Refractive Index

From the previous study most of the compound on the surface layer of fly ash is siliceous compound. This compound has the refractive index about 1.81. By consulting with the table of the instrument manufacturer, this compound is considered to be transparent.

Besides the particle appears no indication of any reflectivity under the light microscope. The picture also shows that greater than 85-90% is non-agglomerated spheres. Therefore it can be concluded that the size distribution is measured by using transparent parameter.

2) Sample Preparation

Wetting a mixing of the sample requires the selection of proper combination of the solvent and a surfactant. Water is used since fly ashes in this study are not autopozzolanic. Precise measurement of sample quantity is not necessary for satisfactory operation of the instrument since there is a function that is used to determine the amount of sample required for optimum measurement. Therefore low concentration of fly ash sample is prepared so that the dispersion process can work effectively.

The dispersing agent that used in this study is Tritonx100. It is a nonionic surfactant with a pH of about 6 to 8. The optimum amount of this chemical is obtained by plotting the curve between the amount of the dispersing agent and the particle size distribution. The curve that gives the highest amount of fine particle is considered to be the curve of optimum amount of dispersing agent. The ultrasonic wave is applied outside the circulation system. Each sonication is undergone about 30 minutes before measuring the particle size. The sample preparation method is described as following;

1. Prepare 10% by weight of Tritonx100
2. Weigh 200 mg of fly ash and add it to 60 ml. deionized water.
3. Add 10 ml of 10% Tritonx100 to the well-mixed sample and stir it.
4. Place sample flask in the ultrasonic bath for 30 minutes.
5. Immediately pipette the sample into the recirculator.

6. Run three tests with 30 seconds duration. The result is accepted only if its repeatability of the size distribution data is observed.

4.3.7 Loss on Ignition

The loss on ignition (LOI) test is the standard method for determination of the carbon content of fly ash. Fly ash sample is dried overnight at 140 °C to drive off water absorbed in interstitial space and then weighed before being placed in an ashing furnace for several hours at 750 °C. The sample is then reweighed and the loss in weight is assumed to be due to the carbon initially in the sample.

Particle size of carbon of raw feed fly ash was determined by sieving the fly ash and the amount of carbon retained in each size range is also measured by LOI test. Raw feed fly ash was sieved into different size: #40, 50, 60, 80, 100, 140, 200, 230, 325, and 500. Particle size distribution of fly ash measuring by dry sieving method was conducted by calculating the weight percentage of fly ash retained on the sieve. Size distribution of carbon was conducted by calculating the weight percentage of carbon burnt out at 750°C of each sieve.

4.3.8 Contaminants from Grinding Process

The grinding process may introduce chemical to fly ash. This is because the media or arm and bowl of attritor can wear off during grinding. The contaminant may effect the behavior of fly ash mortar or concrete. In this study, two types of media were used: zirconium bead and carbon steel. Their properties are shown in Table 4.1. Both media has higher hardness than fly ash so they can be used as a grinding media. Fly ashes,

which were ground by ceramic mortar, were used as a control fly ash since the ceramic mortar does not wear off during grinding. The elemental analysis of fly ashes, which were ground by using zirconium beads and carbon steel, were compared with this control fly ash. Element of three series of fly ashes were analyzed using XRF.

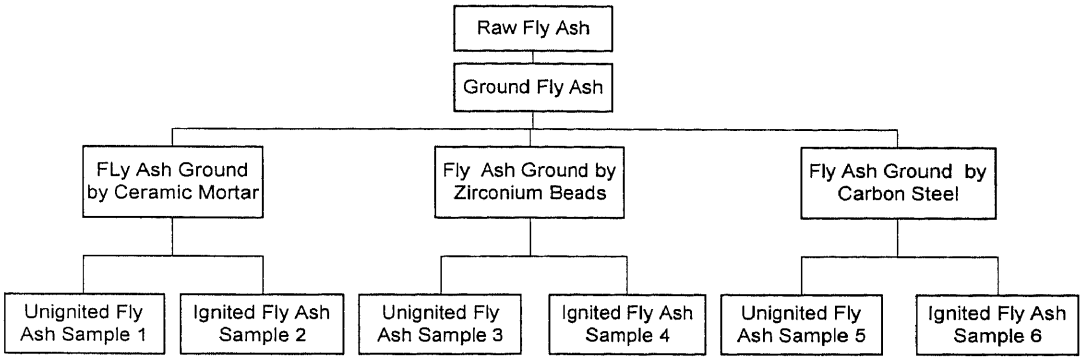

Figure 4.5 Organized Chart of Grinding Procedure Using Different Media

Table 4.1 Properties of Grinding Media

Media	Size (mm)	S.G.	Hardness	Cost	Color	Remark
Zirconium Silicate	2.0-2.5	3.85	MOHS7.0	Moderate	White	-
Carbon Steel	1.25-2.00	7.8	Rockwell C62-66	Low	Grey	Ferrous Oxide

4.3.9 Strength Development of Ground and Fractionated Fly Ash Mortar

Three types of fly ashes (MO, GPU, BOI) were ground into different size ranges by using grinding conditions obtained from grinding process program. Four sets of ground fly ashes are used as a replacement of cement 15%, 25%, 35% and 50% by weight of cementitious materials. The compressive strengths of ground fly ash mortar will be

tested at 3, 7, 14, 28, 60 and 120 days. The 2x2x2 cube is used to determine the compressive strength of ground fly ash mortar. Strength development of fly ash mortars using different size range of fly ash will be compared between each other in order to analyze the effect of particle size of fly ash on the strength of mortar. The strength development of fly ash mortars at different percent replacement of ground fly ash will be plotted and compared. The result is expected to show the effect of percent replacement of ground fly ash on the strength development of mortar. The relationship between compressive strength of fly ash mortar and percentage of cement replacement are plotted to obtain the optimum percentage of each series. The mix that uses the highest amount of fly ash with strength of the matrix surpassing that of the control mortar at 28 days is considered as the optimum percentage for that fly ash mortar. The mix proportion of this test program is shown in following table.

Table 4.2 Mix Proportion of Processed Fly Ash Mortar

Ingredients	Ground Fly Ash (by weight)		
	0	25 %	35 %
Cement	1.00	0.75	0.65
Fly Ash	-	0.25	0.35
Sand	2.75	2.75	2.75
Water	0.50	0.50	0.50
Water/(Cem+FA)	0.50	0.50	0.50

4.3.10 Quantitative Structural Study of Fresh Fly Ash Cement Paste by Image Analysis

In order to know in detail the changes in the pore structure of fly ash pastes, the size distribution of capillary pores in hardened fly ash paste and cement paste were

determined by ESEM image analysis. Three types of fly ashes with different fineness: Cement, MOG125, MOG2, and GPU2G1 were used in the mix.

Sample Preparation

The paste specimens were prepared from 25% of fly ash and 75% of Type I Portland cement. The water cement ratio of all paste was 0.50. The mixture was kept inside the plastic container until the observation period: 3, 7, 28 and 250 days. The sample preparation for 5-minute paste analysis was different from samples at older ages since the paste was not hardened yet. To catch the instant picture of this sample, it was hardened by freezing with liquid nitrogen. The mixture was put into plastic bag and soaked in liquid nitrogen for 5 minutes. Then the sample was cut to a thin slice and observed immediately with ESEM. The temperature and the pressure in the chamber were adjusted to -20 °C and 2.5 Torr. The other specimens for image analysis were prepared by cutting a thin slice from the middle of each past specimen. No coating or finishing is applied in order to keep the surface untouched. The microstructure examination was carried out under Environmental Scanning Electron Microscope (ESEM) with an acceleration voltage of 20 kV.

Image Analysis

Micrograph at 400x and 1000x of each specimen were obtained. The structure is composed of solid grains appearing in white and large pores and interconnected pores appearing in black. Normally the gray scale of the untouched image does not show a clearl separate peak for the pore. Therefore the gray level was selected for each image by

adjusting the threshold level. The pore size determined as a diameter of a circle of area equal in area to that feature was calculated by Image Analysis program. The upper limit of size is 10 microns which is the largest size of capillary pores. The lower limit is a function of pixel size. In this program, the minimum is set at 7 pixels and the minimum size of a 7-pixel pore feature accessible at 1000x is approximately 0.8 microns in diameter. This limit is also applied to image with lower magnification since the pore size obtained with this magnification is usually larger.

With assumption that the fraction of area of pore is equal to the fraction of volume of pore in the specimen. Therefore, the pore area is considered as three-dimensional volume of each pore. The total pore size distribution of the paste is obtained from multiplying the pore size distribution with the total porosity of the pastes. The method of porosity measurement is described in separate section.

Methods of Porosity Measurement

The liquid displacement technique is used in this study. Paste specimen is vacuum saturated in water for 1 day and weigh in the saturated, surface dry condition (Ws). The buoyant weight of the sample (Wb) is then measured by suspending it in the water. The water is then removed by oven drying the sample at 110°C to constant weight (Wd). The mass of water lost from saturation for drying is an estimate of the evaporable water content in the specimen. The percent porosity can then be calculated as equation.

$$\text{Porosity (\%)} = (Ws - Wd)/ (Ws-Wb) \times 100$$

The pore size distribution is calculated as follows.

Total Pore Size Distribution (%) = Porosity x Pore Size Distribution from Image analysis

4.3.11 Quantitative Analysis of the Calcium Hydroxide in Fly Ash Cement Paste by X-ray Diffraction

This test is aimed to determine the mount of calcium hydroxide generating during the hydration process of fly ash cement paste. The hydration processes of fly ashes, which have the same mineralogical compounds but treated with different method, were examined. The ground (MOG1, MOG2) and raw feed (MO) of wet bottom fly ash were observed. The cement pastes (water/binder ratio of 0.50) were cured in plastic containers at a temperature of 20 °C and vacuum environment for different period of time (2, 3, 4, 5, 8, and 12 hrs, 1, 3, 7, 14, 28 days). The hydration stopped when it was soaked in acetone and dry ground. The samples were subsequently dried at 60 °C for 3 hours. Then, the samples were dried, ground by ceramic mortar for 10 minutes to obtain homogeneity of the grain size below 50 microns and filled into specimen holder by backpacking for XRD analyses. Quantitative x-ray powder diffraction (QXRD) analysis of calcium hydroxide was carried out using straight model for area phase type. The XRD scans were run at 0.05° steps, and with a 1 second per step.

4.3.12 Investigation of Hydration Reaction and Pozzolanic in Ground Fly Ash Cement Paste by X-ray Diffraction Method

The reaction between components of the fly ash and cement were studied by means of X-ray diffraction technique of different mixtures during their curing. Mixture were prepared with 25% cement replacement by weight by fly ash and with 0.50 water cement

ratio. Fly ash was mixed with cement and water in the same manner as mixing the mortar. The fly ash cement pastes were cured in plastic containers at a temperature of 20 °C and vacuum environment for different period of time (2, 5 hrs, 1, 3, 7, 14, 28 days). The hydration stopped when it was soaked in acetone and ground. The samples were subsequently dried at 60 °C for 3 hours. Before XRD measurements the samples were dried, ground by ceramic mortar for 10 minutes to obtain homogeneity of the grain size below 50 microns and filled into specimen holder by backpacking for XRD analyses. The XRD scans were run at 0.02° steps, and with a 4 second per step. Phases formed at different ages were identified by reference to the ICDD Minerals Powder Diffraction files.

4.3.13 Microstructure Examination of Fly Ash Cement Paste

The development of morphology and micro-chemical features in each ground and unground fly ash mortar will be monitored at selected curing ages using a scanning electron microscope (ESEM). A small piece of ground fly ash mortar will be examined under high magnification at different age of 1, 3, 7, 14, 28 and 250 days.

4.3.14 Study the Effect of Carbon in Fly Ash on Fresh and Hardened Mortar

In order to see the effect of carbon content on the properties of fly ash mortar, the amount of carbon in fly ash will be varied. Two types of carbon removal technique are used; Thermal Process and STI process. For the Thermal Process, carbon in low NO_x fly ashes (GPU) was adjusted to 0, 6, and 12 %. The fly ash with 6% carbon will be prepared by mixing unburned fly ash which has 12% carbon with burned fly ash which has no carbon.

Using STI process, carbon in BO the dry-bottom fly ash was adjusted to 1.45 and 4.5%. The particle size and mineralogical component of fly ash after going through the carbon removal process will be studied. They were then ground to have the same particle size distribution. The ground and unground modified fly ashes will be tested for air entraining absorption, and were used as cement replacement.

The effect of residual carbon content in ground and unground fly ashes on the strength of mortar will be investigated. Two series of mortars will be prepared: ground and unground fly ash mortars. Mixtures containing 25 and 35% of fly ash as cement replacement will be prepared. Microstructure of the interface between carbon and cement paste will be observed by ESEM and EDS analysis. Compressive strength of mortar will be measured after 1, 3, 7, 28 and 60 days. The result will provide the effect of residual carbon content in the fly ash on the strength development of fly ash mortar.

4.3.15 The Interaction of Carbon in Fly Ash with Air Entraining Admixture by Using ASTM 311

The objective of this test is to investigate the difference in adsorptive capacity between ground and unground fly ashes. This behavior is measured by the consumption of air entraining admixture (AEA) by fly ash. If AEA is absorbed by fly ash, there will be less air content in the matrix. Air content is measure by using gravimetric method (ASTM C138). Two series of fly ashes are used: unburned ground fly ash and burned ground fly ash. They are GPU2, GPU2I, GPU2G, and GPU2GI. The burn ground fly ash series is used as a control since it does not have carbon. A test modified by Stephen Lane is used in this experiment. Specific gravity of cement, sand and fly ash are measured by using ASTM C128. Air entraining agent used in this study is vinsol resin.

CHAPTER 5

RESULTS AND DISCUSSION

5.1 Grinding Process

The Attritor HSA-10 was used to perform the batch dry grinding process in this study. The grinding process is achieved in a stationary tank by means of rotating shaft and arms that agitate the media into a random state. As a result, the grinding media brakes the fly ash into small particles. To achieve the desired size of fly ash, the material-to-media and grinding time were varied while the type and size of grinding media (zirconium bead of 2.5-mm diameter), volume of media (2 liters), and stirring speed (1000 RPM) were held constant. At least three grinding times were used for each fly ash. The carbon steel beads and zirconium beads were chosen as grinding media. The media that poses less contamination to ground fly ash was used throughout the program. After selecting the media type, MO, GPU2O and BOT fly ash were ground into different size. During each intermission a small amount of sample was taken out to determine the particle size distribution by optical method. The PSD from different grinding was plotted in the same graph, hence tracking the PSD of fly ash in the process.

5.1.1 Contaminants from Grinding Process

The XRF elemental analysis of fly ashes ground with different media is shown in Table 5.1. Fly ash used in this contamination study is low NO_x fly ash (GPU). Control fly ash was raw fly ash hand ground by ceramic mortar and pestle. Fly ash ground by using zirconium beads is GPU2GZR. Fly ash ground by using carbon steel is GPU2G5SS. Iron was a major concern in this investigation because it wears off from arm and bowl of

Attritor during grinding process. It can be seen from Table 1 that even fly ash ground by zirconium beads which does not contain iron, has higher iron content than that of control fly ash. The additional amount comes from the grinding bowl and arm. The fly ash sample ground by steel balls has the highest iron content as expected. Iron affects the behavior of mortar. To lessen the contaminant from grinding process, the zirconium bead will be used as the grinding media throughout the experiment.

Table 5.1 Chemical Analysis of Ground Low NO_x Fly Ash Using XRF (Super Q)

Element	Normalized Concentration(%)		
	Sample #1 gpu2o	Sample #3 GPU2GZr	Sample#5 gpu2g5ss
Na	2.542	2.320	2.494
Al	32.824	29.176	26.568
Si	45.351	45.202	40.216
K	2.528	2.498	2.278
Ca	6.630	6.852	5.915
Fe	15.239	17.382	24.680
Total(%)	100	100.000	100.000

5.1.2 Observation of Particle Size Distribution of Ground Fly Ashes at Different Grinding Times

Three types of fly ashes were used in this study; Wet Bottom fly ash (MO), Low NO_x fly ash (GPU2O), and Dry Bottom fly ash (BOT). These raw fly ashes were ground with different ratios of media to fly ash. In each batch, the particle size distribution of fly ash product during the grinding process was observed and plotted in the same graph to track the change in particle size distribution.

5.1.2.1 Wet Bottom Fly Ash (MO): The particle size distributions of ground wet bottom fly ashes at different grinding times with different media to fly ash ratio, 2.5:1

and 2:1 are discussed here. Figure 5.1 shows the change in size distribution of ground wet bottom fly ash using a 2.5:1 media-to-fly ash ratio. It can be seen that raw fly ash (MO) has a considerable amount of fine particle about 50% finer than 10 microns. Therefore, it takes less grinding time for one that has more coarse particles. When longer grinding time is used, the size distribution shifts toward smaller size. The rate of decreasing size is high during the first period of grinding and slows with time. From Figure 5.1 the difference in volume percentage between 5-min line and raw line is higher than that of 10-min line and 5-min line. As grinding time increases, the distance between the lengthening grinding time curves becomes smaller and then negligible which means that the particles can no further be ground. This resulting particle size distribution at 30 min. is the finest one that can be achieved within the 2.5 μm media.

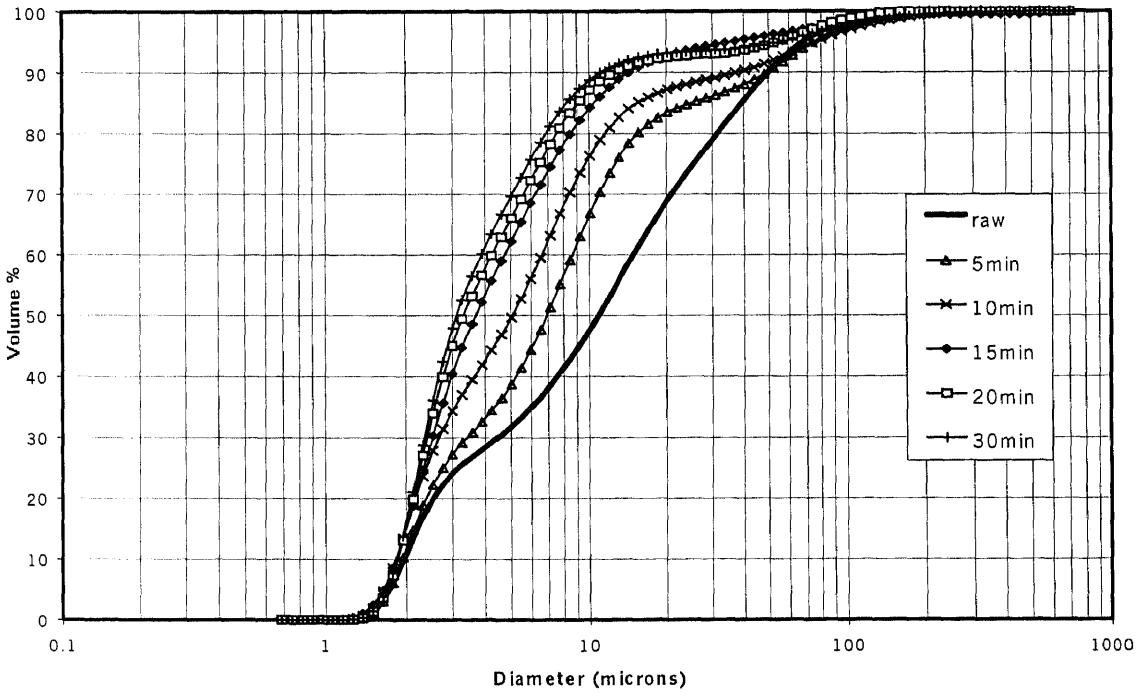

Figure 5.1 Cumulative Particle Size Distribution of Ground Wet Bottom Fly Ash (Run#1) Grinding at 1000 rpm, 2.5 mm Zr beads, Zr:FA = 2.5:1 by volume

The changes in size distribution during grinding process can be illustrated more clearly in Figure 5.2, a plot of differential particle size distribution. It can be seen that distribution of MO has peak at 2.5 microns and 15 microns. The 2.5-micron peak represents the fine portion and the 15–micron peak represents the coarse portion in raw fly ash. Within the first five minutes of grinding process, most of the coarse particles were crushed to particle sizes smaller than 30 microns. The 5-min distribution has three peaks: 2-5 microns peak, the 8.5-microns peak, and the coarse peak. The coarse particles were ground and formed the middle peak. As grinding proceeds, the remaining particles that were crushed from the first period were ground further. Thus, the middle peak of distribution with longer grinding time shifts to the finer size and finally meets the peak at 2.5 microns. The 2.5 microns size was the smallest size that grinding of this fly ash can yield with this method. As seen from the distribution, there is no change in volume of particle size smaller than 2.5 microns. The coarse peak at 60 microns could be the particles that have yet been ground. This peak, which still existed even in longer grinding time, could be the raw portion that sticks to the wall or the corner of the bowl. The height of this peak also degraded as grinding proceeds but its position remains the same. It can be explained that the coarse particles that stick to the wall were ground to fine particles instantly after they were introduced to the grinder.

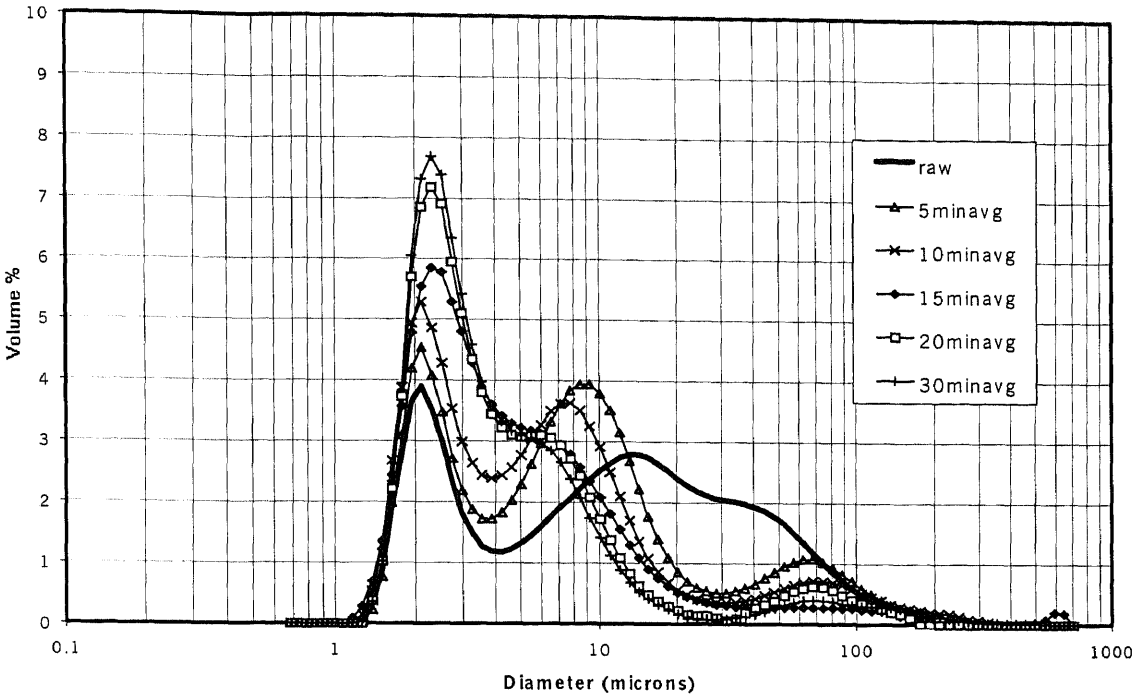

Figure 5.2 Differential Particle Size Distribution of Ground Wet Bottom Fly Ash (Run#1) Grinding at 1000 rpm, 2.5 mm Zr beads, Zr:FA= 2.5:1 by volume

The distributions of 20-min and 30-min fly ashes do not differ much. Only the height of a peak at 60 microns decreases. At this point it can be concluded that the 30-min distribution is the finest distribution for this grinding condition and media. Further grinding only wastes energy and degrades the media and arm of attritor.

Figure 5.3 presents the change in size distribution of ground wet bottom fly ash using 2:1 of media-to-fly ash ratio (run#2). It follows the same trend as the fly ash ground by using ratio of 2.5:1. However, the 20-min and 30-min lines of this run have more of coarse particles than grindings using ratio of 2.5:1. This difference is more noticeable in Figure 5.4. The heights of peak at 60 microns of 20-min and 30-min distributions are equal to that of the raw fly ash. This portion may be the coarse particles that never got into contact with media. However, if this is the case, this peak should be

lower in a run with longer grinding time. This unexpected peak could be an error of the size measurement or sampling method.

The major difference between distribution of run number one and number two is that the peak at 2.5 microns of 20-min distribution of the latter is lower than that of run number one. Also the 30-min distribution of run number two still has coarse particles size between 20 to 40 microns where there are almost no particles within this range in run number one. The explanation of these differences is that the amount of media in run number 2 of 2:1 is not enough to grind all fly ash down to below 20 microns. Even fly ash ground further, for another 10 minutes, did not significantly change it distribution. Therefore the 20-min grinding produces the finest distribution obtainable from grinding condition number two.

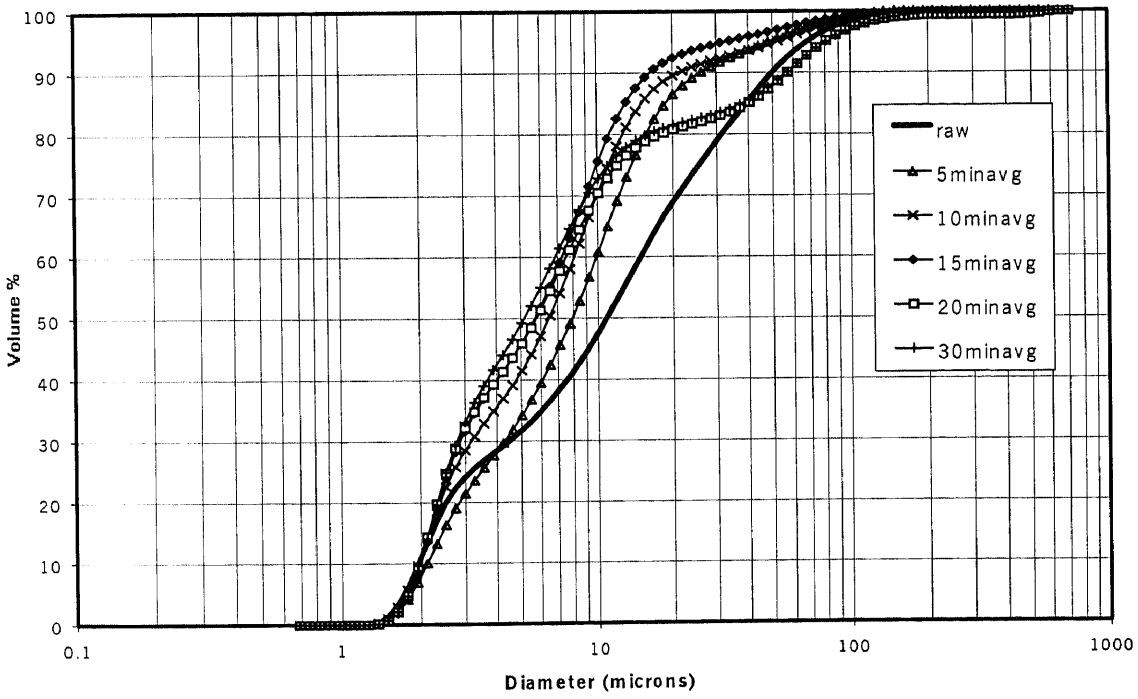

Figure 5.3 Cumulative Particle Size Distribution of Ground Wet Bottom Fly Ash (Run#2) Grinding at 1000 rpm, 2.5 mm Zr beads, Zr:FA=2:1 by volume

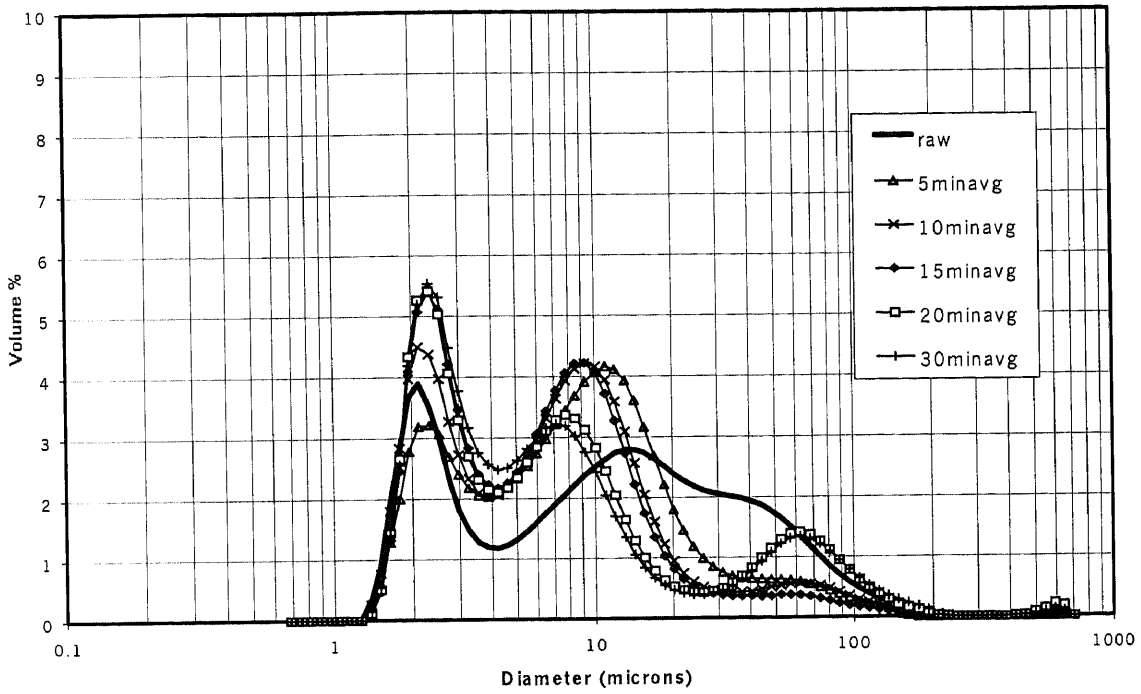

Figure 5.4 Differential Particle Size Distribution of Ground Wet Bottom Fly Ash (Run#2) Grinding at 1000 rpm, 2.5 mm Zr beads, Zr:FA=2:1 by volume

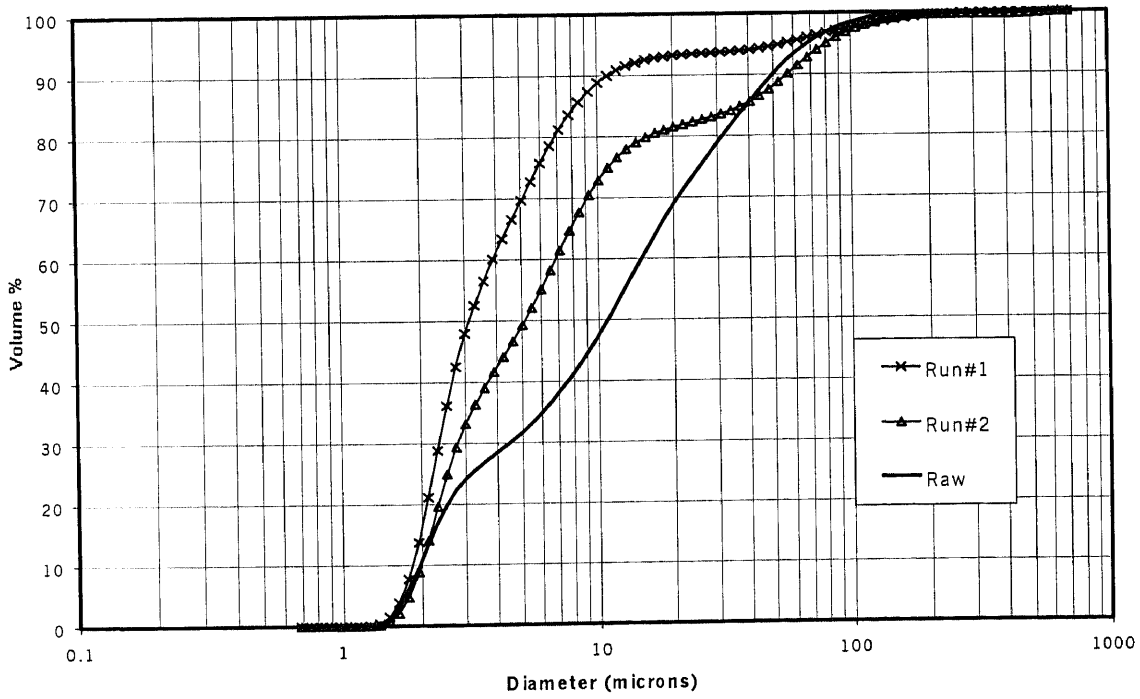

Figure 5.5 Comparison of Cumulative Particle Size Distributions of Wet Bottom Fly Ashes at 30 minutes with Different Media/Fly Ash Ratio; Run#1(2.5:1) and Run#2 (2:1)

Comparing the distributions after 30 minutes of grinding from run number one and number two, in Figure 5.5, the particle size distribution of run number 1 is finer than that of run number 2 because of higher media-to-fly ash ratio. The grinding condition of run number one was chosen to prepare fly ashes to different fineness for the following tests with optimum grinding time of 20 minutes.

5.1.2.2 Low NO_x Fly Ash (GPU2O): Low NO_x fly ash was ground with 2:1 media to fly ash ratio and their size distribution at 5, 10, and 20 minutes were observed. Figure 5.6 and 5.7 show the cumulative and differential particle size distribution of ground low NO_x fly ash, respectively. In Figure 5.6, the particle size of raw GPU2O fly ash ranges from 1.5 to 450 microns. About 50% of particles are finer than 30 microns, hence the GPU2O is considered coarser than wet bottom fly ash. Because the low NO_x furnace produces fly ash with a high amount of unburned coal (12%) which is porous, brittle and large in size, it is easily ground. Within five minutes, the particle size of this fly ash is reduced significantly compared to that of the 5-min grinding of the wet bottom fly ash (MOG). GPU2O can be ground to below 10 microns within 20 minutes. The volume percentage of particles at 2.5 microns is about 11%, which is higher than that of MOG fly ash. A finer distribution could be obtained if finer media was used. Another point is that the peak at 60 microns did not occur in any of these distributions. Since the distributions of ground fly ashes with different grinding times are distinguishable, their grinding conditions were chosen to prepare the low NO_x fly ashes to study the effect of fineness on strength of fly ash mortar.

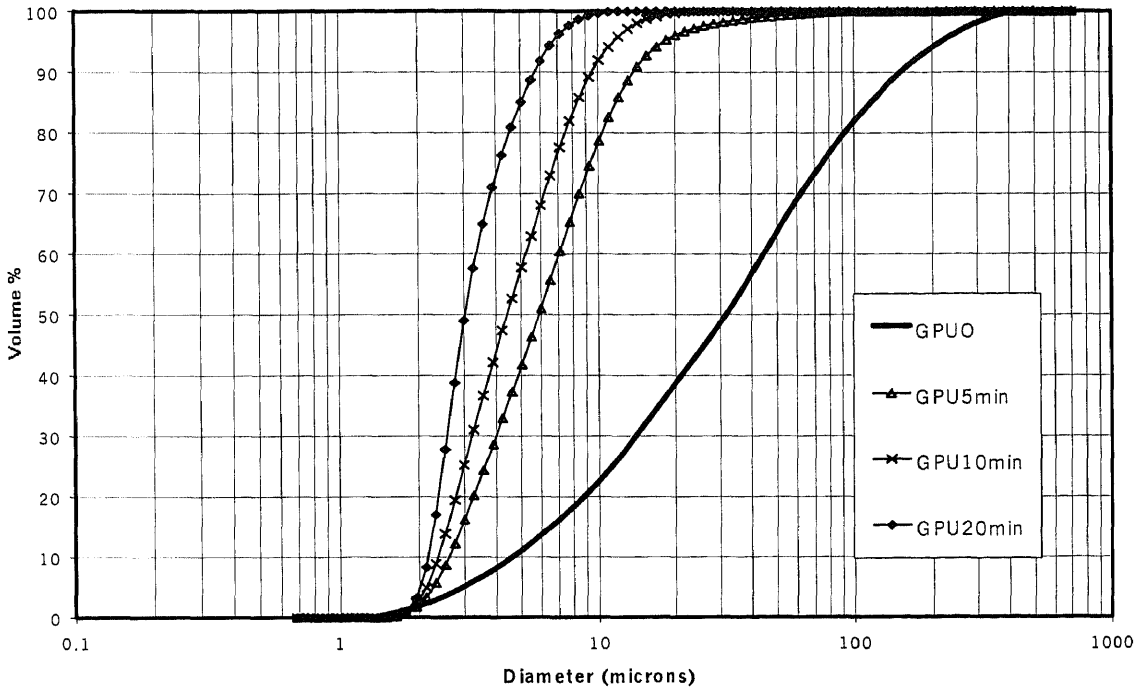

Figure 5.6 Cumulative Particle Size Distribution of Ground Low NO_x Fly Ash Grinding at 1000rpm, 2.5 mm, Zr beads, Zr:FA = 2:1 by volume

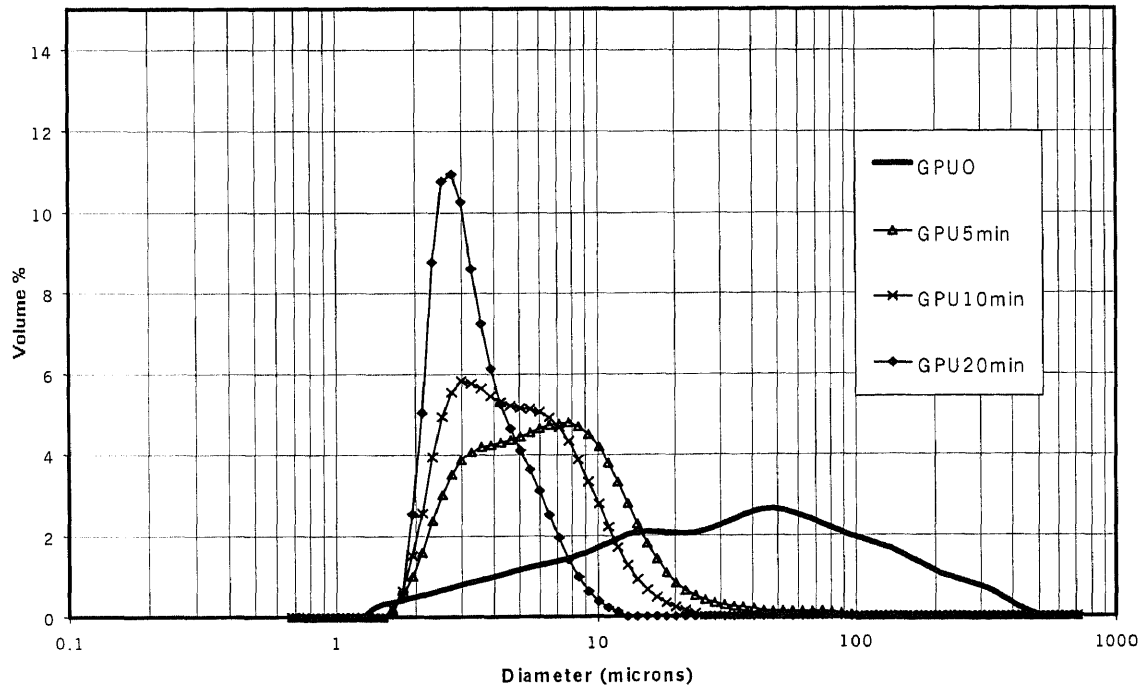

Figure 5.7 Differential Particle Size Distribution of Ground Low NO_x Fly Ash Grinding at 1000rpm, 2.5 mm, Zr beads, Zr:FA = 2:1 by volume

5.1.2.3 Dry Bottom Fly Ash (BOT): The size distribution of the raw BOT fly ranges from 1.5 to 450 microns. About 50% of particles are finer than 25 microns. It was ground using three different media to fly ash ratios; 2.5:1, 2:1, and 1:2 and their size distributions were observed at 1, 3, 5, 10, 15, and 30 minutes. The cumulative and differential particle size distribution of ground BOT fly ash ground with 2.5:1 media to fly ash ratio are shown in Figure 5.8 and 5.9, respectively. From Figure 5.8, the size distribution hardly changes within the first five minutes. It takes 10 minutes before a difference is noticeable even when high ratios of media to fly ash are used. In Figure 5.9, it can be seen that the 10-min, 20-min and 30-min lines have peaks at 2.5, 10, and 60 microns. When the longer grinding time was used, the volume percentage at 2.5 microns increased. The highest percentage at this peak, which is 9 %, occurred when fly ash was ground for 30 minutes. Another observation is that the volume percentage at 60 microns hardly changes at first 15 minutes. This coarse peak only drops after grinding for 30 minutes but it still exists to considerable extent. It can be a result of insufficient mixing during grinding process.

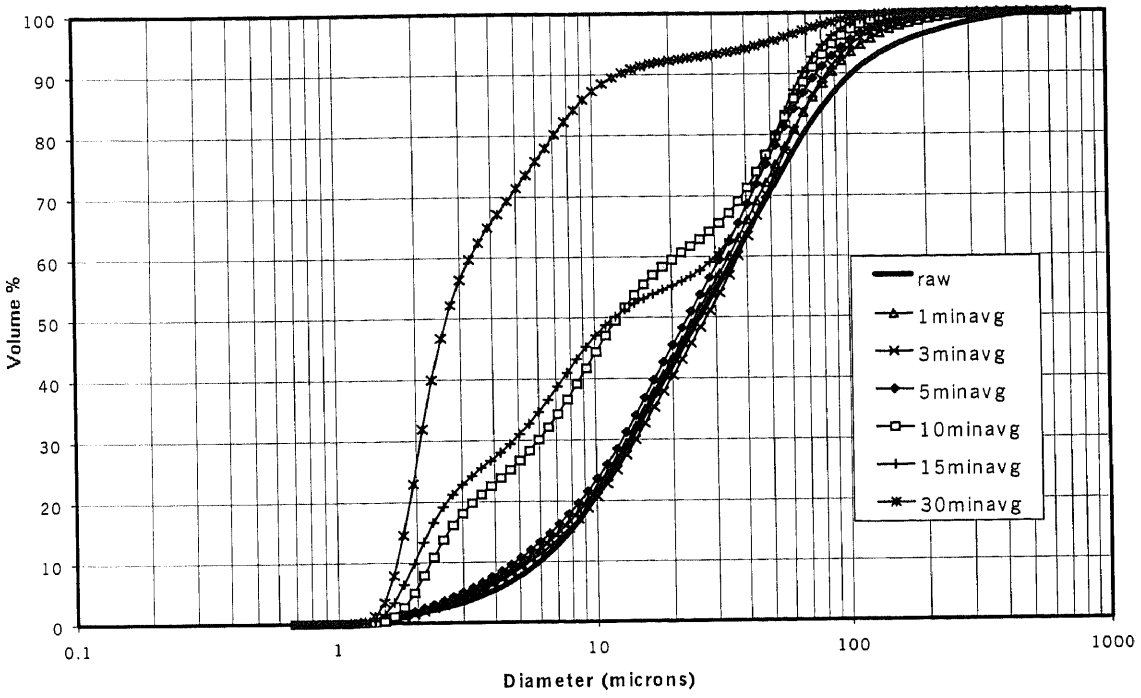

Figure 5.8 Cumulative Particle Size Distribution of Ground BOT Fly Ash (Run#1) Grinding at 1000 rpm, 2.5 mm Zr beads, Zr:FA = 2.5:1 by volume

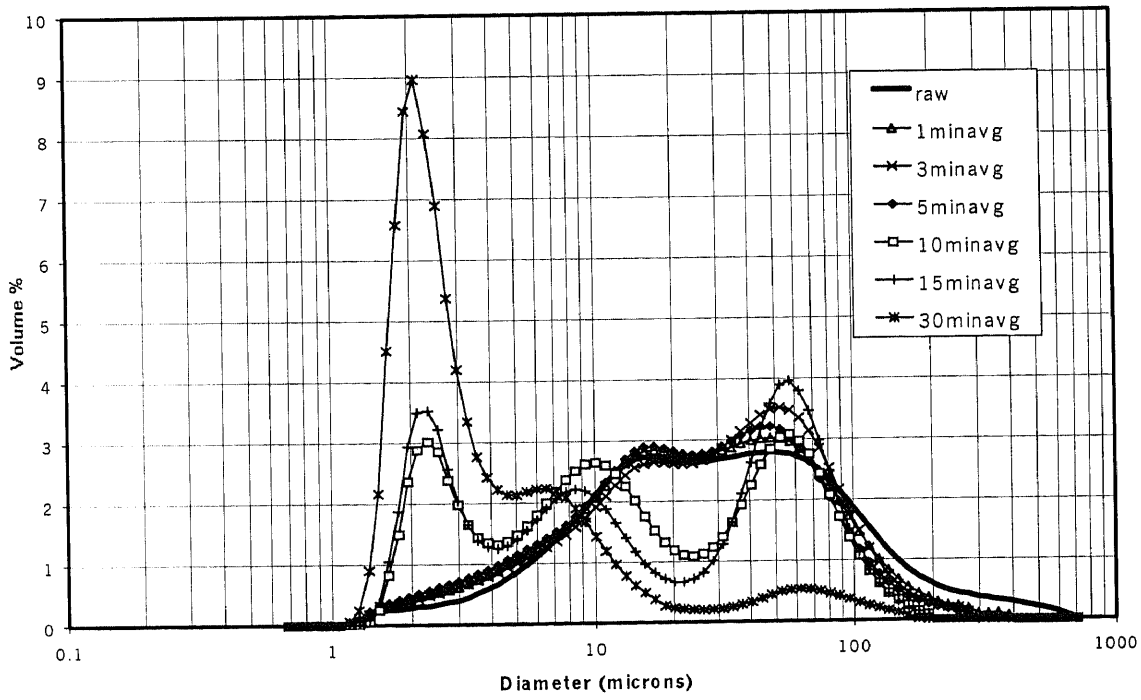

Figure 5.9 Differential Particle Size Distribution of Ground BOT Fly Ash (Run#1) Grinding at 1000 rpm, 2.5 mm Zr beads, Zr:FA = 2.5:1 by volume

The cumulative and differential size distributions of ground fly ash using a 2:1 media to fly ash ratio are shown in Figure 5.10 and 5.11, respectively. The change in size distribution after grinding is more significant than the previous run even through a lower ratio was used. At 1 minutes grinding time, the coarse particles, above 200 microns, were ground while the finer particle were essentially untouched. The distribution retained its original shape excepting the increasing volume of particles of 45 microns. The additional volume at the 45-microns comes from grinding coarse particles. As grinding proceeds, these particles were ground further. The coarse peak position gradually moved towards finer size and the volume of particles at the fine peak increased. The fly ash obtained after grinding for 20 minutes still maintains its bimodal shape. Most of its particles are less than 20 microns. The fine peak at 2.5 microns emerged after 3 minutes grinding time. This condition yielded fine particles faster than previous condition but the maximum volume percentage at 2.5 microns was lower (6.5%). It should be noticed that in run number 2 the peak at 60 microns did not appear. This may be because the mixture was mixed thorough enough during the process.

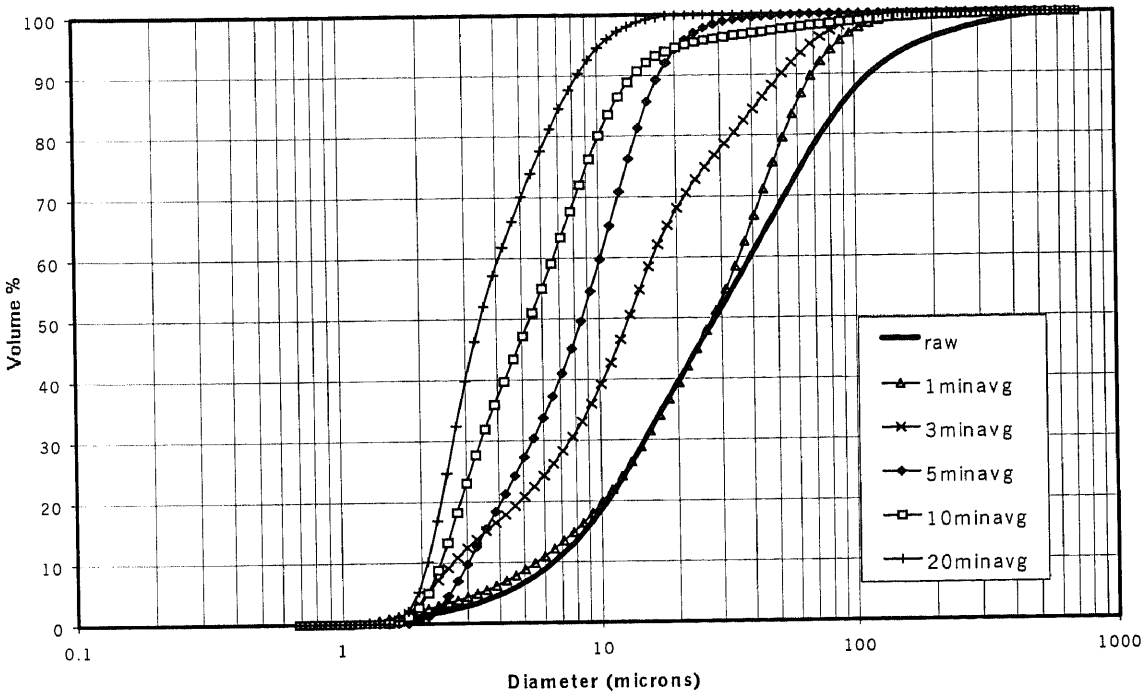

Figure 5.10 Differential Particle Size Distribution of Ground BOT Fly Ash (Run#2), Grinding at 1000 rpm, 2.5 mm Zr beads, Zr:FA=2:1 by volume

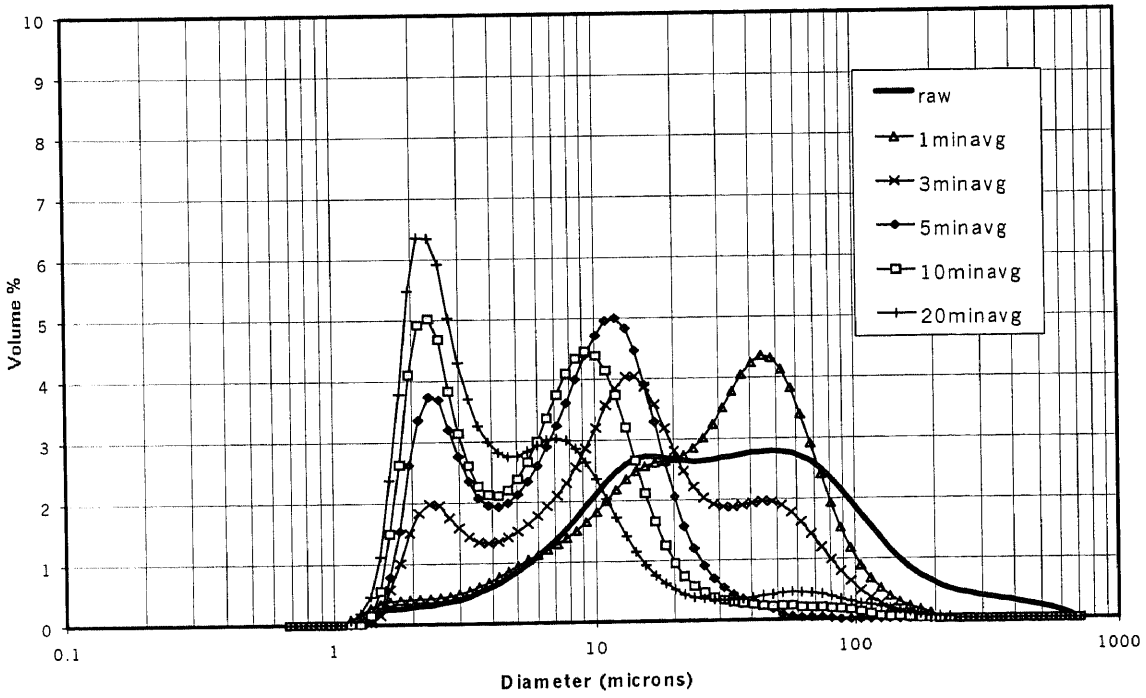

Figure 5.11 Differential Particle Size Distribution of Ground BOT Fly Ash (Run#2), Grinding at 1000 rpm, 2.5 mm Zr beads, Zr:FA=2:1 by volume

Figure 5.12 shows the distribution of ground fly ash in run number 3, which has media to fly ash ratio of 1:2. Unlike run number 1 and 2, their distributions were not altered much from that of raw fly ash. Within the first 10 minutes, the fine portion maintains its distribution while some of coarse particle were ground. Only after 20 minutes did fine particles of 2.5 microns in size, which were not in the raw fly ash, appeared. However, the amount of this fine portion is very low. The fineness does not improve much with longer grinding. It is assumed that the ratio of media to fly ash is so low that there is less chance for fly ash to contact with media. Hence, this ratio is not sufficient to grind fly ash to below 10 microns.

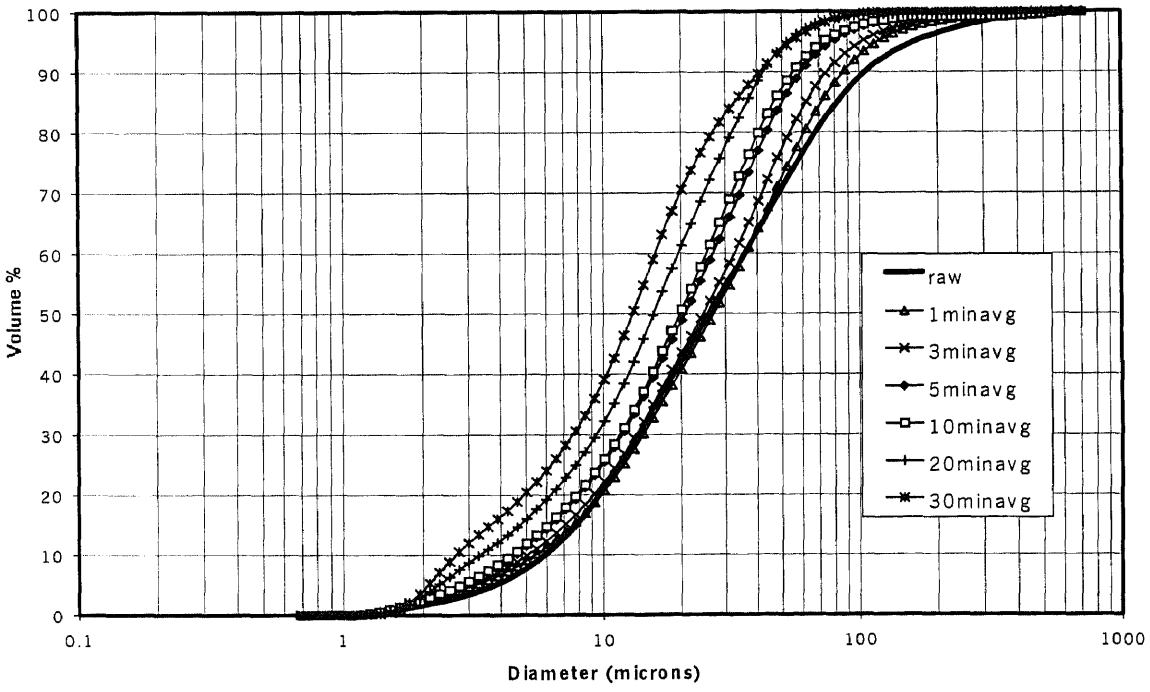

Figure 5.12 Differential Particle Size Distribution of Ground BOT Fly Ash (Run#3), Grinding at 1000 rpm, 2.5mm Zr beads, Zr:FA = 1:2 by volume

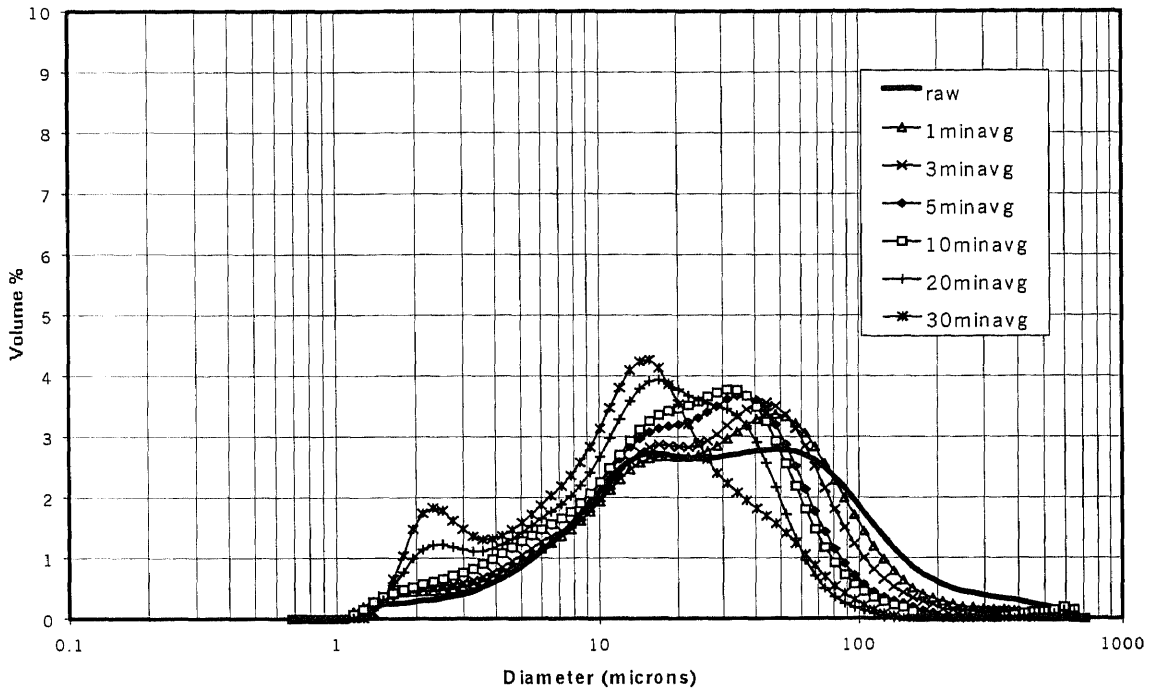

Figure 5.13 Differential Particle Size Distribution of Ground BOT Fly Ash (Run#3), Grinding at 1000 rpm, 2.5mm Zr beads, Zr:FA = 1:2 by volume

The comparison of the size distributions of fly ashes after 10 minutes of each run is shown in Figure 5.14. Run number one provides finer distribution than the others. Thus, it can be concluded that the higher the media to fly ash ratio, the higher volume percentage of fine particles can be obtained. However, the condition with high ratio of media to fly ash does not mix well enough. Therefore, it still contains higher percentages of coarse particles. Since the goal of this grinding process is to obtain the fly ash having size smaller than 10 microns, therefore the condition of run number two will be used to grind BOT fly ashes. The grinding condition in run number three is not efficient to be used since their distributions do not change much with times.

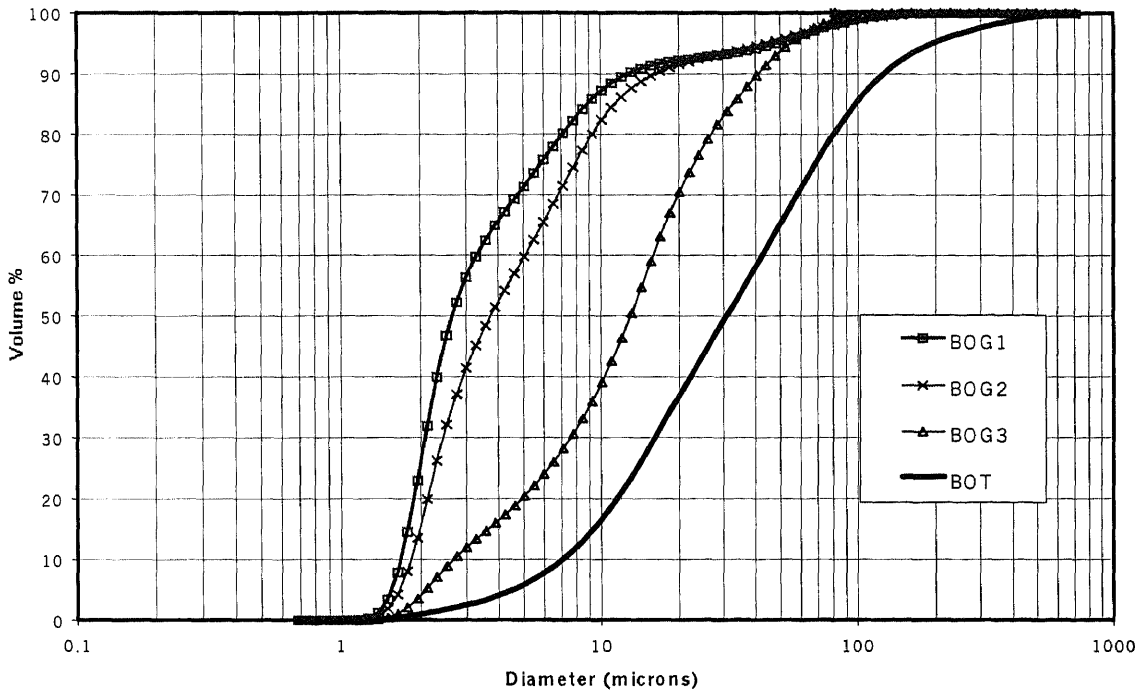

Figure 5.14 Comparison of Differential Particle Size Distribution of BOT Fly Ash at 10 minutes with Different Media/Fly Ash Ratio; (Run#1 (2.5:1), Run#2 (2:1), and Run#3 (1:2))

5.2 Particle Size Distribution of Processed Fly Ashes

5.2.1 Particle Size Analysis of Dry Bottom Fly Ashes (HO91)

The cumulative particle size distributions of dry bottom fly ash 91 are shown in Figure 5.15. Their differential particle size distributions are shown in Figure 5.16. Original dry fly ash 91 was fractionated into seven distribution ranges and was ground into two distribution ranges. Figure 5.15 shows that the particle size of fly ashes varied from 1.5 - 25 microns to 1.5 - 350 microns. The HOG911 has the highest proportion of particle size, less than 3 micron. It is also seen from Figure 5.15 that the distribution curves of ground fly ash are different from those of fractionated fly ashes. The ground fly ashes, i.e. HOG911 and HOG912, have higher amounts of fine particles and higher amounts of coarse particles. The HOG911 and HOG912 distributions are steep at the beginning and then start to flatten at about 80% of total volume. This means that 80% of ground fly ash is fine and the particles are about the same size. But, there is still some coarse fly ash, which is probably the result of incomplete grinding process. The HOG911 fly ash was ground longer than the HOG912 fly ash. Their differential curves also support this idea.

Comparing within the fractionated fly ash itself, it can be seen from Figure 5.16 and Table 5.2 that the H3F91 has the smallest peak size and the smallest mean diameter. The peak size is defined as a particle size that has the highest volume percentage. The mean diameter is defined as the size that has 50% of particles smaller than this size. The H1C fly ash has the largest peak size and the largest mean diameter. From Figure 5.15, it can be seen that the distributions of all fractionated fly ashes have the same trend. Their slopes are steep and their sizes vary within narrow range or the particle size within the same type tends to be uniform.

Figure 5.16 shows that there is not much different among the size distributions of H6F91, H7F91, H10F91 and H11F91. Their ranges overlap at the upper and lower end and their peaks are close. Only the finer fly ashes have higher amounts of fine particles and lesser amounts of coarse particles. Therefore, these four groups of fly ashes are not good representatives of fractionated fly ash since they are quite similar and their size distributions do not differ much. The distributions of H3F91 and H1C91 fly ashes are much different. They have no overlapping range and the distribution of H1C91 is ten times broader than that of H3F91. Also, the H1C91's peak value is lower than that of H3F91. Therefore, the particle size of H3F91 is finer and more uniform than that of H1C91.

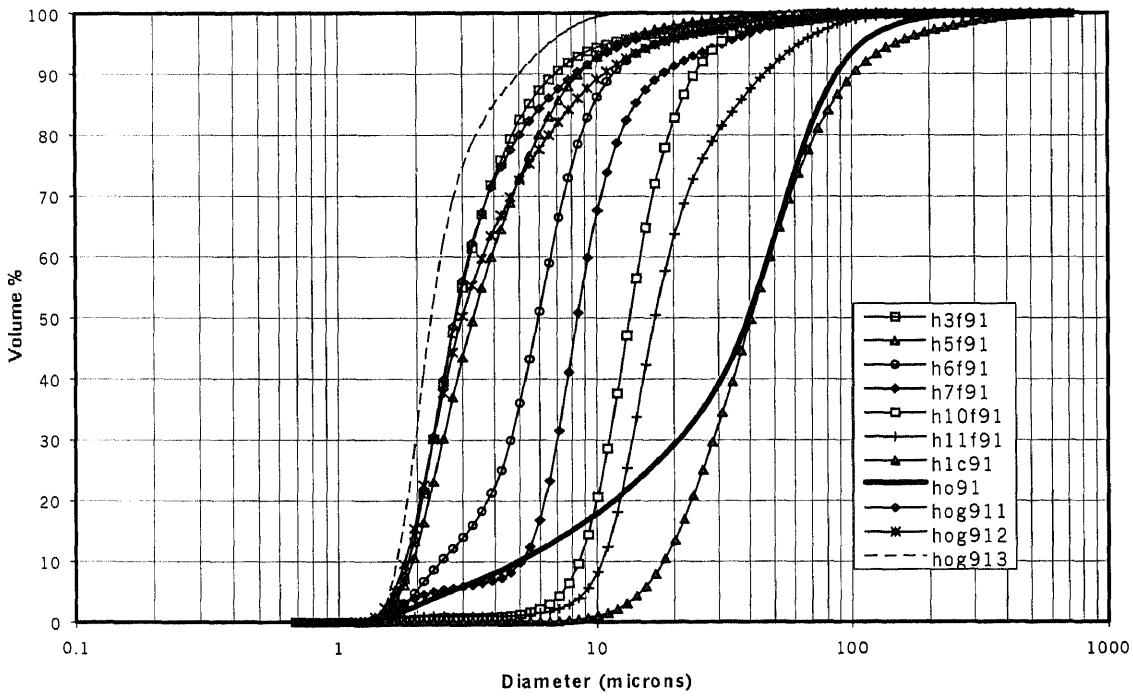

Figure 5.15 Cumulative Particle Size Distribution of Dry Bottom Fly Ashes 91

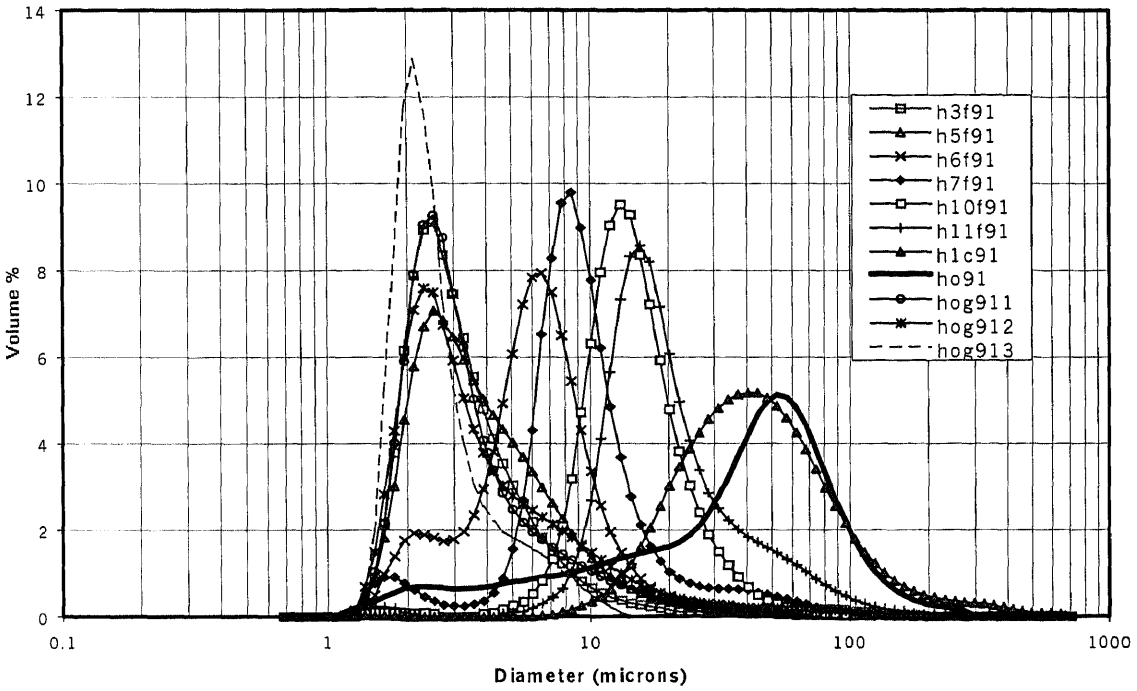

Figure 5.16 Differential Particle Size Distribution of Dry Bottom Fly Ashes 91

Table 5.2 Analysis of Particle size Distribution of Dry Fly Ashes 91

Type of Fly Ash	Range (microns)	95%UL of Differential curve	90% UL of Differential Curve	Peak Size (microns)	%Diff. Volume at Peak Size	Size at 50% (microns)
HO91	1.2-352	2.1-146	2.5-114.1	57	1.21, 4.2	35.53
H3F91	1.5-22	1.7-10.1	1.9-7.8	2.8	9.4	3.1
H5F91	1.5-37	1.8-14.3	1.9-11.0	2.8	7.7	3.5
H6F91	1.5-31.1	1.9-15.6	2.3-13.08	7.1	8.3	6.3
H7F91	1.2-88	1.9-40.4	2.8-28.5	9.3	9.8	9.2
H10F91	1.5-104.7	5.5-48	7.7-37.0	14.3	9.0	14.8
H11F91	1.5-124.5	7.8-57.1	11.0-88.0	17	7.8	19.8
H1C91	7.1-497	13.1-191.9	15.5-135.7	44	5.1	39.6
HOG911	1.2-88	1.6-20.2	1.8-13.1	2.3	8.8	2.8
HOG912	1.2-124.5	1.7-34	1.8-22.0	2.5	7.3	3.3

5.2.2 Particle Size Analysis of Dry Bottom Fly Ashes (HO95)

The cumulative particle size distributions of dry bottom fly ash 95 are shown in Figure 5.17. Their differential particle size distributions are shown in Figure 5.18. The original dry fly ash 95 (HO95) was fractionated into two series. The analysis of size distribution is given in Table 5.3. The first fractionating batch of the original dry fly ash 95 yielded the H7F95 fly ash as the fine portion and H7C95 fly ash as the coarse portion. The second fractionating batch yielded H8F95 as the fine portion and H8C95 as the coarse portion. From Figure 5.17 and 5.18, it can be seen that the fine portion ranges within 1.5 to 25 microns and the coarse portion ranges within 1.5 to 700 microns. The H7F95 fly ash has more fine particles than H8F95. The coarse portion of the H7 series, which is H7C95, is coarser than H8C95 as expected. This is because the HO95 can be fractionated easier and a higher proportion of the fine material separated, hence, leaving coarse portion coarser. However, the H7F95 curve is flat after 10 microns, which means that this fly ash consists of some particles bigger than 10 microns. This portion takes about 7% of total volume. It should not result from insufficient fractionating since the sorting condition, which uses less rotating speed, yields less coarse material. It may come from contamination during fractionating or improper size measurement. It can be seen from Figure 5.17 and 5.18 that the H7C95 has the highest amount of coarse particles. The H7C95 has the same trend as that of HO95 but it has less fine material.

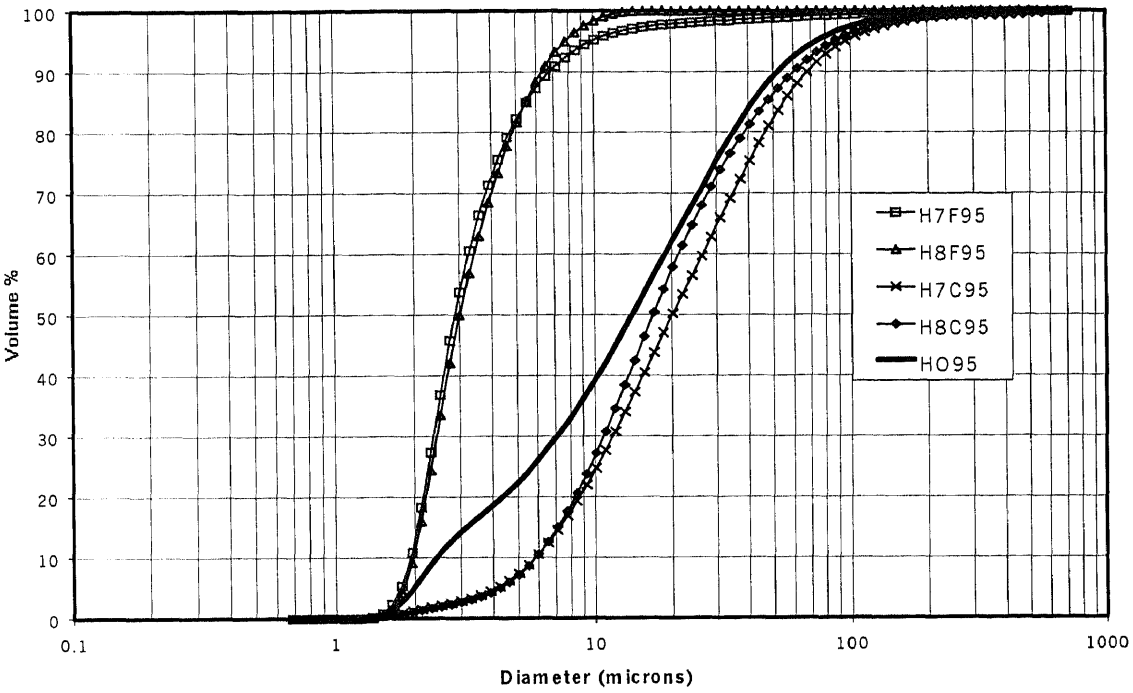

Figure 5.17 Cumulative Particle Size Distribution of Dry Bottom Fly Ashes 95

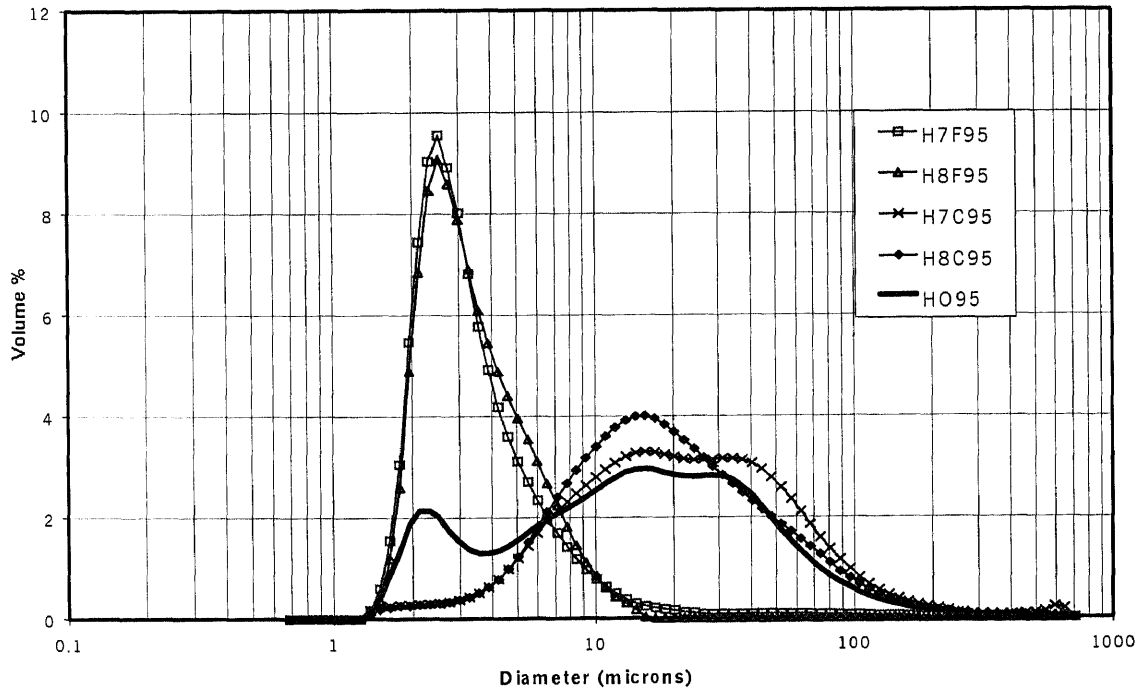

Figure 5.18 Differential Particle Size Distribution of Dry Bottom Fly Ashes 95

Table 5.3 Analysis of Particle size Distribution of Dry Fly Ashes 95

Type of Fly Ash	Range (microns)	95%UL of Differential curve	90% UL of Differential Curve	Peak Size (microns)	%Diff. Volume at Peak Size	Size at 50% (microns)
HO95	1.5-352	1.9-148	2.5-114	2.5, 44	1.77,2.72	19.3
H7F95	1.5-26.2	1.8-12.0	1.9-9.2	2.75	9.51	3.2
H8F95	1.5-15.6	1.9-9.3	2.0-8.5	2.75	9.14	3.3
H7C95	1.5-296	3.0-135.7	4.6-104	16.9	3.33	21.2
H8C95	1.5-352	3.3-296	5.0-148	16.9	3.67	20.2

Comparison of Particle Size Analysis between Original Dry Bottom Fly Ashes 91 (HO91) and Dry Bottom Fly Ashes 95 (HO95)

The cumulative and differential particle size distributions of raw feed dry bottom fly ashes 91 and 95 (HO91 and HO95) are shown in Figure 5.19. Comparing the particle size distributions of these fly ashes, it is seen that the distributions are different even though they were taken from the same plant. This reflects changes in the furnace conditions. The HO95 batch has a higher amount of fine particles than the HO91 batch. HO91 fly ash has 20% of the total volume finer than 10 microns and 40% for HO95.

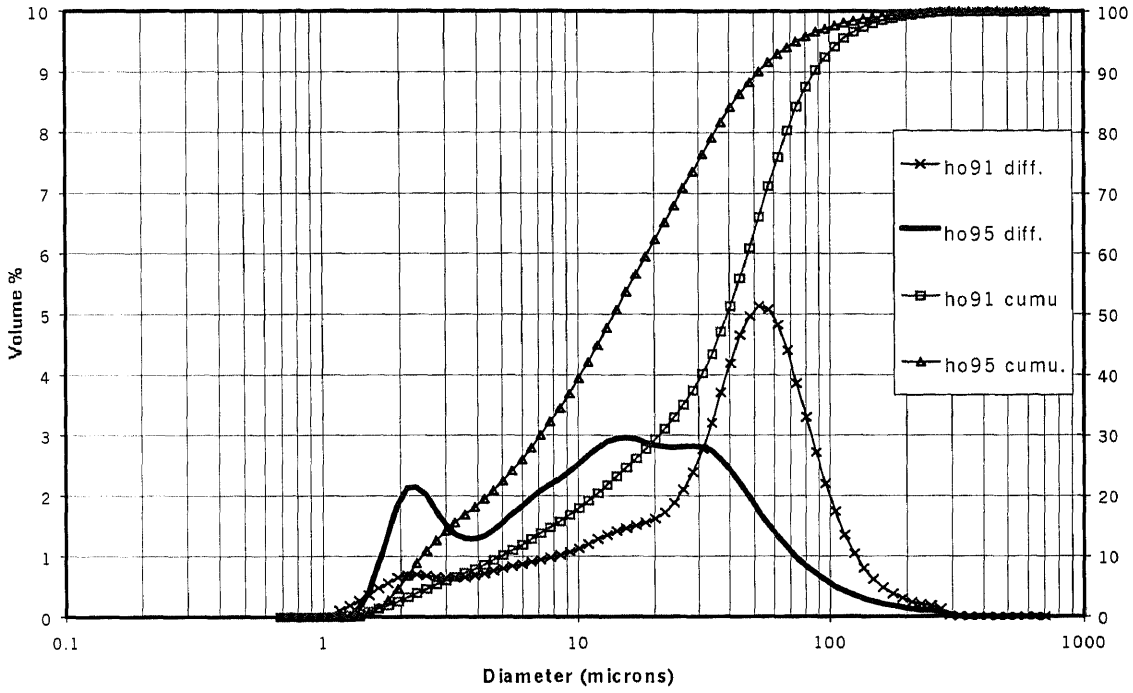

Figure 5.19 Particle Size Distribution of Raw Feed Dry Bottom Fly Ashes 91 (HO91) and Raw Feed Dry Bottom Fly Ash 95 (HO95)

5.2.3 Particle Size Analysis of Wet Bottom Fly Ash (MO91)

Wet fly ash 91 underwent series of fractionating processes. The finer portion was subjected to further fractionation. This procedure yielded seven classes of fractionated fly ash; M13F91, M14F91, M15F91, M16F91, M17F91, M18F91, M18C91, and MO91. The cumulative particle size distributions of wet fly ash 91 are shown in Figure 5.20 and the differential particle size distributions are shown in Figure 5.21. It can be seen from Table 5.4 that the M13F91 has the smallest peak size and the smallest mean diameter. The M18C91 fly ash has the largest peak size and the largest mean diameter. From Figure 5.20, M13F91 has the steepest slope, indicating that its particle size is uniform. The curve that gives the widest range is that of MO91, the original feed fly ash.

Figure 5.21 shows the differential particle size distribution of these fly ashes. The M13F91, M14F91 and M15F91 have more than 85% of total volume smaller than 10 microns. These three fly ashes have high percentage of particle at their peak size. The M13F91 gives the highest percentage of particles in the fine range. It is the finest and most uniform fly ash of the batch. The other fly ashes, M16F91, M17F91, M18F91, M18C91, are not good products of classification since they have broadened range and their ranges overlap each other. They should not be used to compare among each other.

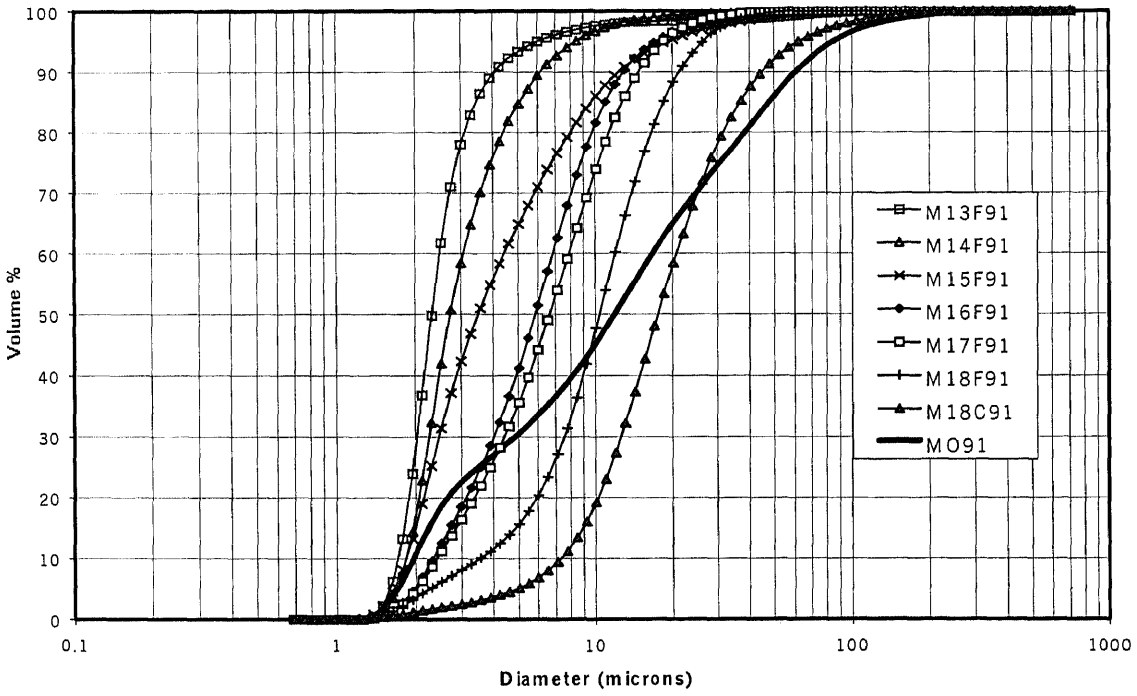

Figure 5.20 Cumulative Particle Size Distribution of Wet Bottom Fly Ashes 91

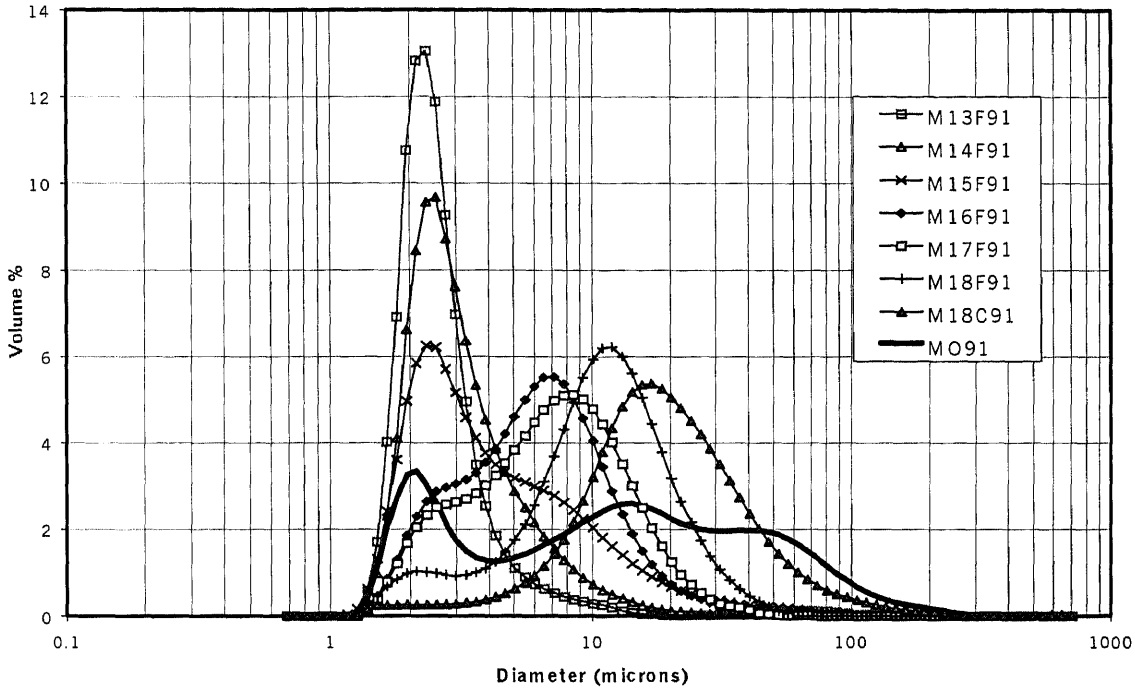

Figure 5.21 Differential Particle Size Distribution of Wet Bottom Fly Ashes 91

Table 5.4 Analysis of Particle size Distribution of Wet Bottom Fly Ashes 91

Type of Fly Ash	Range (microns)	95%UL of Differential curve	90% UL of Differential Curve	Peak Size (microns)	%Diff. Volume at Peak Size	Size at 50% (microns)
MO91	1.5-700	1.8-135.7	1.9-104.7	2.3,14.3	3.24,2.4	13.87
M13F91	1.5-15.6	1.6-7.1	1.8-5.5	2.52	13.09	2.51
M14F91	1.5-26.2	1.7-11.5	1.9-8.5	2.75	9.62	2.98
M15F91	1.5-104.7	1.6-31.1	1.8-20.1	2.52	6.38	3.72
M16F91	1.5-124.5	1.9-37	2.1-26.2	7.7	5.23	6.49
M17F91	1.5-74	1.9-28.5	2.1-22	9.25	4.97	7.35
M18F91	1.5-62.2	1.9-37	2.3-28.5	12.0	6.24	11.17
M18C91	1.5-296	3.5-114	6.0-80.7	17.0	5.05	20.25

5.2.4 Particle Size Analysis of Wet Bottom Fly Ashes (MO95)

The wet bottom fly ash 95 was processed by two different ways, fractionating and grinding. In the fractionating process, raw wet bottom fly ash was fractionated into four ranges (M8F95, M9F95, M12F95, and M13F95) and only the fine portion of each step was analyzed. In the grinding process, the raw bottom fly ash was ground to yield the MOG1 fly ash. The M8CG1 and M8CG2 are the ground fly ashes obtained from grinding the coarse fly ash left from M8F95 processing.

The cumulative particle size distributions of fractionated fly ash 95 and ground fly ash 95 are shown in Figure 5.22 and 5.23, respectively. Their differential particle size distributions are shown in Figure 5.24 and 5.25. Comparing among the fractionated fly ash, the M8F95 is the finest distribution. It has the highest volume peak but the same range as the other two fly ashes. The mean diameters of M8F95, M9F95, M12F95, and M13F95 are 3.31, 3.21, 3.64, 3.6 microns, respectively. Since the size distributions of these fly ashes are not significantly different, they will not be used in the study of the fineness effect on the properties of fly ash mortar. Comparing the ground fly ashes, their curves are similar but that of M8CG1 is a little bit out of the group. It can be seen more clearly from Figure 5.23 that although the MO95, which is primary fly ash of MOG95, is finer than the M18C, which is the primary of M8CG1, M8CG1 fly ash is the finest ground fly ash. This may be because it was subjected to longer grinding time than M8CG2 and MOG195. The mean diameters of MOG, M8CG1, M8CG2 are 3.43, 2.88, 3.39 microns, respectively

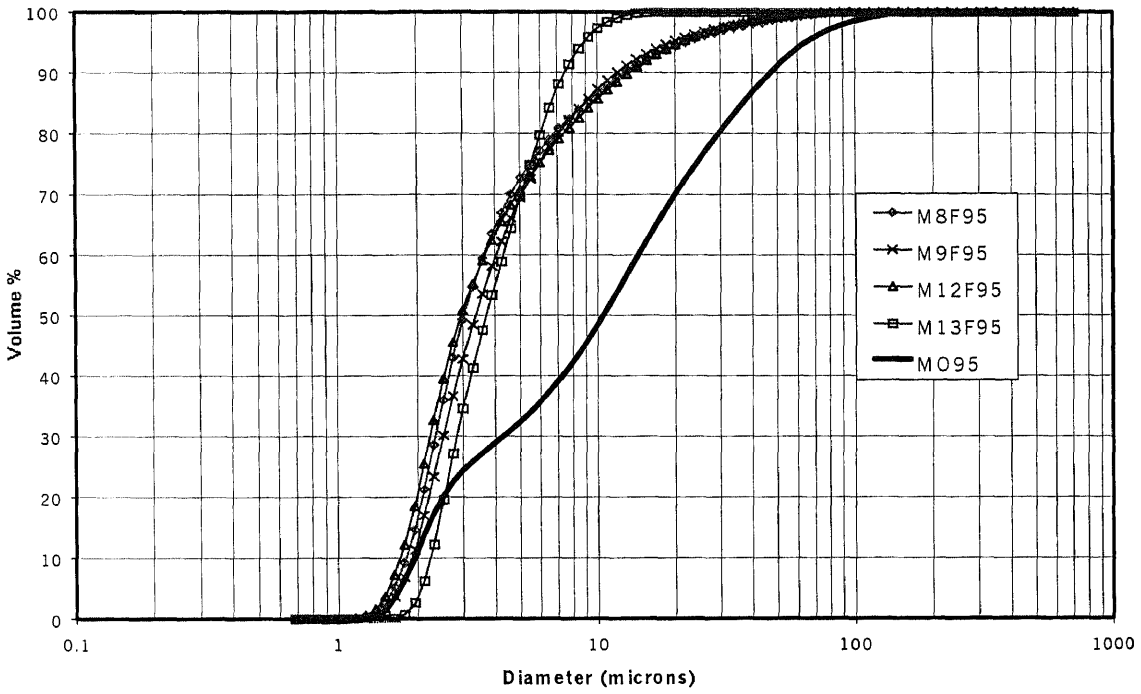

Figure 5.22 Cumulative Particle Size Distribution of Fractionated Wet Bottom Fly Ash 95

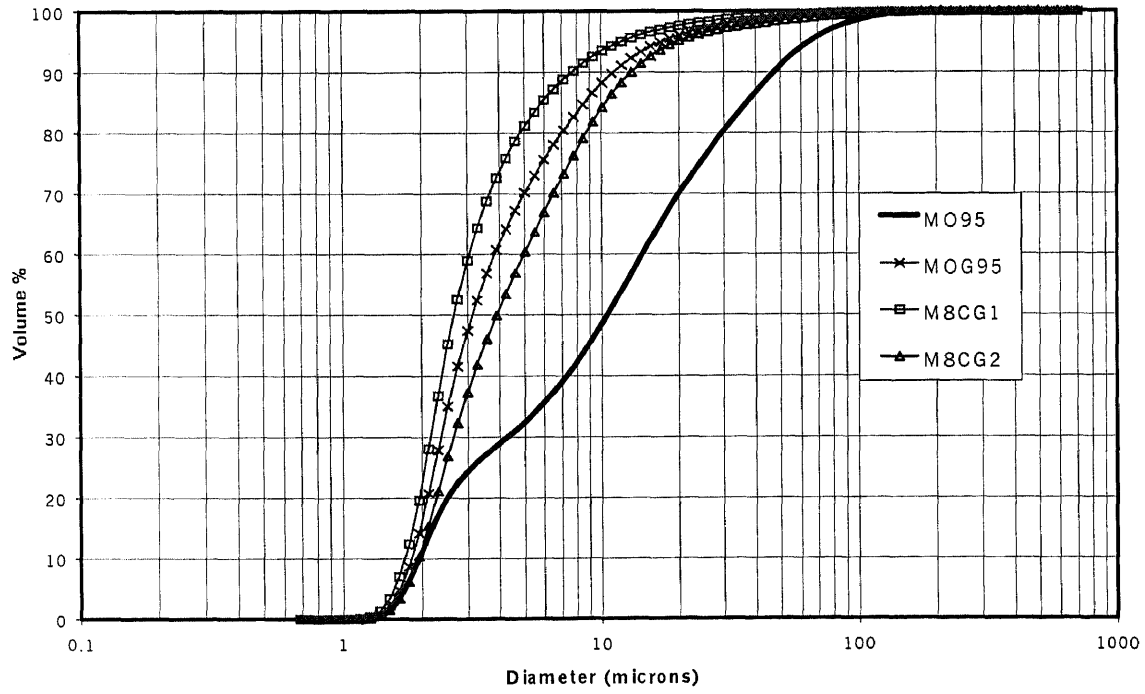

Figure 5.23 Cumulative Particle Size Distribution of Ground Wet Bottom Fly Ashes 95

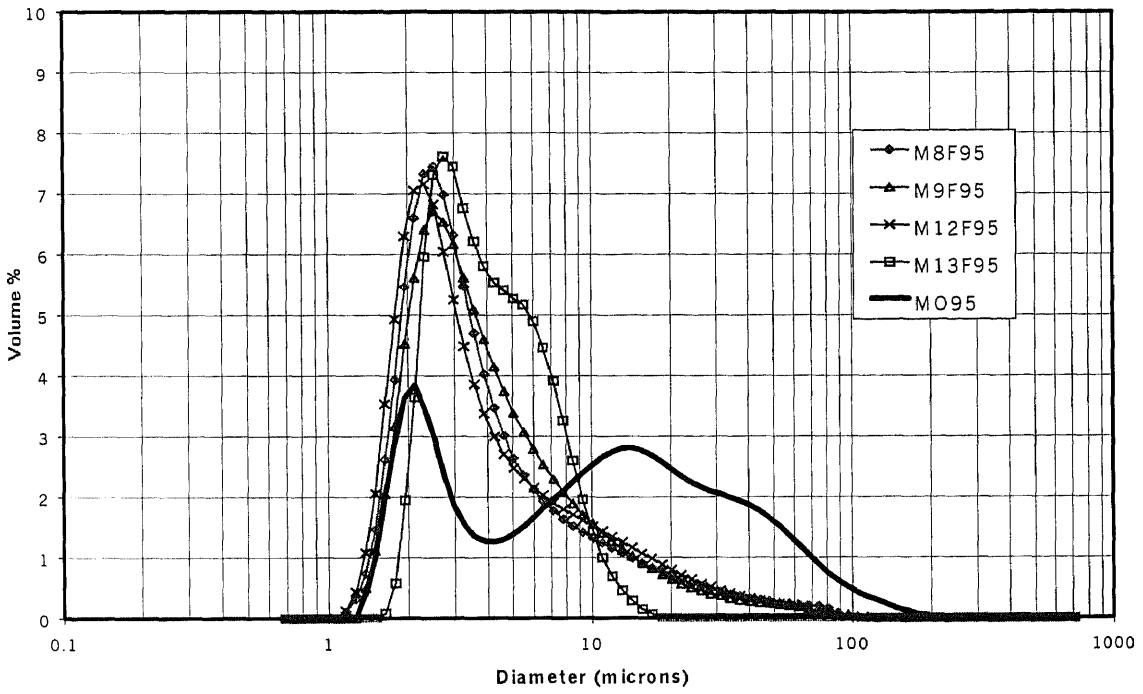

Figure 5.24 Differential Particle Size Distribution of Fractionated Wet Bottom Fly Ashes 95

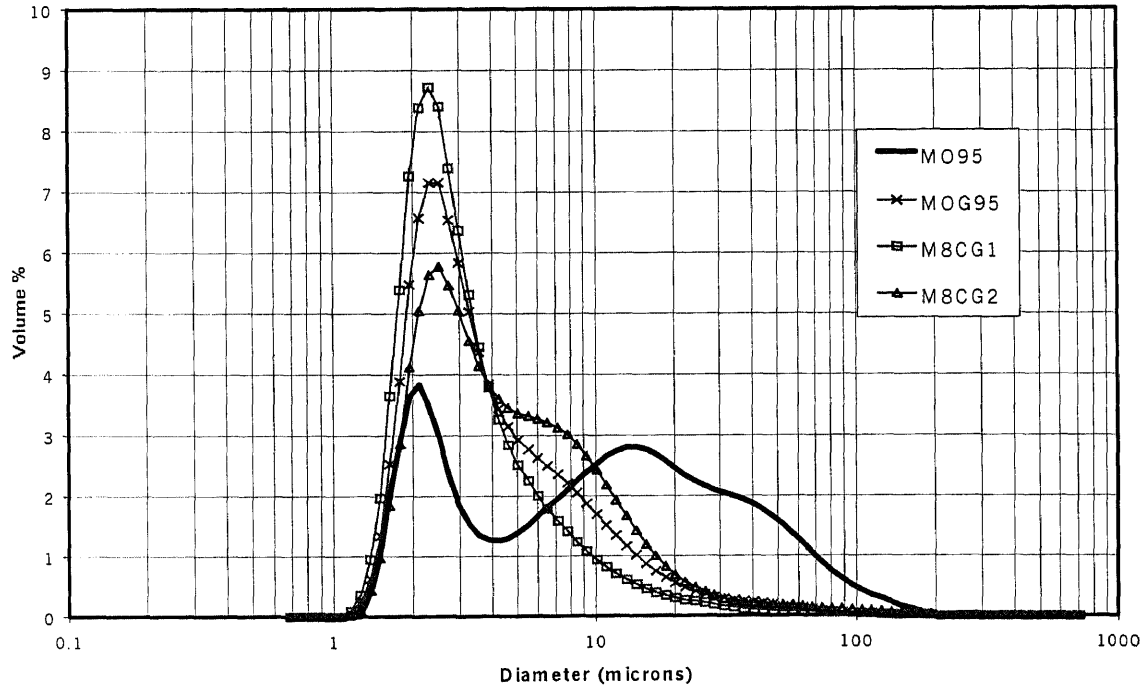

Figure 5.25 Differential Particle Size Distribution of Ground Wet Bottom Fly Ashes 95

Table 5.5 Analysis of Particle size Distribution of Wet Fly Ashes 95

Type of Fly Ash	Range (microns)	95%UL of Differential curve	90% UL of Differential Curve	Peak Size (microns)	%Diff. Volume at Peak Size	Size at 50% (microns)
MO95	1.5-148	1.7-80	1.9-62.2	2.31	4.15	10.57
M8F95	1.2-114	1.6-370	1.8-24	2.75	7.45	3.31
M9F95	1.5-114	1.7-31.1	1.8-20.2	2.75	6.88	3.64
M12F95	1.2-88	1.6-33	1.7-22	2.52	7.25	3.21
M13F95	1.6-16.9	2.1-11.0	2.3-9.3	2.75	7.6	3.6
MOG95	1.2-148	1.6-31	1.8-20.2	2.75	7.14	3.43
M8CG195	1.2-74	1.6-16.9	1.7-13.6	2.5	8.61	2.88
M8CG295	1.2-124.5	1.6-31.1	1.8-20	2.5	7.23	3.39

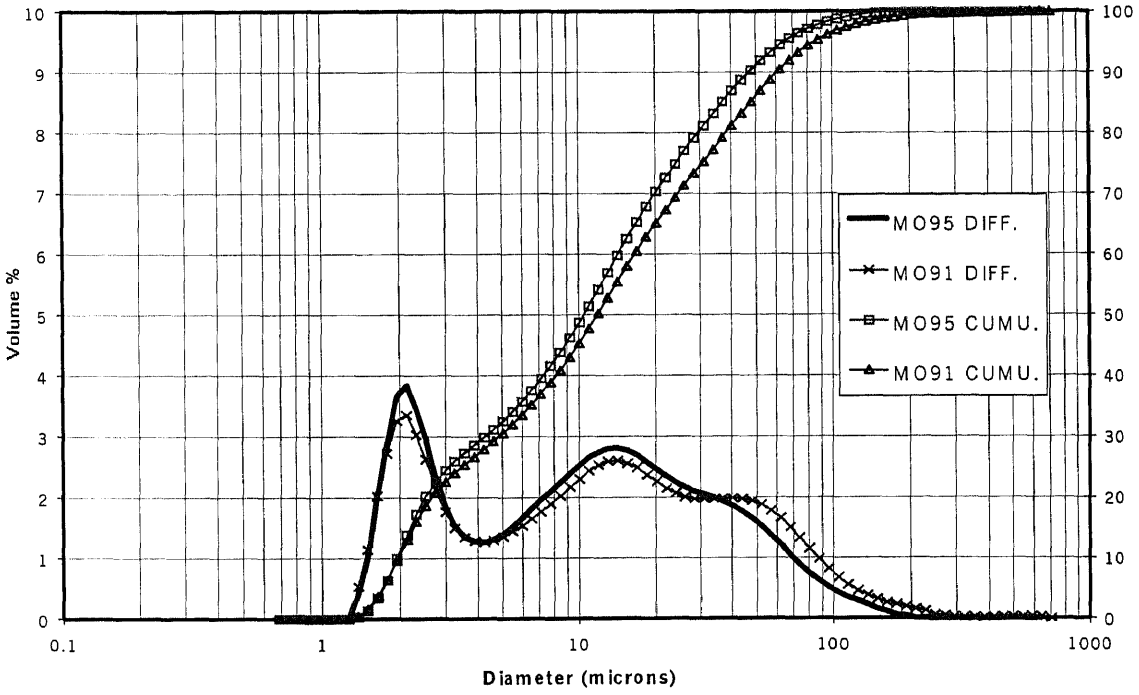

Figure 5.26 Particle Size Distribution of Wet Bottom Fly Ashes 91 and 95

The change in size distribution of fly ash generated at different times, 1991 and 1995, was also investigated. The cumulative and differential particle size distributions of raw wet bottom fly ashes generated at different time (MO91 and MO95) are shown in

Figure 5.26. Comparing the particle size distributions of these fly ashes, it is seen that the size distributions of these ashes are similar. This means that the fly ash formation has not been changed over the sampling period.

From the original feed, the raw wet bottom fly ash 95 (MO95) was ground into three ranges: MOG1, MOG2, and MOG3. As shown in Figure 5.27, the MOG1, and MOG2 have particle size smaller than 20 microns while the MOG3 still has large portion of coarse particles. The MOG1 has about 100% of particles finer than 10 microns while the MOG2 has about 95% and the MOG3 has about 84%. The finest ground fly ash in this series is MOG1. The mean diameters of MOG1, MOG2, and MOG3 are 2.7, 3.2, and 5.0 microns, respectively. These three fly ashes were used in the study of the effect of fineness on the strength of ground wet bottom fly ash mortar.

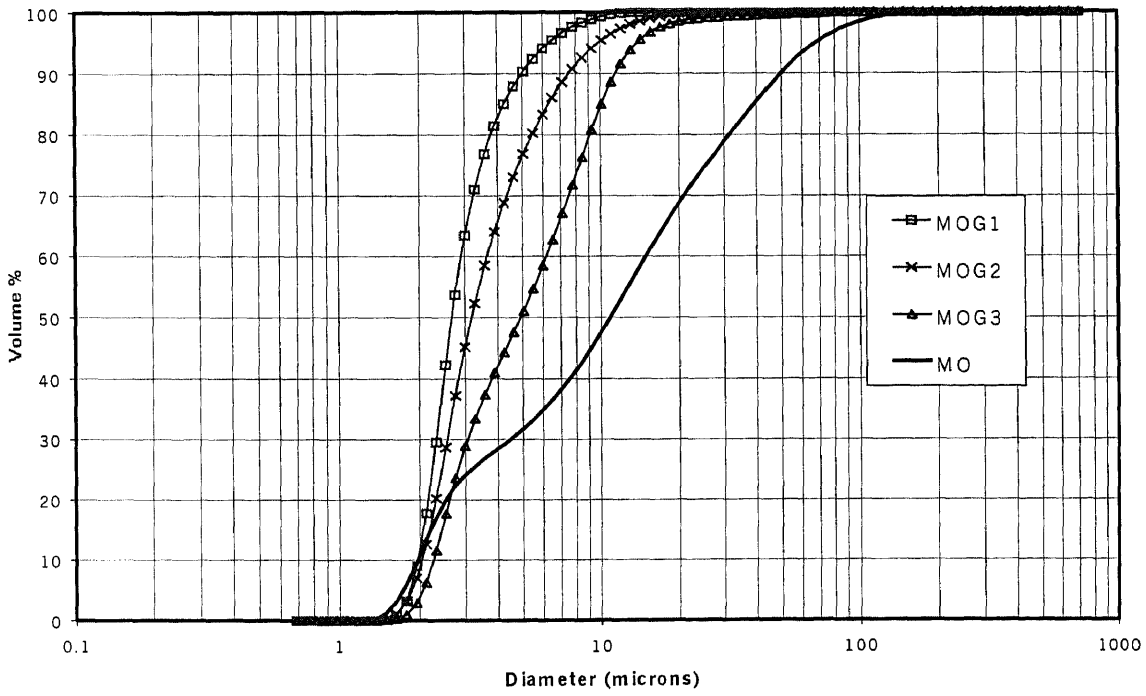

Figure 5.27 Cumulative Particle Size Distribution of Ground Wet Bottom Fly Ashes (MOG)

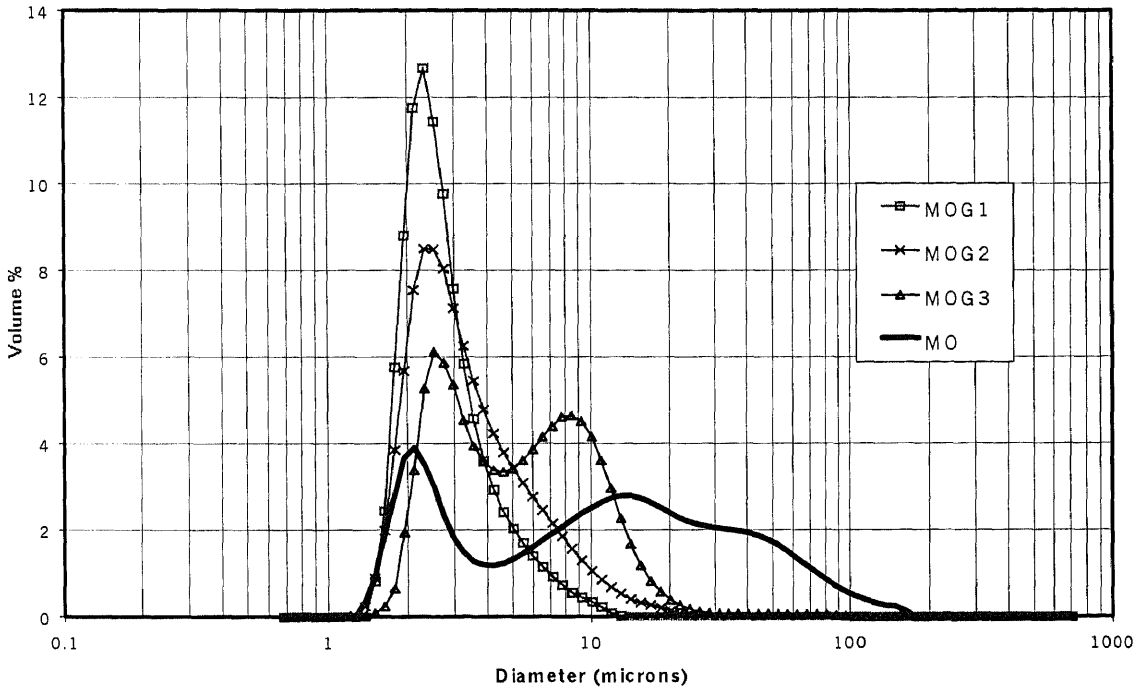

Figure 5.28 Differential Particle Size Distribution of Ground Wet Bottom Fly Ashes (MOG)

Table 5.6 Analysis of Particle size Distribution of Ground Wet Bottom Fly Ashes

Type of Fly Ash	Range (microns)	95%UL of Differential curve	90% UL of Differential Curve	Peak Size (microns)	%Diff. Volume at Peak Size	Size at 50% (microns)
MO	1.3-161.4	1.5-88.0	1.73-67.8	2.1, 14.3	3.9, 5.9	11.0
MOG1	1.6-14.7	1.5-13.8	1.8-6.5	2.3	12.6	2.7
MOG2	1.3-22.0	1.7-7.7	1.8-10.1	2.3	8.5	3.2
MOG3	1.3-95.9	1.9-17.0	2.1-14.27	2.5	6.1	5.0

5.2.5 Particle Size Analysis of Dry Bottom Fly Ashes Treated with STI Process (BOT)

The dry bottom fly ash (BOT), which its carbon was removed by STI process, was ground to be BTG1, BTG2 and BTG3 fly ashes. The cumulative particle size distributions of fly ashes are shown in Figure 5.29. Their differential particle size distributions are shown in Figure 5.30. The mean diameters of BTG1, BTG2, and BTG3 are 2.6, 3.8, and 13.1 microns, respectively. Comparing between these fly ashes with the wet bottom fly ashes, the BTG series is much coarser although they were ground using the same grinding condition. The BTG1 has about 87% of particles in finer than 10 microns while the BTG2 has about 82%. The BTG3 is much coarser than these two fly ashes. It has only 38% of their particles finer than 10 microns. They will be used in the study of fineness effect on the strength of ground dry bottom fly ash mortar.

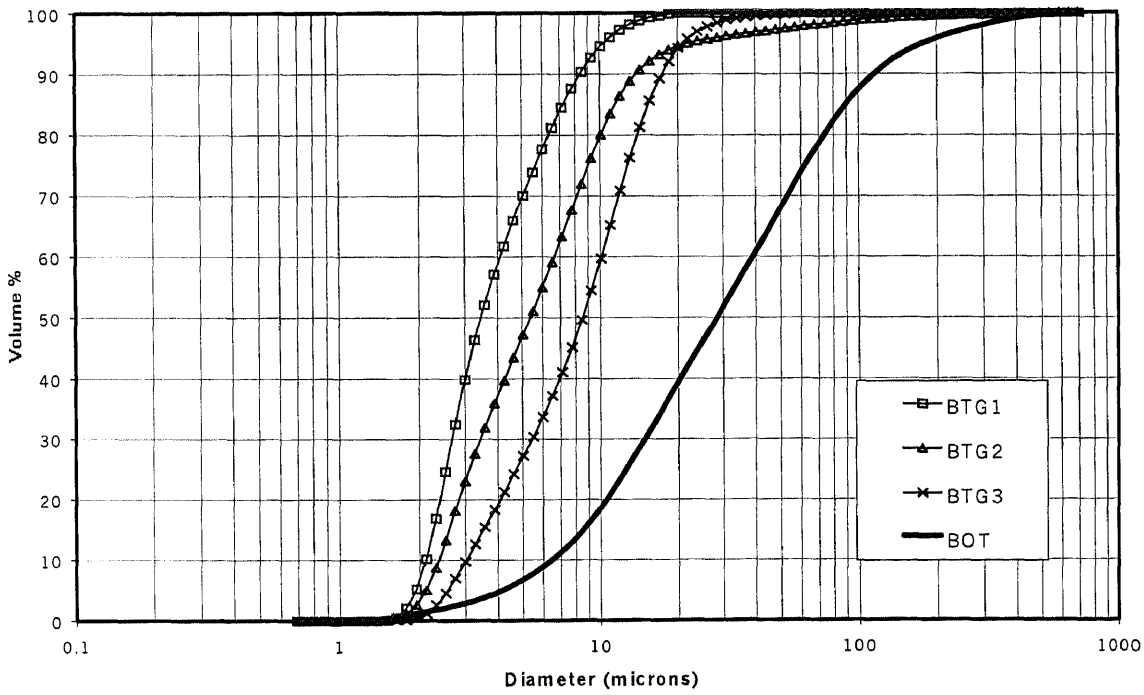

Figure 5.29 Cumulative Particle Size Distribution of Ground Dry Bottom Fly Ashes (BTG)

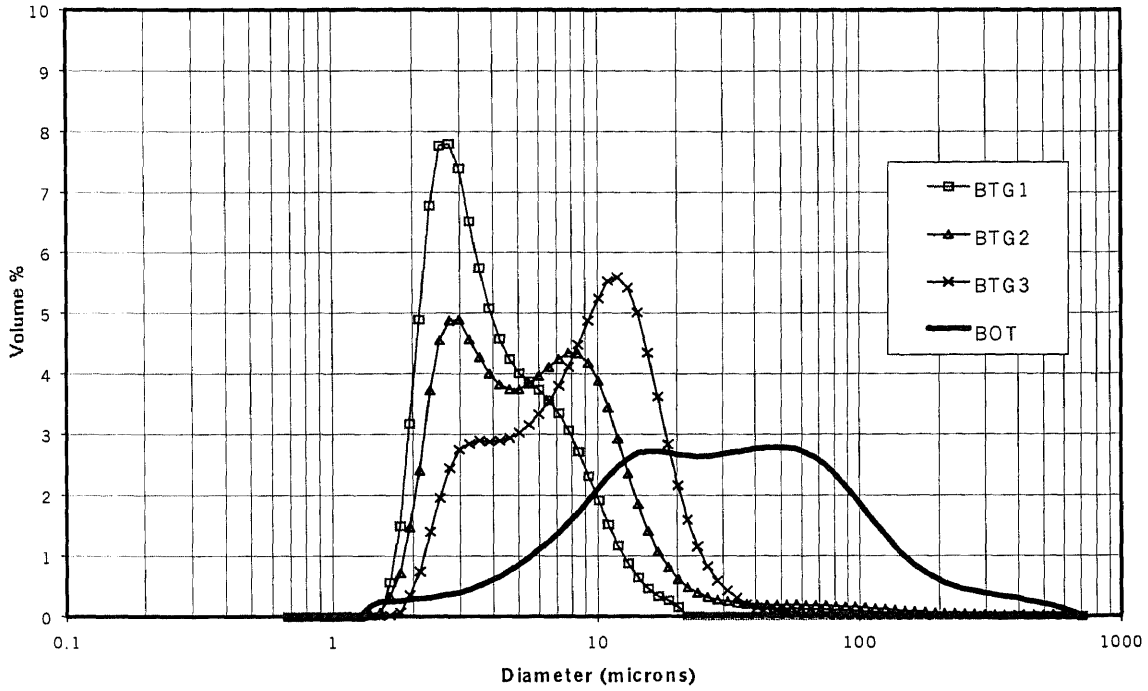

Figure 5.30 Differential Particle Size Distribution of Ground Dry Bottom Fly Ashes (BTG)

Table 5.7 Analysis of Particle size Distribution of Dry Bottom Fly Ashes

Type of Fly Ash	Range (microns)	95%UL of Differential curve	90% UL of Differential Curve	Peak Size (microns)	%Diff. Volume at Peak Size	Size at 50% (microns)
BOT	1.4-645.6	3.5-80.7	2.1-57.1	48.0	2.79	31.1
BTG1	1.1-191.9	1.4-74.0	1.6-47	2.12	8.96	2.6
BTG2	1.1-228.2	1.6-74.5	1.7-44	2.12	6.36	3.8
BTG3	1.4 -135.7	1.8-67.8	2.1-57.1	15.56	4.26	13.1

5.2.6 Particle Size Analysis of Low NO_x Fly Ashes (GPU2O)

The low NO_x fly ash (GPU2O) was also ground in three series, GPU2G1, GPU2G2 and GPU2G3. The cumulative particle size distributions of fly ashes are shown in Figure 5.31. Their differential particle size distributions are shown in Figure 5.32. Comparing this series to the MO series and BOT series, even though their primary raw fly ash (GPU2O) is coarser, the finest ground fly ashes, which is GPU2G1, is finer than those fly

ashes in BOT series and about the same as those fly ashes in MOG series. This is because the coarse portion of low NO_x fly ash is unburned coal, which is more brittle than glassy fly ash and therefore easier to grind. There is no portion coarser than 20 microns in the GPU series of ground fly ashes. The GPU2G1 has 100% of particles finer than 10 microns while the GPU2G2 has about 92%. The GPU2G3 has about 80% of particles finer than 10 microns. The mean diameters of GPU2G1, GPU2G2, and GPU2G3 are 3.0, 4.5, and 7.0 microns, respectively. They will be used in the study of fineness effect on the strength of low NO_x fly ash mortar.

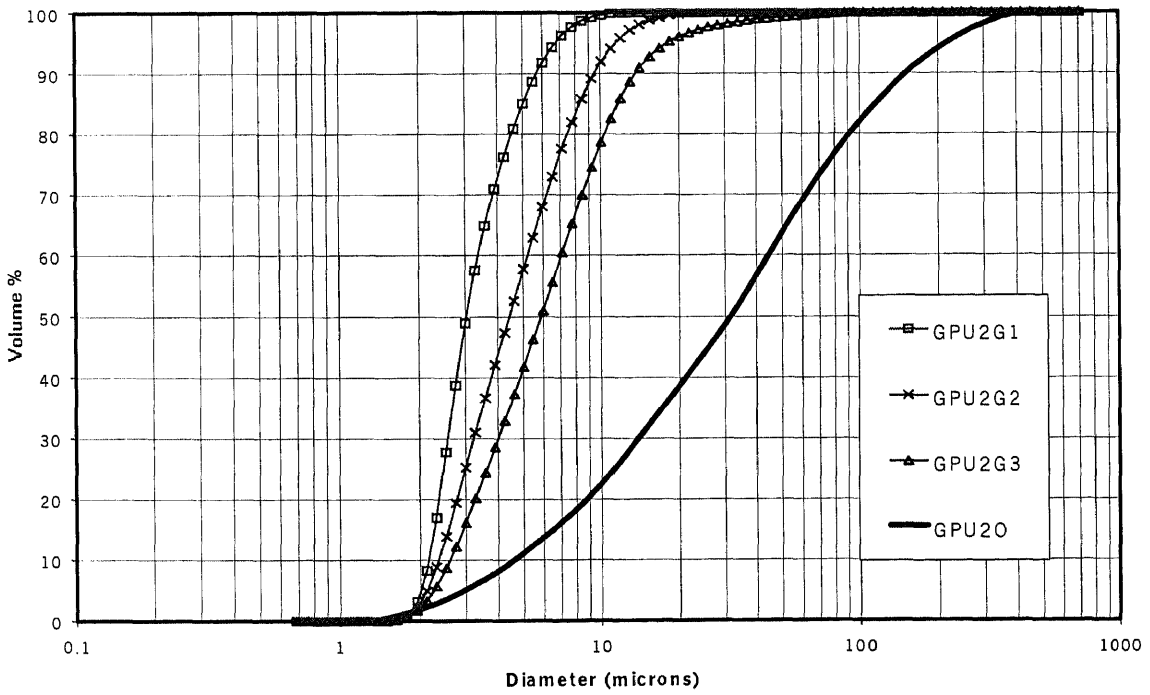

Figure 5.31 Cumulative Particle Size Distribution of Ground Low NO_x Fly Ashes (GPU2G)

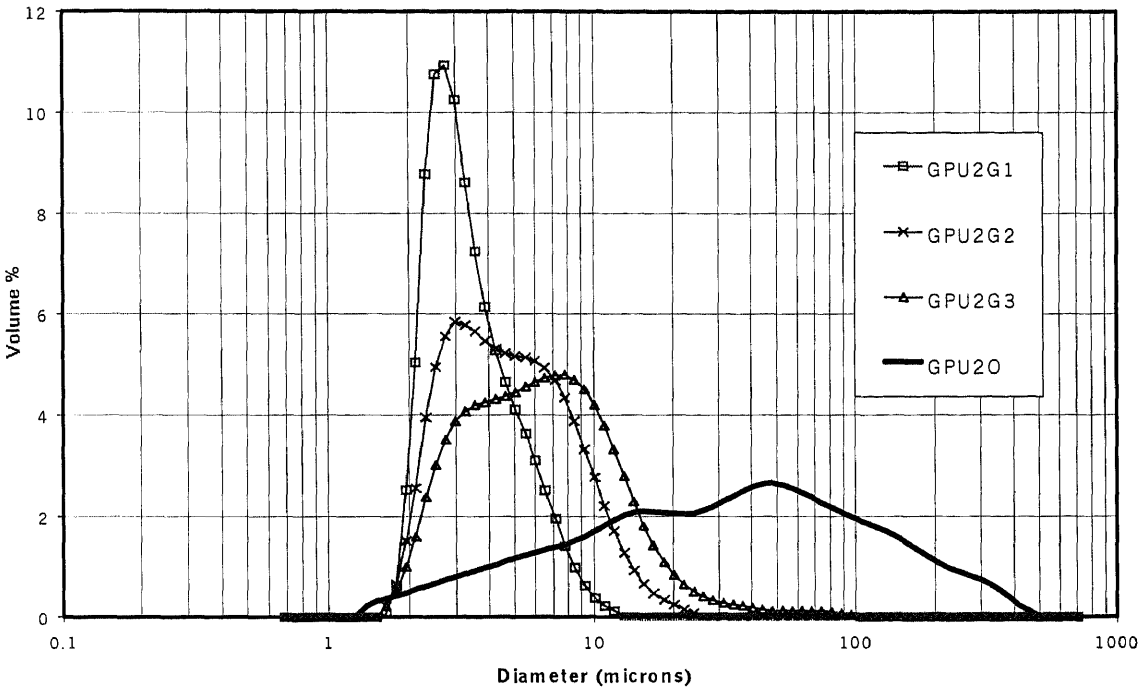

Figure 5.32 Differential Particle Size Distribution of Ground Low NO_x Fly Ashes (GPU2G)

Table 5.8 Analysis of Particle size Distribution of Low NO_x Fly Ashes

Type of Fly Ash	Range (microns)	95%UL of Differential curve	90% UL of Differential Curve	Peak Size (microns)	%Diff. Volume at Peak Size	Size at 50% (microns)
GPU2O	1.3-543	2.1-271.4	3.0-228	47.98	2.6	31.1
GPU2G1	1.6-12	1.8-7.7	2.0-6.5	2.55	10.9	3.0
GPU2G2	1.6-24	2.0-13.1	2.1-12	3.0	5.8	4.5
GPU2G3	1.6-95.5	2.0-26.2	2.3-18.5	7.78	4.8	7.0

5.3 Chemical Composition and Mineralogy of Processed Fly Ash

5.3.1 Bulk Chemical Composition

The chemical and physical properties of original feed fly ash and its ground fly ashes were determined. With the knowledge on the chemical characteristics of each fly ash, one can analyze the effect of these parameters on the strength of ground fly ash mortar. Table 5.9 shows the chemical composition of fly ashes, and cement used in this study. Sample CEM is locally available Portland cement type I. The HO and BO fly ashes are the fly ashes from the original feed of dry bottom ash but from different plants. The BOT fly ash is the dry bottom fly ash (BO), which has its carbon removed with STI process. The MO fly ash is wet bottom fly ash. The GPU2O fly ash is the low NO_x ash. H3F and M13F are the finest fly ash samples of dry and wet bottom ash respectively. Only one ground fly ash from each series was analyzed in comparison with its primary fly ash. MOG1 is the ground fly ash of the wet bottom MO fly ash. M8CG1 is the ground fly ash, which had the coarsest wet bottom ash (M18C) as its primary fly ash. BTG1 is the ground fly ash resulting from BOT. GPU2G1 is the ground fly ash which has as its primary fly ash the low NO_x fly ash from plant II (GPU2O).

The major differences among the raw feed of these fly ashes are the LOI content and the amount of oxides. The LOI content is the loss on ignition of material after burnt at 750 C. It is presumed that the LOI content is the amount of unburned coal in fly ash. The HO, BO, and MO fly ashes have LOI about 2.05 to 4.57 % of carbon, while the GPUO fly ash has LOI of about 12.5 % of carbon. ASTM recommends that to be suitable for concrete the fly ash should be less than 4% of carbon. The trouble with using fly ash with high carbon content in concrete is that the carbon particle in fly ash, which is

extremely porous, could lower the strength of concrete and absorb chemical additives such as water reducing agent, air entrained agent, etc. as reported by Freeman (1997), Gao (1997), and Hornain (1992). By accepting this percentage as a limitation, the GPU2O fly ash fail to meet this requirement, while the others pass. Another point that should be noted is that the LOI content is not just carbon. In fact, it primarily is unburned coal. Its particle is so porous that it has adverse effect on concrete property. However, it is also has a positive effect by being a source of oxides. Since coal contains similar chemical compounds as fly ash does, part of the oxide content in chemical analysis of fly ash comes from unburned coal. Therefore it is possible that the sum of oxide and LOI of high carbon fly ash would exceed 100%.

Table 5.9 Chemical Composition of Dry Bottom Fly Ashes (%)

Type	SiO_2	Al_2O_3	Fe_2O_3	CaO	K_2O	MgO	Na_2O	SO_3	LOI
CEM	20.07	8.84	1.41	60.14	0.86	2.49	0.28	2.53	0.73
HO	52.25	26.72	5.43	1.67	1.67	0.69	0.28	0.93	2.75
H3F	49.89	26.94	5.43	2.99	1.76	0.99	0.33	1.69	4.97
HOG	45.55	30.01	8.54	4.22	1.66	1.37	0.43	N/A	2.75
MO	41.54	27.74	14.83	6.89	2.07	1.43	1.17	3.13	2.05
M13F	38.93	23.35	12.13	5.68	1.65	1.56	1.96	5.06	2.67
MOG1	39.36	25.54	17.48	9.84	1.66	1.39	1.04	N/A	2.05
GPU2O	34.00	15.42	12.13	4.44	1.10	0.47	0.44	2.44	12.50
GPU2G1	33.19	15.31	13.56	4.56	1.13	0.47	N/A	2.06	12.50
BO	41.80	39.96	5.02	1.15	3.07	0.88	N/A	N/A	4.57
BOT	43.06	41.4	5.04	1.05	3.28	1.06	N/A	N/A	1.45
BTG1	42.89	42.5	8.04	1.20	3.19	1.09	N/A	N/A	1.45

Another difference between these fly ashes is the SiO_2, Al_2O_3, and Fe_2O_3 content. According to ASTM C-618 (1990), all fly ashes in this study are classified as class F fly

ash since the total amount of oxide, SiO_2, Al_2O_3 and Fe_2O_3 is higher than 70%. The class F fly ash is considered as a non-autopozzolanic fly ash because it cannot start the reaction unless it reacts with $Ca(OH)_2$. Since the cement paste has abundant $Ca(OH)_2$, shown as calcium oxide content in Table 5.9, these class F fly ash can be used with cement as a source of silicon, aluminum, and iron compounds.

The MO fly ash and HO fly ash have slightly different chemical composition. The major differences are the SiO_2, Al_2O_3 and Fe_2O_3 contents. The HO fly ash has about 10 % higher silica content than that of the MO fly ash. The CaO content of HO fly ash varies from 1.67% to 4.22% while MO fly ash, the variation is from 6.89% to 9.84%. Fe_2O_3 content of MO fly ash is almost three times higher than that of the HO fly ash.

The low NO_x fly ash (GPU2O) has a different chemical composition from the dry bottom fly ash (HO) even though they were generated from the dry bottom furnace. This is because the chemical compositions of their primary coal are different. The carbon content in GPU2O fly ash was high as expected from fly ash generated from incomplete combustion. The BO and BOT fly ashes have high silica and alumina content and low iron content as does HO fly ash. This is typical composition for fly ash generated from dry bottom boiler. The SiO_2 and Al_2O_3 of BO and BOT fly ashes are slightly different. The LOI content of BO fly ash is three times higher than BOT fly ash because the unburned coal was separated out by using STI process.

The chemical composition of fractionated fly ash is different from that of raw fly ash. Fractionated fly ashes (H3F, M13F) commonly have high percentage of LOI. This is due to the fact that carbon is lighter than most fly ashes and through the centrifugal process, gravitational separation yields larger carbon particles with the smaller size fly

ash. Ravina (1980) also had the same observation, that the finest particle of fly ashes have the highest LOI values. Most of the fractionated fly ashes have slight variations in the oxide compositions from their primary fly ashes. This result agrees with the report of Hemming and Berry (1986) that the chemical composition of Class F fly ash changes when the mean diameter changed.

Comparisons of ground fly ashes with original raw ashes did not show any other major variation on most of its chemical compositions except that the amount of Fe_2O_3 that tends to increase in the ground fly ashes. This Fe_2O_3 is believed to come from the wear of the steel balls, arms, and bowl of the attritor during grinding process. Other observed variations of chemical compositions are the slight increase of SO_3 that is attributed to the concentration of certain chemicals on smaller particle size of fly ash. All ground fly ashes have same percentage of LOI as their primary fly ash because the grinding process does not remove the carbon content.

Nonetheless, not all of silica, alumina, and iron oxide participate in pozzolanic reaction. This is because some of them are in a crystalline phase, which does not become chemically available in normal cement paste. Hence, the percentage of the silicon, alumina, and iron compounds cannot be used to determine the pozzolanic activity of that fly ash. This property can only be measured by the increased strength relative to that of the control cement paste. The contents of these compounds could be used to indicate the maximum percentages of the compounds that the whole particle of fly ash can release.

It can be concluded from the chemical analysis that these fly ashes are class F. Their major differences are the LOI content and the oxide content (silica, alumina, and iron content). The fly ash from low NO_X fly ash (GPU20) has LOI content exceeding the

available limit for use in concrete while those of the MO, HO, and BO fly ashes are in the acceptable range. It has been found that the unburned coal also has a positive effect as it contributes oxides to fly ash. The fractionated fly ash has higher LOI content but comparable oxide content as its primary ash. The ground fly ash has higher percentage of Fe_2O_3 than its primary ash. It is believed that the increasing amount is received from the wear off of arms and bowl of grinder during grinding process. The other chemical compounds of ground fly ash are in the same range as its feed fly ash.

5.3.2 Mineralogy of Processed Fly Ashes

5.3.2.1 Mineralogy of Raw Feed Fly Ashes: The XRD patterns of raw feed fly ashes, MO, GPU2O, and BO are shown in Figure 5.33, 5.34, and 5.35, respectively. From the phase identification, these raw ashes are typical fly ashes from a bituminous coal. The principal phases are quartz (SiO_2), mullite ($3Al_2O_3$-$2SiO_2$), spinel (magnetite, Fe_3O_4), hematite (Fe_2O_3), and glass (non-crystalline).

The major crystalline phases found in these ashes are mullite, quartz, hematite, and anhydrite. Mullite, a common phase in low-lime fly ashes, was detected in all fly ashes at 16.43, 25.97, 26.26, 35.28, 40.87 2-theta angle. Its presence confirms that these three fly ashes are Class F fly ash. Quartz (20.85, 26.65 2-theta angles) and hematite (24.12, 33.11, 35.61 2-theta angles) in these fly ashes are those unreacted quartz and hematite from coal. They directly pass from coals to the fly ashes without any change in their structure because they can withstand the combustion temperature, which is around 1000 °C due to its high thermal stability. Anhydrite ($CaSO_4$) was detected at 25.44, 31.37, 38.64 2-theta angles. This phase could form from the reaction between SO_2 and

CaO. SO_2 is obtained from the oxidation process of pyrite (FeS_2). CaO could form from decomposition of calcite ($CaCO_3$) at 900 °C or form from the dehydration of gypsum presenting in the coal. The generation of the CaO is not known since the mineralogy of the primary coals is not analyzed. The rest of lime phase that did not react with sulfur dioxide became free lime in fly ash.

In practical, the glass constituent in fly ash is of most interest. It is considered to be reponsible for pozzolanic activity (Fraay 1989). Most of glass phases in fly ash are amorphous aluminosilicate. The glass phase appears in XRD pattern as a halo. Since the glass phase has short range order, it does not give the sharp peak in the XRD pattern. The XRD patterns from these three fly ashes show the presence of halo at the same position, 17 to 35 2-theta angles. The area of these haloes, which was considered as the glass content of each fly ash, was used to compare the pozzolanic action among these fly ashes.

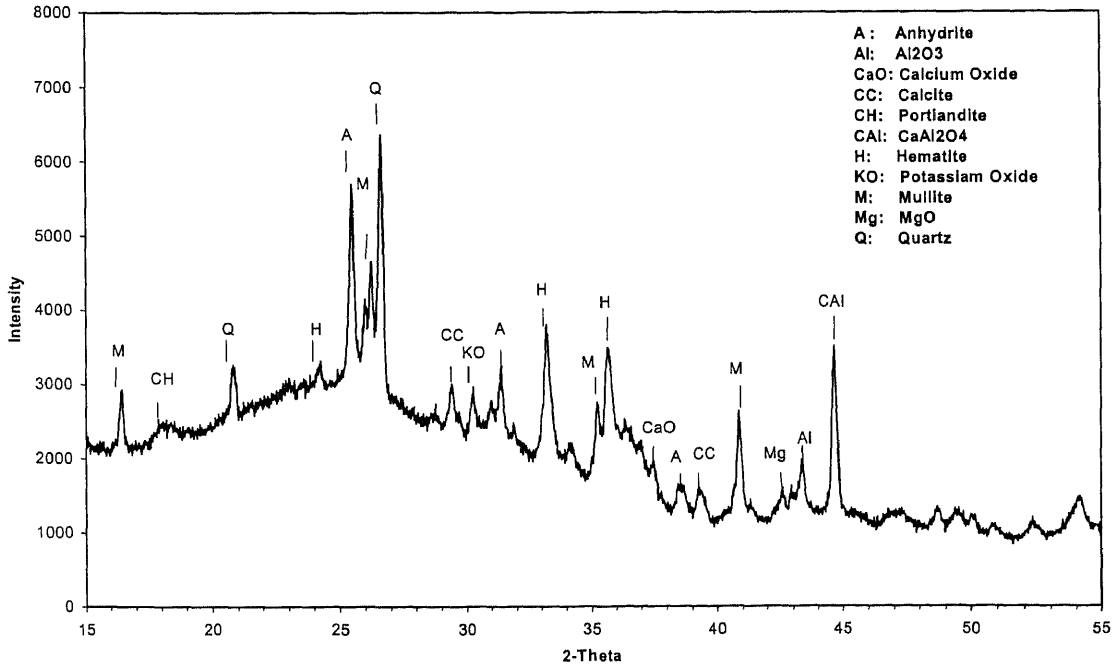

Figure 5.33 XRD Pattern of Wet Bottom Fly Ash (MO)

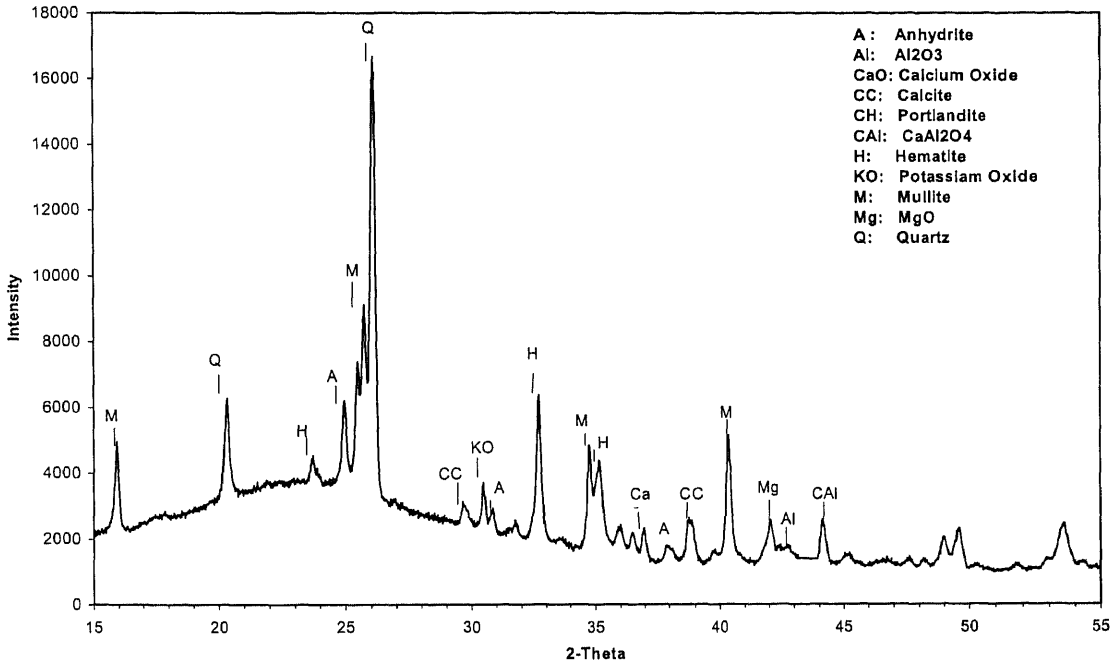

Figure 5.34 XRD Pattern of Low NO_x Fly Ash (GPU2O)

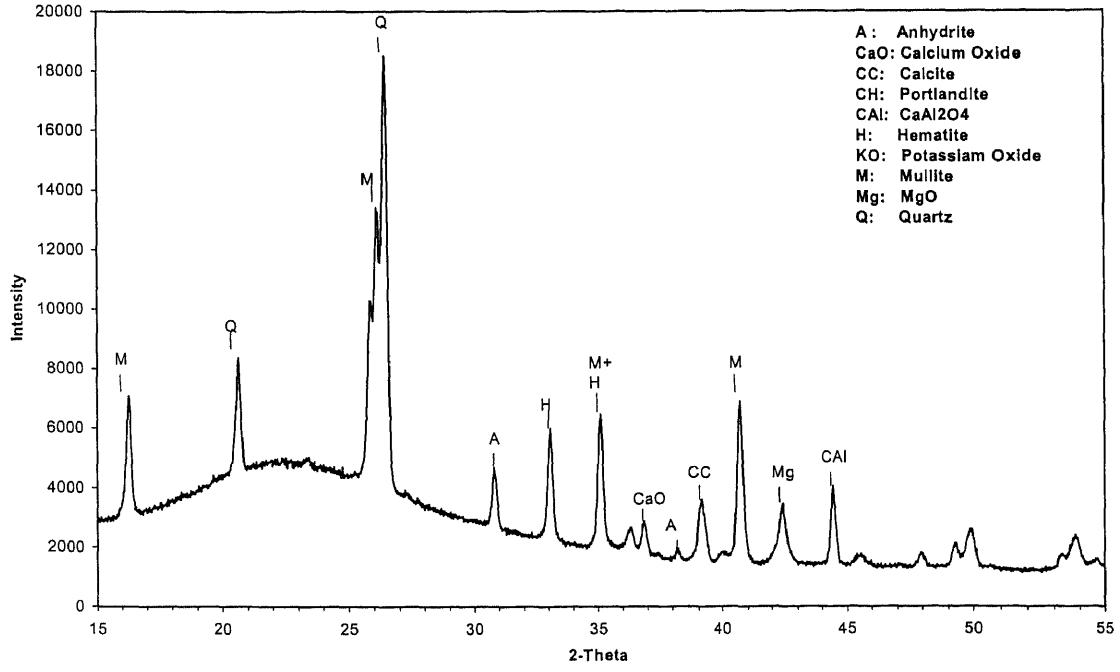

Figure 5.35 XRD Pattern of Dry Bottom Fly Ash (BO)

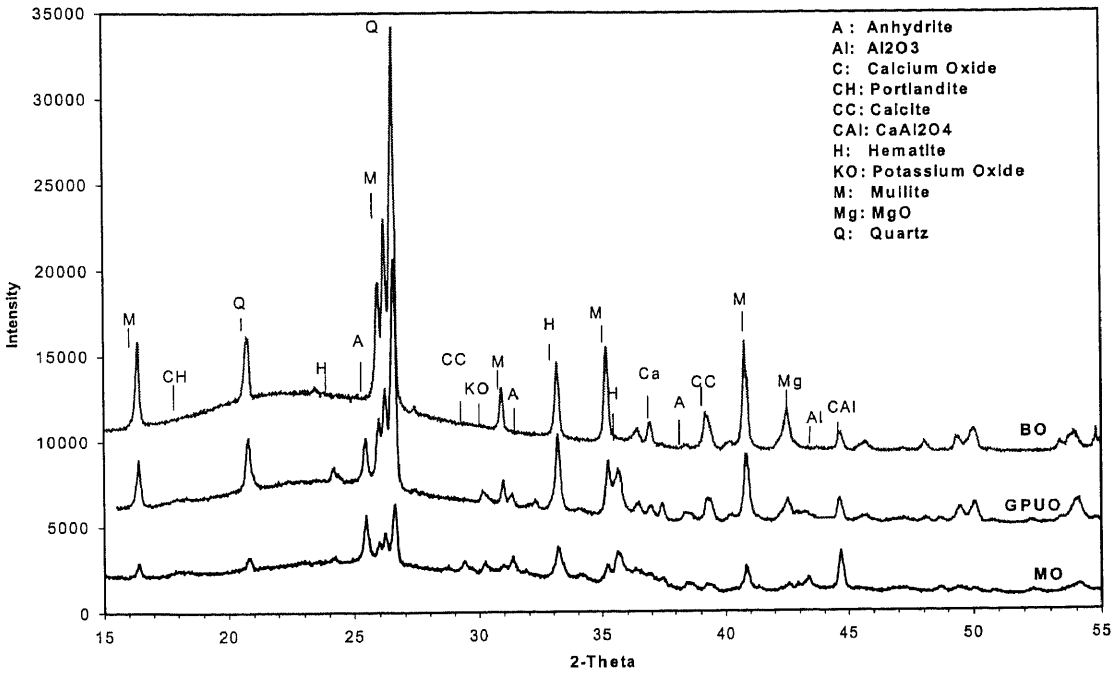

Figure 5.36 Comparison of XRD Patterns of Raw Feed Fly Ashes

Figure 5.36 shows the comparison of XRD patterns of fly ashes from different furnace: MO, BO, and GPUO. The BO fly ash and GPUO fly ash generating at low temperature, 1300-1600°C (Kautz, 1984), have high intensity of quartz, mullite, and hematite. This temperature is lower than the melting point of quartz which is 1600 °C therefore the quartz in the ground coal could pass directly to the fly ash. In the wet bottom furnace that has high temperature (1700°C), quartz and mullite in coal melt down completely and became the constituents in bottom ash instead of fly ash (Fraay, 1989). As a result, the MO fly ash generating from wet bottom furnace tends to have the total amount of crystalline constituents less than that of the BO fly ash generating from dry bottom furnace. It has been found that the crystalline phase does not contribute pozzolanic action to cement paste because it cannot be dissolved in high pH (Fraay,

1989). According to his finding, the BO and GPUO fly ashes would possess less pozzolanic activity than the MO fly ash.

The quantitative comparison between glassy phase and crystalline phase of these fly ashes was done by calculating the percentage of phase constituent from the halo and peak area of XRD pattern. The area under the peak of the graph is defined as percentage of crystalline phase. The glassy phase is defined as an area of halo in the graph, which is the area under the base line of peak and above the background curve. The percentage of glassy phase of each fly ash is shown in Table 5.10.

Table 5.10 Percentage of Amorphous Phase and Crystalline Phase in Each Fly Ash

Type of Fly Ash	Amorphous Phase (%)	Crystalline Phase (%)
MO	51.62	48.38
M13F	54.89	45.11
M18C	48.33	51.77
MOG1	50.27	49.73
M8CG1	45.04	54.96
M8CG2	46.04	53.96
GPU2O	46.95	53.05
GPU2G	42.86	57.14
GPU2COAL	63.55	36.45
BO	50.05	49.95
BOT	45.21	54.79
BTG1	42.55	57.45

By comparing the areas of halos of three types of raw feed fly ash, the MO fly ash has the highest percentage of amorphous phase and the Low NO_x fly ash has the lowest one which is in agreement with Fray's study. However, this result cannot be used to compare the pozzolanic activity among these raw fly ashes. This is because they are the phase percentages of the whole particle. Some phases are not participate in pozzolanic

reaction since they embed deep inside the big particle. This phase percentage could be used to determine the pozzolanic activity of fine or ground fly ashes such as MOG1, GPU2G, and BTG1. This is because at this fineness, the glassy phases are more liberated. From the result in Table 5.10, the order of pozzolanic activity of fly ash from low to high is BTG1, GPU2G, and MOG1. This result suggests that the MOG1 fly ash is the most reactive fly ash in this study

Comparing among the amorphous phase of the fractionated fly ashes from wet bottom furnace, the fine fly ash, M13F, has the highest percentage while the coarse has the lowest percentage. This result agrees with the study by Kautz (1984) that the fine fly ash has more glassy phase. It is shown that the amorphous percentages of the ground fly ashes are lower to those of their primary fly ashes. This is because the grinding process introduces the metal, which is the crystalline phase to the ground fly ash. Consequently, the amorphous phase in ground fly ashes are low.

The GPU2O fly ash has lower percentage of amorphous phase than the MO fly ash. This can be the case since it was generated in the low temperature furnace as explained earlier. The result also shows that the unburned coal portion in GPU2O fly ash, so called GPU2COAL, has high percentage of amorphous phase. Therefore, the unburned coal would increase the pozzolanic activity of fly ash. However, many studies found the lower strength of mortar incorporating with high carbon. The adverse effect could come from the physical feature of the unburned coal particle. Because most of them are large particle, so they are not well distributed in the mixture and had less possibility to react with other chemical compounds in cement paste. This factor hinders

the benefit of its reactivity. When it is ground to finer particle, the unburned coal could have more area for pozzolanic action, hence, increasing the strength of fly ash mortar.

The percentage of amorphous phase of BO fly ash is also lower than that of MO fly ash. This is because it was generated from dry bottom furnace as well as low NO_x fly ash. Therefore it tends to have lower pozzolanic activity as well. The BOT fly ash, which was treated by STI process, has less percentage of amorphous phase. The reason is that the unburned coal portion that has high amorphous phase was removed out after treatment.

The percentage of amorphous phase may not be an effective mean to determine the pozzolanic activity during early age for raw or coarse fly ash. This is because it is the bulk percentage of amorphous phase of the whole particle. In coarse particle, it would take a long period of time for essential elements in the pozzolanic action such as Si and Al to diffuse out. The percentage of glassy phase may be high but if this phase embeds inside the fly ash particle, it will not participate in pozzolanic action at the early age. While in finely ground fly ash, it can diffuse into the pore solution in shorter time, therefore, this percentage value can be used to determine its pozzolanic activity since the early age of fine ground fly ash.

5.3.2.2 Mineralogy of Fractionated Fly Ashes: Figure 5.37 shows the comparison between the XRD pattern of fine fractionated fly ash (M13F), coarse fractionated fly ash (M18C) and raw feed fly ash (MO). Unlike the ground fly ash, the mineralogy of the primary fly ash and the fractionated fly ash are not the same. Their compositions are different depending on the formation of the particle. The fine fraction of fly ash has less

crystalline phase and more glassy phase than the coarse fraction. Quartz and mullite were found in lesser intensity in fine fly ash than those found in coarse fly ash. The intensities of other constituents are also lower in fine fly ash. As a result, the fine portion should have higher reactivity than coarse portion. Since the MO fly ash is consisted of 50% of fine portion, thus, it still has high intensity of crystalline peaks. Another major difference between the XRD patterns of fine and coarse fly ashes is that the XRD pattern of fine fly ash has much higher intensity of $CaAl_2O_4$ peak than that of coarse fly ash and raw fly ash. This phase may precipitate in the same chamber that fine particle forms and deposit on the fine fly ash surface, subsequently.

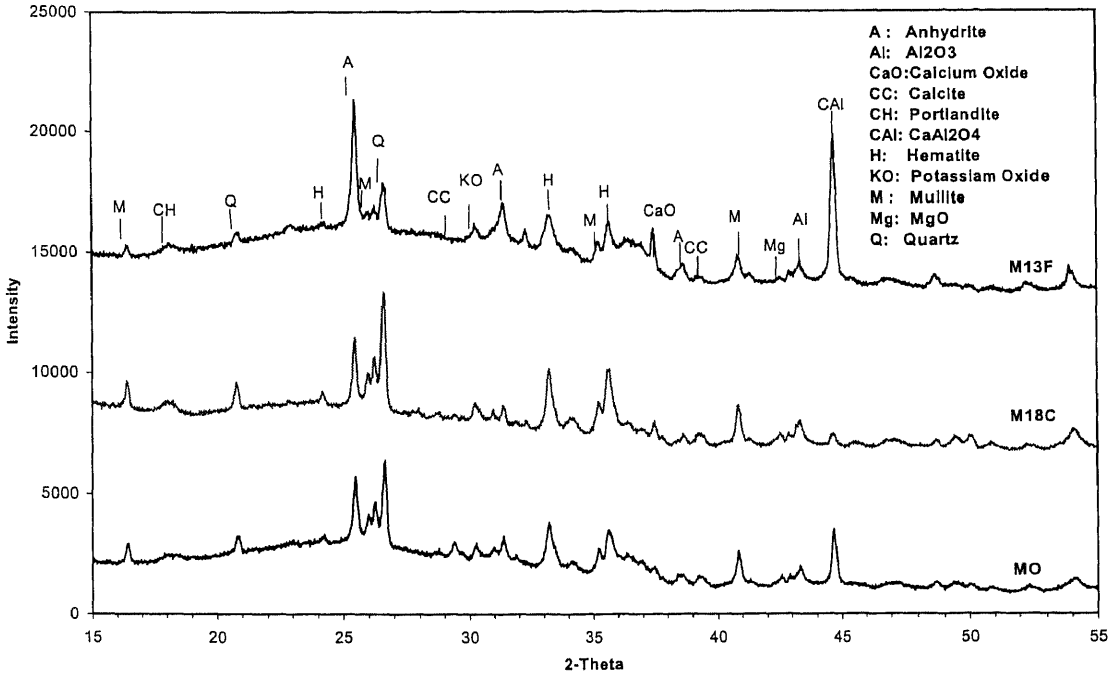

Figure 5.37 Comparison of XRD Patterns of Fractionated and Raw Feed Fly Ashes

5.3.2.3 Mineralogy of Ground Fly Ashes: The comparison of XRD patterns of ground fly ashes (M8CG1, M8CG2) and their primary feed fly ash (M8C) are shown in Figure 5.38. Most particle of primary fly ash (M8C) has particle size in range between 10 to 30 microns while that of M8CG1 and M8CG2 fly ash has size below 20 microns. The M8CG1 fly ash was ground to finer particle size than that of M8CG2 fly ash. It can be seen from Figure 5.38 that the XRD patterns of the M8CG1 and M8CG2 fly ashes are very close. Also, all peaks in XRD patterns of ground fly ash match with that of M8C fly ash except one peak at 29.6 2-theta. This peak also does not appear in XRD pattern of raw feed fly ash (MO). Therefore, this phase should generate during the grinding process. The identification process reveals that this phase is calcite, which is formed from the reaction between $Ca(OH)_2$ and CO_2. The presence of this phase in ground fly ash is possible since the high temperature in grinding process may initiate the reaction. The $Ca(OH)_2$ may come from the reaction between CaO and H_2O which is moisture in fly ash. The $Ca(OH)_2$ subsequently reacted with CO_2 in air to form $CaCO_3$. Because of its presence, the percentages of crystalline phase in M8CG1 and M8CG2 are higher than that in M18C as seen from Table 5.10. The M8CG1 fly ash has higher intensity at this 2-theta angle than the M8CG2 fly ash. It can be explained that grinding fly ash for longer time renders more formation of $CaCO_3$

In general, it can be said that the other crystalline constituents do not change during the grinding process. From Table 5.10, the percentages of amorphous phase of M8CG1 and M8CG2 fly ash are very close. The mineralogy that obtained from XRD technique is of the whole particle. Therefore the phase percentage does not depend on the fineness of ground fly ash. Despite of having the same percentage of amorphous

phase, the pozzolanic activity of M8CG1 would be higher since it has larger surface area to reactive.

The comparison of XRD patterns of ground fly ashes (MOG1, MOG2) and their primary feed fly ash (MO) are shown in Figure 5.39. It can be seen that the XRD pattern of MOG1 and MO are very similar but that of MOG2 is different in many peaks. In MOG2 fly ash has no anhydrite since its peaks at 25.5, 31.2, and 43.2 2-theta are undetectable. This phase is found in both MOG1 and MO fly ash. The loss of anhydrite may be due to the reaction going on during the grinding process or due to the error during the sampling. As the XRD pattern of MOG2 is still questionable, the comparison between phase percentage of MOG1 and MOG2 is not done. The high intensity at CAl or $CaAl_2O_4$ peak is also found in ground raw fly ash as well as the ground coarse fly ash.

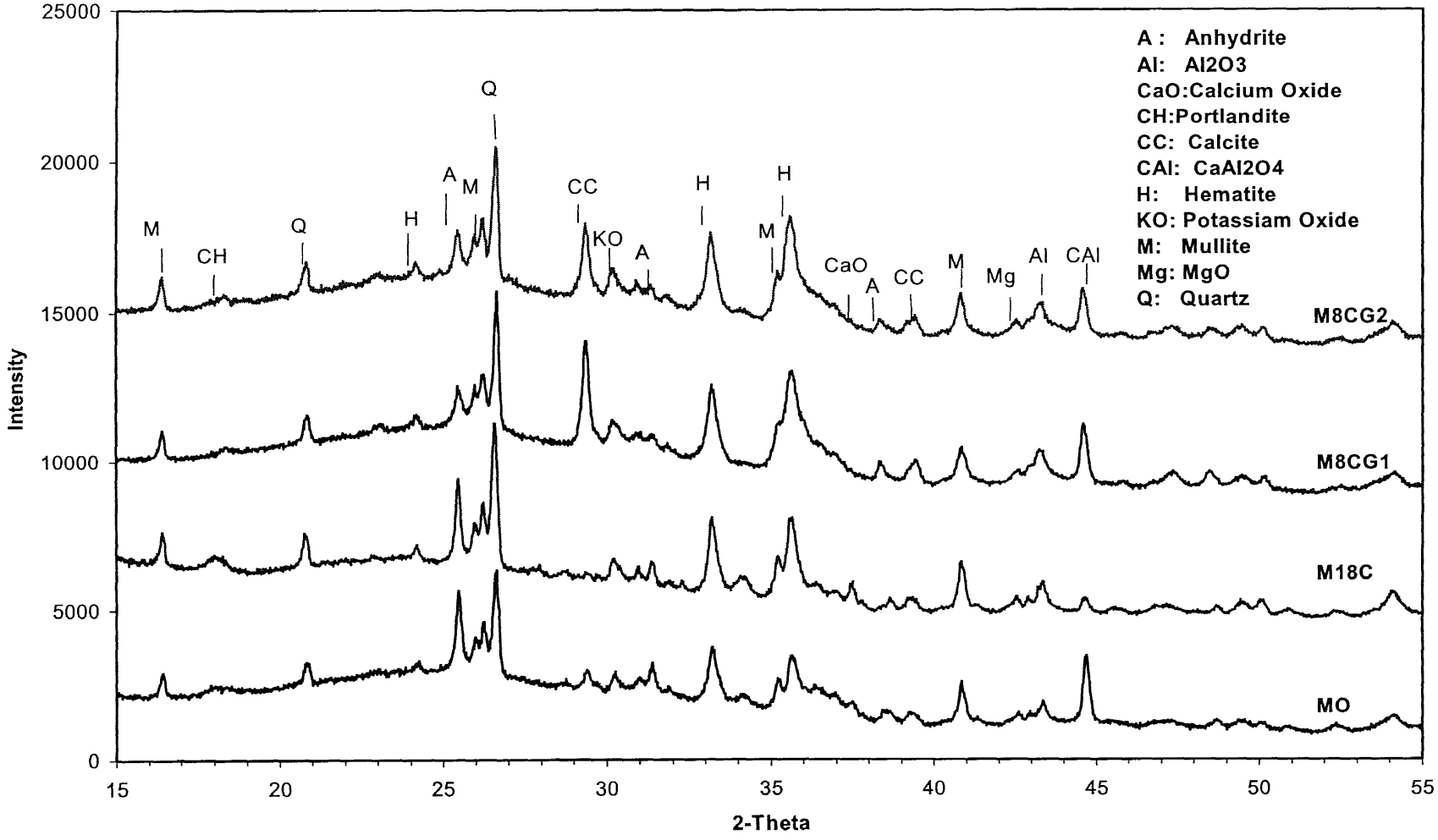

Figure 5.38 Comparison of XRD Patterns of Ground and Coarse Wet Bottom Fly Ashes

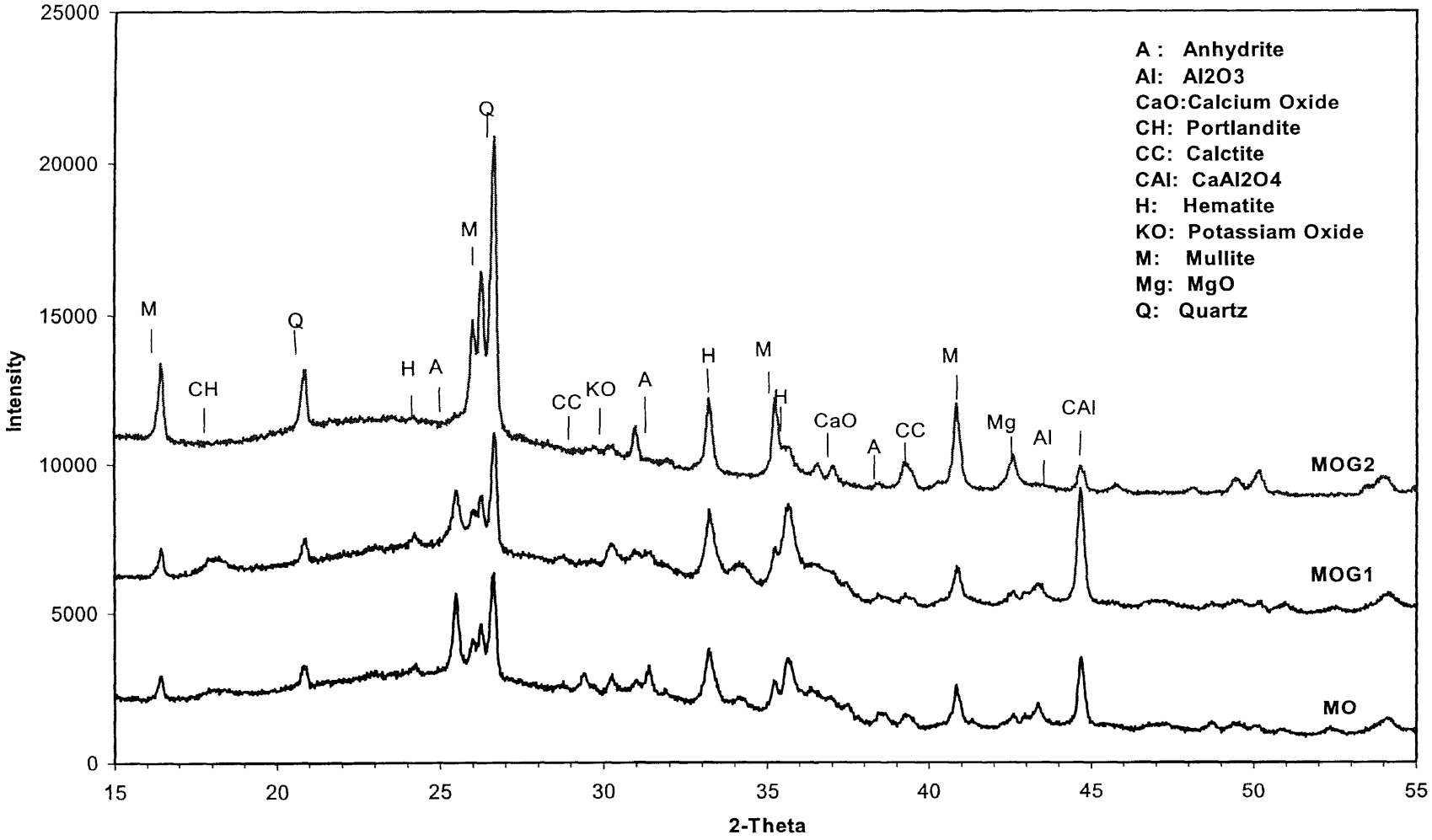

Figure 5.39 Comparison of XRD Patterns of Ground and Raw Wet Bottom Fly Ashes

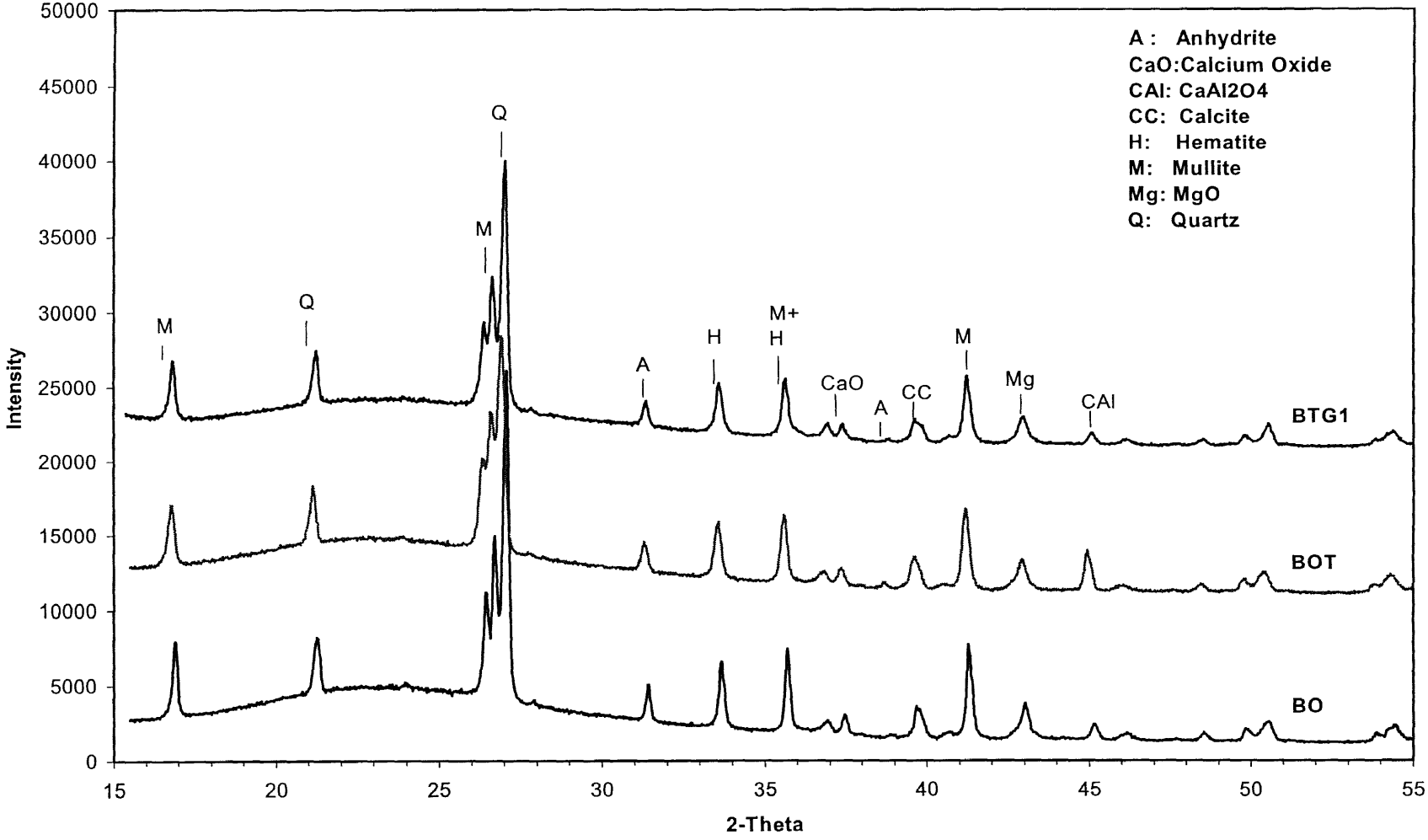

Figure 5.40 Comparison of XRD Patterns of Ground and Raw Dry Bottom Fly Ashes

There are many conclusions that can be drawn from these results. The phase percentage can be used to determine the pozzolanic activity of fine or ground fly ash but not for raw fly ash due to its hidden phase. The ground wet bottom fly ash has higher amorphous phase than the ground low NO_x fly ash and ground dry bottom fly ash. In fractionated fly ash, the glass content of the fly ash increased as the average particle size was reduced. Unlike fractionated fly ash, the fineness of ground fly ash does not influence their phase content. Still, it helps increasing the pozzolanic property of fly ash by increasing the surface area. The grinding process may initiate the reaction, which forms the additional crystalline phase in ground fly ash. The other phases that they have the same intensity as their primary fly ash.

5.4 Morphology and Elemental Analysis of Surface of Fly Ash

5.4.1 Morphology of Fly Ashes

5.4.1.1 Wet Bottom Fly Ash (MO)

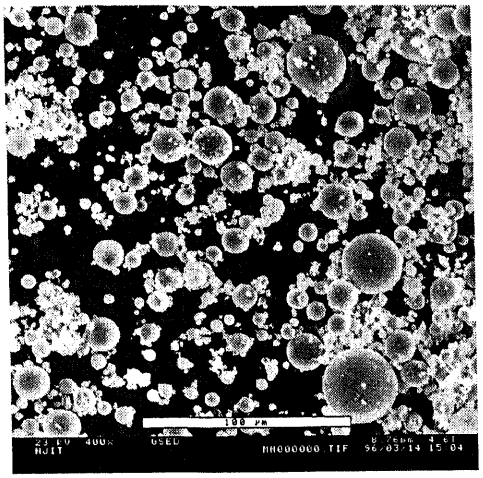

(a) Raw fly ash, 400x

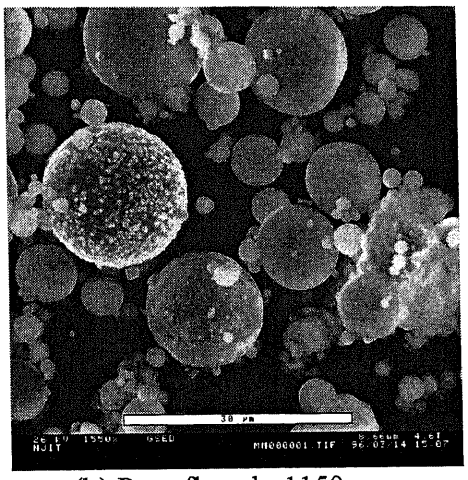

(b) Raw fly ash, 1150x

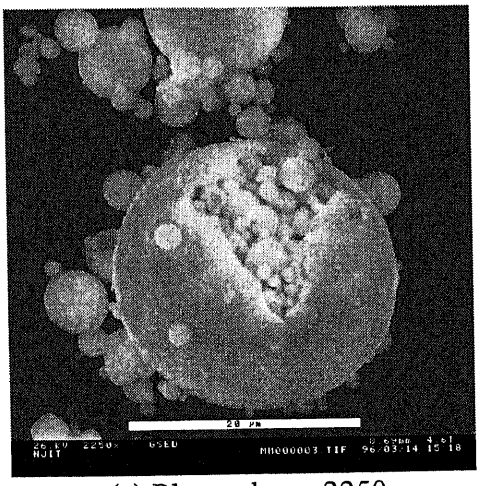

(c) Plerosphere, 2250x

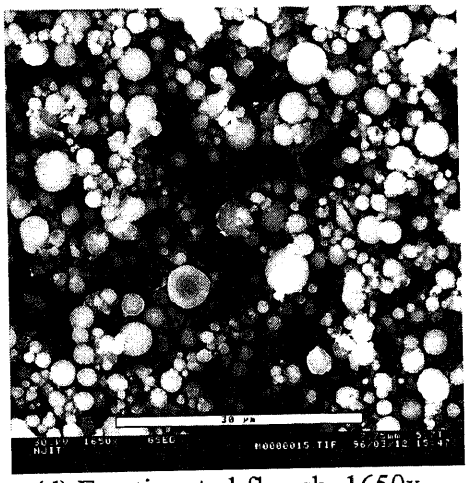

(d) Fractionated fly ash, 1650x

Figure 5.41 Micrograph of Wet-Bottom Fly Ash: (a) Raw fly ash, 400x; (b) Raw fly ash, 1150x; (c) Plerosphere, 2250x; (d) Fractionated fly ash, 1650x

Figure 5.41(a) shows the micrograph of some raw bottom fly ash particles with 400 magnification. There are several features that can be distinguished from the picture, which includes nice smooth spheres without surface precipitation, spherical particles with irregular surface or surface precipitation, conglomerates, and fused particles. Most particles are spherical and have smooth surface. The irregular particle is hardly seen in this wet bottom fly ash. With high magnification in Figure 5.41(b), the micrograph shows that the surface of fly ash has unknown particles deposited on it. The plerosphere and hollow particle is shown in Figure 5.41(c).

Figure 5.41(d) shows the micrograph of fine fractionated fly ash. It can be seen that all of them are spherical. Most particles are smaller than 10 microns. This result agrees with the PSD of M13F that its particle is not larger than 10 microns and its cut size is about 5 microns. Conglomeration of these particles may occur but their bond may be broken by dispersing agent in circulator of size analyzer.

The micrographs of coarse fly ashes are shown in Figure 5.42(a) to 5.42(d). Their particle sizes are larger than 50 microns. It is shown in PSD of MO fly ash that about 20% of its volume are the particles in this range. The coarse portions appeared in size analysis could be the unburned coal with fine particles fixed on it (Figure 5.42(a)), single sphere (Figure 5.42(b)) and the conglomerate of fine fly ash (Figure 5.42(c)). In a closer look of clusters, it can be seen that the fine particles are attached together (Figure 5.42(d)). This can be the case since the finer particle may be fused together during the combustion process. The bond within this cluster is so strong that they cannot be separated with the dispersing agent or sonic wave applied during sample preparation of particle size measurement

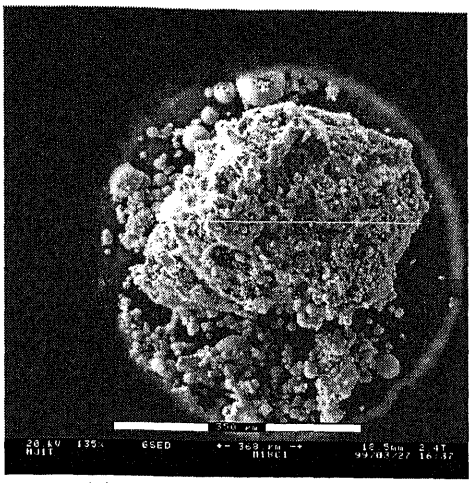

(a) Unburned coal, 135x

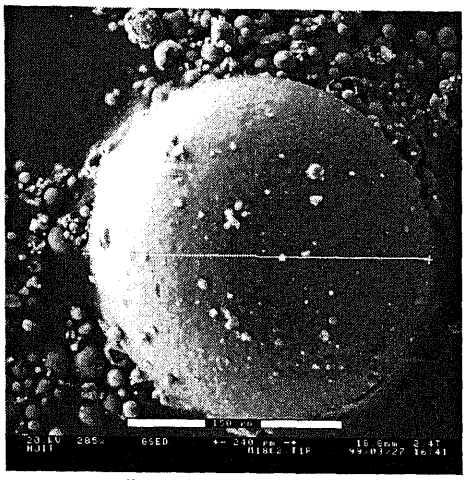

(b) Big Sphere, 285x

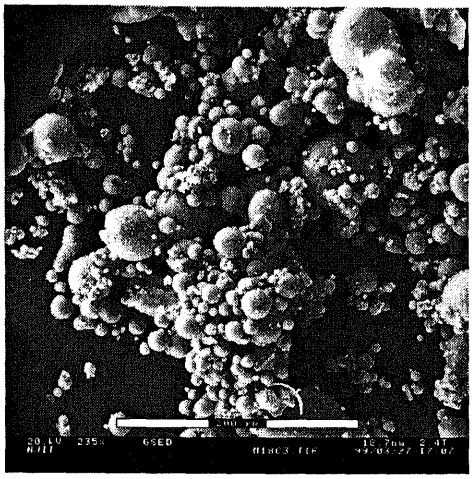

(c) Cluster of fine particles, 235x

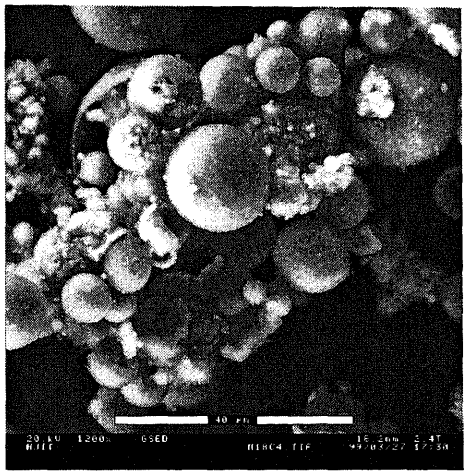

(d) Cluster of fine particles, 1200x

Figure 5.42 Micrograph of Wet Bottom Fly Ash: (a) Unburned Coal in Coarse Fly Ash, 135x; (b) Big Sphere in Coarse Fly Ash, 285x; (c) Cluster of Fine Particles in Coarse Fly Ash , 235x; (d) Cluster of Fine Particles in Coarse Fly Ash, 1200x

Figure 5.43(a) shows the morphology of ground wet bottom fly ash (MOG1) in general. The particles can be distinguished into two categories, broken fragment and sphere fragment. The sphere fragment is mainly fine particles that were not crushed during the grinding process. This may be because the media is too big to grind the fine

particle. The evident of spherical particle are shown more clearly in Figure 5.43(b) and 5.43(c). The portion that was crushed the most is the coarse portion. The residues from grinding the coarse particle could be shell shaped fragments originated from cracking of cenospheres and plerospheres and solid fragments originated from solid particles (Figure 5.43(b) and 5.43(c)). As measured from the picture, these broken particles are smaller than 10 microns (6.9, 7.9, and 8.9 microns). When the conglomeration of fine fly ash was ground, it yields the smaller clusters as shown in Figure 5.43(d). The remainder of the cluster is believed to be the core of the cluster.

The micrograph of ground fly ash originated from coarse fly ash is shown in Figure 5.43(e) and 5.43(f). Most of them are angular particles which are believed to be part of the big sphere particle. However, the spherical particles, which are very fine, still exist. They may be the fraction that broken down from conglomeration.

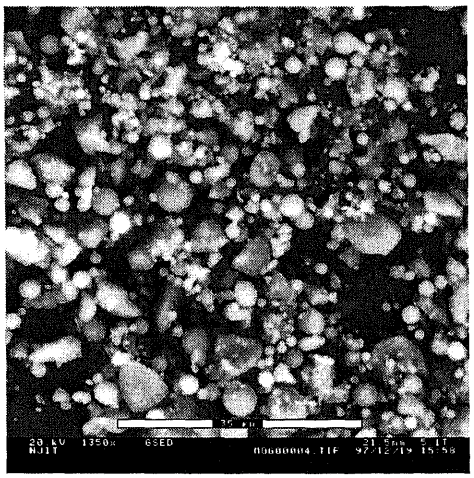

(a) MOG1, 1350x

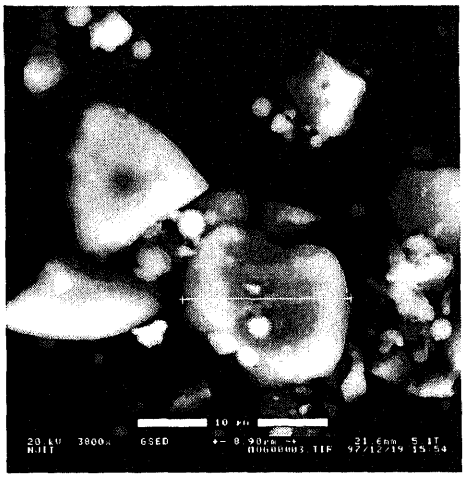

(b) MOG1, 3800x

(c) MOG1, 1600x

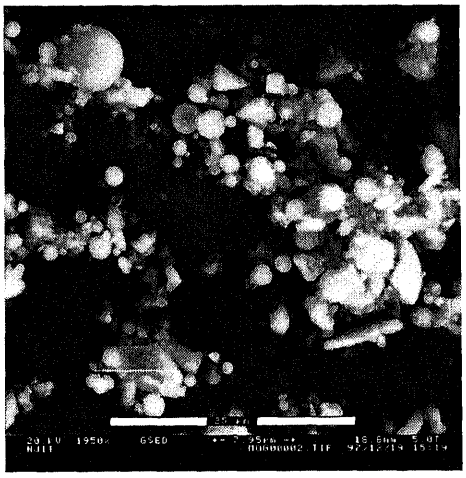

(d) MOG1, 1950x

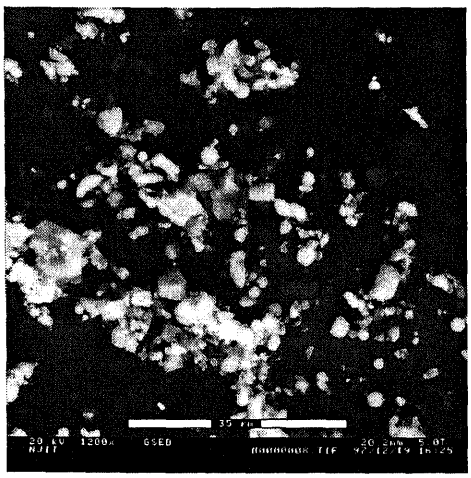

(e) M8CG1, 1200x

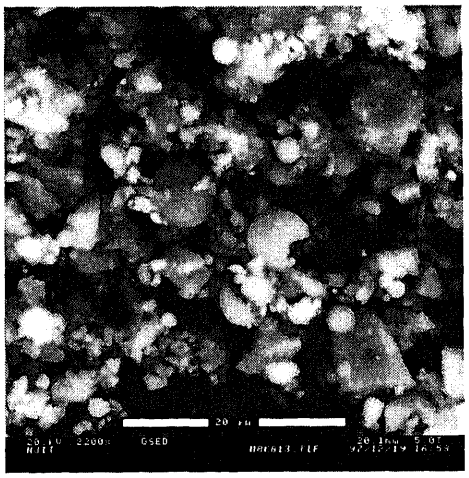

(f) M8CG1, 2200x

Figure 5.43 Micrograph of Ground Fly Ash: (a) MOG1, 1350x; (b) MOG1, 3800x; (c) MOG1, 1600x; (d) MOG1, 1950x; (e) M8CG1, 1200x; (f) M8CG1, 2200x

5.4.1.2 Low NO_x Fly Ash (GPU): Representative portions of the low NO_X fly ashes were examined. This fly ash has significant content of non-spherical oversize particles, as seen in Figure 5.44(a), but the finer particles are mostly spherical (Figure 5.44(b)). Figure 5.44(c) shows a cluster of conglomerated fine particle and a big plerosphere, which is about 50 microns. In Figure 5.44(d), a big porous particle is believed to be an unburned coal. It can be seen that there are fine particles inside the pores. These fine particles may adhere to the pore of the unburned coal when they mix together. A closer look of unburned coals that has fine particles attached to them is shown in Figure 5.44(e), 5.44(f). It can be seen that the pores can be as small as 1 microns or as big as 30 microns. Their size range is considered as the size of the air pore (>5 μm) (Mindess, 1981). Therefore, the higher number of small pore presenting in this raw fly ash can be responsible to the high porosity, low durability, low mechanical property in mortar that it incorporating with. Micrograph of the fly ash treated by thermal process (GPU2I) is shown in Figure 5.45(a) and 5.45(b). There is no evident of big and porous particle shown in this figure. The unburned coal was removed in the complete combustion at 750 °C and enough oxygen content of the thermal process. Since the temperature in the burning process is not above the melting point, the fly ash particles should not fuse together in this process. The clusters that found in the fly ash should be the clusters formed in the previous combustion. The residue of the process consists of mostly fine spherical particles.

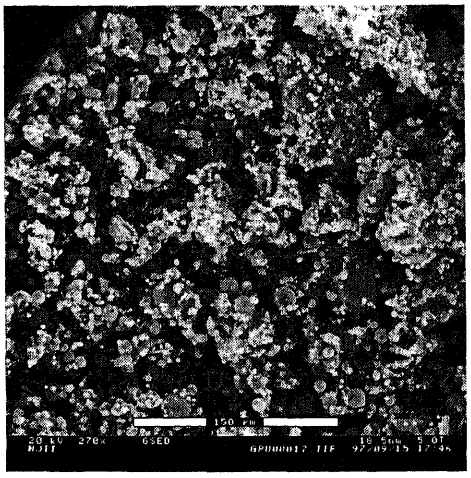

(a) GPU2O, 270x

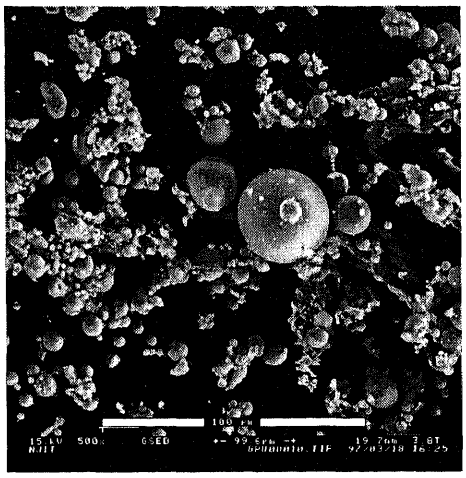

(b) GPU2O, 500x

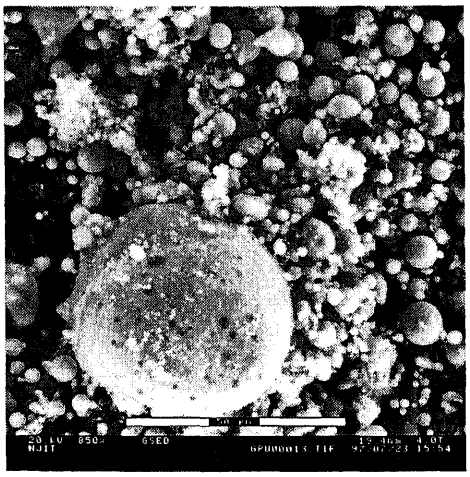

(c) GPU2O, 850x

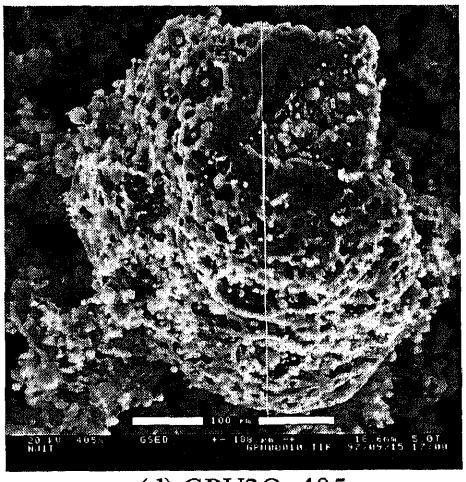

(d) GPU2O, 405x

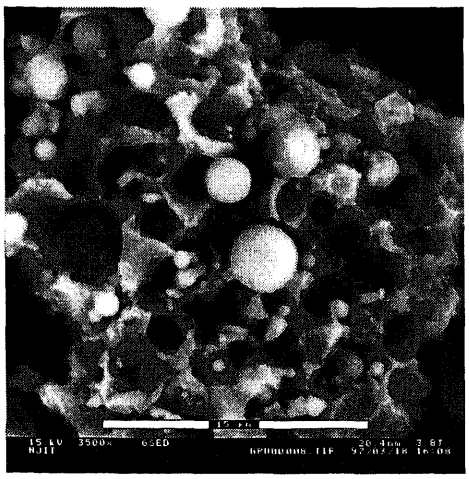

(e) GPU2O, 3500x

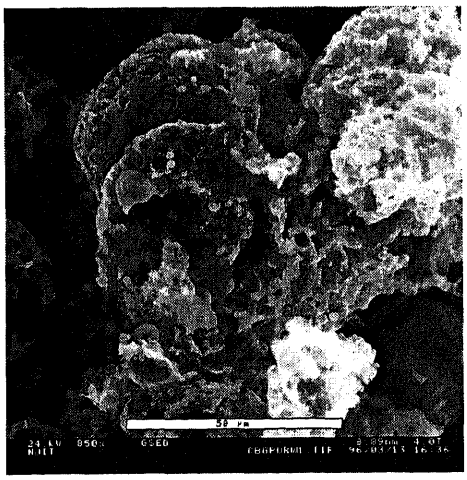

(f) GPU2O, 850x

Figure 5.44 Micrograph of Low NO_x Fly Ash (GPU2O): (a) 150x; (b) 500x; (c) 850x; (d) 405x; (e) 3500x; (f) 850x

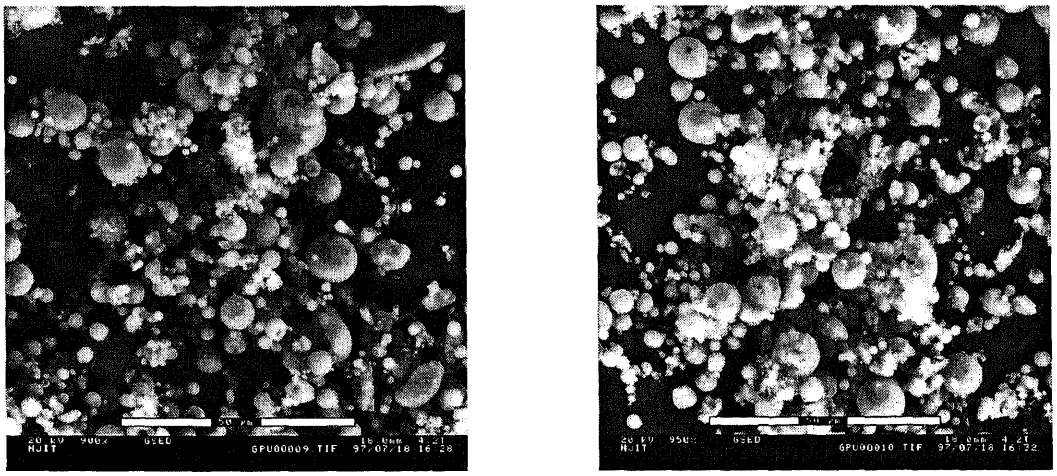

(a) 900x (b) 950x

Figure 5.45 Micrograph of Ignited Low NO_x Fly Ash (GPU2I): (a) 900x, (b) 950x

Micrograph of ground Low NO_x fly ash is shown in Figure 5.46. As might be expected, angular particles predominate over the remaining intact spheres. The phenomenon of plenosphere breaking in fly ash is observed as a shell shape in Figure 5.46(b) and 5.46(c). Previous study by Frias and de Rogjas (1996) found that the plerosphere broken during the stirring or vibrating of mortar leaves particle rests with empty hollows and partially broken spheres. They found that these broken plerosphere directly influence mortar porosity. The porosity increases due to the increase of broken sphere. Different from their research, the broken plerosphere by grinding process does not leave empty hollows or partially broken sphere, the whole plerosphere was crushed down to pieces. The fineness of these pieces increases with longer grinding time. The micrograph of ground low NO_x fly ashes subjected to 5, 10, 20 minutes are shown in Figure 5.47(a)-(b), 5.46(e)-(f) and 5.46(a)-(d), respectively. The empty hollows or partially broken sphere are not visible even in fly ash underwent a rupture process for the lowest degree (5 minutes) and having their particle size below 40 microns. However, the conglomerate of fine particle fused still exists and responsible for the particle between

10-40 microns as seen from Figure 5.47(b). This result suggests that the plerosphere are so brittle because it has hole inside that it can be broken easier than other fused particles. The mortar incorporating with fly ash from grinding process should not have porosity increased since there is no hollow sphere in ground fly ash.

Another particle that may introduce a pore to the matrix of mortar is the unburned coal in fly ash. Unlike the plerosphere, the unburned coal particle in raw fly ash has pore on the surface and its size is in a wider range. Most of its pores are smaller than 10 microns. The fly ash particles, cluster of fine particles, and unburned coal were ground to size below 40 microns (Figure 5.47(a)). The porous unburned carbon particles are not shown in all ground fly ash. It is believed that broken pieces of these porous particles are so brittle that they are all broken into solid pieces.

The micrographs at low magnification of GPU2G1 (Figure 5.46(a)), GPU2G2 (Figure 5.46(e)), and GPU2G3 (Figure 5.47(a)) fly ashes were used to analyze the effect of grinding time on fineness of fly ash. It can be seen that fly ash ground for longer time is finer than the one with shorter time. The cluster of fine particle is smaller and the number of fine particles increases.

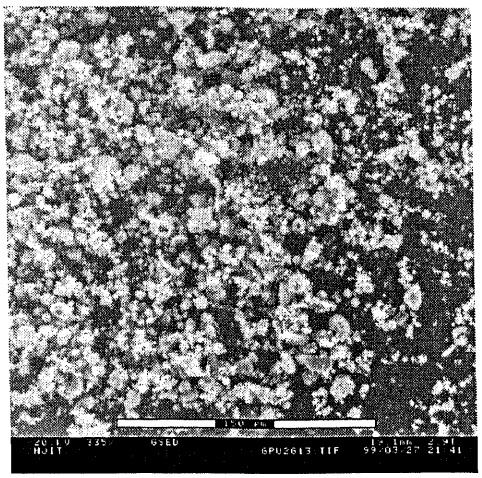

(a) GPU2G1, 335x

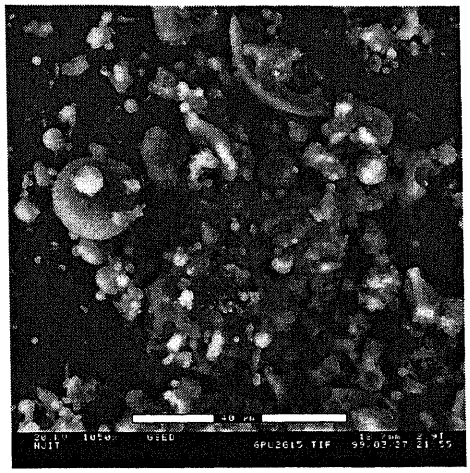

(b) Plerosphere in GPU2G1, 1050x

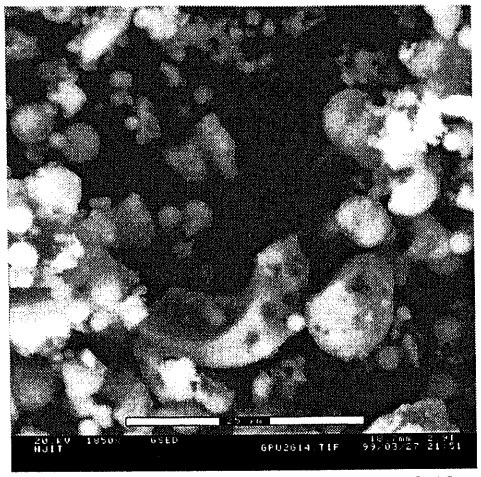

(c) Plerosphere in GPU2G1, 1850x

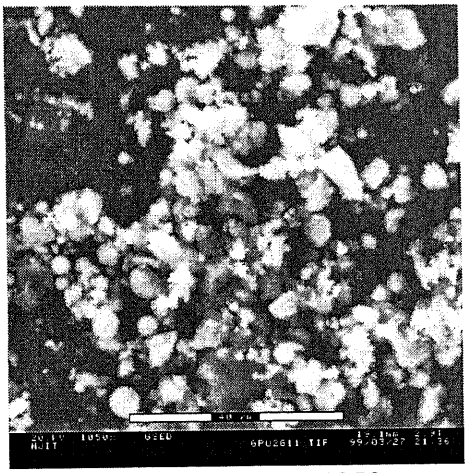

(d) GPU2G1, 1050x

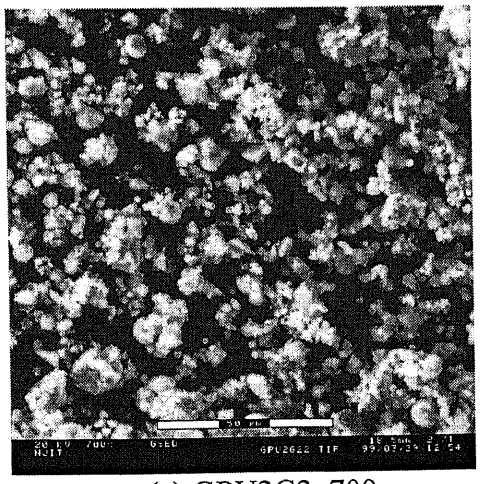

(e) GPU2G2, 700x

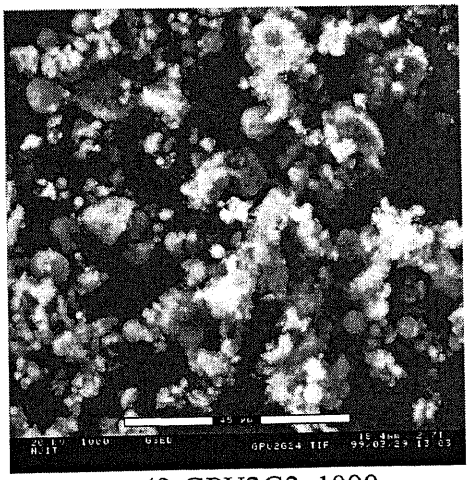

(f) GPU2G2, 1000x

Figure 5.46 Micrograph of Ground Low NO_x Fly Ash: (a) GPU2G1, 335x; (b) GPU2G1, 1050x; (c) GPU2G1, 1850x; (d) GPU2G1, 1050x; (e) GPU2G2, 700x; (f) GPU2G2, 1000x

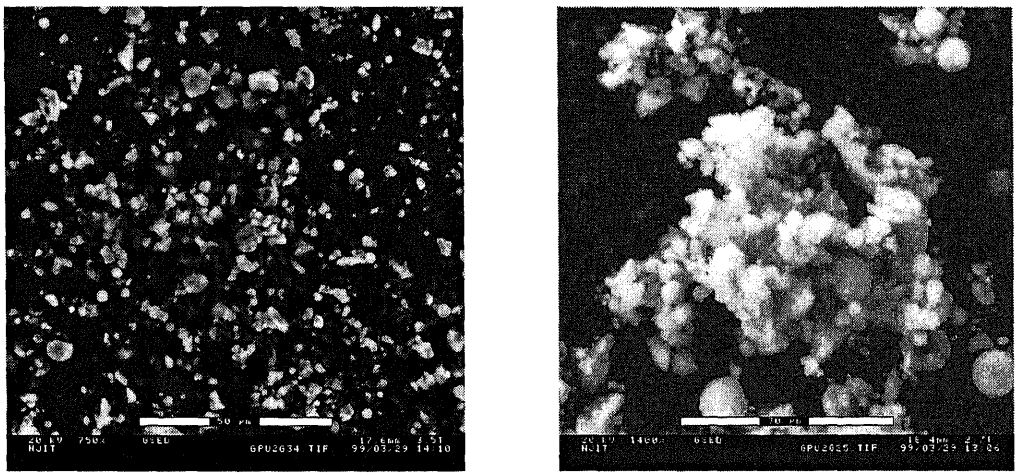

(a) GPU2G3, 750x (b) GPU2G3, 1400x

Figure 5.47 Micrograph in Ground Low NO_x Fly Ash (GPU2G2): (a) 750x, (b) 1400x

5.4.1.3 Dry Bottom Fly Ash (BO): Micrograph of BO fly ash is shown in Figure 5.48. It can be seen that most of their particles are spherical. There is lesser amount of unburned carbon shown in the micrograph than that found in GPU2O fly ash. This result consents with its low LOI content (4.5%). The big plerospheres are also found in this fly ash. Single particle, which is finer than 10 microns is hardly found in the raw feed of BO fly ash. This result agrees with its particle size distribution that only 16% of them have particle size smaller than 10 microns. They fused together and formed a cluster occupying most of the volume of this fly ash (Figure 5.48(a) and 5.48(b)). These clusters have width in 70-120 microns range. The cluster in Figure 5.48(a) has about 111 microns in width.

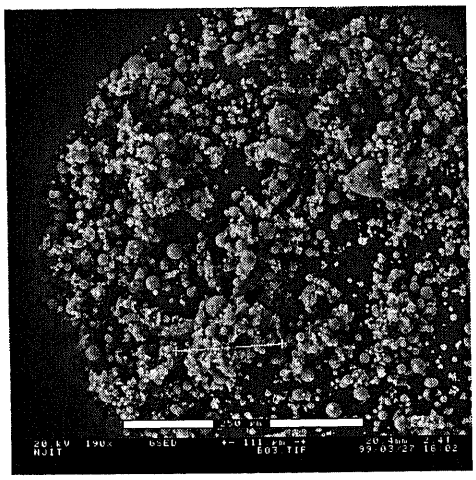

(a) BO, 190x

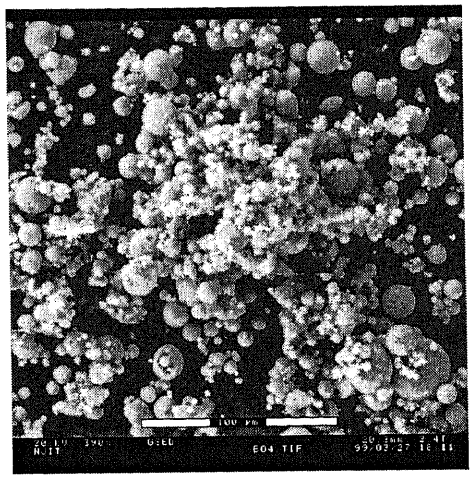

(b) BO, 390x

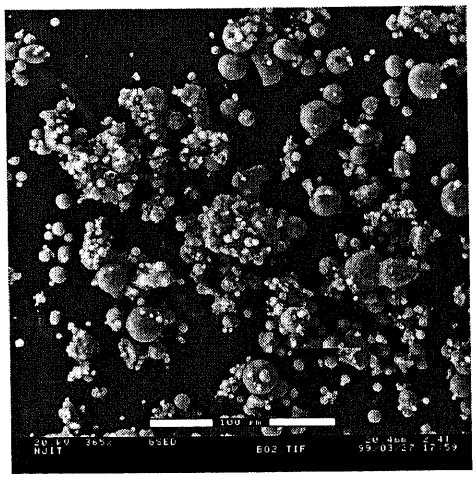

(c) BO, 365x

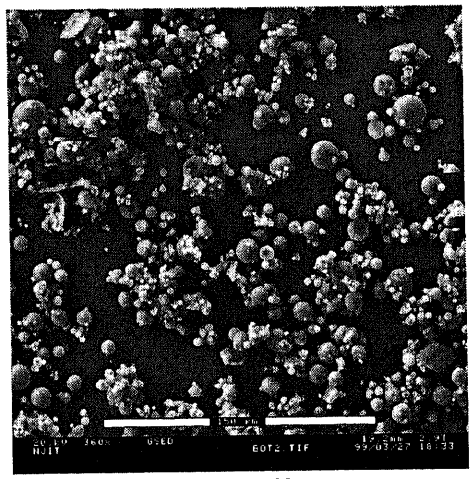

(d) BOT, 360x

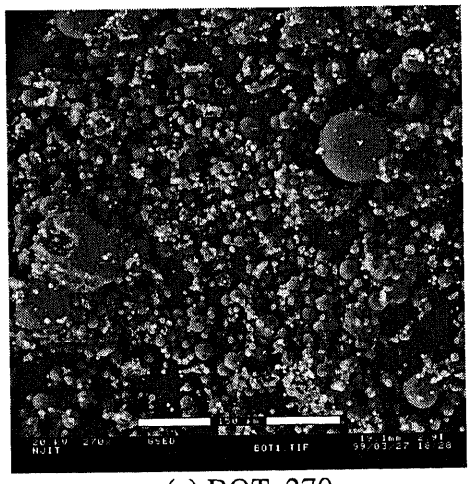

(e) BOT, 270x

Figure 5.48 Micrograph of Raw Dry Bottom Fly Ash: (a) BO, 190x; (b) BO, 390x; (c) BO, 365x; (d) BOT, 360x; (e) BOT, 270x

Figure 5.48(d) and 5.48(e) shows the micrograph of BOT fly ash. It was treated with STI Process and posses about 1.47% in LOI content. This technique removes only the unburned carbon, which is found as big particle in fly ash. Therefore, the BOT fly ash has less percentage of coarse particles than BO fly ash. The big particles that were left in the treated fly ash (BOT) as shown in Figure 5.48(e) are the big spheres, the plerospheres and the clusters of fine particles.

The morphology of fly ashes subjected to grinding with different media to fly ash ratio was studied. It can be seen from Figure 5.49(a) that the most of particle appearing in BTG1 fly ash are cluster of fine particles. Their size range is between 10-30 microns. Small portion of fine particles and angular particles are detected (Figure 5.49(b)). The remaining of cluster that was ground is shown in Figure 5.49(b). The size of this cluster is dramatically reduced when it was ground with higher media to fly ash ratio. In the micrograph of BTG2 fly ash, most particles are angular and smaller than 10 microns and some cluster of fine particles still exist (Figure 5.49(c) and 5.49(d)). The cluster is hardly found in BTG3 fly ash (Figure 5.49(e) and 5.49(f)). This result shows that the grinding process is more efficient when high media-to-fly ash ratio is used.

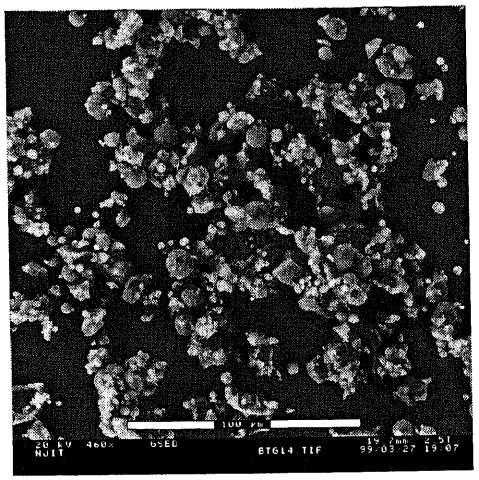

(a) BTG1, 460x

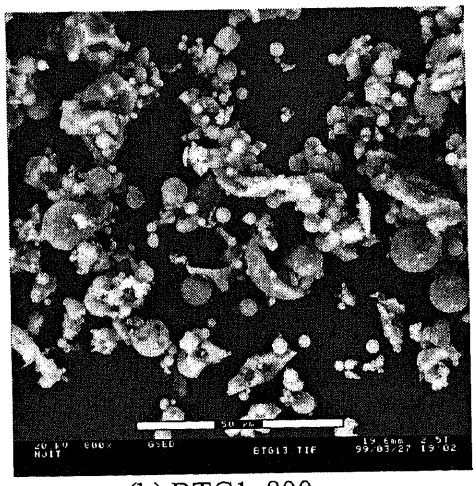

(b) BTG1, 800x

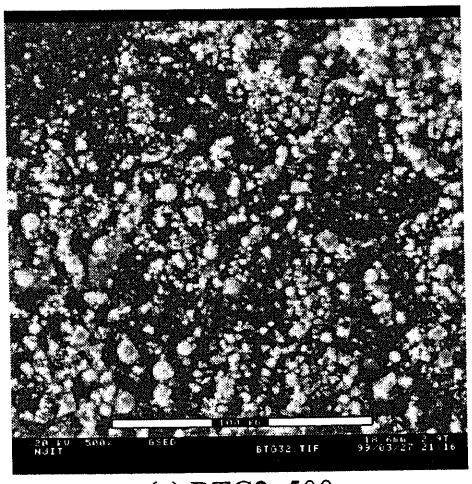

(c) BTG2, 500x

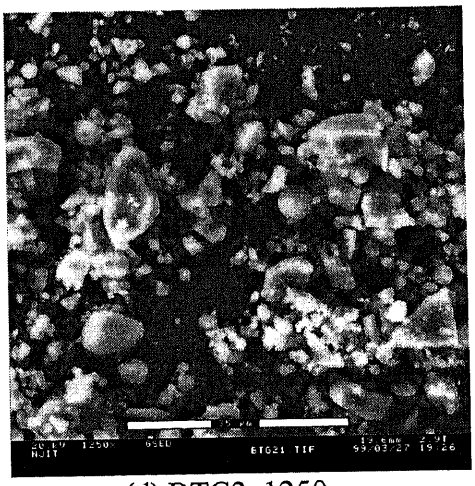

(d) BTG2, 1250x

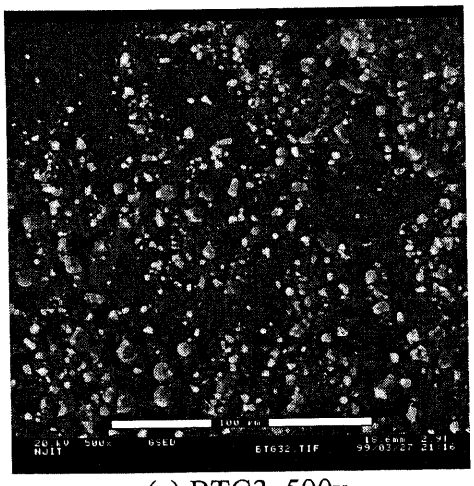

(e) BTG3, 500x

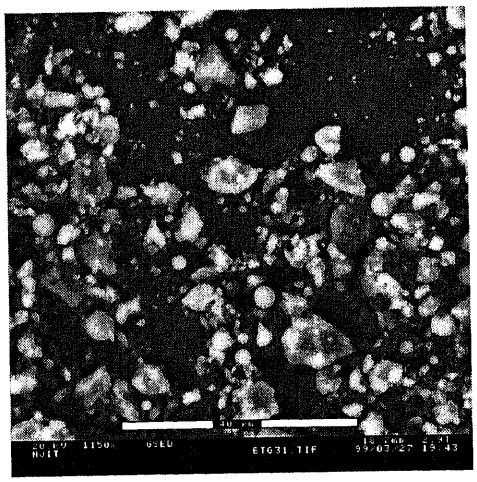

(f) BTG3, 1150x

Figure 5.49 Micrograph of Ground BOT Fly Ash: (a) BTG1, 460x; (b) BTG1, 800x; (c) BTG2, 500x; (d) BTG2, 1250x; (e) BTG3, 500x; (f) BTG3, 1150x

5.4.2 Elemental Mapping of Low NO_x Fly Ash

Table 5.11 Chemical Analysis of Low NO_x Fly ash by EDX/ESEM (%)

Element	Cluster of Particle	Porous Particle	Irregular Particle	GPU2G (1)	GPU2G (2)
Magnification	2150	3500	375	2150	4950
Al	14.89	9.43	9.55	18.5	18.24
Ca	5.01	3.05	30.51	5.21	6.02
Fe	5.54	3.64	12.51	13.81	13.27
K	1.60	1.13	1.68	2.01	2.2
Mg	-	0.77	0.79	-	1.4
Na	1.50	0.68	0.72	1.5	1.68
O	21.44	13.23	11.48	20.28	20.76
S	-	2.46	2.87	1.85	1.98
Si	22.37	14.60	14.16	35.38	33.32
Ti	1.09	0.98	2.11	1.47	1.12
C	26.56	50	13.61	-	-
SUM	100	99.97	99.99	100	99.99

The chemical analysis of particular particles in raw and ground low NO_x fly ash determined by EDX is shown in Table 5.11. This is aimed to determine the type of particle and its pozzolanic activity. Three types of particles, which are mostly found in low NO_x fly ash, were examined. It includes a cluster of fine particles, a porous particle, and an irregular particle. The element mapping of these fly ashes are shown in Figure 5.50 to 5.54. The area that has the element is shown as a dark dot while the area that does not have the element is shown in white dot. Among these elements, silicon, aluminum, oxygen, and carbon are the element, which has highest content. Normally, the oxygen is high since it is part of oxide in fly ash. The percentage of carbon could be the carbon in organic substance of coal particle or residue carbon from the combustion process, which cannot be distinguished by this instrument. The other oxides will be analyzed along with their mapping in each fly ash.

Figure 5.50(a) shows the image of a cluster of many very fine spheres and element mapping of the low NO_x fly ash (GPU2O). In small spherical particles, the mappings of silicon and aluminum have the highest density of pixels and they appear in the same area. This means that the fine particle is consisted of the phase of these two elements. This phase could be crystalline phase such as mullite which is $Al_6Si_2O_{13}$ or amorphous phase because they are also detected by XRD. In some area, silicon is found without aluminum and other elements. The mineral phases in that area could be quartz. The area that has the quartz phase does not participate in pozzolanic reaction. Therefore, the more number of quartz found on the surface of fly ash the lower the pozzolanic activity it has. In this cluster, there is no quartz in the shown area.

There exist some spheres that have low concentration of these elements but have iron and calcium predominant on their surface instead. There are two spheres that are covered with iron. This number is far less than the number of spheres covered with silicon and aluminum. The result agrees with its chemical analysis that shows low percentage of iron and calcium. The mapping of K element shows the pixel scattering all over the map but in very low density. This is because this fly ash has only 1.6% of potassium element.

The EDX also reveals the element of glue-like material that bridges these spheres together. It is found that they have low content of silicon and aluminum, hence, they are not the fused fly ash. They could be the unburned coal because the coal has lesser concentration of the silicon and aluminum than that of fly ash. Some area of the bridge has high calcium content. This means that the salt could be a bridging phase in the cluster.

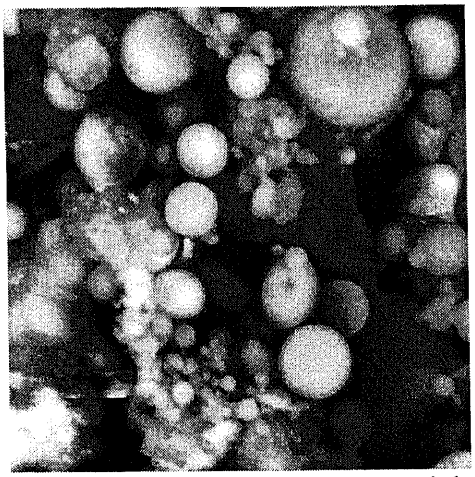

(a) Image of Cluster of Fine Particle

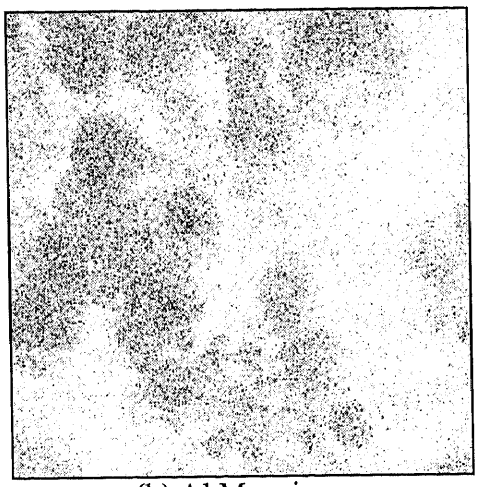

(b) Al Mapping

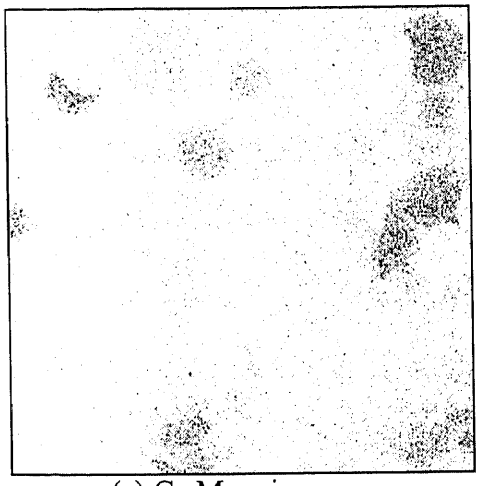

(c) Ca Mapping

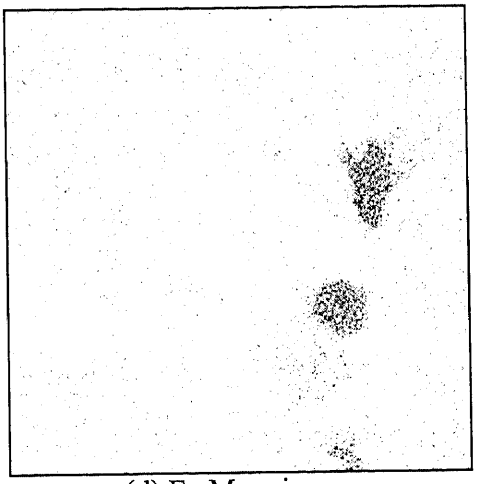

(d) Fe Mapping

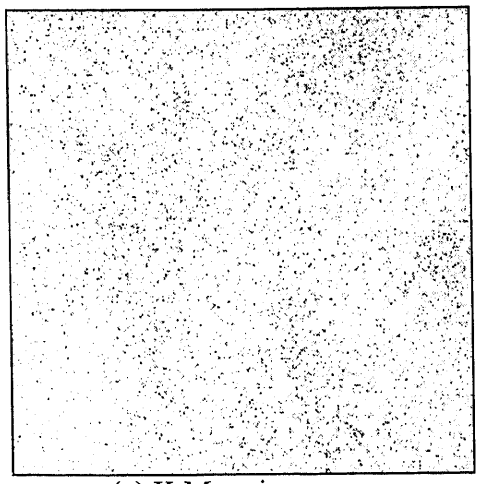

(e) K Mapping

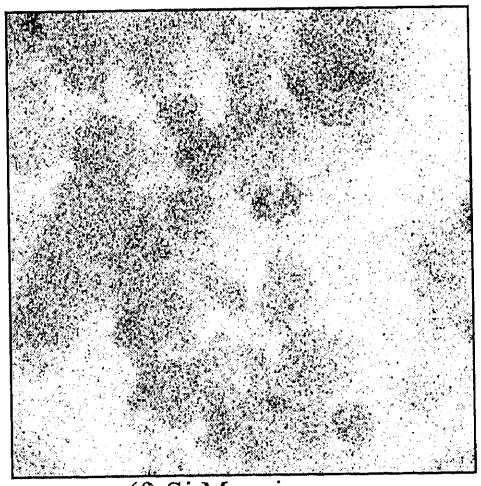

(f) Si Mapping

Figure 5.50 Elemental Mapping of Cluster of Fine Particle in Low NO_x Fly Ash (GPU2O)

Figure 5.51 shows a porous particle in the low NO_x fly ash (GPU2O). Both mapping of carbon and its elemental analysis reveal that it is composed of carbon, silicon and aluminum. Therefore, it is not made of carbon as it has been misunderstood. The carbon content belongs to the porous particle since it does not appear on the sphere of fly ash. So, the percentage of carbon in the elemental analysis is contributed by this particle. According to the elemental analysis of coal, the coal is composed of carbon and similar elements as that of fly ash but they are in lower percentage. Therefore, this particle could be an unburned coal particle.

The micrograph of irregular particle at low magnification is shown along with its element mapping in Figure 5.52. This particle has about 131 microns in width. Its surface is rough. From the mapping of aluminum and silicon elements, they are found more on the boundary of the particle than in the particle itself. The area that these two elements present corresponds with the area that spherical fly ashes present on the fly ash and the nearby area. Therefore the silicon and aluminum content in elemental analysis come from the sphere not the irreular particle. The high density of calcium in the area of this particle suggests that it is mostly consisted of calcium.

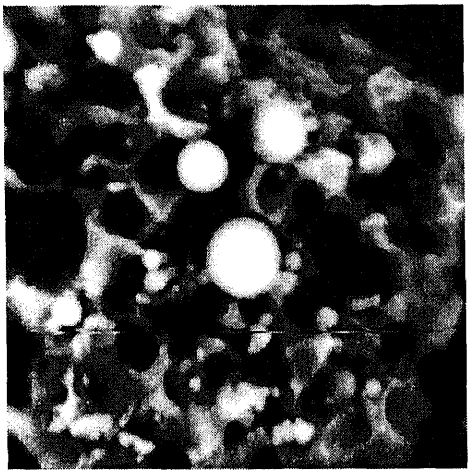

(a) Image of Porous Particle

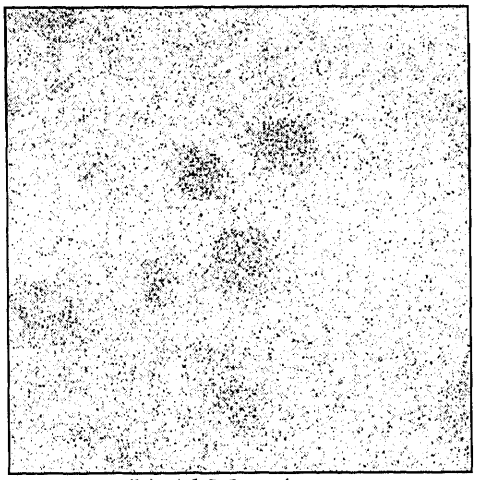

(b) Al Mapping

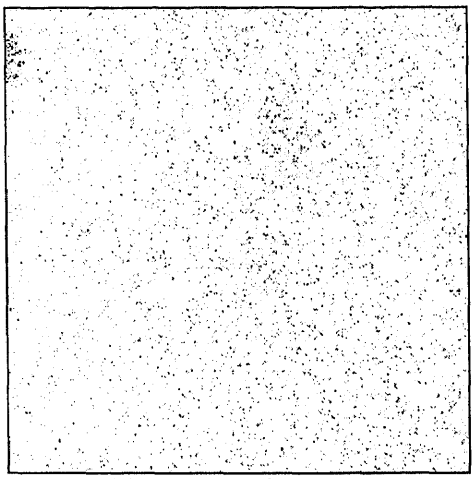

(c) Ca Mapping

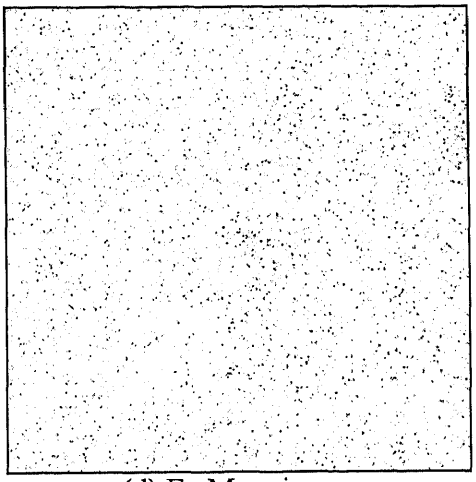

(d) Fe Mapping

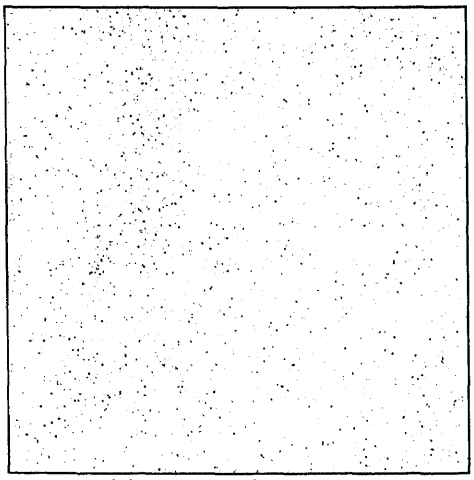

(e) C Mapping

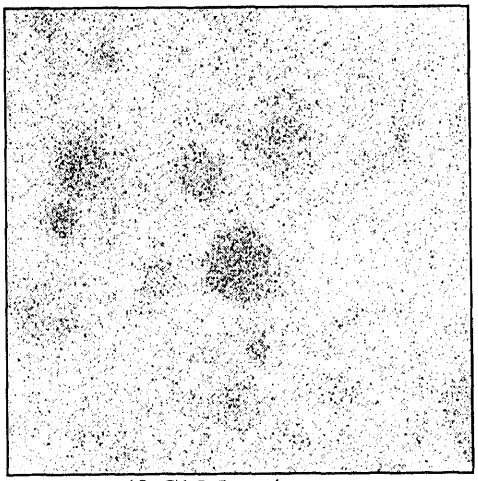

(f) Si Mapping

Figure 5.51 Elemental Mapping of Porous Particle in Low NO_x Fly Ash (GPU2O)

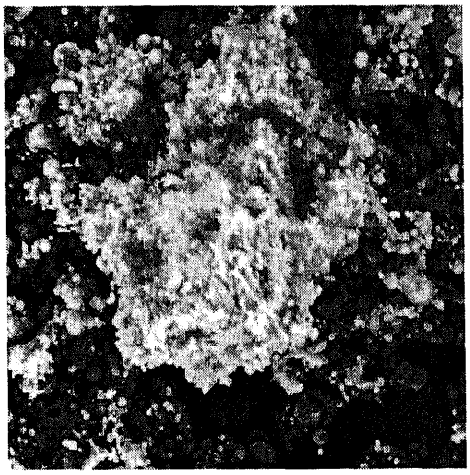

(a) Image of Irregular Particle

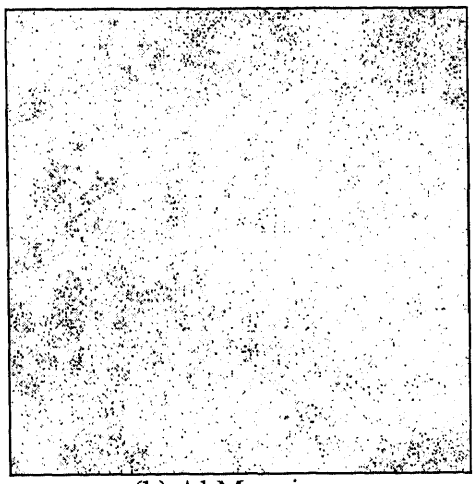

(b) Al Mapping

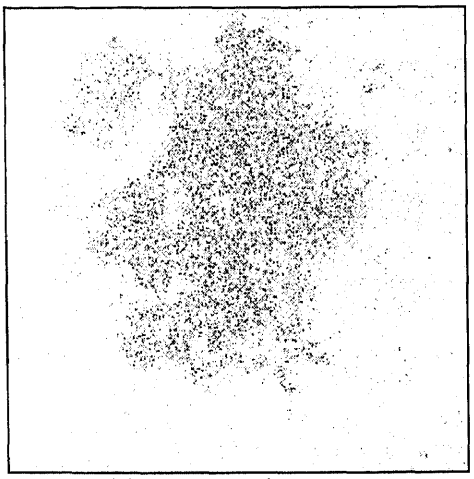

(c) Ca Mapping

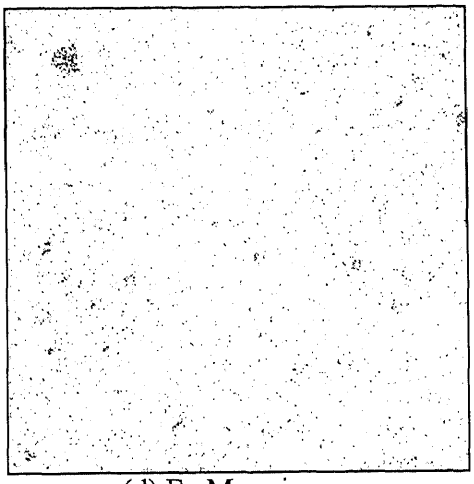

(d) Fe Mapping

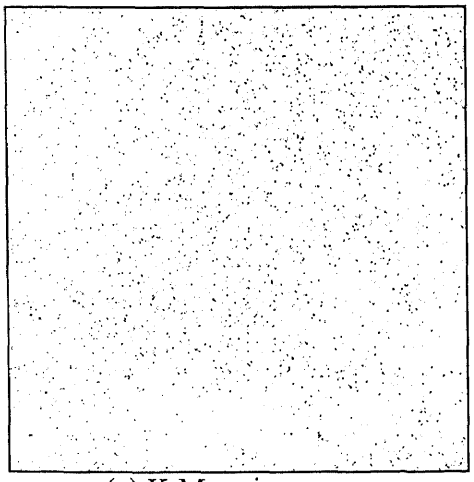

(e) K Mapping

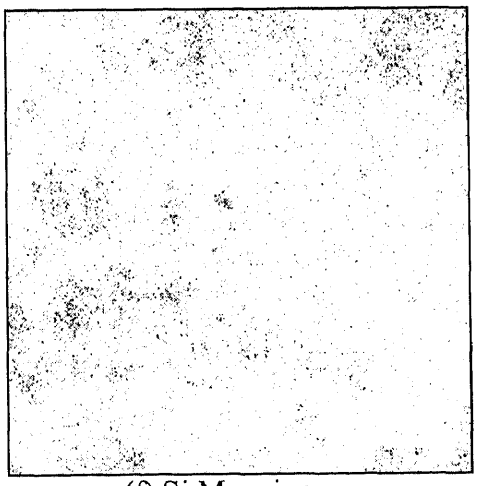

(f) Si Mapping

Figure 5.52 Elemental Mapping of Irregular Particle in Low NO_x Fly Ash (GPU2O)

The ground low NO_x fly ash was examined at high magnification (2150 and 4950) in order to observe the surface chemistry of broken sphere. The difference between these two conditions is the area that it projects to. The micrograph taken with higher magnification examines smaller area than the lower one. It can be seen from Table 5.11 that their chemical compositions are similar meaning that they are quite homogeneous.

Figure 5.53 presents the micrograph of ground low NO_x fly ashes at 4950 magnification and its element mapping. Again, the silicon and aluminum appear in the same area. It should be noted that they also appear on the surface of broken fragment. This means that the silicon and aluminum are found both outside and inside the fly ash particle. However, there are some particles covered with silicon only as shown in the center of silicon mapping. It could be quartz phase which cannot release the elements essential for the pozzolanic action of fly ash. Some area of the iron mapping shows the high intensity of pixel which suggests the present of particle made of iron. It is believed that this iron-rich particle wore of from the bowl and arm during grinding process.

Another set of element mapping of ground fly ash is shown in Figure 5.54. The present of silicon, aluminum, and iron in fly ash could be seen more clearly with the boundary of the fly ash area. It can be seen that the silicon and aluminum are found more inside the perimeter. The spot that has high intensity of silicon but no aluminum content is not found in this micrograph. The iron element is also found more inside the boundary. Some spots of high density of iron are found in small angular pieces. They could be the piece wearing of from arm and bowl or the broken piece from solid sphere.

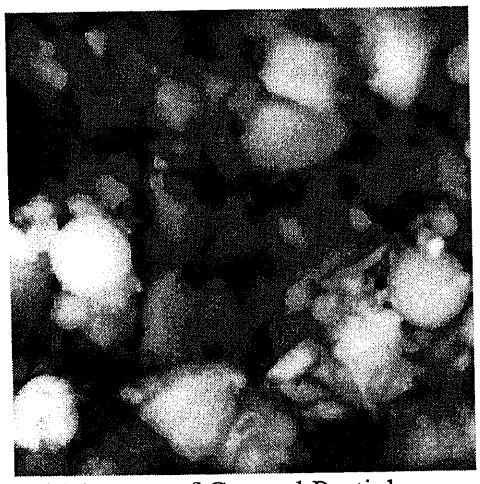

(a) Image of Ground Particles

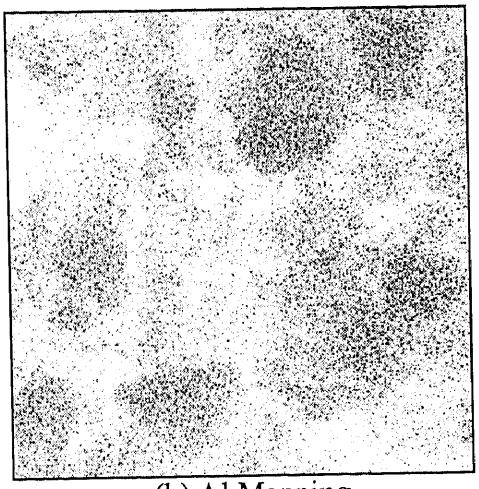

(b) Al Mapping

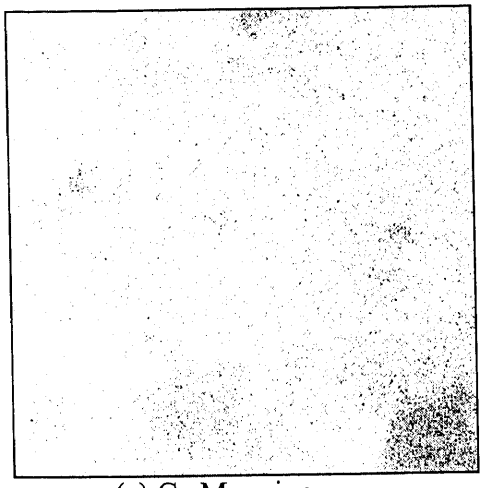

(c) Ca Mapping

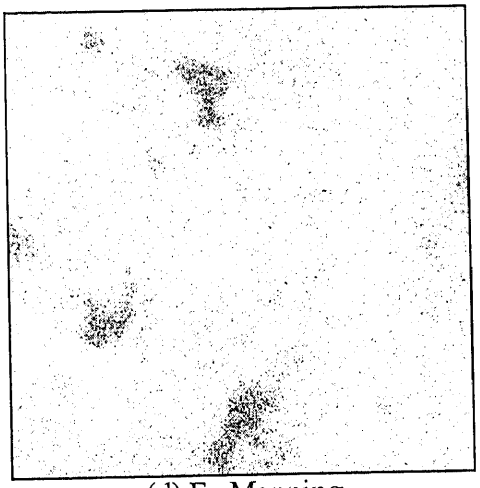

(d) Fe Mapping

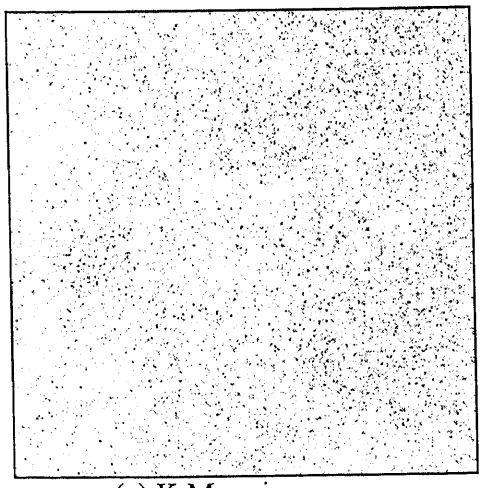

(e) K Mapping

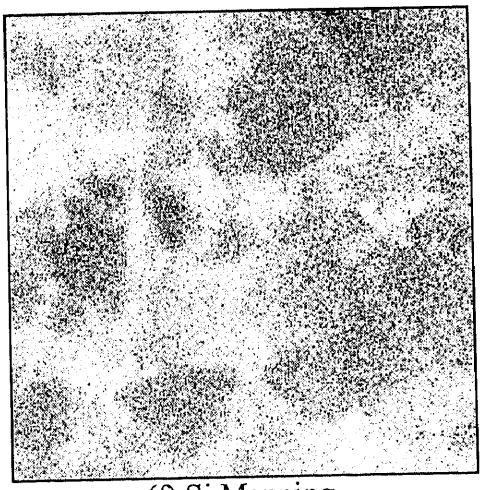

(f) Si Mapping

Figure 5.53 Elemental Mapping of Ground Particle in Low NO_x Fly Ash (GPU2G), (4950X)

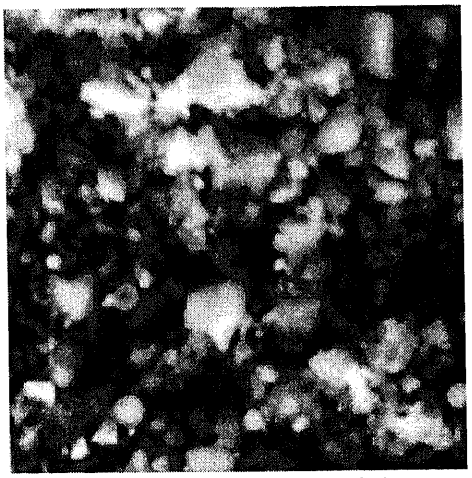

(a) Image of Ground Particles

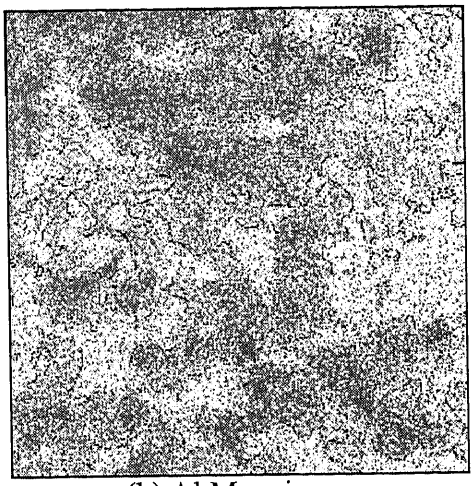

(b) Al Mapping

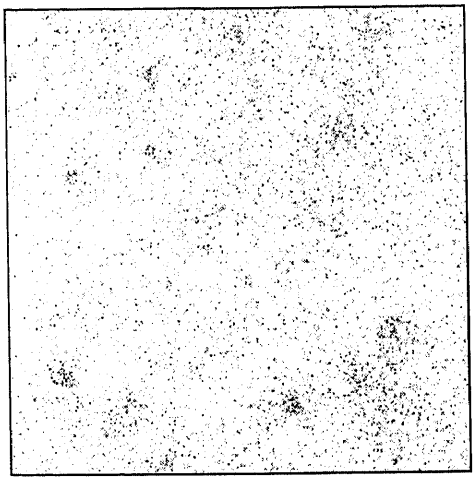

(c) Ca Mapping

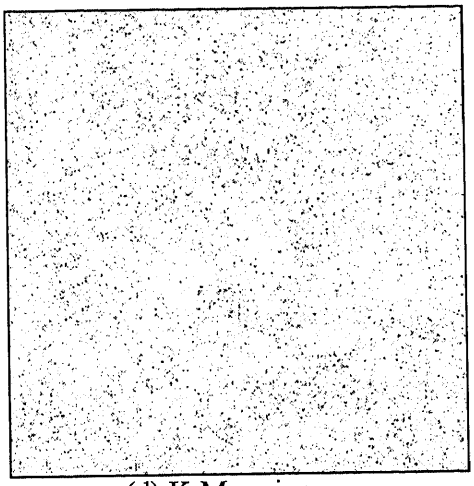

(d) K Mapping

(e) Fe Mapping

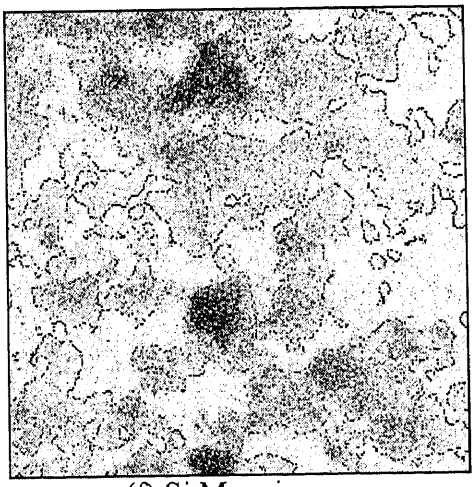

(f) Si Mapping

Figure 5.54 Elemental Mapping of Ground Particle in Low NO_x Fly Ash (GPU2G), (2150X)

5.5 Effect of Fly Ash on Hydration Process

5.5.1 Hydration Process of Fly Ash Paste Within 24 Hours

The effect of fly ash on hydration process was observed during the first 24 hours. The cement in the paste, composed of 60 to 65% of alite and 20 to 30 % of belite, reacts with water and forms calcium silicate hydrate (C-S-H gel) along with calcium hydroxide ($Ca(OH)_2$) as shown in the following equations (Lea, 1971).

$$2\ C_3S + 6\ H_2O \rightarrow C\text{-}S\text{-}H + 3\ Ca(OH)_2$$

$$2\ C_2S + 4\ H_2O \rightarrow C\text{-}S\text{-}H + Ca(OH)_2$$

Since the C-S-H gel is in a noncrystalline form, it cannot be detected directly from XRD pattern. The hydration process was observed by reduction of XRD peak intensities of the major crystalline components of portland cement such as C_3S and C_2S and the increased of the XRD peak intensity of $Ca(OH)_2$, so called CH. The C_3S has a sharp XRD line at 51.88 2-theta angle. The most intense diffraction peak for $Ca(OH)_2$ in the XRD occurs at 4.90 °A d-value or at 18.09 2-theta angle.

Figure 5.55 shows the phase changes during the first 24 hours of the hydration of cement paste. In the plain cement paste the $Ca(OH)_2$ formed after 5 hours of hydration and its peak intensity at 18.09 2-theta angle gradually increased over 24 hours. At the same time, the peak intensity of C_3S gradually decreased suggesting the consumption of C_3S during the curing process.

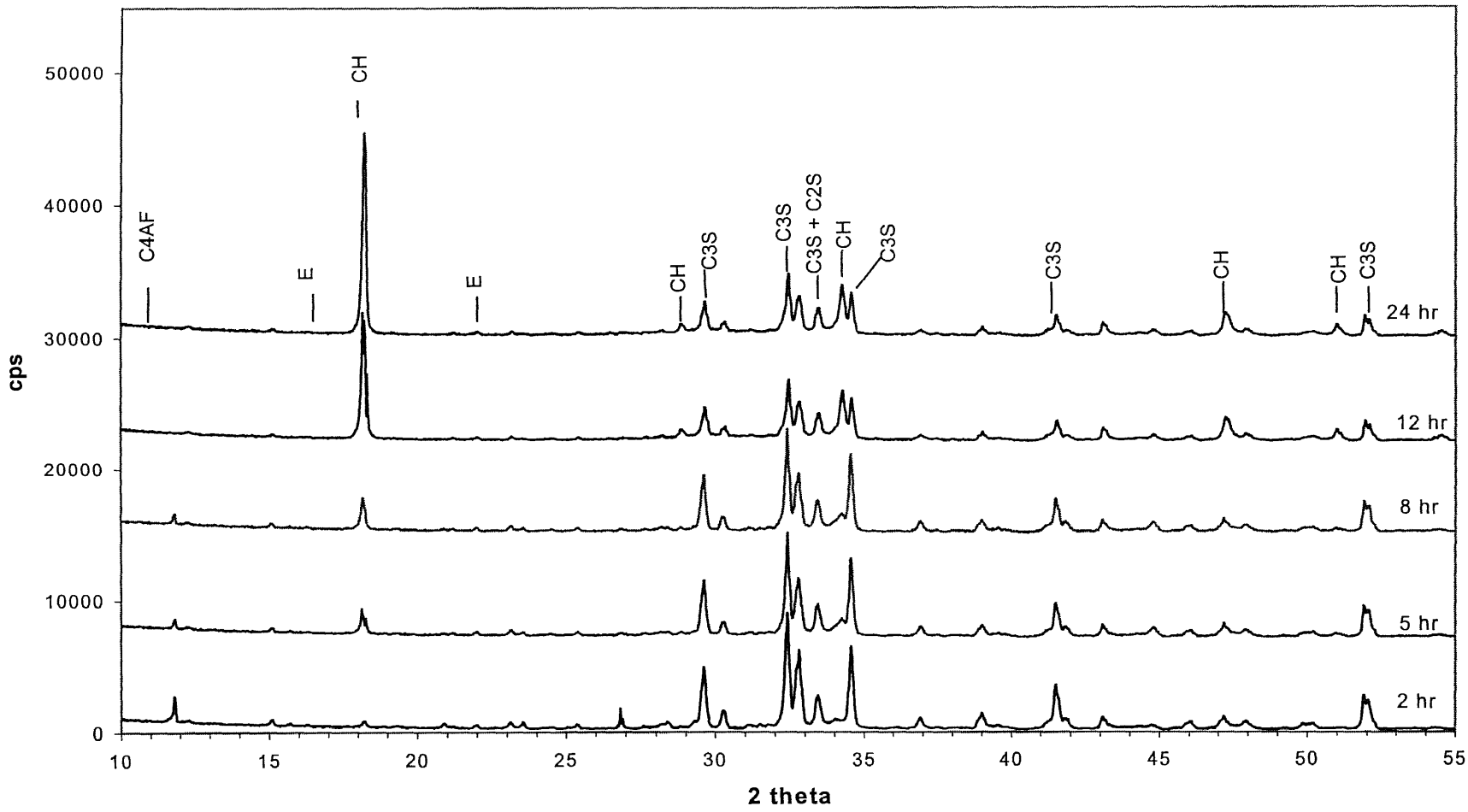

Figure 5.55 XRD Patterns of Cement Paste within 24 Hours

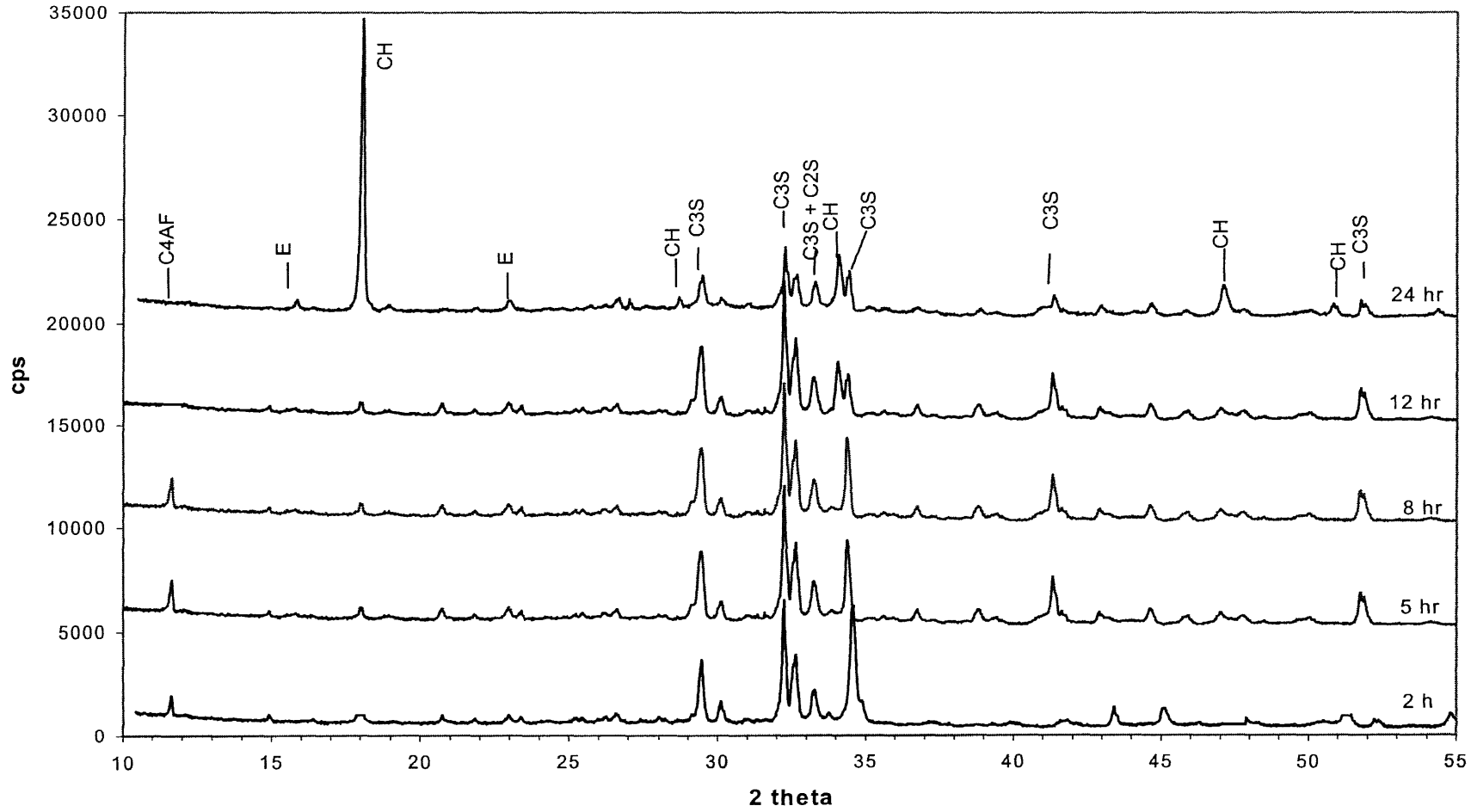

Figure 5.56 XRD Patterns of MO Fly Ash Paste within 24 Hours

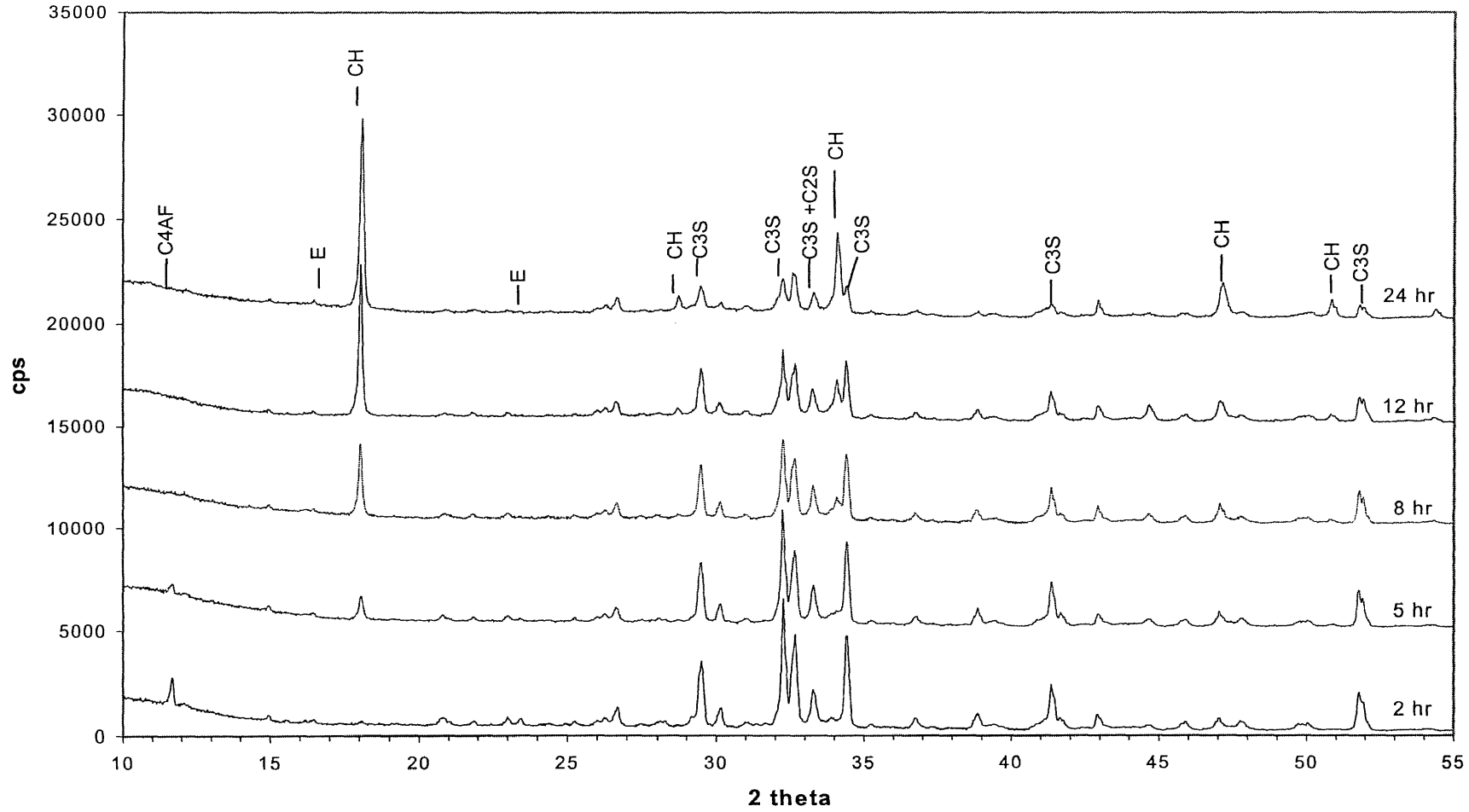

Figure 5.57 XRD Patterns of MOG1 Fly Ash Paste within 24 hours

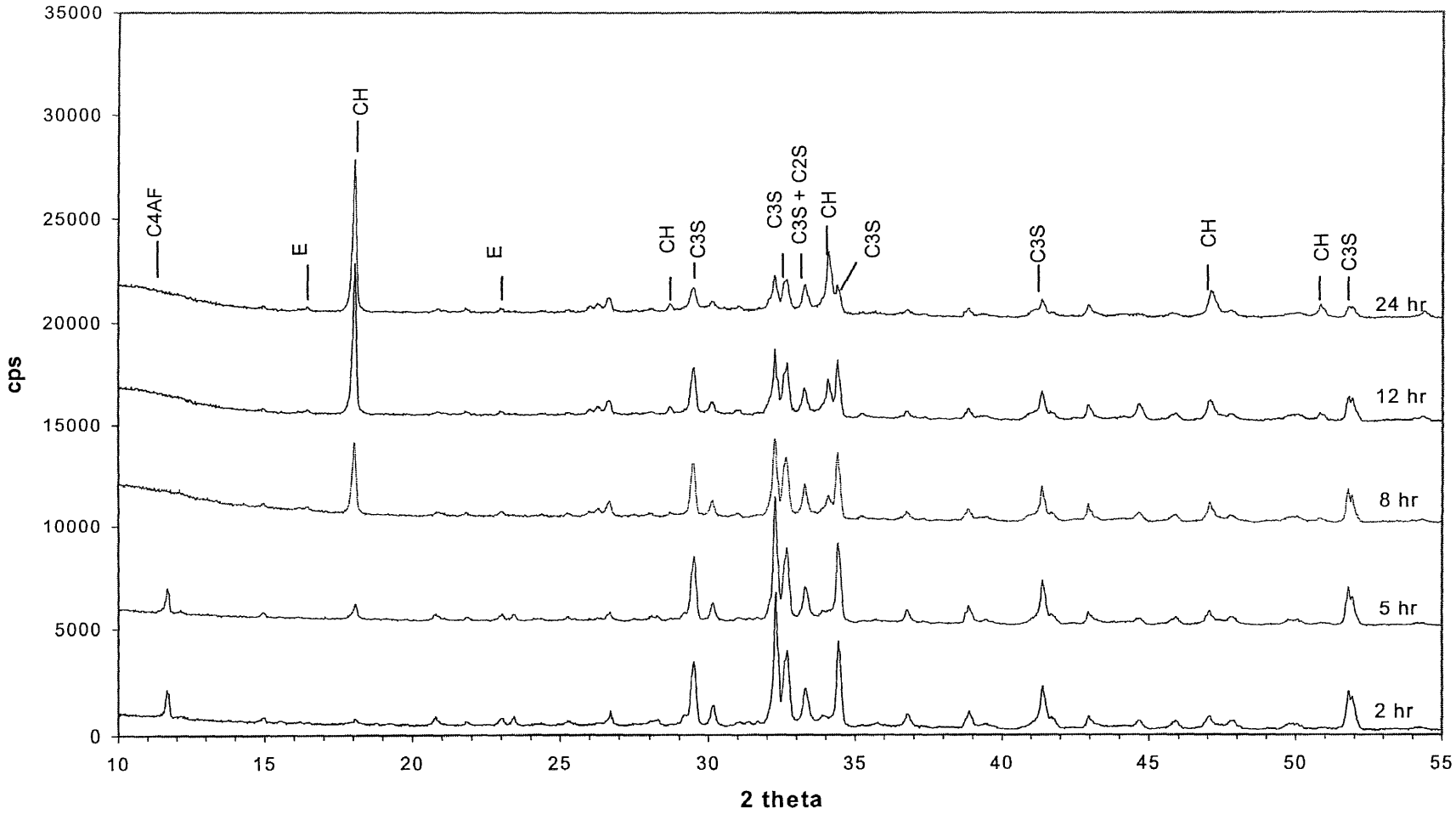

Figure 5.58 XRD Patterns of MOG2 Fly Ash Paste within 24 Hours

Figure 5.56, 5.57, and 5.58 show the phase change occuring in the first 24 hours of MO, MOG1, and MOG2 fly ash pastes, respectively. The $Ca(OH)_2$ formation of raw fly ash cement paste was hardly observable up to the 12th hour. Between the 12th and 24th hour, the content of $Ca(OH)_2$ in this sample rapidly increased. The C_3S peak intensity began to decrease at the same time as the formation of $Ca(OH)_2$ started. The This suggests that the hydration process with raw feed fly ash has a longer dormant period than that of the control or ground fly ash mixes. However, the longer delay in hydration process did not occur in the pastes containing ground fly ash (MOG1, MOG2). The formation of $Ca(OH)_2$ was detected in these ground fly ash pastes at the 5th hour and gradually increased, just like plain cement paste. All pastes show no sign of ettringite within 24 hours.

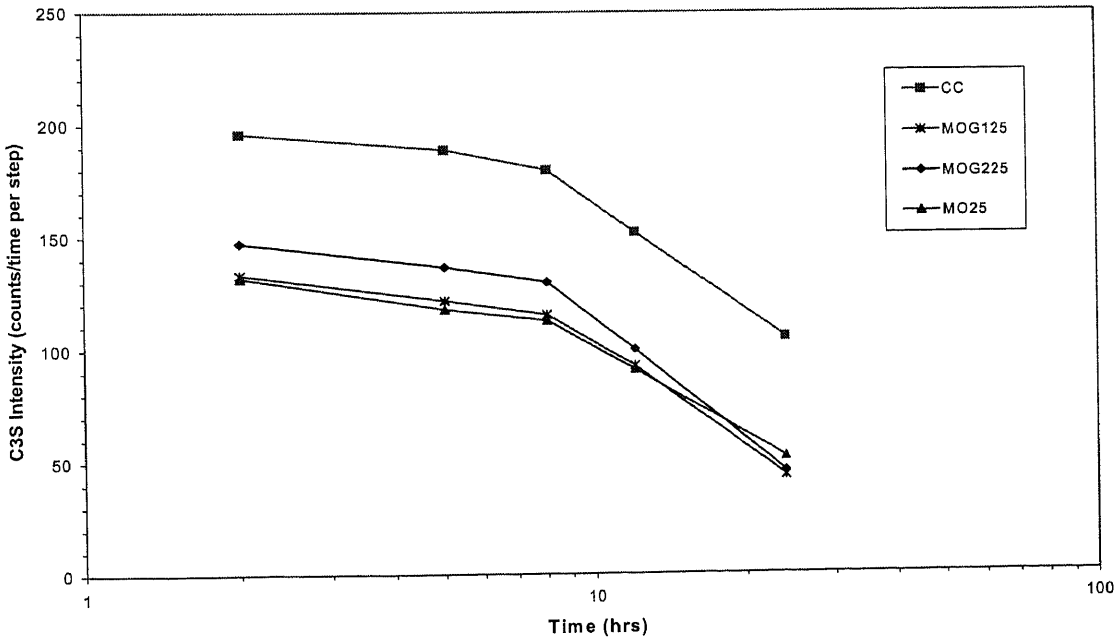

Figure 5.59 Relative C_3S Content versus Age of Different Fly Ash Pastes

The quantitative assessment of C_3S was made by measuring the area under the peak between from 51.3 to 52.1 2-theta angles. The amount of C_3S in the paste depended on the amount of cement in that paste. The initial intensity of C_3S in fly ash paste should be less than that of pure cement paste because the added fly ash dilutes the cement content. This is also the mechanism by which fly ash lowers the heat of hydration. In this study, the mineralogy of the paste during the first 2 hours was not examined because there is no other reaction, except the intensive hydrolysis of C_3S. According to Mindess (1981), during the hydrolysis stage, the calcium ion and hydroxide ions are rapidly released from the surface of C_3S grain. After their concentrations reach critical values, the hydration products, C-S-H gel and $Ca(OH)_2$, form rapidly at the expense of C_3S during the acceleration period.

The first measurement was done after two hours in order to observe the decreasing in C_3S content during the so called acceleration stage. It was found that from the 2nd to the 8th hour, the C_3S intensity of all pastes decreased slowly. Between 8th hour to 24th hour, the C_3S intensity of all pastes decreased rapidly. This result suggests that the dormant period of these pastes was extended to 8 hours after mixing and the acceleration period began after the 8th hour. The extended dormant period was not solely caused by fly ash since the plain cement paste also had its dormant period delay. It is suspected that the delay is caused by the chemical compounds of this cement. As seen from Figure 5.59, the intensity of C_3S in MOG225 paste was unexpectedly higher than those of other fly ash pastes during the dormant period. This could mean that of C_3S in this fly ash paste has low hydrolysis rate, hence, less consumption of C_3S during this period.

During the acceleration period when the C_3S is reacting vigorously, the fineness of fly ash had a strong influence on the consumption of C_3S. The ground fly ash pastes, MOG125 and MOG225, had a slightly higher rate of reduction of C_3S than MO25 pr plain cement pastes. The reduction rate of C_3S in MOG1 was higher than that of MOG2 and MO. This is explained by the fly ash dispersing the cement grain throughout cement paste, thus exposing cement to hydration.

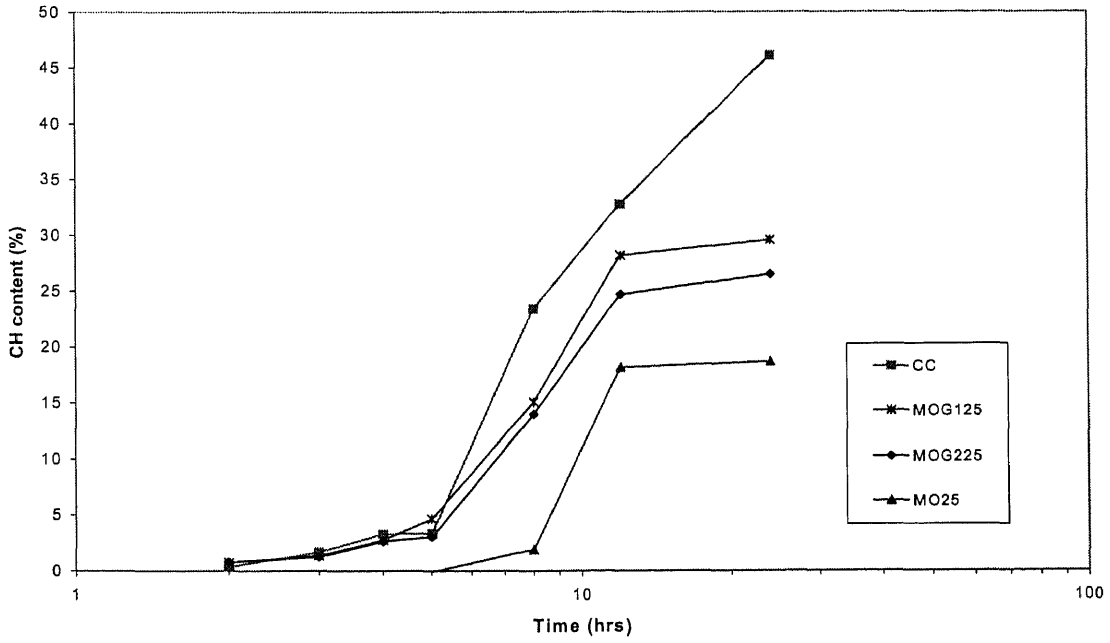

Figure 5.60 Relative Calcium Hydroxide Content at Early Age of Different Fly Ash Pastes

The increasing of $Ca(OH)_2$ in hydrating pastes can be seen more clearly in Figure 5.60. The $Ca(OH)_2$ contents of ground fly ash pastes and cement paste was low during the first 5 hours. The $Ca(OH)_2$ content of cement paste was slightly higher than that of ground fly ash pastes. After the 5th hour, the $Ca(OH)_2$ content of cement paste and ground fly ash pastes increased significantly but their C_3S contents have not been

diminished much. Due to the precipitation of $Ca(OH)_2$ and C-S-H, the levels of calcium ion and hydroxide ion in the pore solution were reduced. When their concentrations were low enough, the C_3S started to react. In case of raw fly ash paste (MO), the $Ca(OH)_2$ was undetectable during the first 5 hours. It was at the 8th hour that the $Ca(OH)_2$ content in MO fly ash paste started to increase at the same rate as that of cement paste. The $Ca(OH)_2$ content in fly ash pastes increased at the high rate for 14 hours. After of that it became stagnant while that of cement paste continued to increase.

At the end of this period, the paste that made of the finest fly ash in this study did not show a $Ca(OH)_2$ content as high as that of cement paste. This is because about 25% of cement was replaced by fly ash, which had not chemically reacted at this age. The fly ash particles physically disperse the cement grains making them available for hydration. It was observed that the presence of finer fly ashes enhance the hydration process, indicating by a higher $Ca(OH)_2$ content in the paste that used finer fly ash. This may be because the finer fly ash could deflocculate and liberate more cement grains to hydrate. The evidence of this assumption can be seen from the finer pore structure of fine fly ash paste at 1 day. This will be discussed further in chapter 5.7. This increased of $Ca(OH)_2$ content in fine fly ash pastes consequently increase the nucleation effect of fly ash because of the more hydration product precipitating on fly ash particles. Hence, the increasing nucleation effect would increase the strength at the later age.

5.5.2 Hydration Process of Fly Ash Paste at Later Age

Figure 5.61 shows the phase transformation in cement paste at 1, 3, 7, 13, and 28 days. The mineralogy of the pastes were observed at these intervals in order to observe the

phase changes corresponding to the strength of their mortars at the same time. In the plain cement paste the $Ca(OH)_2$ was still present in high intensity at all ages. The C_3S gradually declined suggesting the consumption of C_3S was in progress throughout the period of 28 days. The other hydration products, formed during this later age, was ferrite phase (C_4AF) and ettringite (C_4ASH). The C_4AF peak, from 11.8 to 12.2 2-theta angles had a low intensity at 3-day paste and it remained the same after that. At the same time, the ettringite peaks were also detected and its intensity decreased with time.

The XRD patterns in the later ages of MO25, MOG125, and MOG225 are shown in Figure 5.62, 5.63, and 5.64, respectively. Since these fly ash pastes were composed of 75% cement, their XRD patterns are very similar to that of cement. Thus, the cement hydration products are the dominant phases in the fly ash paste. Besides the hydration products and cement component, peaks of the crystalline phases of fly ash also appeared between 25 to 27 2-theta angles. It can be seen that the intensity of these crystalline phases did not changed during this period. This supports the hypothesis that the fly ash crystalline phase did not dissolve nor participate in the chemical reaction. The only phase that is involved in the pozzolanic reaction is the amorphous phase of the fly ash. Due to the low percentage of fly ash in the paste, it is not possible to comment on whether the broad halo of the amorphous phase has undergone any changes due to the pozzolanic activity. Moreover, the intensity of amorphous phase in the fly ash paste may not be the result of amorphous phase in fly ash alone. It might be an indication of the pozzolanic products forming in the paste.

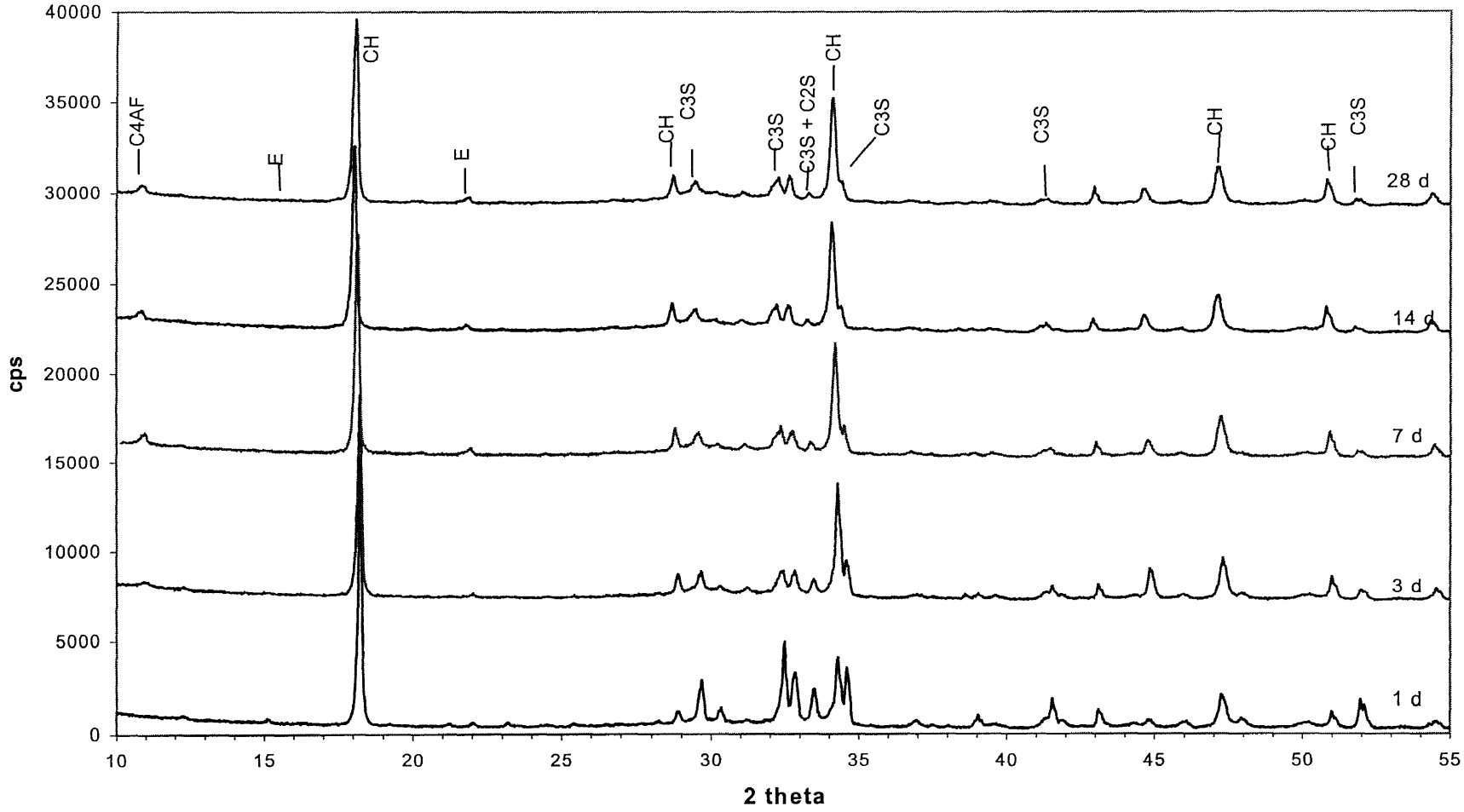

Figure 5.61 XRD Patterns of Cement Paste at Later Age

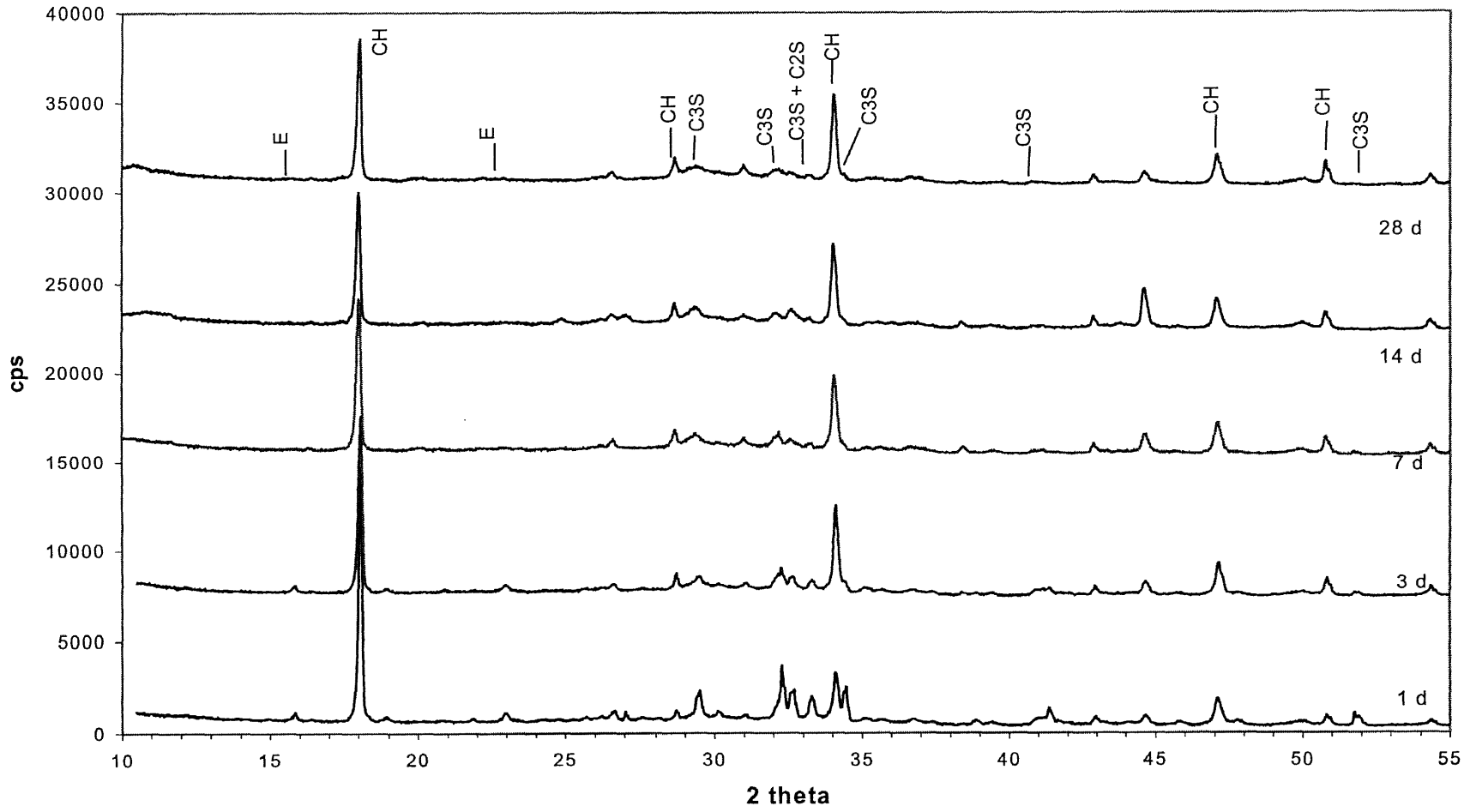

Figure 5.62 XRD Patterns of MO25 Fly Ash Paste at Later Age

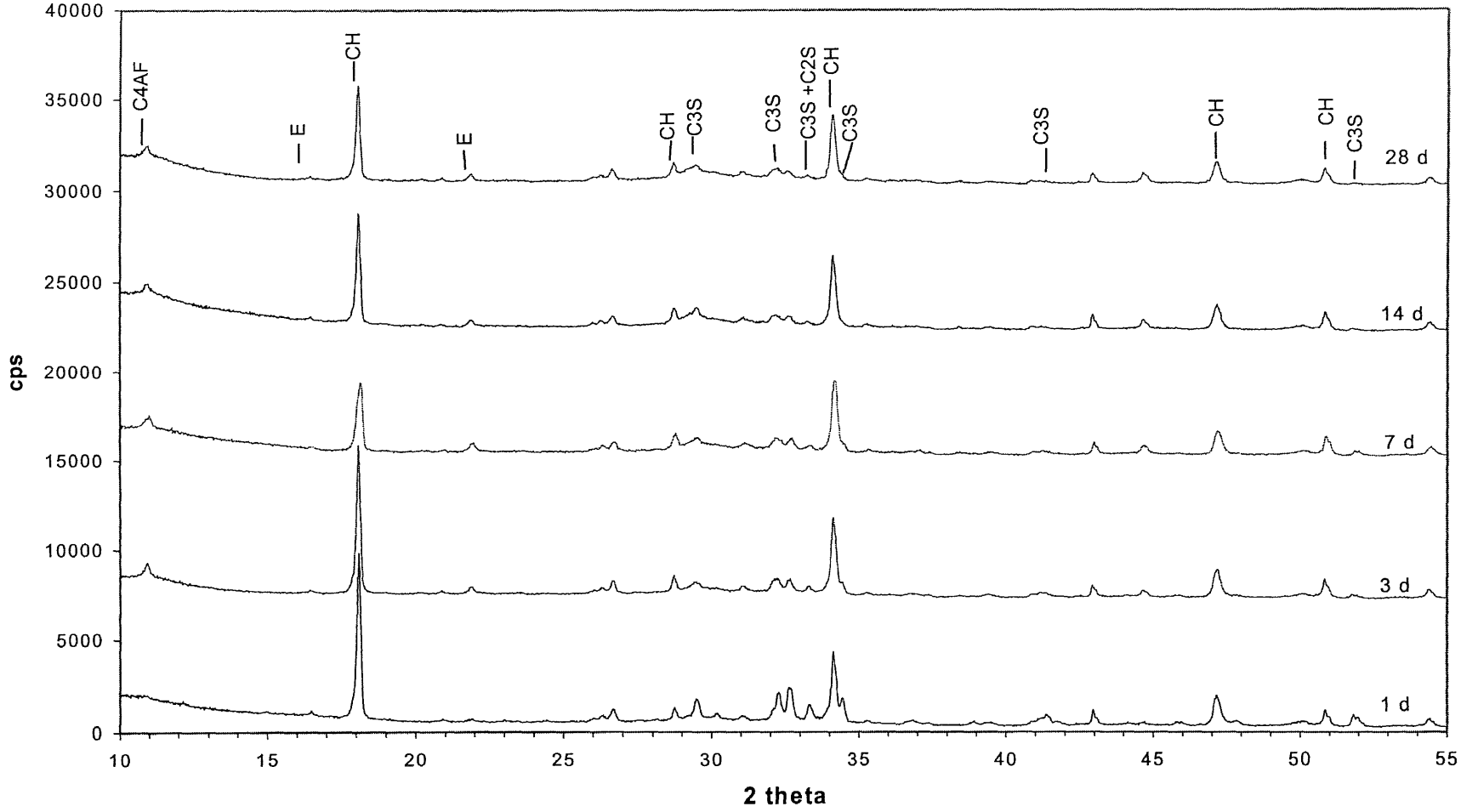

Figure 5.63 XRD Patterns of MOG125 Fly Ash Paste at Later Age

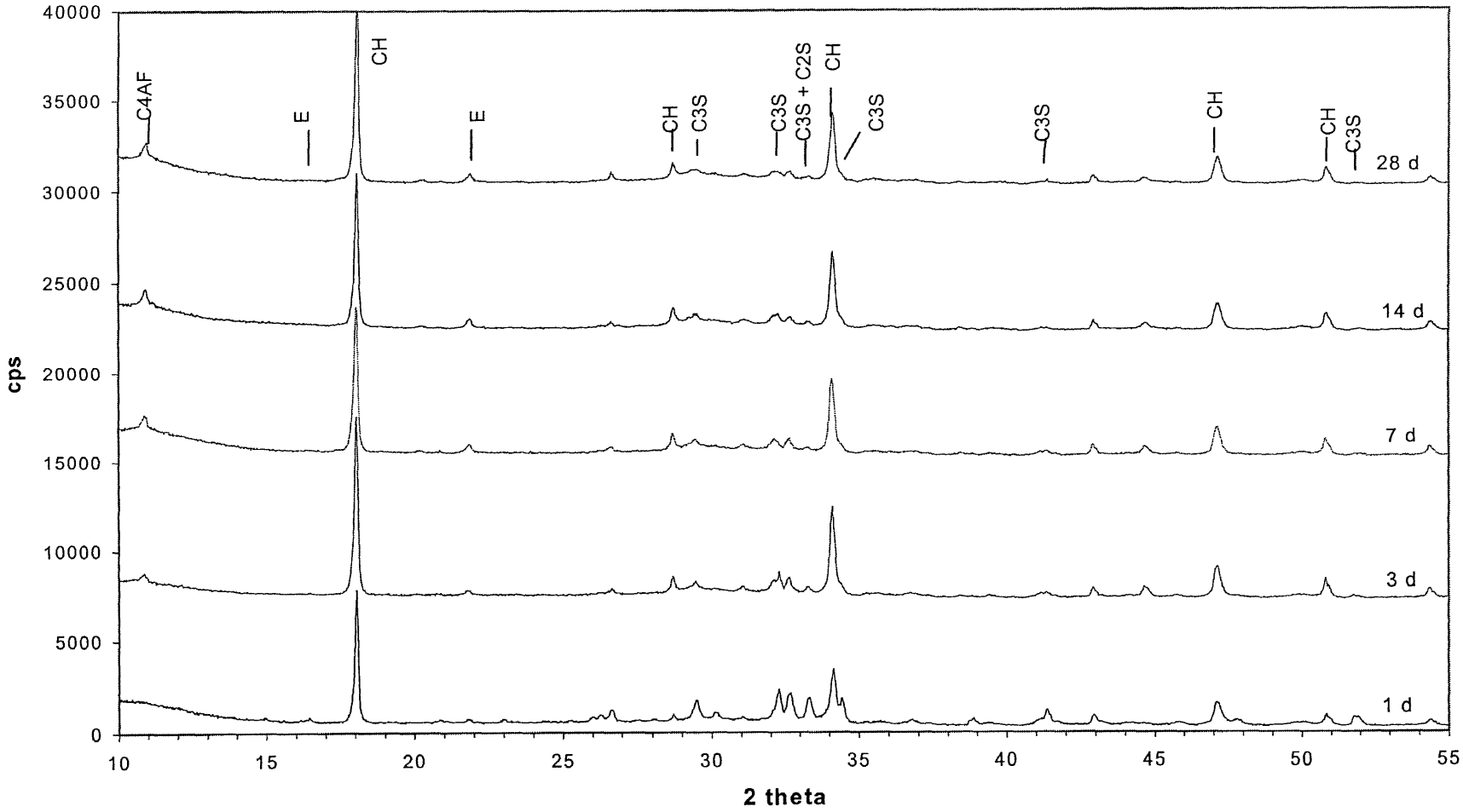

Figure 5.64 XRD Patterns of MOG225 Fly Ash Paste at Later Age

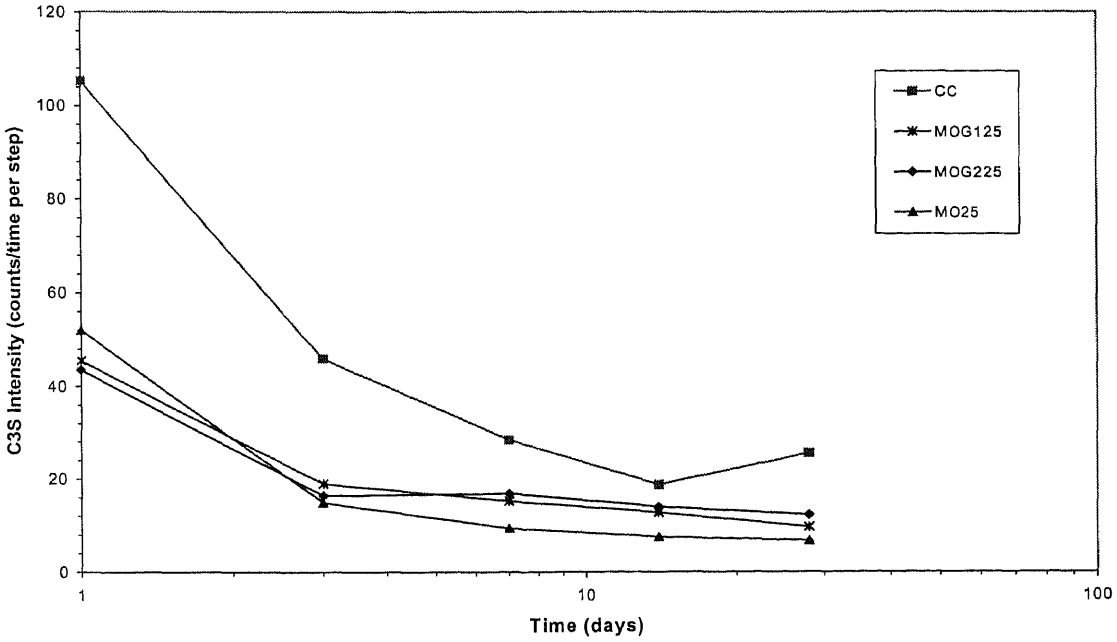

Figure 5.65 Relative C_3S Content at Later Age of Different Fly Ash Pastes

Up to 28 days of curing, the XRD pattern of fly ash pastes did not provide any direct confirmation of pozzolanic products such as C-S-H (II). This is because most of them are in a noncrystalline phase. In this study the changes in content of $Ca(OH)_2$ was used to indicate the change in hydration of cement and pozzolanic reaction fly ash paste.

Figure 5.65 shows that the C_3S intensities of cement dropped sharply during the first three days and continuing to decrease at a slower rate after the 3rd day. After 14 days, there is very little changed. The reduction of C_3S was consistent with the increasing strength gain measured by mortar cube from compression experiments. The change in C_3S intensity of fly ash pastes followed the same trend as that of cement paste. However, the rate of reduction was slower and it started to level off after the 3rd day. This result indicates that the cement hydration process in fly ash pastes completed earlier

than that of cement paste presumably because of the lower cement content resulting from replacement by fly ash.

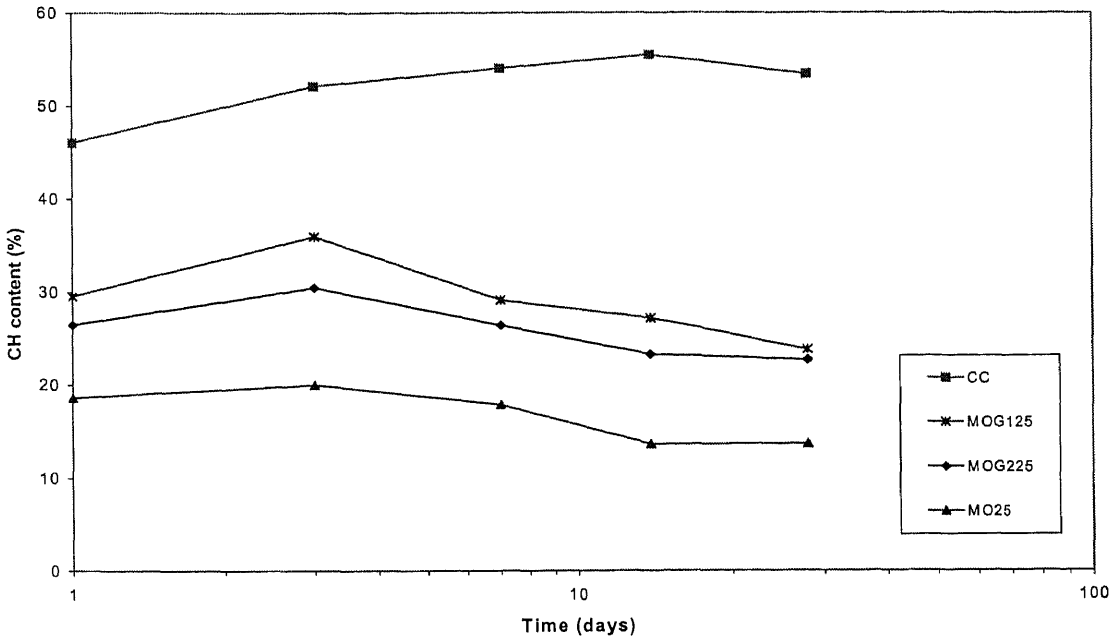

Figure 5.66 Relative Calcium Hydroxide Content at Later Age of Different Fly Ash Pastes

The $Ca(OH)_2$ content of all pastes after 1st day are shown in Figure 5.66. The $Ca(OH)_2$ of ash-containing pastes were lower than the cement paste. The cement paste curve showed an increase in $Ca(OH)_2$ content throughout the 28th day period. Whereas, the $Ca(OH)_2$ content of fly ash pastes starts to decline after three days. At the same time, the C_3S contents of fly ash paste decreased slightly meaning that cement hydration was taking place and the $Ca(OH)_2$ content should have increased. However, Figure 5.66 shows a decrease in the $Ca(OH)_2$ content. The $Ca(OH)_2$ formed was depleted by the pozzolanic reaction of the fly ash. The pozzolanic reaction is described by the following formula (Mindess, 1981).

$$Ca(OH)_2 + SiO_2 / Al_2O_3 + H_2O \rightarrow C\text{-}S\text{-}H\ (II)$$

Figure 5.66 also shows a comparison of the $Ca(OH)_2$ content of the pastes containing fly ashes with different fineness showed that their $Ca(OH)_2$ content consistently decreased after the 3rd day. This would suggest that the pozzolanic action of these fly ashes starts at a very early age regardless of their sizes. The pastes containing unprocessed fly ash also showed an indication of pozzolanic action at the 3rd day. It was found, however, that the fineness of fly ash had an effect on the reduction rate of the $Ca(OH)_2$. The $Ca(OH)_2$ content of MOG125 fly ash paste dropped more rapidly than those of coarse fly ash pastes (MOG225 and MO25). The reason is that the fine fly ash has a larger surface area to provide the silica and alumina compounds for pozzolanic activity. These compounds reacted and consumed $Ca(OH)_2$. The reduction of $Ca(OH)_2$ content in all fly ash pastes became subtle with age. This may be because the dissolution of essential reactant compounds from the fly ash and cement were hindered by the thickening layer of hydration products.

In summary, the XRD studies show that the fly ash pastes have different cement hydration rates described by the of C_3S consumption and $Ca(OH)_2$ formation rates. Over 24 hours, the fly ash paste has less hydration product than cement paste, which may be due to dilution effect of fly ash. The finer fly ash is found to generate more of hydration product. It is assumed that this is due to the dispersion effect of fly ash, fine fly ash particles dispersing cement grains to finer grains, hence, promoting the hydration reaction of cement. This could explain the higher strength at early age of the finest fly ash paste.

The hydration process of fly ash pastes show to imperceptible after the third day, whereas those of cement pastes were still increasing. There was a reduction of $Ca(OH)_2$ content in fly ash pastes after the third day. This consumption was likely to be due to the pozzolanic action of fly ash. To compare the pozzolanic actions among pastes with different fineness of fly ash, the $Ca(OH)_2$ consumption was used as an indicator of pozzolanic action. It is found that for all fly ash pastes the pozzolanic action started at ages as early as 3 days regardless of their fineness. As a result, their pozzolanic action could contribute the strength to the paste at early age as well. It is also found that the fineness of fly ash had an effect on the pozzolanic action rate. The paste containing finer fly ash showed higher pozzolanic activity rate than the paste containing coarse fly ash.

5.6 Microstructure Study of Processed Fly Ash in Cement Pastes

An extensive investigation of processed fly ash reactions was done by using Environmental Electro Scanning Microscope (ESEM). The changes in microstructure of ground fly ash paste (MOG1, MOG2, GPU2G1) and fine fractionated fly ash paste (M13F) were examined immediately after mixing from 1 to 3 days, 7 to 14 days, 28, and 260 days. The summary of properties of the hydration products of portland cement compounds are summarized in Table 5.12.

Table 5.12 Properties of Hydration Products of Portland Cement (Mindess, 1981)

Compound	Composition (Ca:Si:Al:S)	Crystallinity	Typical Crystal Dimensions in Pastes	Morphology in Pastes
C-S-H	-	Very poor	1x0.1 μm less than 0.01 μm	Spines; unresolved morphology low porosity striated material
Calcium Hydroxide (CH)	-	Very good	0.01 to 0.1 mm	Long slender prismatic needles
Ettringite	1:0.76:0.36:0.5	Good	10x0.5 μm	Thin needle

At the Beginning of the Hydration Process

The sample preparation for 5-minutes analysis was different from samples at older age since the paste was not hardened yet. To catch the instant picture of liquidated sample, the sample was hardened by freezing with liquid nitrogen. This is also in order to arrest the hydration reaction of the paste. Otherwise the microstructure may change by the intensive hydration process that occurs during the observation. Figure 5.67 (a) shows the micrograph of cement paste after five minutes of hydration. The elemental mapping is shown in Figure 5.68 with the elements appearing in black. Their microstructure in the

microstructure section showed that the fly ash particles in the paste were not covered with hydration products. The large prism-like structures, about 30 microns in size, were found in abundance. Their features resemble that of cement grain. The elemental mapping showed that this grain has calcium content higher than the other constituents. However its ratio of Ca:Si:Al:S did not correspond to that of cement which was obtained from XRF; 1:0.12:0.04:0.08 against the ratio of 1:0.33:0.15:0.04 for cement. This may be because this elemental analysis result is of the whole square area which the other compounds forming during this stage may exist. According to the morphology, the prism like structure could be considered a cement grain. Since they are found in abundance, implying that the cement particles had not dissolved completely at this age. This plentiful unreacted cement particles in the paste could cause the low strength at this early age.

Figure 5.67(b) shows the 5-minutes microstructure of fly ash cement paste using MOG1 fly ash at the same magnification as that of cement paste. There was no hydration product precipitating on to the fly ash particles as in aged fly ash paste. This confirms that the hydration was arrested by freezing with liquid nitrogen. The micrograph shows that there were fewer numbers of cement grains in fly ash paste as a result of dilution effect of fly ash. Moreover, the cement grain appears in smaller size. It is assumed that the presence of the fly ash particle, during mixing disperses the cement grains to finer grains. This mechanism will be discussed in the pore size distribution section. It can be seen from the micrograph of fly ash paste that the pores between these grains are occupied by small spheres of fly ash resulting in smaller pore size in fly ash paste.

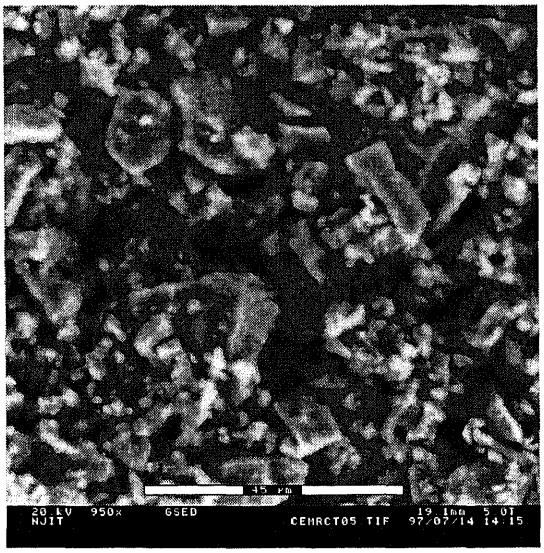

(a) Cement Paste (950x)

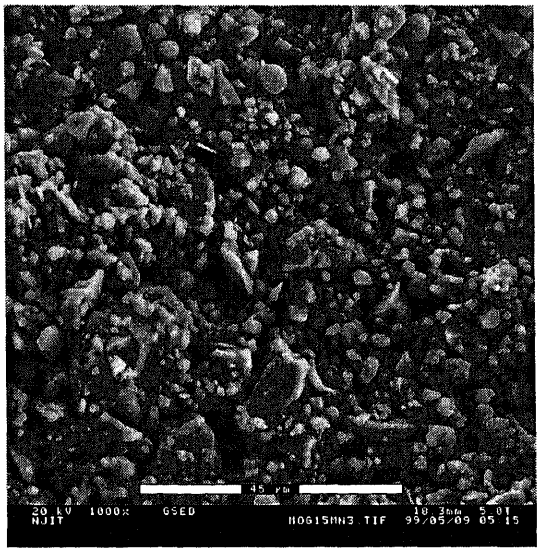

(b) MOG125 Paste (1000x)

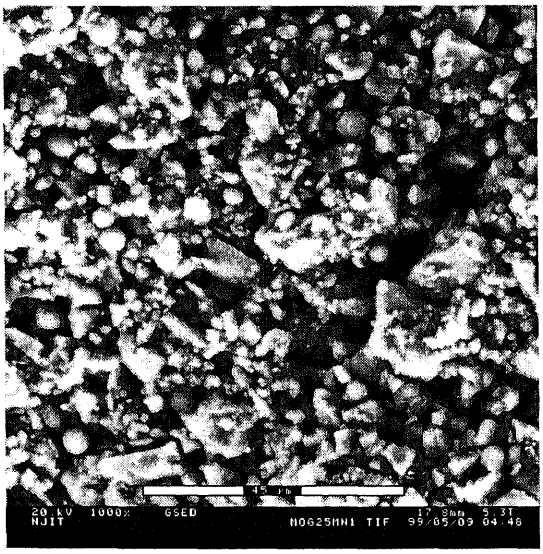

(c) MOG225 Paste (1000x)

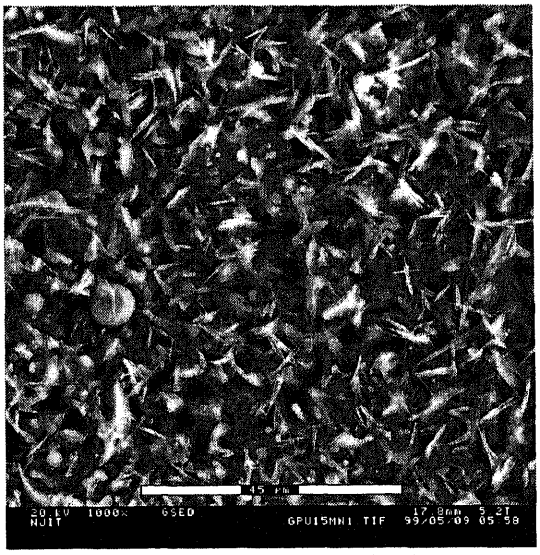

(d) GPU2G25 Paste (1000x)

Figure 5.67 Microstructure of Paste at 5 minutes (a) Cement Paste (950x), (b) MOG125 Paste (1000x), (c) MOG225 Paste (1000x), (d) GPU2G25 Paste (1000x)

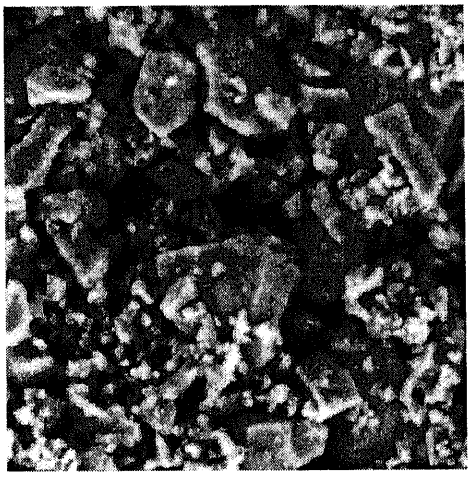

(a) Image of Cement Paste

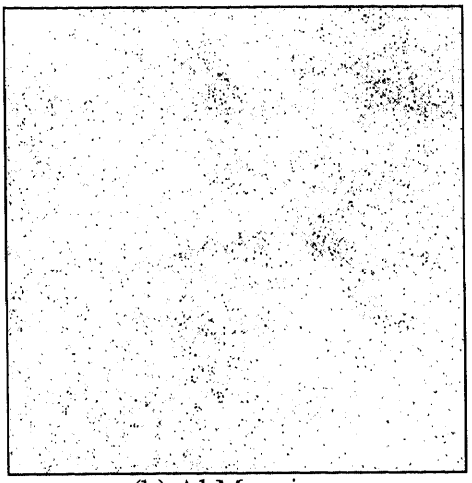

(b) Al Mapping

(c) Ca Mapping

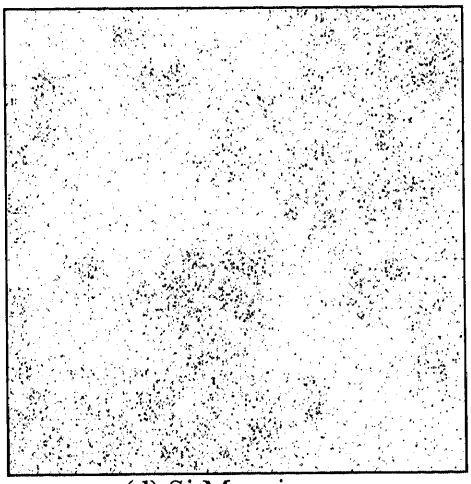

(d) Si Mapping

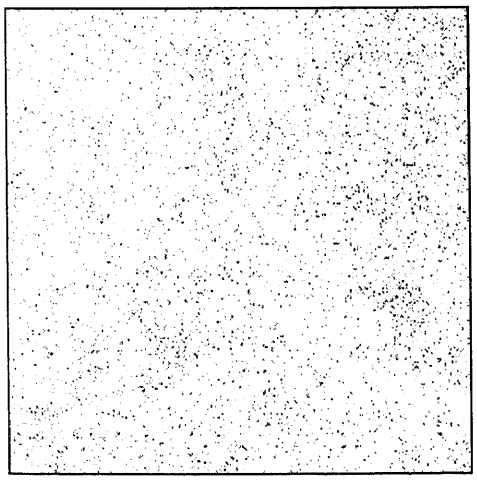

(e) K Mapping

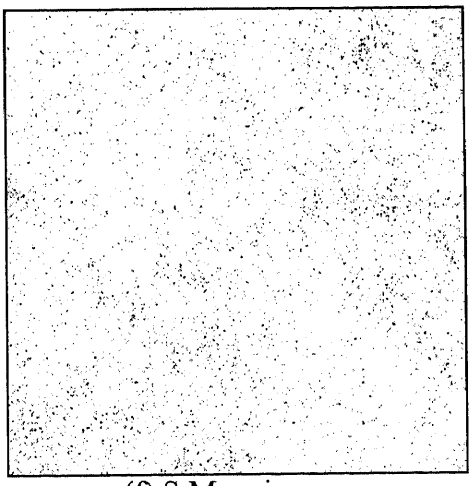

(f) S Mapping

Figure 5.68 Microstructure and Element Mapping of Cement Paste at 1 day (900x)

During the first 3 days

Figure 5.69(a), 5.69(b) and 5.69(c) show the microstructures of cement pastes at one day. Its paste is composed of irregular shape particles, which are supposed to be unreacted cement grains. These grains are smaller than in the earlier picture because their outer have undergone some of the hydration reaction. Within three days there were many needle-like particles widespreading among fuzzy particles covering the grains. The elemental analysis by Energy Dispersive X-ray indicates that these needle-like particles are ettringite, and the fuzzy particles are C-S-H gel.

Figure 5.70(a), 5.71(a), and 5.72(a) illustrate the low magnification microstructure of MOG125, MOG225, and GPU2G125, respectively. At this magnification, the overall structure, distribution of fly ash, crystals, grains, and pores of the paste can be observed. The MOG1 and MOG2 pastes are dense while that of GPU2G1 is porous. The number of pores between clusters of particles in GPU2G1 was evident which corresponds to its high porosity at this age. The big particle with crystal shape in GPU2G1 is assumed to be calcium hydroxide precipitating from the calcium-rich pore solution during sample preparation. The calcium hydroxide grains that normally result from the hydration reaction are small particles embedded among the clusters.

The fly ash appears as a single spherical particle and a cluster of spheres distributed around the paste. Angular particles of ground fly ash cannot be seen since its morphology is very close to that of other crystal structures. Close examination of all fly ash pastes reveal that the fly ash particles act as sites for growth and deposition of hydration products. Most small spheres were covered with slightly fibrous particles. The morphology of this feature closely resembles to the morphology of C-S-H gel. Aimin

(1994) has suggested that the fibrous features on the fly ash particles at early stages of hydration is C-S-H gel. However, at this stage the fibrous layer appeared to be very thin. Its thickness was less than 1 μm. A few needle-like structures were also observable but fewer than in normal cement paste. The EDS analysis showed that there was a significant amount of Si in these needles, with Ca:Si:Al:S = 1:0.86:0.44:0.13. According to the chemical composition of hydration products in Table 5.12, this ratio is close to that of the ettringite composition, except for the Sulfur content.

The nucleation stage of fly ash mortars begins immediately after mixing and continues as long as there is product precipitating on the surface. This concept was proposed by Cao, Ho and Guirguis (1990), and Gopalan (1993). They suggested that strength contribution of fly ash mortar up to 28 days can be attributed to this nucleation factor and the strength after 28 days can be attributed to pozzolanic action of fly ash. However, they did not investigate the nucleation process in microscopic scale, which was done in this study.

As a result of the dispersion and nucleation phenomena, the distance between adjacent grains and the porosity of the paste could be lowered, which indirectly increases its strength of the cement paste. Nonetheless, at this age, the precipitation rate of hydration product is slow and large gaps between grains are observed. Noticeably, 1-2 μm gaps are present between particles. The presence of large numbers of these small pores has an adverse effect on its strength because they lower the density of the paste.

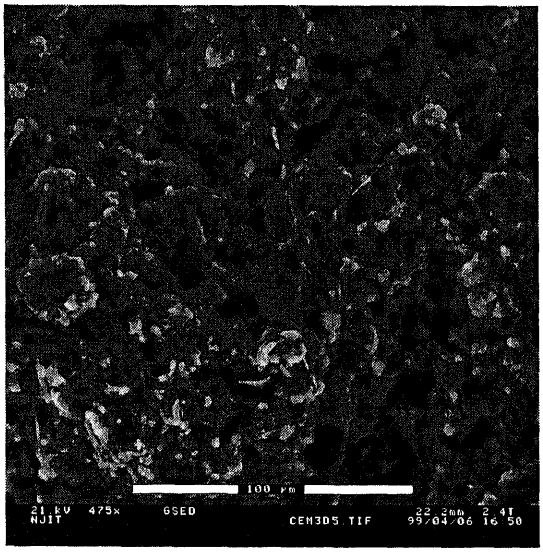

(a) 475x

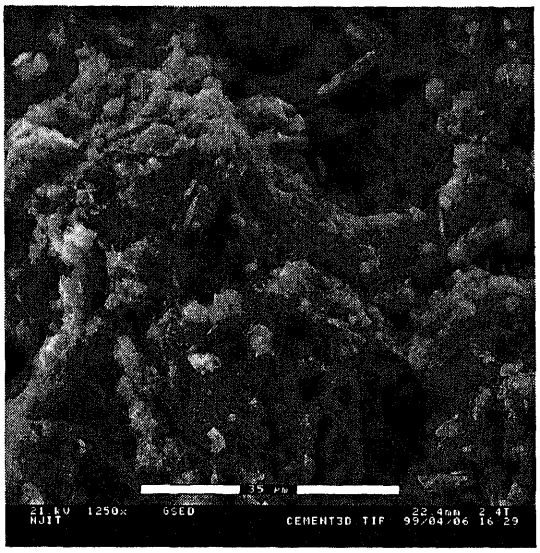

(b) 1250x

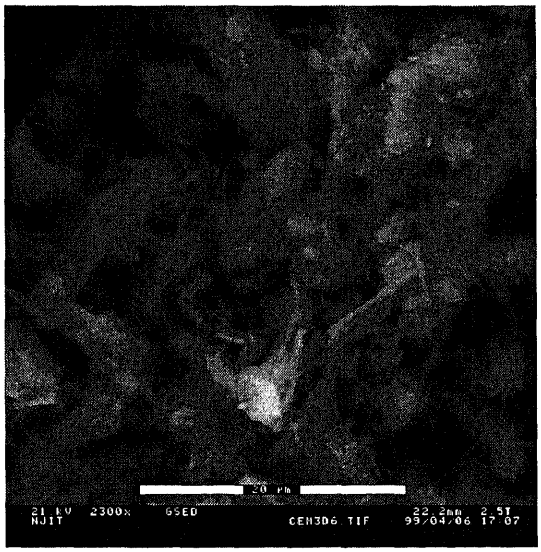

(c) 2300x

Figure 5.69 Microstructure of Cement Paste at 1 day, (a) 475x, (b) 1250x, (c) 2300x

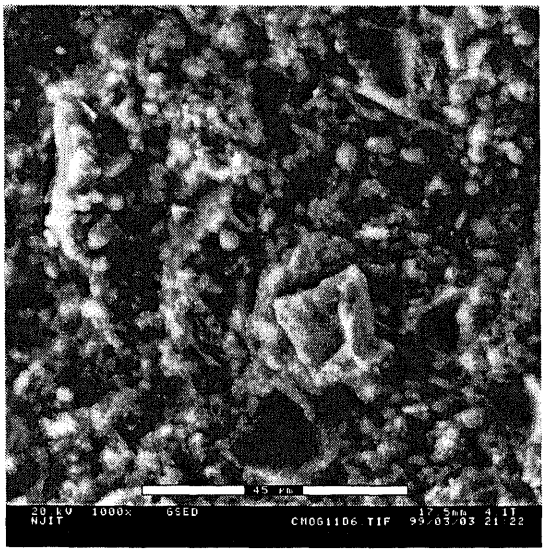

(a) MOG125 at 1 day, 1000x

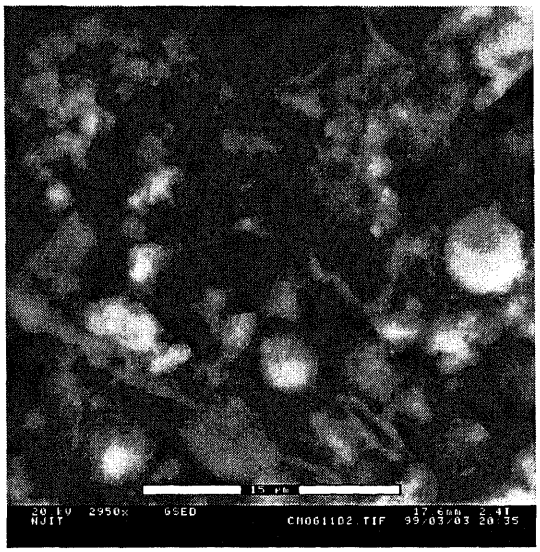

(b) MOG125 at 1 day, 1450x

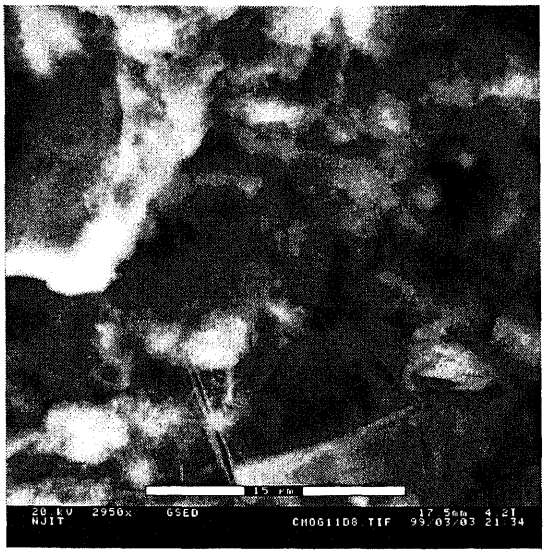

(c) MOG125 at 1 day, 2950x

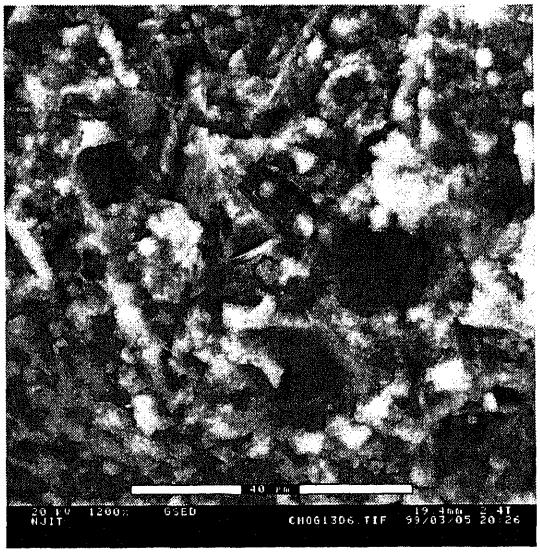

(d) MOG125 at 3 days, 1200x

Figure 5.70 Microstructure of Fly Ash Paste at 1-3 day, (a) MOG125 at 1 day, 1000x, (b) MOG125 at 1 day, 1450x, (c) MOG125 at 1 day, 2950x, (d) MOG125 at 3 day, 1200x

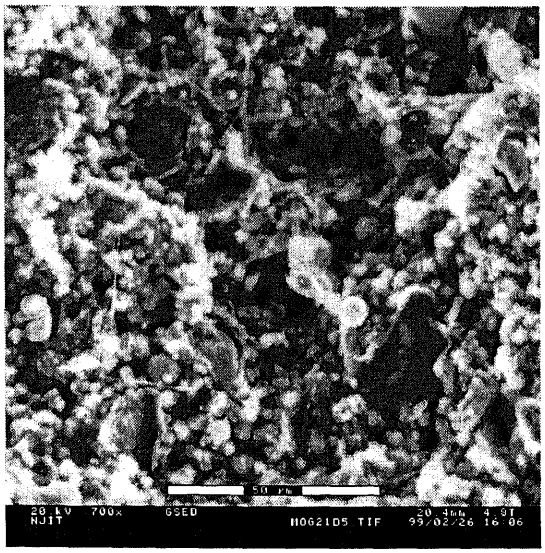

(a) MOG225 at 1 day, 700x

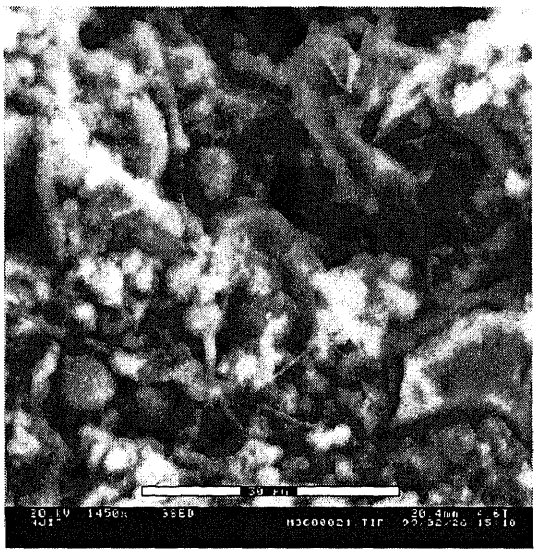

(b) MOG225 at 1 day, 1450x

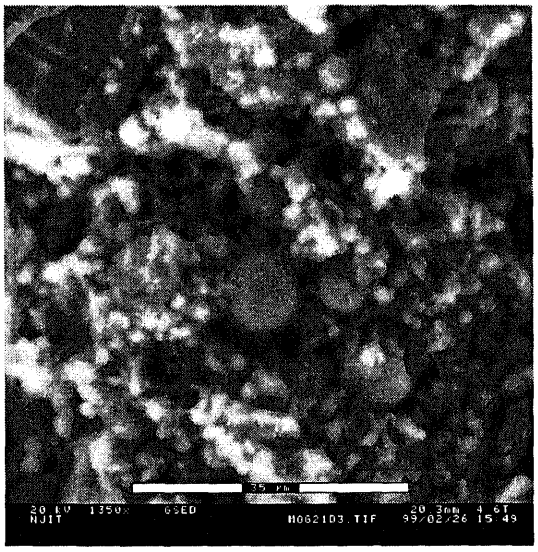

(c) MOG225 at 1 day, 1350x

Figure 5.71 Microstructure of Fly Ash Paste at 1-3 day, (a) MOG225 at 1 day, 700x, (b) MOG225 at 1 day, 1450x, (c) MOG225 at 1 day, 1350x

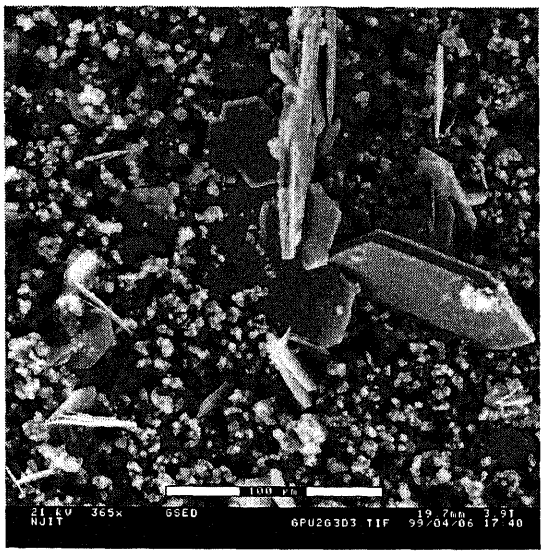

(a) GPU2G125 at 1 day, 365x

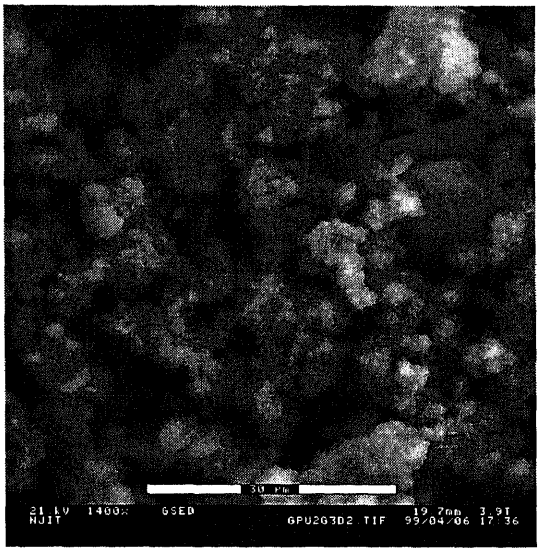

(b) GPU2G125 at 3 day, 1400x

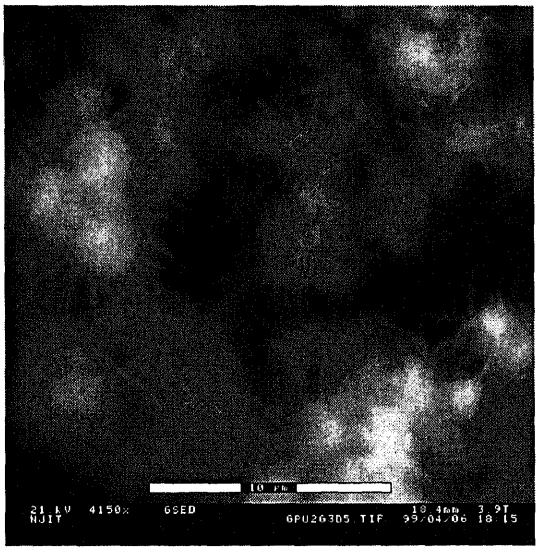

(c) GPU2G125 at 3 day, 4150x

Figure 5.72 Microstructure of Fly Ash Paste at 1-3 day (a) GPU2G125 at 1 day,365x ; (b) GPU2G125 at 3 day, 1400x; (c) GPU2G125 at 3 day, 4150x

7-14 days

Between 7 to 14 days, the microstructure of cement paste do not change from that of the 3-day paste much. However, their strength increases significantly during this period. This could be a result of the interconnection between the hydration products on fly ash.

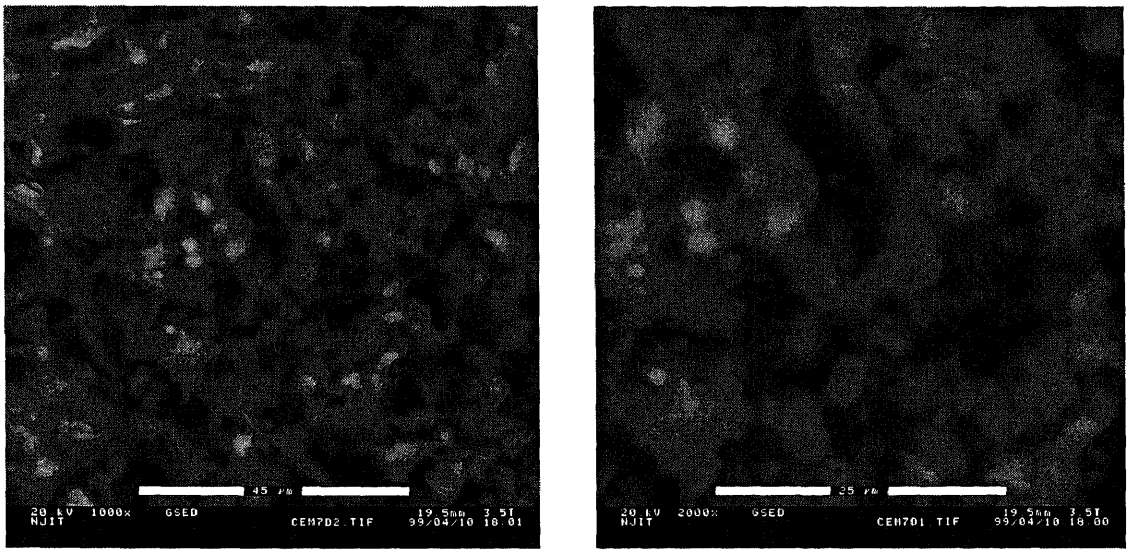

(a) 1000x (b) 2000x

Figure 5.73 Microstructure of Cement Paste at 7 day: (a) 1000x, (b) 2000x

The ground fly ash paste became denser than the younger paste, as seen from the microstructure, because of the formation of ettringite and acicular features (C-S-H gel) on the surface of fly ash. The breaking down of the glass structure of fly ash is probably hindered by this precipitating layer (Fraay, 1989). This layer also obstruct the pozzolanic activity of ground fly ash. To observe the pozzolanic action of fly ash, one may either examine the formation of its products or the deterioration of its source, fly ash. Unfortunately, the pozzolanic product, C-S-H type II, has similar morphology to that of C-S-H type I from the cement hydration, therefore the pozzolanic product cannot be distinguished by its morphology. The alternative method is to observe the damage on the surface of the fly ash. Since most of fly ash particles were covered by the hydration product, so it is always not possible to observe the fly ash surface. However, some fly ash particles in 14-day paste of MOG2 were not covered with layers. There is no

indication of etching on their surface, which means that the pozzolanic reaction of this particle has not occurred. Nonetheless, the pozzolanic action of other fly ash particles, which were obscured, might be in progress but could not be observed. At this point, the pozzolanic action of the pastes at this age could not be confirmed by their microstructure.

With or without the pozzolanic action, the compression tests showed the rate of strength was still increasing while that of normal cement mortar had slowed by this time. The process that accounts for the difference is the nucleation effect of fly ash, which continually reduces the pore size of the paste from the beginning of the reaction.

As seen from micrograph, Figure 5.74, the layer covering the fly ash spheres became complex since the hydration product continuously precipitates. The hydrated grains from nearby structures interconnected with each other reducing the gaps or pores between the grains in fly ash pastes. This phenomenon explains the higher early strength in mortars using finer fly ash. In pastes with finer fly ash, there are more particles able to act as a nucleus for hydration product than in pastes with coarse fly ash. The higher the number of nucleus, the higher the nucleation effect and the denser the paste is. However, this distribution of fly ash particles was not quantitatively analyzed in this study because crushed particles could not be differentiated because they have feature similar to hydration products. The conclusion drawn from this is that the higher strength at early age in ground fly ash paste is caused by the nucleation effect.

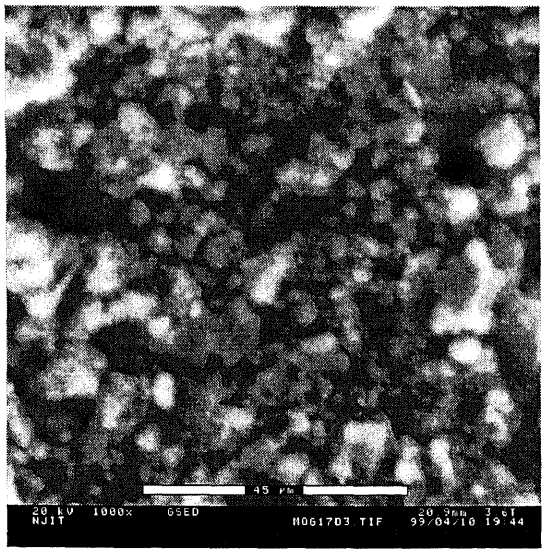

(a) MOG125 at 7 day, 1000x

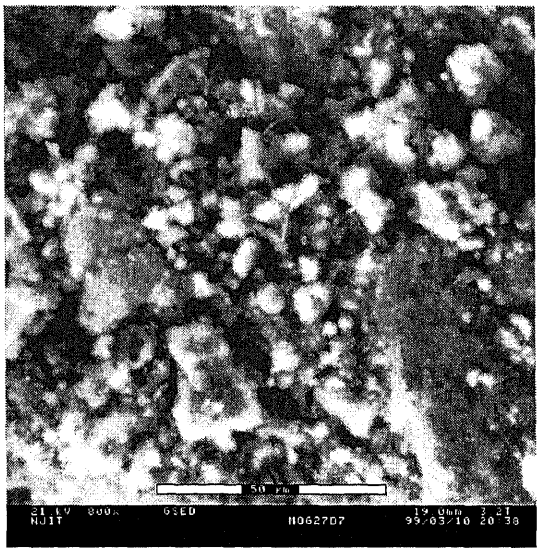

(b) MOG225 at 7 days, 800x

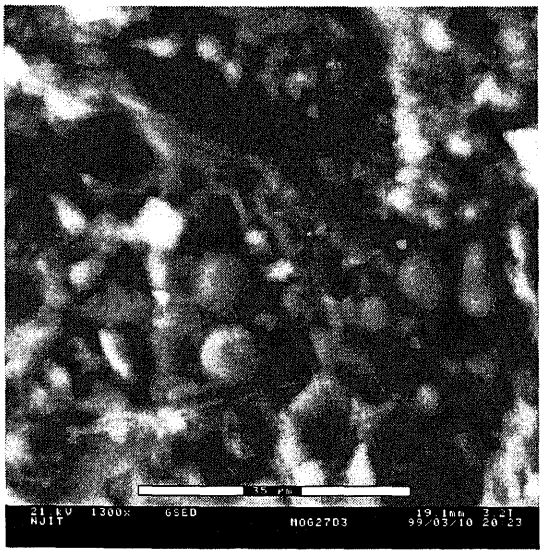

(c) MOG225 at 7 days, 1300x

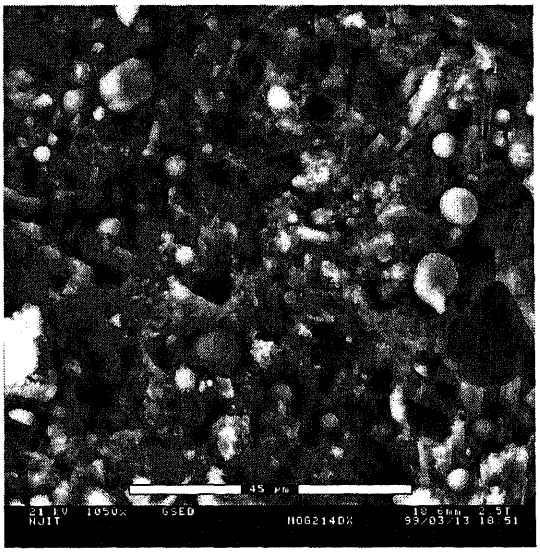

(d) MOG225 at 14 days, 1050x

Figure 5.74 Microstructure of Fly Ash Paste at 7-14 days, (a) MOG125 at 7 day, 1000x; (b) MOG225 at 7 days, 800x; (c) MOG225 at 7 days, 1300x; (d) MOG225 at 14 days, 1050x

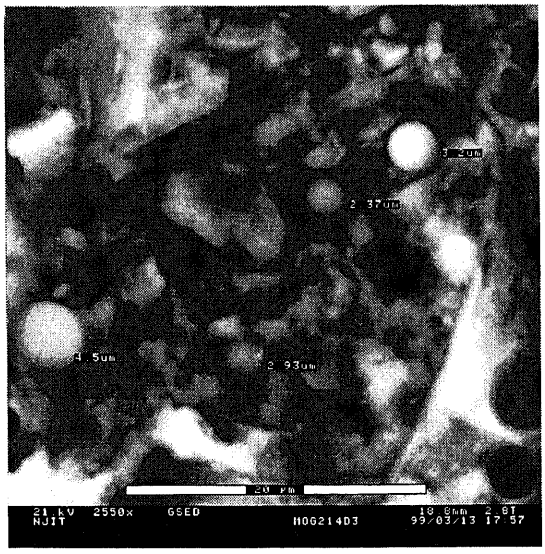

(a) MOG225 at 14 days, 2550x

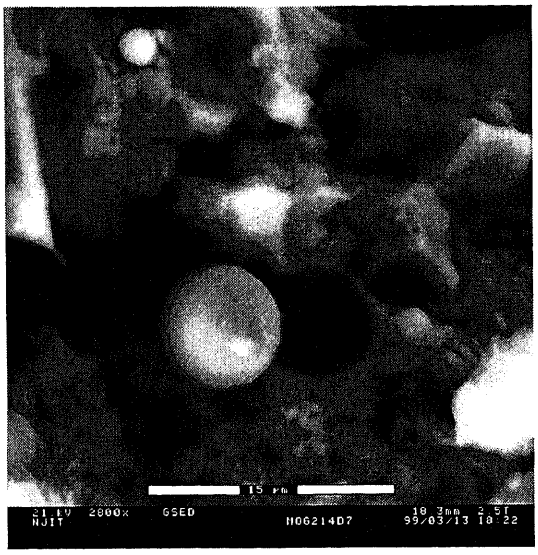

(b) MOG225 at 14 days, 2800x

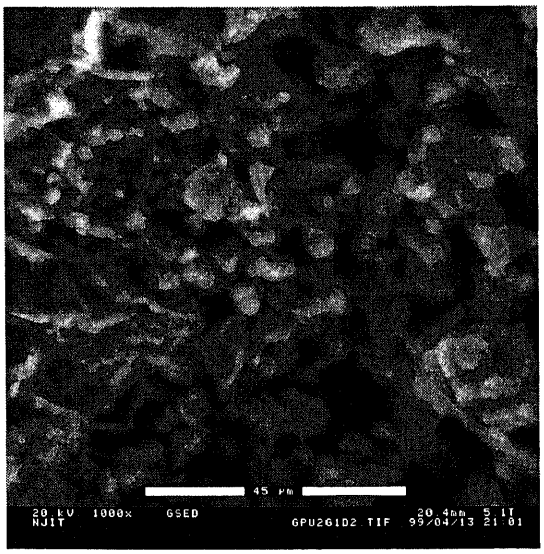

(c) GPU2G125 at 7 days, 2150x

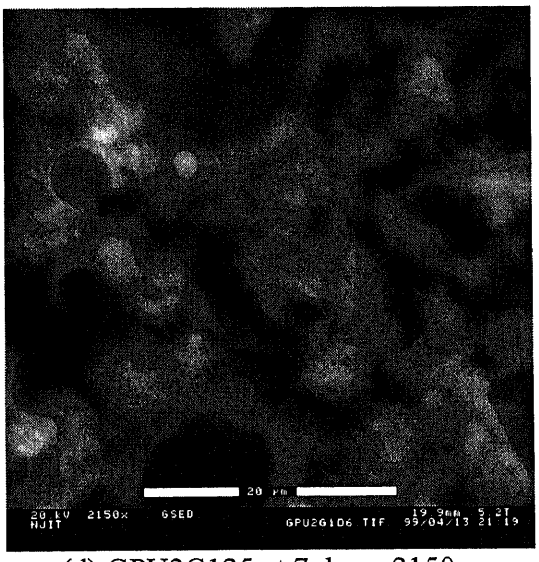

(d) GPU2G125 at 7 days, 2150x

Figure 5.75 Microstructure of Fly Ash Paste at 7-14 days, (a) MOG225 at 14 days, 550x; (b) MOG225 at 14 days, 2800x; (c) GPU2G125 at 7 days, 2150x; (d) GPU2G125 at 7 days, 2150x

28 days and beyond

Figure 5.76(a), 5.76(b) show the microstructure of cement paste at 28 days. By 28 days, the number of angular portlandite crystals ($Ca(OH)_2$) in cement paste increases significantly. At the same time, the more developed form of C-S-H gel is also present in the pore space. However, the ettringite is still as long slender structure.

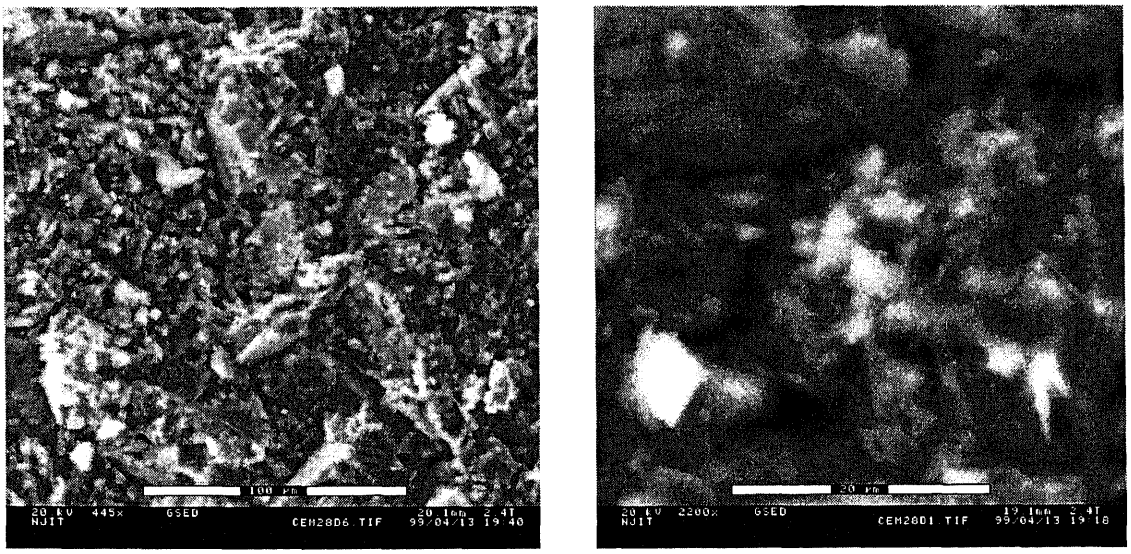

(a) 445x (b) 2200x

Figure 5.76 Microstructure of Cement Paste at 28 days, (a) 445x, (b) 2200x

At this age, the microstructure of ground fly ash paste appears further denser and hydration products are well developed (Figure 5.77(b), 5.78(a), 5.79(a), and 5.80). The amount of angular portlandite ($Ca(OH)_2$ in all ground fly ash pastes increases significantly which was also noticeable in the XRD pattern of the paste. Also present are interparticulate voids have yet to be filled by growing hydration products. This observation suggests that the paste is capable of becoming denser and gaining yet more strength. The pozzolanic product from fly ash itself predominantly fills up those gaps.

In the fly ash pastes, fly ash particles were observed in three forms: particles with damaged surface, particles with smooth surface, and particles with a covering layer. It appears that some fly ash particles have signs of etching on their surface, indicating that they are participating in the pozzolanic action (Figure 5.77(a)). These particles were about 10 microns in size. The remaining structure was a mullite sphere, as reported by Aimin (1994). This strongly suggests that the glass phase on fly ash surface has dissolved out and the crystalline phase, which is mullite in this case, remains intact. The reason why it was damaged is that it was in a high pH environment. However, observing that most of the fly ash particles were not covered with a layer of hydration product, and the surface was still smooth means that they were still unreacted (Figure 5.77(c) and 5.77(d)). Some of them are smaller than 5 microns. This suggests that the finer fly ash does not always lead to higher pozzolanic activity. Other factors may govern the pozzolanic activity of fly ash instead. Another features are the particles, which have a hydration layer covering on their surface. The morphological change on surface of these particles could not be seen. The pozzolanic action may or may not have occurred on its surface. According to the observation reported by other researchers (Cao, Ho, and Guirguis (1990), Aimin (1994), and Fraay (1989)), the pozzolanic action occurs on the inner shell of fly ash first. Then the silicon and aluminum which dissolve out from the glass phase of fly ash diffuse out of the shell and react with calcium hydroxide in the pores to form the C-S-H gel (Fraay, 1989). Therefore, it is possible that these particles may be participating in pozzolanic reaction.

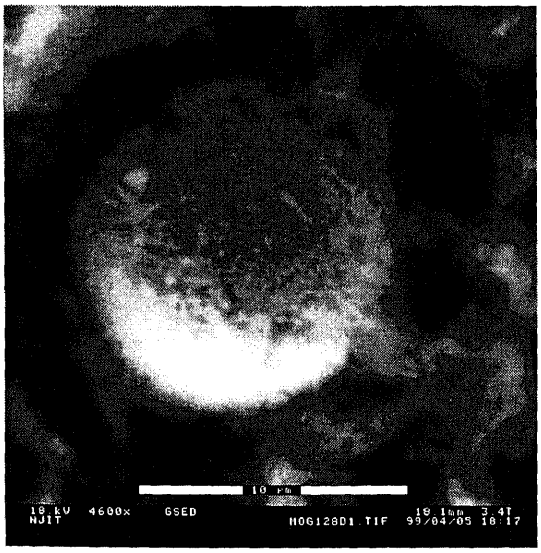

(a) MOG125 at 28 days, 4600x

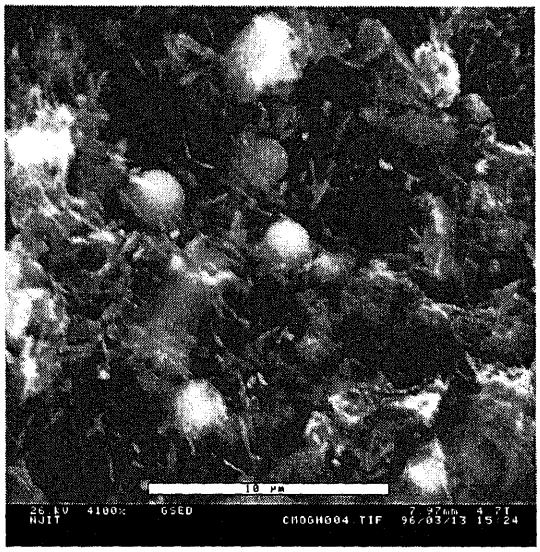

(b) MOG125 at 45 days, 4100x

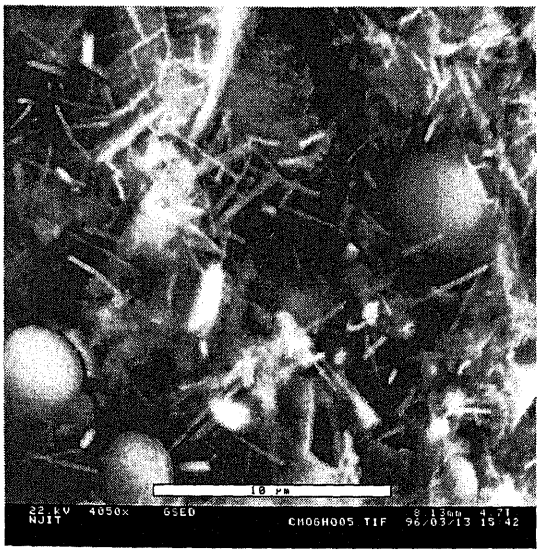

(c) MOG125 at 45 days, 4050x

(d) MOG125 at 45 days, 9000x

Figure 5.77 Microstructure of Fly Ash Paste at 28-45 days, (a) MOG125 at 28 days, 4600x; (b) MOG125 at 45 days, 4100x; (c) MOG125 at 45 days, 4050x; (d) MOG125 at 45 days, 9000x

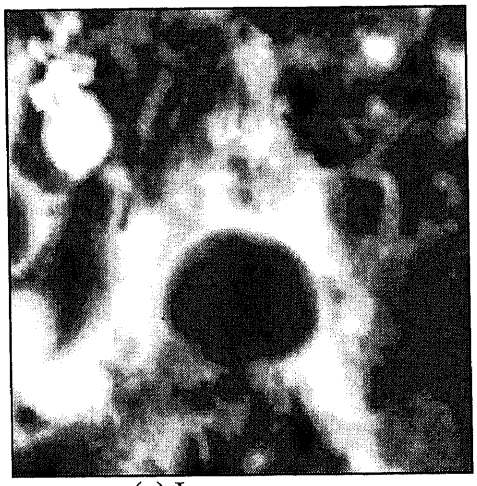

(a) Image

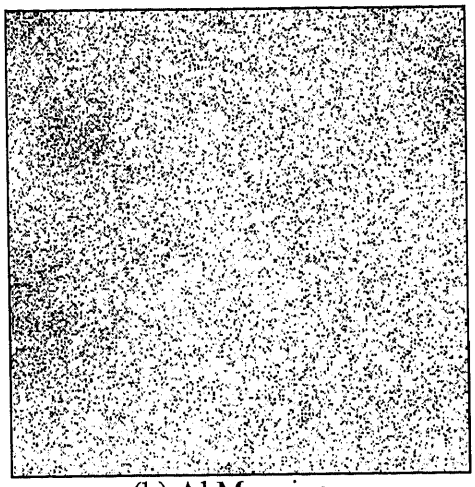

(b) Al Mapping

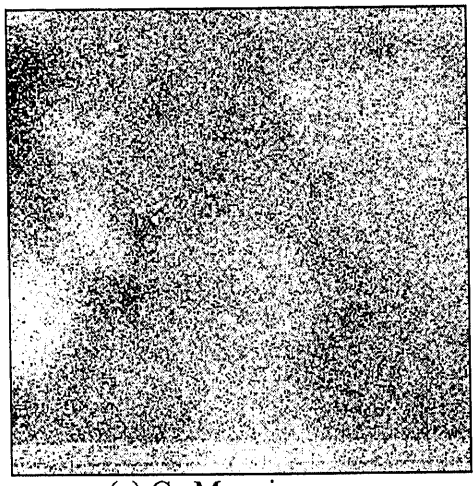

(c) Ca Mapping

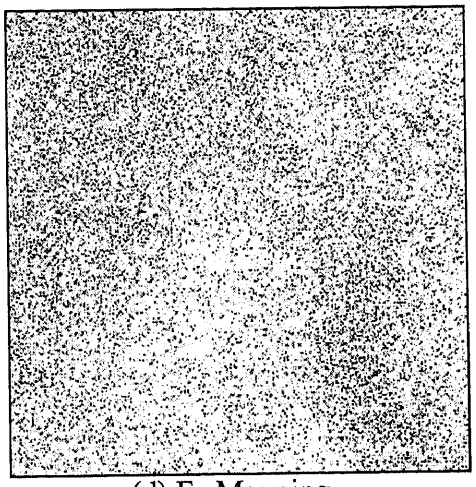

(d) Fe Mapping

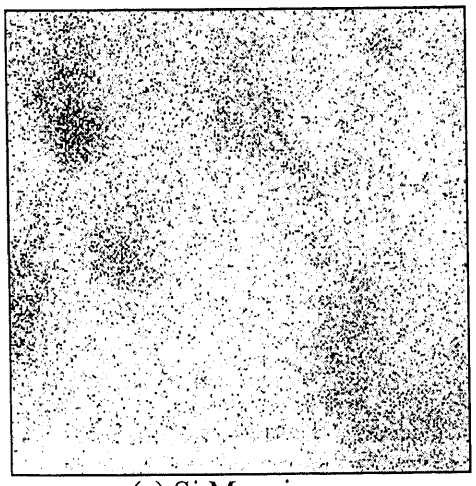

(e) Si Mapping

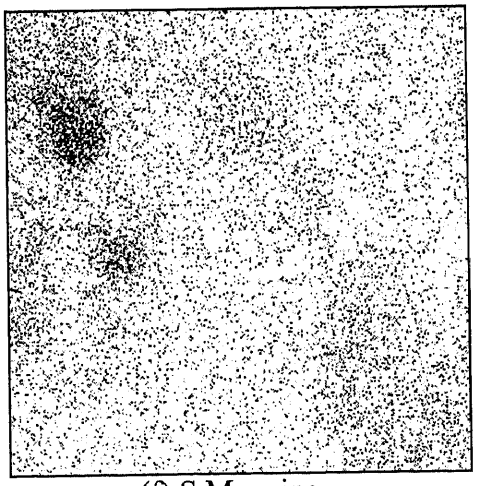

(f) S Mapping

Figure 5.78 Microstructure and Element Mapping of MOG125 at 28 days (3500x)

The elemental mapping of MOG125 at 28 days is shown in Figure 5.78. The selected image was an area around a fly ash particle, which had already loosened out. The image was selected in order to show the diffusing of elements from the fly ash particle. The elements are appearing in black on this mapping. From the picture it can be seen that the Ca was found in high concentration in the area close to the fly ash particle. The concentration diminished with distance from the particle. This result is in agreement with the study done by McCarter (1988) in which the calcium ion was absorbed on to the surface of fly ash. The elements, which dissolved from fly ash particle to react with Ca, are Si, Al, and Fe. Most of Si and Fe in the mapping came from the fly ash since the cement had a low percentage of Al, Fe, and Si. The Al, Fe, and Si in cement were 8.84%, 1.41%, and 20.07% while those in MOG1 fly ash are 25.54%, 17.48%, and 39.36% respectively. The mapping of Si and Fe reveals that their concentrations are higher near the fly ash particle. The mapping of Al reveals that a low concentration of Al everywhere except where the fly ash was, indicating that the Al may have not dissolved out from the fly ash even though fly ash has high concentration of Al (>30%). The result from the elemental mapping shows that the fly ash dissociated the essential elements making them available for pozzolanic action.

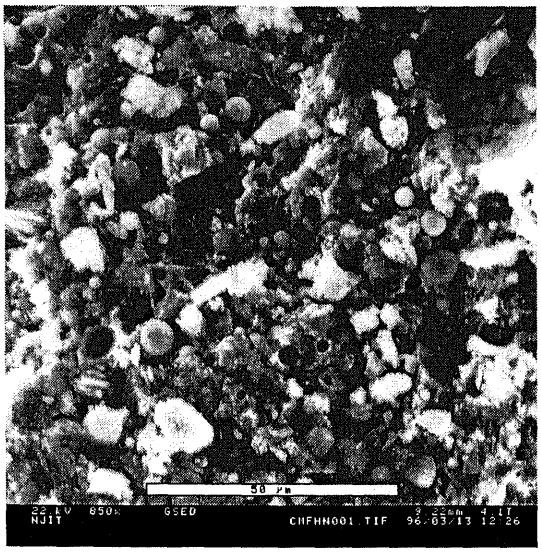

(a) M13F25 at 45 days, 850x

(b) M13F25 at 45 days, 2500x

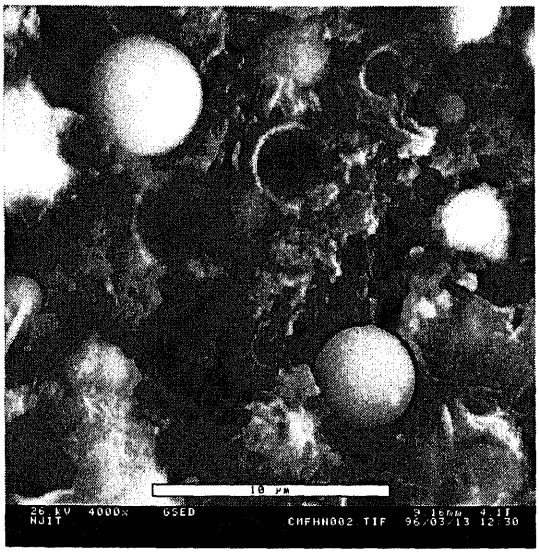

(c) M13F25 at 45 days, 4000x

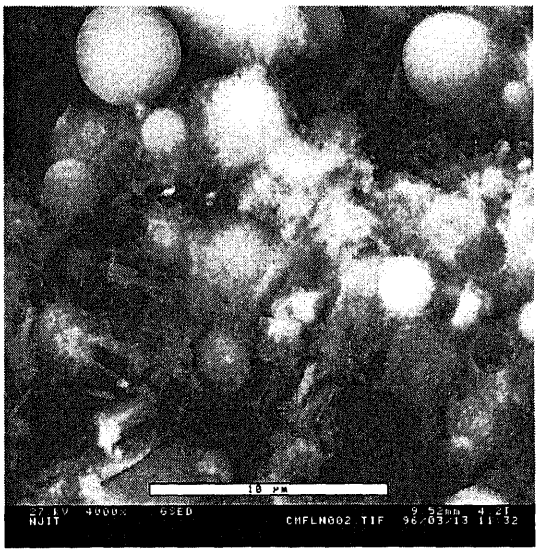

(d) M13F25 at 45 days, 4000x

Figure 5.79 Microstructure of Fly Ash Paste at 28-45 days (a) M13F25 at 45 days, 850x; (b) M13F25 at 45 days, 2500x; (c) M13F25 at 45 days, 4000x; (d) M13F25 at 45 days, 4000x

(a) GPU2G125 at 45 days, 1150x

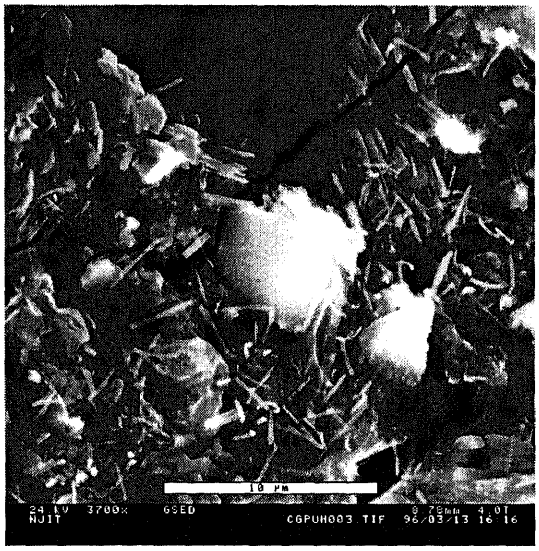

(b) GPU2G125 at 45 days, 3700x

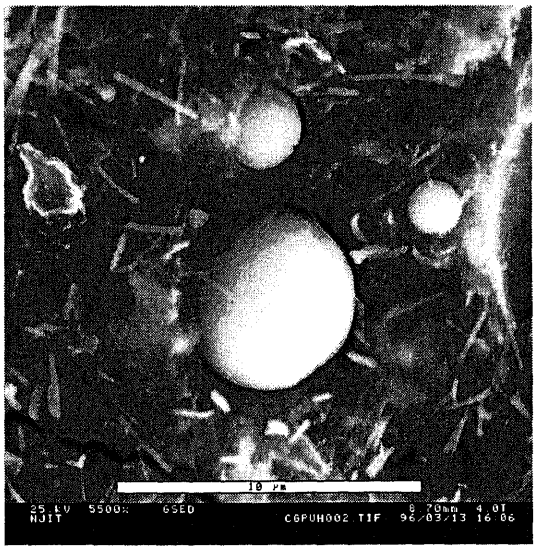

(c) GPU2G125 at 45 days, 5500x

Figure 5.80 Microstructure of Fly Ash Paste at 28-45 days, (a) GPU2G125 at 45 days, 1150x; (b) GPU2G125 at 45 days, 3700x; (c) GPU2G125 at 45 days, 5500x

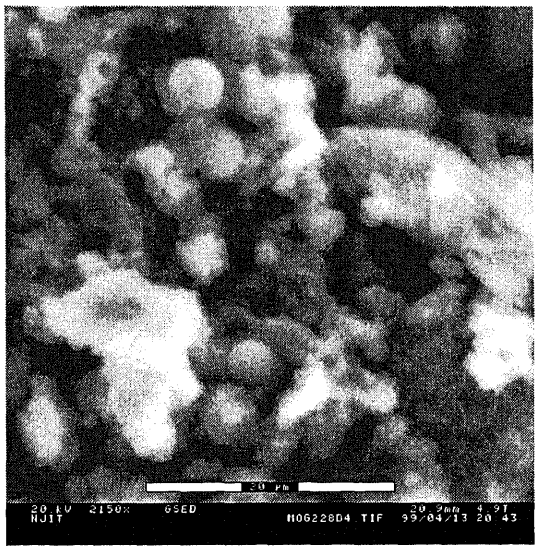

Figure 5.81 Microstructure of MOG225 Fly Ash Paste at 28 days, 2150x

Micrographs of M13F, GPU2G fly ash pastes at this age are shown in Figure 5.79 and 5.80, respectively. They also show that some of their fine particles have not yet reacted. (Figure 5.79(b), 5.79(c), 5.79(d), and 5.80(c)). Figures 5.80(b), 5.80(c) show the micrograph of a broken particle and sphere in ground fly ash paste at 45 days and 28 days, respectively. Both particles are smaller than 10 microns and their surfaces have no evidence of precipitating hydrates. It can be said that the pozzolanic action of fly ash was in progress but the reaction rate could not be obtained from the observation of microstructure. This is because the surface of some many particles cannot be examined. The pozzolanic action occuring at this stage filled the pores near the fly ash particles, reducing the pore volume in the paste, leading to higher strength.

253-day

After curing for a long period of time, all the entire paste structure has been further packed, which corresponds to its relatively high strength. Figure 5.82 shows the

microstructure of cement paste at 253 days. Since the hydration process of the cement paste was already essentially completed, it can be said that this matrix is the representative of the final stage of the cement paste. There was no evidence of segregated particles. They are all bound together and formed a dense texture though some small voids are still present in the paste.

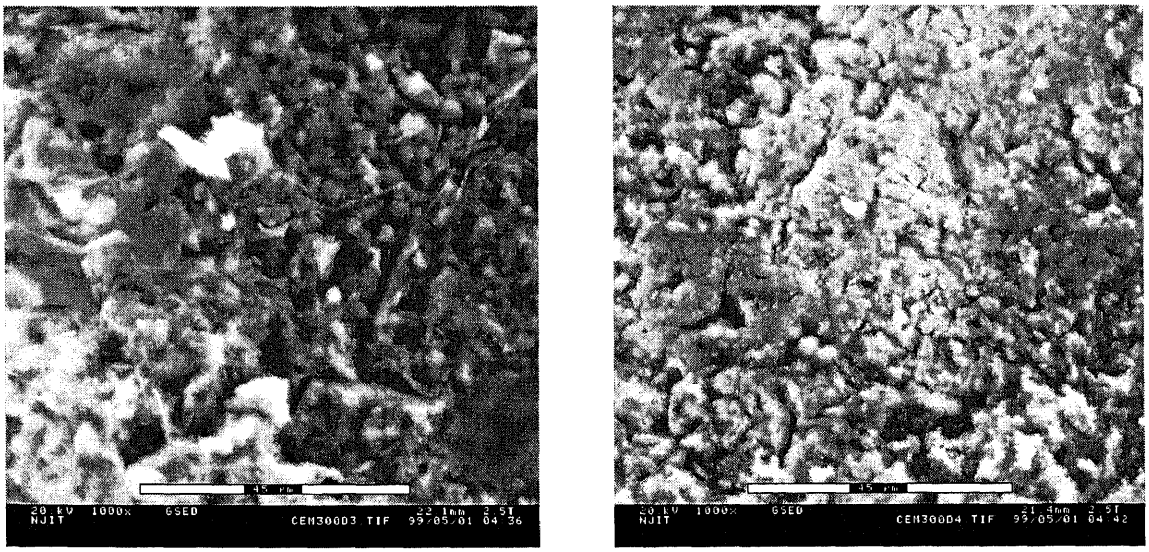

Figure 5.82 Microstructure of Cement Paste at 253 days, 1000x

The microstructure of MOG125, M13F25, and GPU2G125 are shown in Figure 5.83, 5.84, and 5.85, respectively. In Figure 5.83(a) and 5.83(b) , the MOG125 paste had very dense structure. The circular pores seen are believed to be the places occupied by fly ash before they detached. The denser matrix at this age is due to the further growth of hydration and pozzolanic products. The features seen along with the dense matrix of MOG125 paste were ettringite and fly ash particles. It is interesting to see that the fly ash surface was more revealed at this age. It was not covered with the hydration product as that in the earlier paste. This is because the bond between the interconnected matrix is

stronger than the bond between layer and fly ash. Therefore, when the paste was cut during sample preparation, the paste was broken along the weak bond. Whereas in the paste at 45 days, the hydrated layers had not firmly connected with each other, so the broken path occurred between the matrix instead. The fly ash surface so exposed can be used to observe the pozzolanic activity of these fly ash particles. It can be seen that the observed particles have a smooth surface even though they were embedded in the paste for long period of time. These particles include the spheres, as small as 5 microns, and broken spheres of 10 microns. Even though the ground particle had its inside structure exposed to the paste but it did not participate in pozzolanic reaction. These particles were protected from leaching by the thick layer of hydration products that covered them. This result also indicates that the pozzolanic action may not occur in the fly ash covered with hydration layers. It is believed that the pozzolanic action occurs if the pore solution nearby the fly ash particle has a very high pH, which does not depend on the size or the features of the fly ash particle.

Figure 5.84 shows the microstructure of fractionated fly ash paste (M13F25) at the same age. The features are similar to that of MOG125 excepted the broken particles were observed. There were more empty pores shown in this paste. It is believed that these pores were once occupied by fly ash particles. When the particles were detached during the sample preparation, they left the pores in the paste. This could be evidence that the bond between fly ash particle and matrix is weak. Another finding is that fly ash particles as small as 5 microns still had smooth surface at this age. As previously explained, they were not damaged due to the protection by hydration layer. Figure 5.85 shows the microstructure of ground low NO_x fly ash paste (GPU2G125). The paste was

still porous at old age. It is an evident that the matrix has still not been fully developed. It still has room for the products of either pozzolanic or hydration. Since the strength at this age and later age were not measured, the further development in strength by those products is not yet confirmed.

Overall, the microstructure of ground fly ash pastes significantly changed during curing. These observations also show evidence of nucleation process of fly ash at early age and that of fly ash pozzolanic reactions at later age. The fine particle of fly ash fills the pore between the cement grains and it acts as a nucleus for hydration product. The finer the particle the fly ash, the more it refines the pore and the more nuclei for hydration products. The change in pore size of fly ash paste with age is a result of the growth of hydration product. At later age, there are more deposits in the pore, which comes from the pozzolanic action of fly ash. These two phenomena change the overall microstructure of the paste, which indirectly affects the property of the matrix and thereby the strength.

The change in microstructure of fly ash cement paste was observed with time. The investigation reveals that due to its crystallinity the fly ash acts as a site for growth of hydration and pozzolanic products. As seen from micrographs obtained at early age of fly ash paste, the hydrates dissolving from cement grains precipitate on to the fly ash surface. The major constituents was C-S-H gel, ettringite, and $Ca(OH)_2$. At the same time, they precipitate on the surface of cement grains. As the process proceeds, the layer on the fly ash and cement grains becomes thicker. It is believed that at some point the hydration product growing from cement grains and from fly ash particles connect together. This bond contributes strength to the matrix.

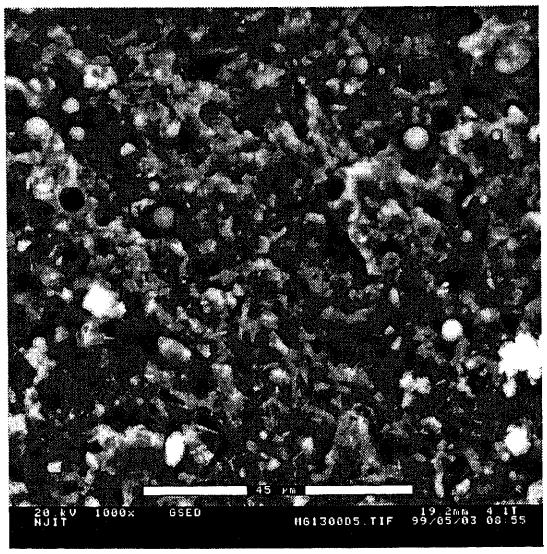

(a) 1000x

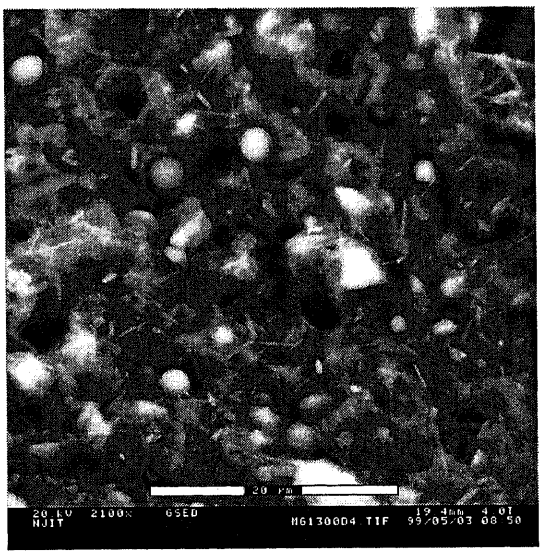

(b) 2100x

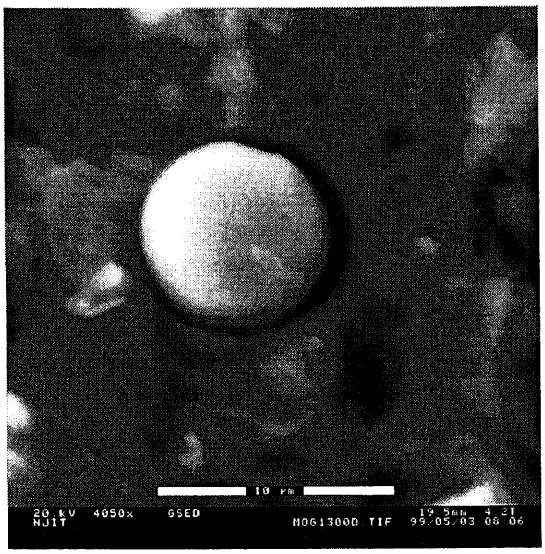

(c) 2150x

(d) 4050x

Figure 5.83 Microstructure of MOG125 Paste at 253 days: (a) 1000x, (b) 2100x, (c) 2150x, (d) 4050x

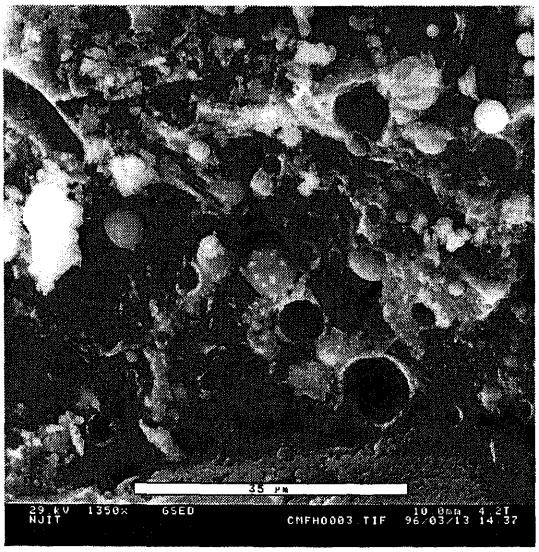

(a) 1350x

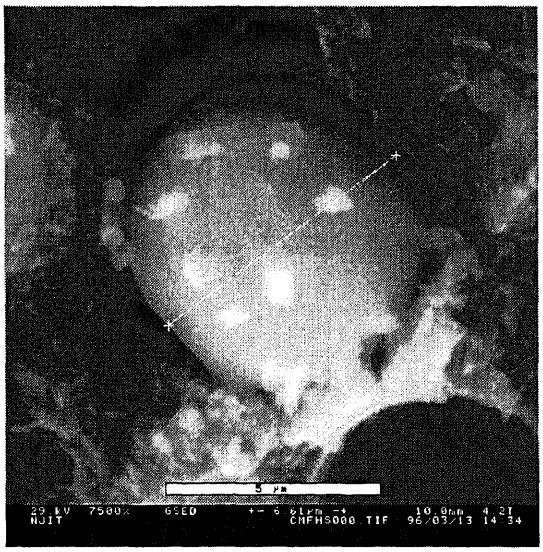

(b) 7500x

Figure 5.84 Microstructure of M13F25 Fly Ash Paste at 253 days (a) 1350x; (b) 7500x

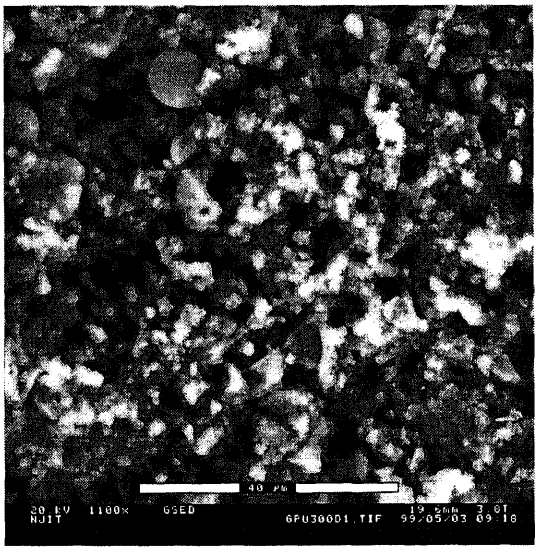

Figure 5.85 Microstructure of GPU2G125 Fly Ash Paste at 253 days, 1100x

5.7 Pore Size Distribution in Fly Ash Cement Paste

The pore size distribution of each paste was obtained by image analysis. This method was modification of the SEM Image Analysis done by Sidney Diamond and Mark E. Leeman (1995). Two images of each paste were obtained by using ESEM. The average of the two was used to analyze the pore size distribution to minimize the chance of getting unrepresentative sample.

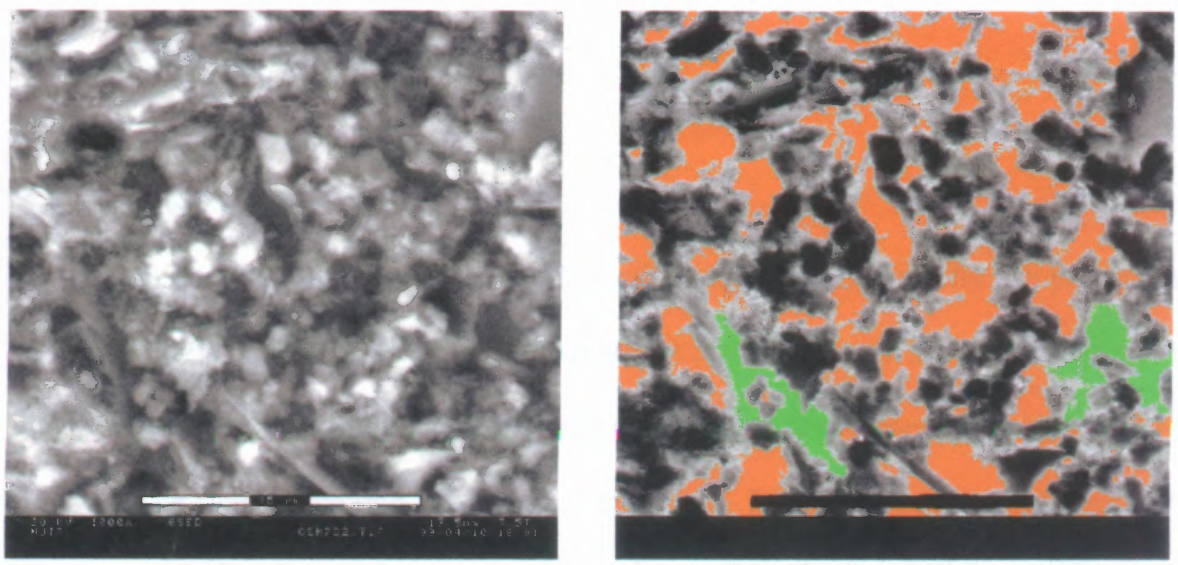

(a) Before Processing (b) After Processing

Figure 5.86 Representative Backscatter Electron Images of 7 days old MOG125 Fly Ash Paste (x1000), (a) Before Processing (b) After Processing

An example of typical Backscatter Electron Image micrographs obtained at 1000x magnification for a water cement ratio 0.50 specimen is shown in Figure 5.86 (a). The structure was composed of solid grains appearing in white and large pores and interconnected pores appearing in dark gray. Some large pores appeared to be the space between hydrated grains. After processing with Image Analysis program, the pores were coded with color depending on their size as shown in Figure 5.86(b). The program also

calculated the pore size as the diameter of a circular area equal to the area of each pore in the micrograph. In this study the size of pores is measured. The upper limit of pore is 10 microns and the lower limit is 0.1 microns as defined by Power (1947). Air voids are bigger than 10 microns. Due to the limitation in distinguishing the pixel, the minimum size that can be measured by this procedure is 0.8 microns. The capillary pore is of interest since it affects the properties of the paste. It was reported by Mehta (1981) that the more percentage of pores larger than 0.1 microns in cement pastes, the lower the compressive strength of mortar.

5.7.1 Porosity of Fly Ash Paste

The porosity at 5 minutes, 3, 7, and 28 days of hardened cement and fly ash pastes are shown in Table 5.13. The porosity of the pastes at 5 minutes is not the actual pore since it was calculated as the volume occupying by air or water. It was used to construct the 5-minutes pore size distribution only. The porosity at 3, 7, and 28 days were obtained by the water displacement method. It is observed that the porosity of all hardened pastes decreased with the progress of age. At 3 days, the porosity of all fly ash pastes was higher than that of cement. Within seven days the porosity of all fly ash pastes was less than that of cement only. Comparing the porosity of ground fly ash from the same source, the one containing finer fly ash had lower porosity than the one with coarser fly ash (MOG1< MOG2). It should be noted that although the GPU2G has finer fly ash than the MOG series, its porosity at an early age was higher. Eventually, its porosity decreased significantly to be lower than the MOG125 paste. Other properties of fly ash may affect the porosity.

Table 5.13 Porosity of Fly Ash Cement Paste (%)

Specimen	Porosity (%)			
	5 min.	3 day	7 day	28 day
Cement	76.01	59.52	58.56	44.25
MOG125	75.05	59.23	54.72	41.71
MOG225	70.03	68.28	55.68	45.25
GPU2G125	70.67	62.31	57.27	40.86

5.7.2 Pore Size Distributions of Different Fly Ash Pastes

Pore size distribution as a function of time of cement paste is shown in Figure 5.87. The pore size distribution of cement paste at 3 days was about the same at 7 days. This result suggests that there was small change in pore size between 3 to 7 days. The hydration products formed during this period may fill the larger void. After 7 days the spaces in the paste were filled further by hydration during that later period.

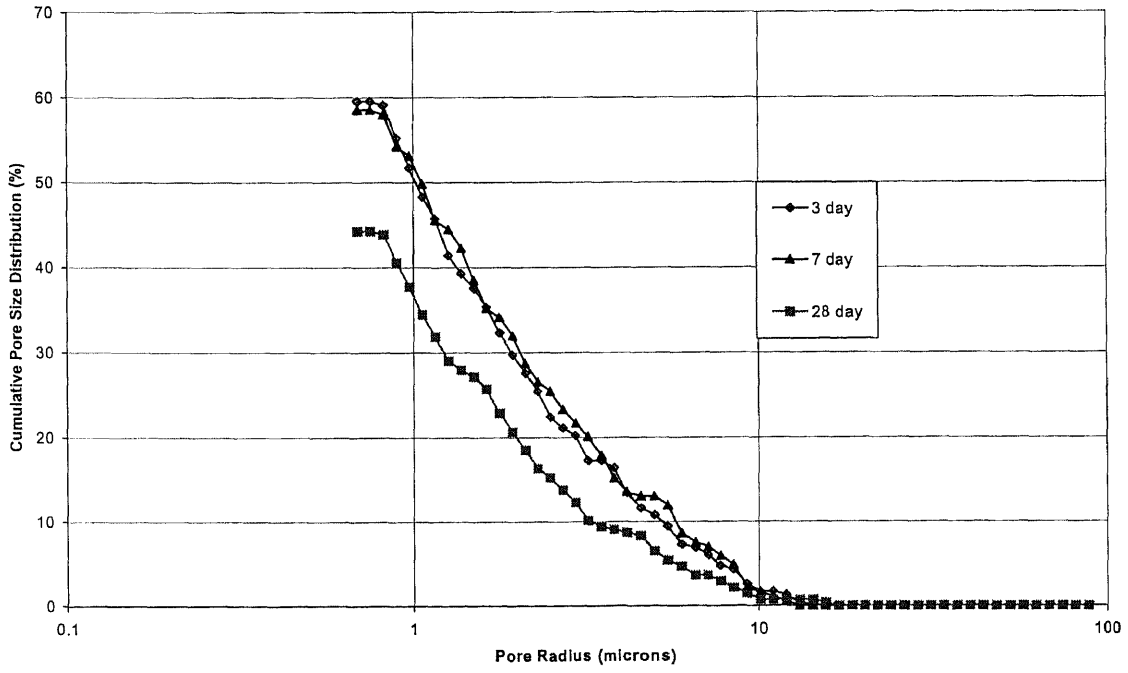

Figure 5.87 Image Analysis Pore Size Distribution for Cement Paste

Figure 5.88, 5.89 and 5.90 show the pore size distribution at different age of MOG125, MOG225, and GPU2G25 pastes, respectively. It is evident that the pores of all fly ash pastes were reduced with time. From 3 days to 7 days, both MOG125 and MOG225 pastes reduced their pore sizes larger than 3 microns reduced but the pore sizes smaller than 3 microns almost had little change. These large pores (> 3 microns) are believed to be the gap between particles. These gaps were smaller because of the growth of hydration products on the particles. Whereas, the pores smaller than 3 microns were not yet filled up yet. At 28 days, the volume percentage of small pores decreased more than that of large pores. This result is due to the formation of both hydration and pozzolainc products. The hydration and pozzolanic products begin to fill the small pores at this time, reducing the pore size.

The pore size reduction at early age in fly ash pastes is the result of the nucleation process. This stage began immediately after mixing and continued until all the cement grains were fully hydrated. The hydrates such as C-S-H gel and $Ca(OH)_2$ dissolving from the cement grains precipitated on to the fly ash surface and cement surfaces. It is expected that the hydration product growing from nearby fly ash particles or cement grains became connected and this bond increases the strength of the matrix. The nucleation effect is present predominantly at the early age because there are many of cement grains ready for hydration. It may diminish at later ages after all cement grains have been hydrated. Hence, the pore size reduction at later age is probably the result of other mechanisms such as the pozzolanic action of fly ash. Cao, Ho and Guirguis (1990), and Gopalan (1993) proposed that this nucleation function was the major contribution to the strength of mortar up to 28 days.

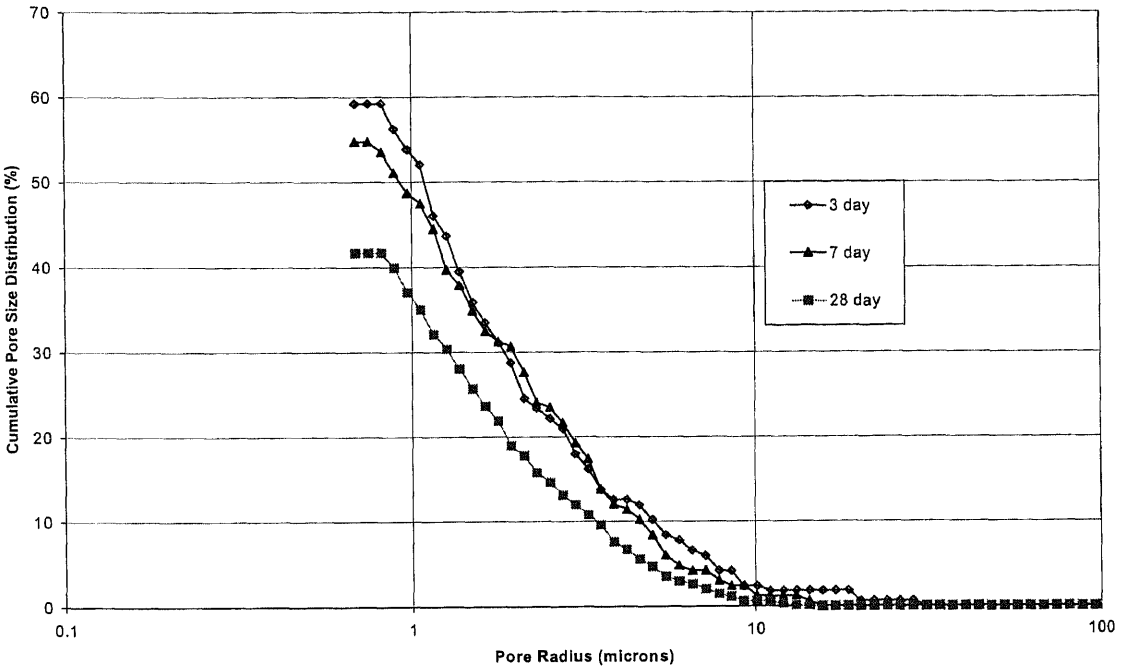

Figure 5.88 Image Analysis Pore Size Distribution for MOG125 Paste

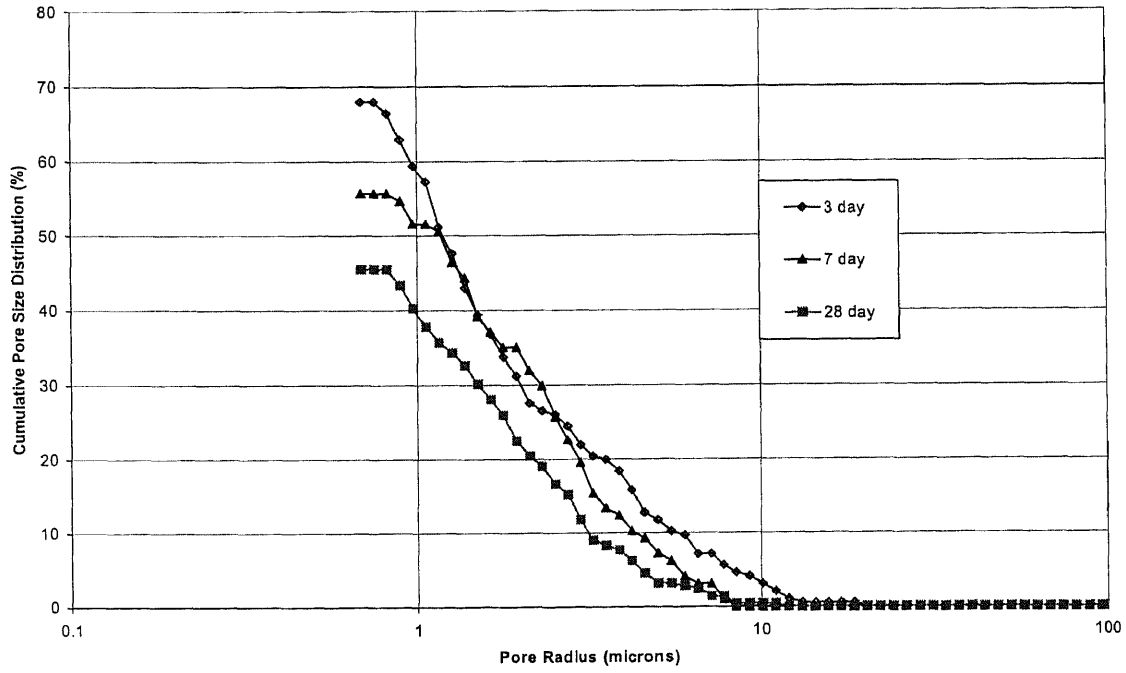

Figure 5.89 Image Analysis Pore Size Distribution for MOG225 Paste

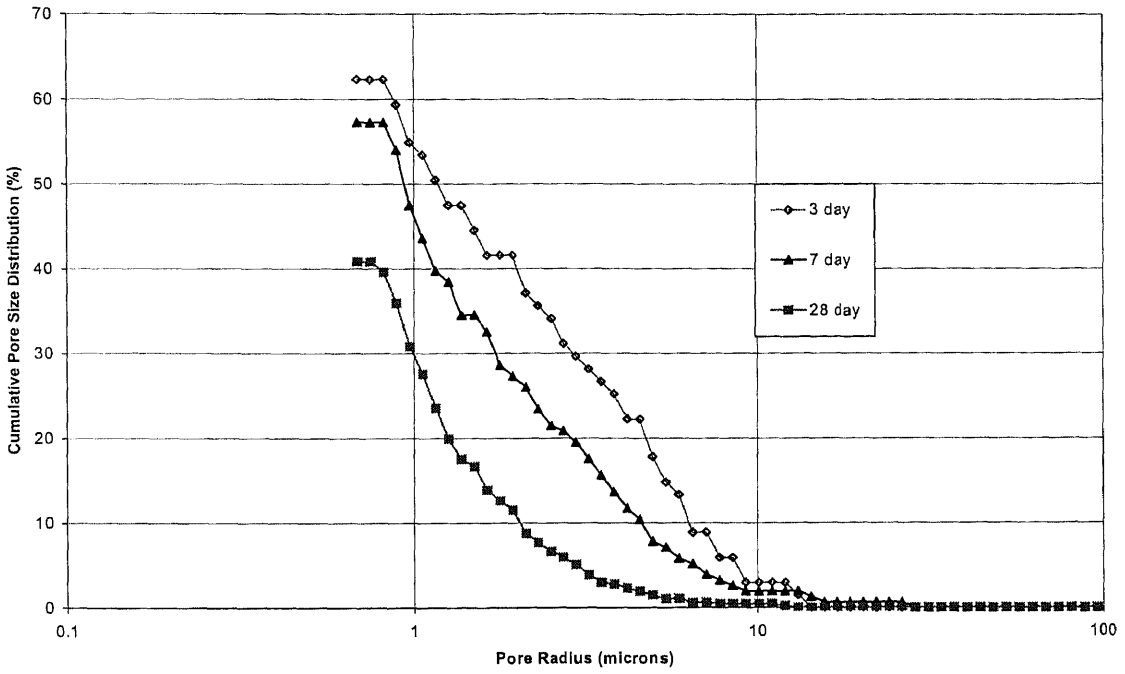

Figure 5.90 Image Analysis Pore Size Distribution for GPU2G125 Paste

5.7.3 Pore Size Distributions of Fly Ash Pastes at Different Time

The pore size distributions of the cement, MOG125, MOG225, and GPU225 at 5 minutes were observed. The sample preparation for 5-minutes analysis was different from samples at older age since the paste was not hardened yet. To catch the instant picture of liquidated sample, the sample was hardened by freezing with liquid nitrogen. This also arrested the hydration reaction of the paste. Otherwise the microstructure would change with the intensive hydration process. In the microstructure section above it was shown that the fly ash particles in the paste were not covered with hydration products at this time, thus it is assumed that the hydration process had not started and the particles shown in the paste were the cement grains and the fly ash particles only. The micrographs of these pastes show that the cement grains were smaller in fly ash paste than in cement

paste. This could be a dispersion function of fly ash that dispersed the cement grains in fly ash paste to finer particle. However, in this study, the grain size of cement was not analyzed since it is difficult to delineate the cement particles, which are overlapping in the micrograph. The pore size distribution in the paste was observed instead.

The pore size distributions of the pastes aged 5 minutes are shown in Figure 5.91. The distributions of pore size in all fly ash pastes were finer than that of normal cement paste. It is assumed that the large particle would yield the large pore size. According to this assumption, the pore in fly ash paste are smaller than that of cement paste. This is because the cement grains in cement paste tended to flocculate and left the large gaps between flocs. But the cement grains in fly ash paste were dispersed due to the action of fly ash in the mixing process. The dispersion of cement grain is expected to be the result of difference in Zeta potential between fly ash and cement (Nagele, 1989). This effect was more pronounced when finer fly ash was used. And the difference in pore size between fine and coarse fly ash paste was shown more clearly on pores larger than 3 microns.

Having finer cement grains may improve the properties of fly ash paste by enhancing the hydration process. It increases the rate of hydration because there will be less amount of unreacted cement enveloped in side the grain. The hydration rate will be investigated in hydration section. Another benefit of having finer cement grains is the modification of pore size. This finer initial porosity is the principal factor determining the development of pore structure at later age.

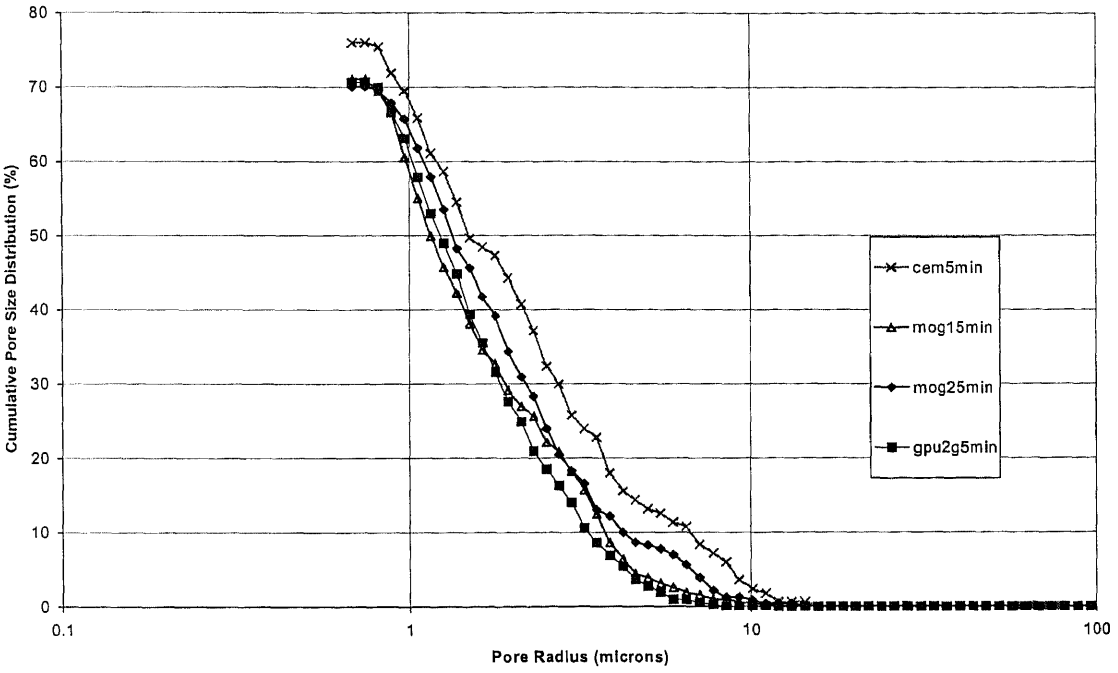

Figure 5.91 Image Analysis Pore Size Distribution of 5 minutes Old Fly Ash Paste

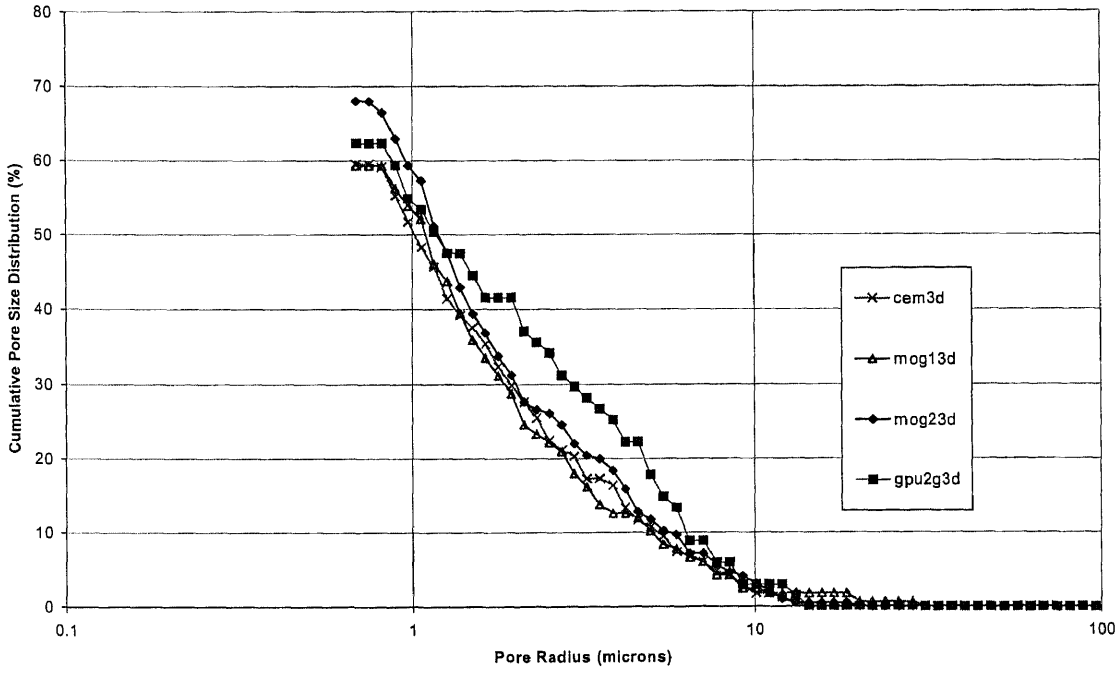

Figure 5.92 Image Analysis Pore Size Distribution of 3 Days Old Fly Ash Paste

The pore size distribution data of the various pastes at 3, 7, and 28 days are plotted in Figures 5.92, 5.93, and 5.94, respectively. Beyond the setting time, the pore size of the paste was reduced due to the nucleation effect of fly ash. This opinion differs from Mehta (1981) who reported that the conversion of large pores to finer pores is a result of pozzolanic action. However, it could not be the only cause since the pozzolanic action normally occurs rather late.

Even though the pore size of cement paste at the beginning was larger than that of fly ash pastes but it became comparable to those of fly ash pastes at 3 days excepting GPU2G125. This is because there was more cement in cement paste (100%) than in fly ash paste (75%) to provide hydration product to fill the pores. As a result, the pore size distribution of cement became equal or smaller than that of fly ash paste within 3 days. Comparing the pore size distributions between fly ash pastes, it can be seen that its distribution decreased as the fineness of fly ash increased (MOG1> MOG2). The decrease in pore size in finer fly ash paste is because it had more numbers of particles acting as a nucleation centers for hydration products.

Mechanical properties of these pastes are usually controlled by pore structure. This relationship had been stated by several researchers, e.g. Aimin (1993). He found that the paste with finer pore size distribution would have higher compressive strength. The result of this study also corresponds with the above concept. The MOG125, and MOG225 fly ash mortars, having the same pore size distribution in their pastes, had about the same compressive strength. Also, the compressive strength of the GPU2G125 mortar, which had coarser pore size distribution than MOG fly ash, was lower. The cement paste had higher early strength due to the two bonds: Coulomb force between

cement grains and interconnection of hydration product (Lagrand, 1994). Unlike the cement paste, the strength at early age of fly ash paste was low. This may be because the binding material has not connected completely or the amount of hydration product was not sufficient to bind them.

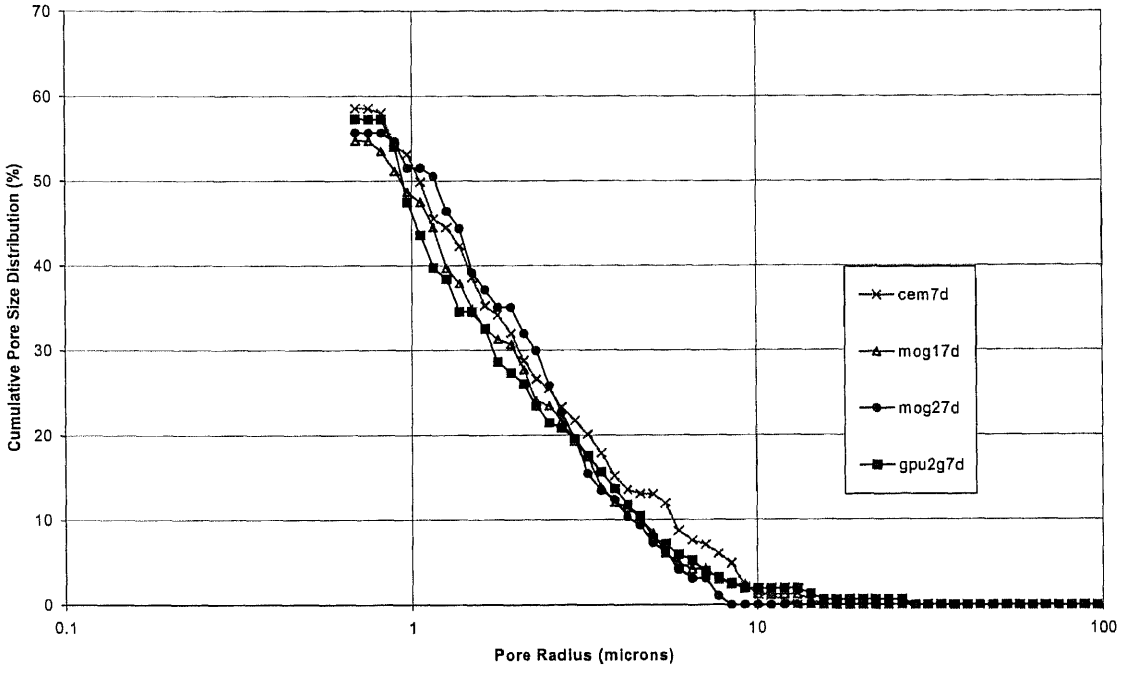

Figure 5.93 Image Analysis Pore Size Distribution of 7 Days Old Fly Ash Paste

At seven days, the pore sizes of fly ash pastes were finer than that of cement paste. As seen from Figure 5.87, the change of pore size distributions between 3 days and 7 days of cement paste was minimal, while those of fly ash pastes were large. The difference in number of pores having size larger than 5 microns between these distributions was clearly seen. The large pores of fly ash pastes were reduced due to the growth of hydration products on the fly ash particles. The conversion of large pores (>5

microns) to smaller pores (<5 microns) can be seen more clearly in the pore size distribution of MOG225 paste (Figure 5.89). At this age, their compressive strengths were still lower than that of cement mortar even though they had finer pore size distributions.

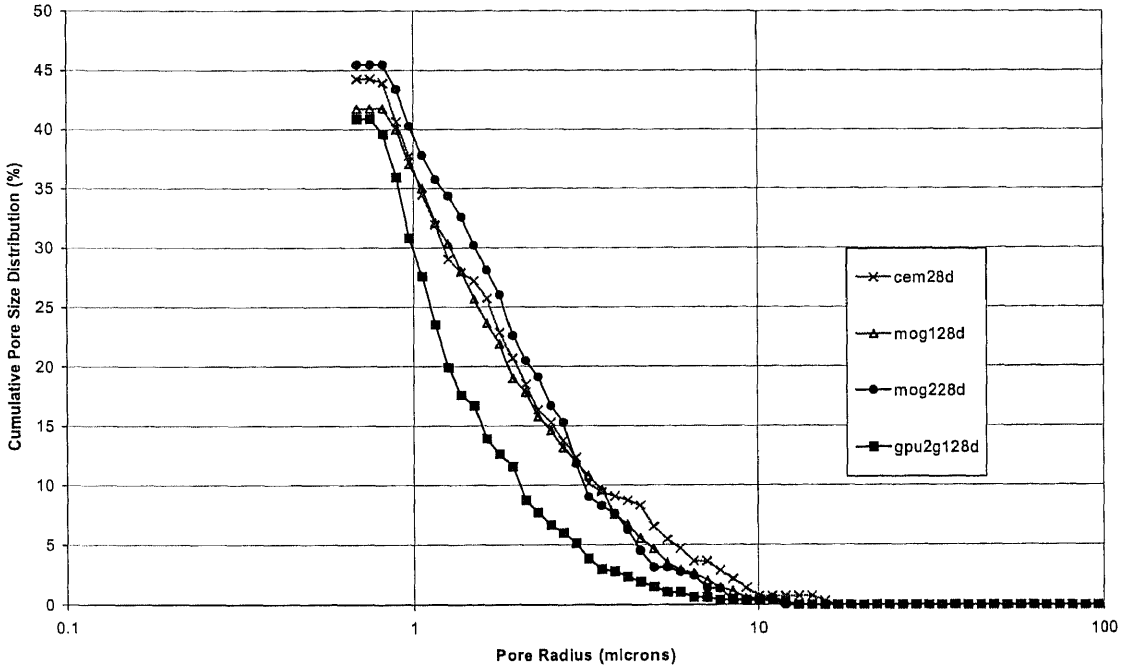

Figure 5.94 Image Analysis Pore Size Distribution of 28 Days Old Fly Ash Paste

By 28 days, the pore size distributions of fly ash pastes were about the same as that of cement paste excepting that they had fewer large pores. At this stage, the products that filled the pores in fly ash paste could be hydration products and pozzolanic products. The hydration process was still in active as seen from the high rate of strength gain of fly ash mortar or thicker layers on the fly ash surfaces. Hence, the nucleation effect of fly ash is a major contribution to the pore reduction at this age. At this period, the

pozzolanic action of fly ash was also in progress. Some particles showed the leaching on their surface. This action may active in other particles but it was not visible as it was hindered by the layer of hydrated products. Since the hydration products and pozzolanic products cannot be differentiated from the images, the effect of both actions on pore size distribution could not be distinguished.

The pore size distribution of MOG125 was finer than MOG225. This result held true at all ages suggesting that the fineness was an important factor contributing to deflocculation, nucleation and pozzolanic action. The pore size distribution of GPU2G125 paste decreased significantly comparing to other fly ash paste at age of 7 days and 28 days.

It can be concluded that the pore size of fly ash paste decreases with time. It is finer than that of cement paste at age of 7 days. The pore reduction was a result of deflocculation, nucleation effect, and pozolanic action. The fineness has positive impact on all three of these processes. It was found that the paste with finer fly ash had finer pore size distribution. The reduction of pore size helps to explain the difference in strength between various fly ash mortars because the denser matrix tends to produce high performance and good durability.

5.8 Strength Development of Ground Fly Ash Mortar

This chapter investigates the effect of percent replacement of ground fly ash used on strength development of ground fly ash mortar, the effect of particle size distribution of ground fly ash on the strength development in each stage, and the optimum percentage for each fineness of ground fly ash. Comparison of strength development between ground fly ash from the same source was done so as to restrain the effect from chemical composition. Three types of fly raw fly ash were used: fly ash from wet bottom boiler, fly ash from dry bottom boiler, and fly ash from low NO_x boiler. They were ground into three batches of ground fly ashes ranging from finest to coarsest. The method of grinding is explained in the chapter 5.1. For wet bottom fly ash, its raw (MO) and coarse (M8C) fly ashes were ground. The MO fly ash was ground into MOG1, MOG2, and MOG3. The coarse fly ash received from classifier was ground in to two batches ranging from fine to coarse: M8CG1 and M8CG2. The raw fly ash from dry boiler (BOT) was ground into BTG1, BTG2, and BTG3. The raw fly ash from low NO_x boiler (GPU2O) was ground into GPU1G, GPU2G, and GPU3G. The ground fly ash mortars were made using a cement replacement at 15%, 25%, 35% and 50% by weight of cementitious materials. Control mortars were mixed in parallel with ground fly ash mortars. The water to cementitious materials ratio was kept at a constant 0.50. The proportion details are shown in Table 4.2. After casting, the molded specimens were left in a humidity room for 24 hours. They were then demolded and cured in saturated limewater until required for testing. The compressive strength of samples was tested at the age of 3, 7, 14, 28, 60, and 120 days.

CC is the control sample. MO, GPUO, and BOT are the mortars with the original feed of wet, dry, and low NO_x fly ashes, respectively. MOG, GPUG, and BTG are the mortars using the original feed of wet, dry, and low NO_x fly ashes in the grinding process. M8CG is the mortar using coarse wet fly ash as raw material in the grinding process. The number "1", "2", or "3" placed after "G" represents the grinding condition of each ground fly ash. The ending number of each sample, i.e. "15", "25", "35", and "50", stands for the percentage of cement replaced by fly ash.

5.8.1 Strength Development of Ground Wet Bottom Fly Ash Mortar

5.8.1.1 Effect of Percent Cement Replacement on Strength Development of Ground Wet Bottom Fly Ash Mortar

5.8.1.1.1 15% Cement Replacement: As seen from Figure 5.95, at the initial stage, the 3-day compressive strength of MOG115, MOG215, and M8CG115 fly ash mortars with 15% cement replacement were higher than control mortar. Those of MOG315, M8CG215 and MO15 fly ash mortar were lower or comparable to that of control mortar. This result is not expected because ground fly ash mortar has less cement than the control. According to the XRD result of ground fly ash cement paste the fly ash did not yield any chemical reaction at this point. This indicates that the physical effect of ground fly ash would be the one that provided the strength. From microstructure observation of ground fly ash cement paste, it can be seen that cement disperses more in the paste with ground fly ash. The dispersion of cement increases hydration rate by generating more fine cement grain for the hydration process. Another benefit is that the dispersion process may help improve the structure arrangement even though there was less cement, but it may be enough to bind the fly ash particles. At 7 days, the compressive strength of

control mortar was higher than ground fly ash mortar. This can be explained by the fact that the highest point of initial strength of control mortar is higher than that of ground fly ash mortar.

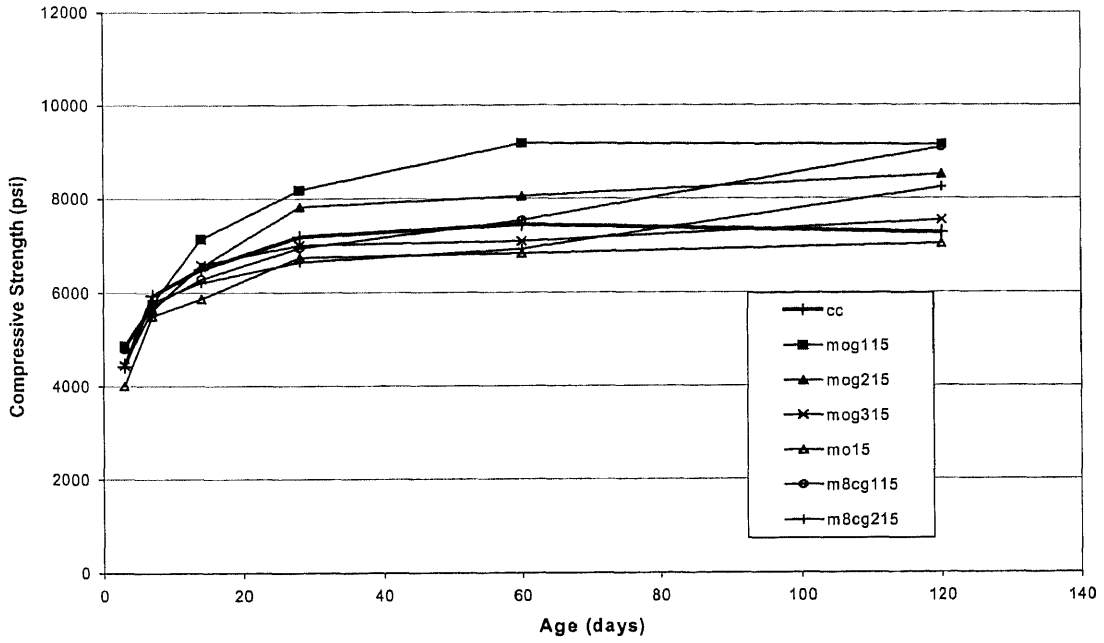

Figure 5.95 Relationship between Compressive Strength of the Ground Wet Bottom Fly Ash Mortar and Age with 15% Replacement of Fly Ash

After 7 days of curing, some of the fly ash mortars have higher strength than control mortar. The compressive strength of MOG115, MOG215 are higher than that of control mortar but MOG315, M8CG115, and M8CG215 are lower. Since MOG315, M8CG115, and M8CG215 use the ground fly ash which still has particles bigger than 10 microns to replace cement, it seems that the pozzolanic activity between fly ash and $Ca(OH)_2$ is not great enough to make up for strength given by the cement hydration.

After 28 days of curing, the slopes of strength development of all mortars become flattened except that of MOG115, which uses the finest ground fly ash. This continued

increasing strength can be the result of more contact area of fly ash for the pozzolanic reaction. However, the rate of increasing strength at this stage is still lower than that in the period from 7 to 28 days due to the obstruction of reaction product on the fly ash surface.

5.8.1.1.2 25% Cement Replacement: The relationship between the compressive strength of mortar containing 25% of ground fly ash and age is shown in Figure 5.96. The evidence of particle size effect on strength still appears in higher-percent cement replacement. It can be seen that when using 25% cement replacement, the strength in the initial stage was lower than that of control mortar. This is expected in fly ash mortar, since at this stage fly ash is still not reactive. The dispersion is not enough to increase strength to the same strength as control. But it can be seen that in the intermediate stage all ground fly ash mortar can surpass the strength of control mortar at an age of 10 to 12 days. They continue to gain strength after 28 days of curing, which is the point that mortar using 15% replacement become flattened. This increasing strength comes from pozzolanic activity, which shows more influence on strength when using a greater percentage of fly ash.

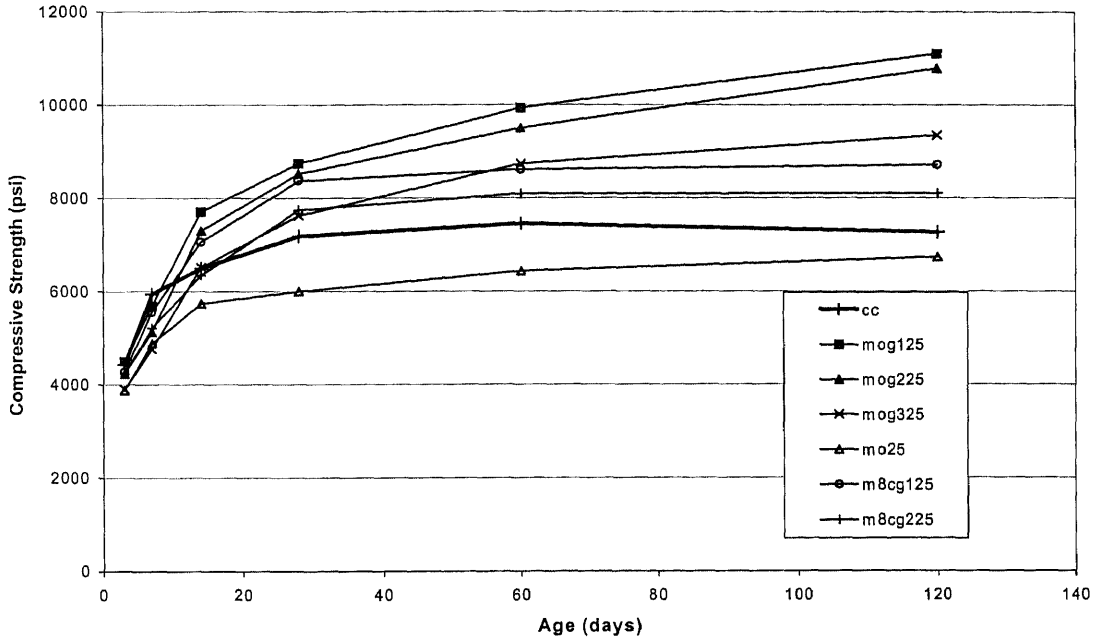

Figure 5.96 Relationship between Compressive Strength of the Ground Wet Bottom Fly Ash Mortar and Age with 25% Replacement of Fly Ash

5.8.1.1.3 35% Cement Replacement: The relationship between the compressive strength of mortar containing 35% of ground fly ash and age is shown in Figure 5.97. The 3-day strength and 7-day strength of ground fly ash mortar using 35% cement replacement were lower than that of control. Only the strength of mortar using fine fly ash (MOG135 and MOG235) can surpass that of control before 14 days of curing. The strength of other mortars took more time to surpass the strength of control. Their rates of gaining strength after 28 days of curing were less than those of mortars with 25%. But the mortar with the finest ground fly ash continued to gain strength after 28 days.

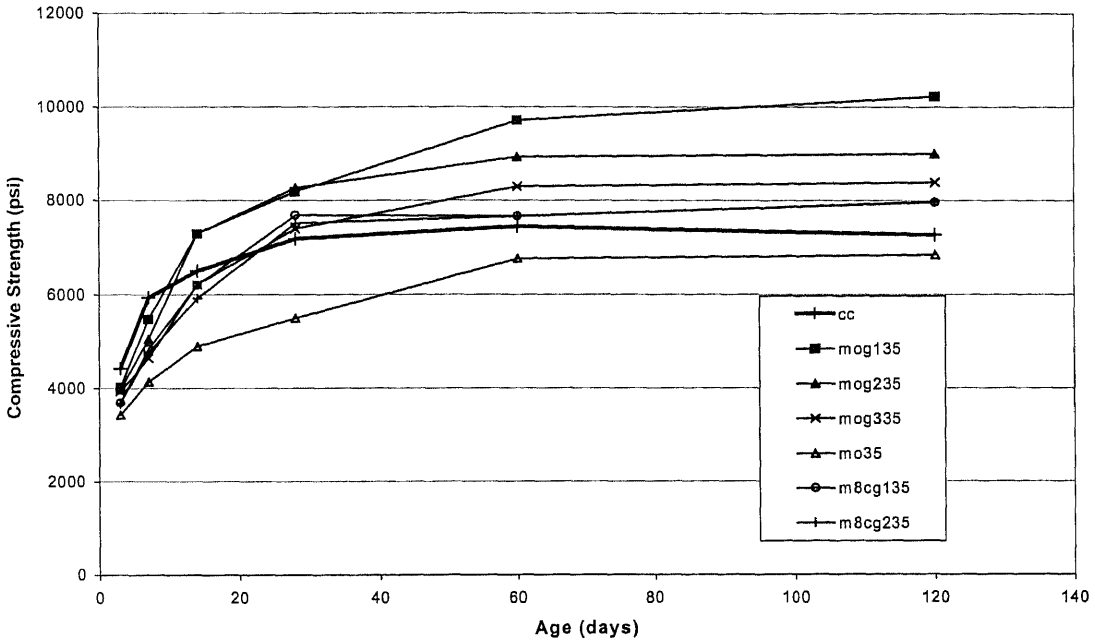

Figure 5.97 Relationship between Compressive Strength of the Ground Wet Bottom Fly Ash Mortar and Age with 35% Replacement of Fly Ash

5.8.1.1.4 50% Cement Replacement: The relationship between the compressive strength of ground fly ash mortar and age is shown in Figure 5.98. It can be seen clearly that all ground fly ash mortar using 50% replacement had lower strength than that of control at any curing age. Their strength development patterns were similar to the ones using lower-percent replacement.

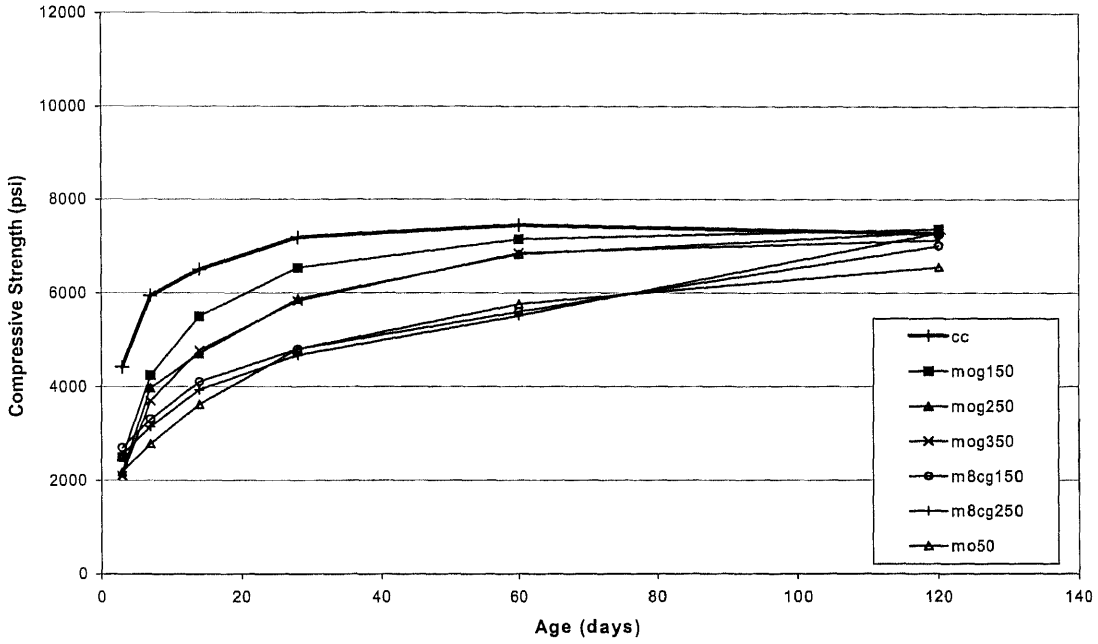

Figure 5.98 Relationship between Compressive Strength of the Ground Wet Bottom Fly Ash Mortar and Age with 50% Replacement of Fly Ash

5.8.1.2 Effect of Fineness of Ground Fly Ash on Strength Development of Ground Wet Bottom Fly Ash Mortar: Relationship between compressive strengths of the ground wet bottom fly ash mortar MOG1, MOG2, MOG3, M8CG1, and M8CG2 and age with different replacement of fly ash are shown in Figure 5.99, 5.100, 5.101, and 5.102, respectively. The 15% replacements of all series had greater 3-day strength than control mortar due to the dispersion effect. But the rate of gaining strength was lower than control, so their 7-day strengths were less than that of control. When comparing different percent replacements of each series, the 25% replacement sample of fly ash mortar had the highest compressive strength at later age or after 7 days of curing. This is the case for all fly ashes regardless of the fineness of fly ash. It can be concluded that the

25% replacement is the most effective percentage, yielding the highest strength of these mixes. The strength of 35% and 50% replacement series are far below that of 25% series.

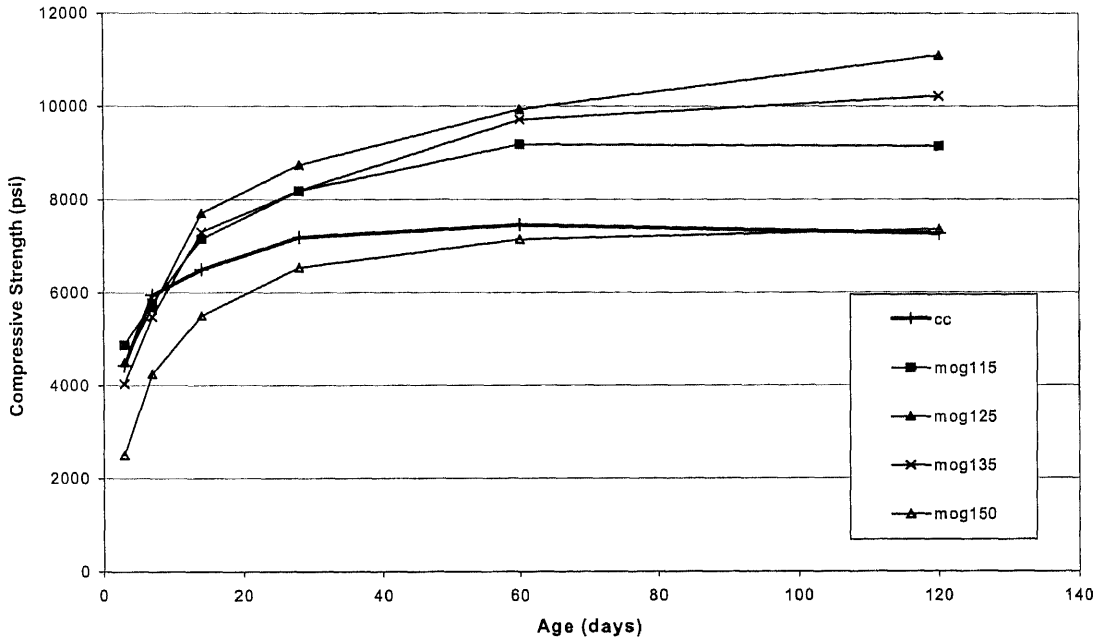

Figure 5.99 Relationship between Compressive Strength of the Ground Wet Bottom Fly Ash Mortar (MOG1) and Age with Different Replacement of Fly Ash

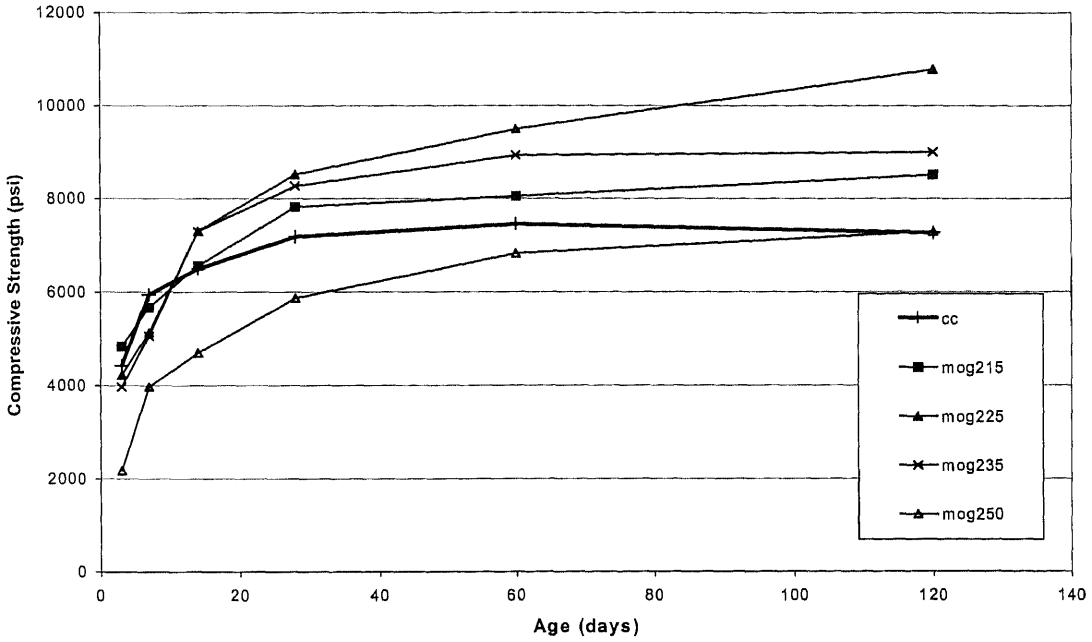

Figure 5.100 Relationship between Compressive Strength of the Ground Wet Bottom Fly Ash Mortar (MOG2) and Age with Different Replacement of Fly Ash

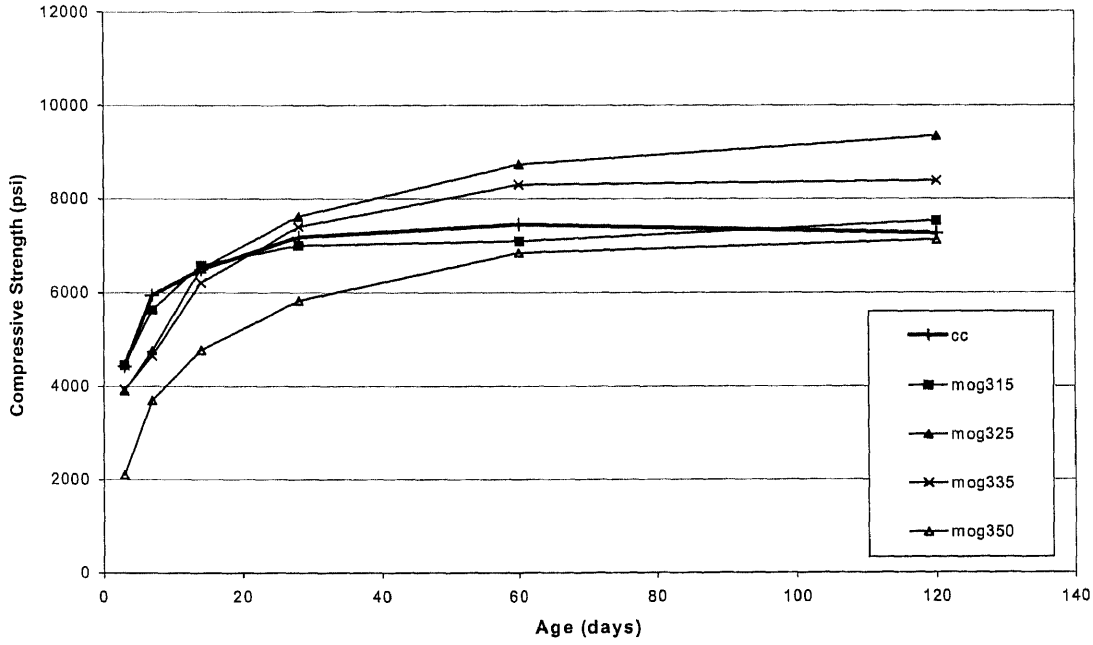

Figure 5.101 Relationship between Compressive Strength of the Ground Wet Bottom Fly Ash Mortar (MOG3) and Age with Different Replacement of Fly Ash

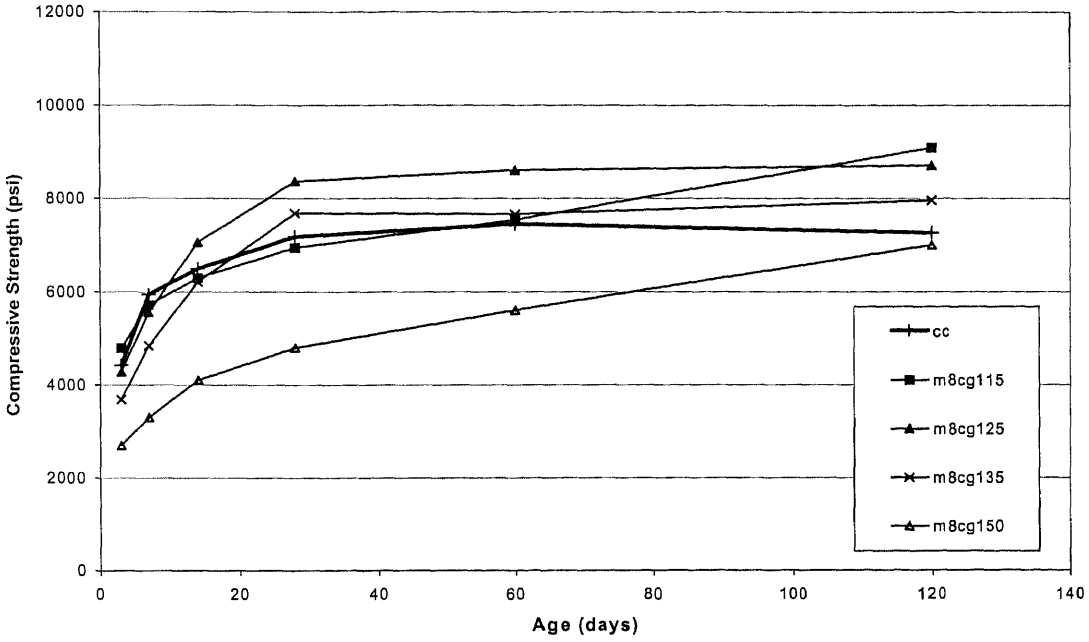

Figure 5.102 Relationship between Compressive Strength of the Ground Wet Bottom Fly Ash Mortar (M8CG1) and Age with Different Replacement of Fly Ash

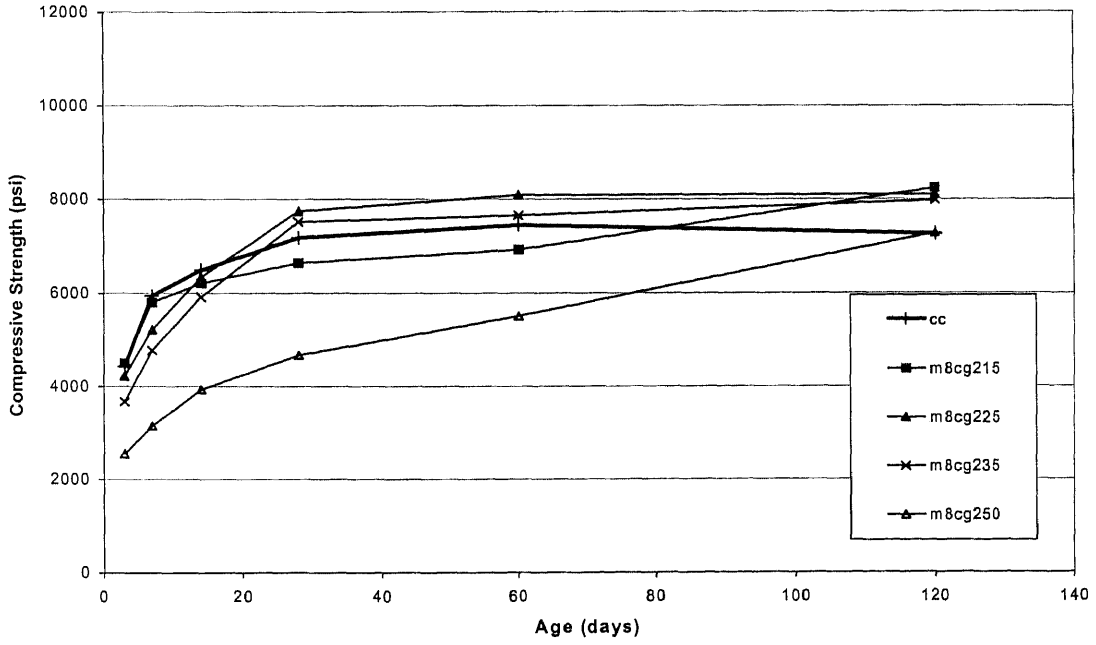

Figure 5.103 Relationship between Compressive Strength of the Ground Wet Bottom Fly Ash Mortar (M8CG2) and Age with Different Replacement of Fly Ash

5.8.1.3 Optimization of the Percentage of Ground Wet Bottom Fly Ash in Mortar:

To find the optimum percentage in each series, the compressive strength of each percentage is plotted against the others in the same graph. The mix that uses the highest amount of fly ash and still surpasses the strength of control mortar at 14 days of curing is considered the optimum percentage for that fly ash mortar. The relationship between relative compressive strength at 14 and 28 days and percent replacement of fly ash is shown in Figure 5.104 and 5.105.

From Figure 5.104, the optimum mix of MOG1 fly ash, which uses the finest fly ash, is 42% replacement. Most of the mix in this series (15%, 25%, and 35%) had much greater strength than control, and the strength of the 50% replacement almost reached the strength of control mortar at 60 days. When 42% replacement was used, its strength surpassed that of control at 14 days. When using coarser fly ash as a replacement, their strength developments were slower and yielded lower strengths than MOG1 fly ash mortar. The optimum mixes for MOG2, MOG3, and M8CG1 are 40%, 25%, and 32%, respectively. The percent replacement of fly ash follows the same order as the fineness of fly ash. The finer the fly ash, the more replacement fly ash can be used in mortar. It can be concluded that the fineness of fly ash has an effect on the optimum percentage of its use.

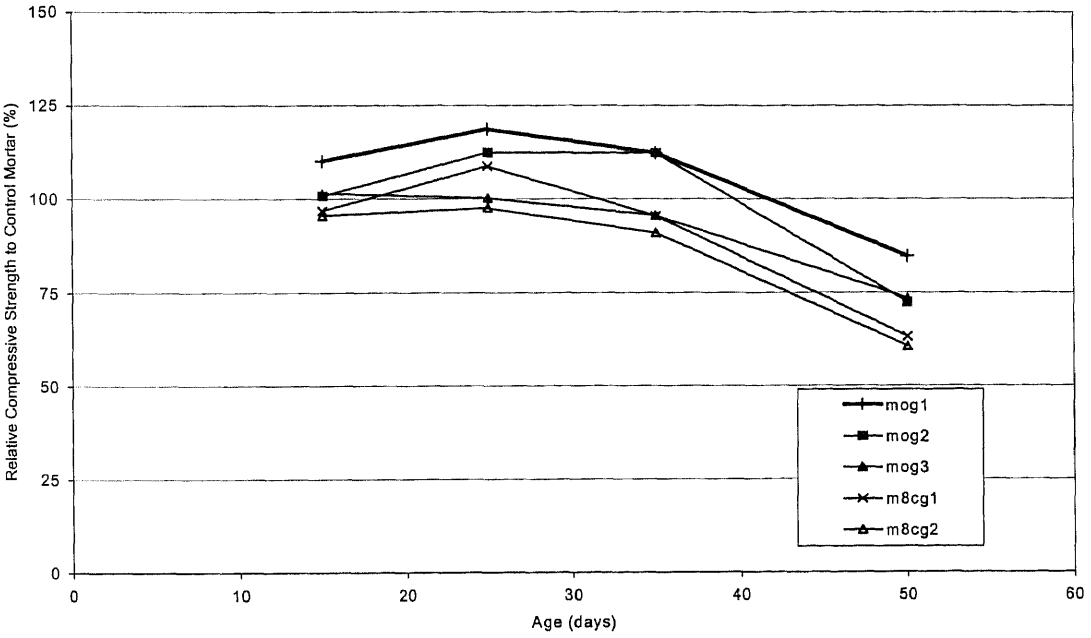

Figure 5.104 Relationship between Relative Compressive Strength at 14 days and Percent Replacement of Fly Ash

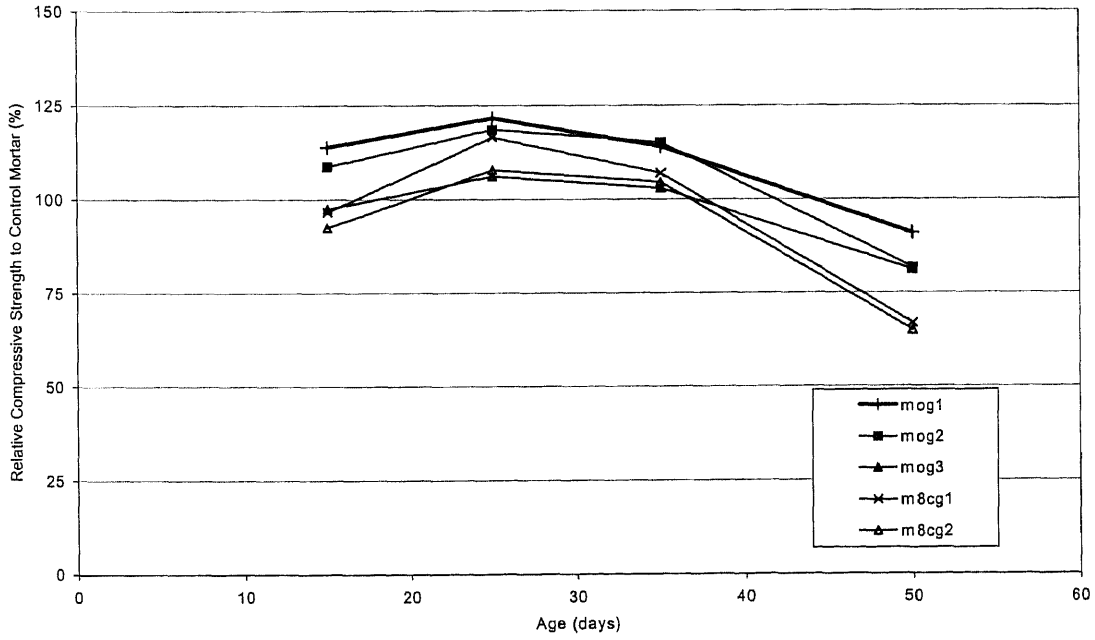

Figure 5.105 Relationship between Relative Compressive Strength at 28 days and Percent Replacement of Fly Ash

5.8.2 Strength Development of Ground Low NO_x Fly Ash Mortar

The strength development of the ground low NO_x fly ash mortar was observed with time. The effects of percent cement replacement and fineness on strength development of ground low NO_x fly ash was studied. The raw low NO_x fly ash was ground into three finenesses: GPU2G1, GPU2G2, and GPU2G3. Two cement replacement percentages were used in the mix: 25% and 35%.

5.8.2.1 25% Cement Replacement: The relationship between compressive strength of mortar containing 25% of ground low NO_x fly ash and its corresponding ages is shown in Figure 5.106. The compressive strength of the raw low NO_x fly ash is lower than that of raw wet bottom fly ash ages less than 14 days and is higher after that. The lower early strength of raw low NO_x fly ash mortar may be due to its possessing high amounts of unburned coal, which is considered a coarse particle. Since fineness has an effect on the dispersion and nucleation functions of fly ash, it makes sense that the wet bottom fly ash mortar, which had finer particle size distribution, had higher early strength. After 14 days, their strength increased significantly. This may be attributed to the higher pozzolanic action of the low NO_x fly ash in its mortar. With this high pozzolanic action, its 60-day compressive strength was almost as high as that of the control.

With 25% replacement of cement by ground low NO_x fly ash, all of their early strengths increased and surpassed the strength of control before 14 days. This may be because the ground low NO_x fly ash was so fine that it enhanced both the dispersion and nucleation effect of the fly ash. Comparing the ground fly ash mortars, the one with finer fly ash had higher compressive strength. At ages later than 14 days, all the strength of the ground fly ash mortars had higher strength than the control. Since the hydration

process in these mortars showed no progress, as seen from the flat slope of strength development of control, the strength contribution must come from the pozzolanic action of the fly ash. It is also noted that the slope of strength development of the fly ash mortar was increasing during the period from 14 to 120 days. This indicates that the pozzolanic action in these fly ash mortars was progressing during that period.

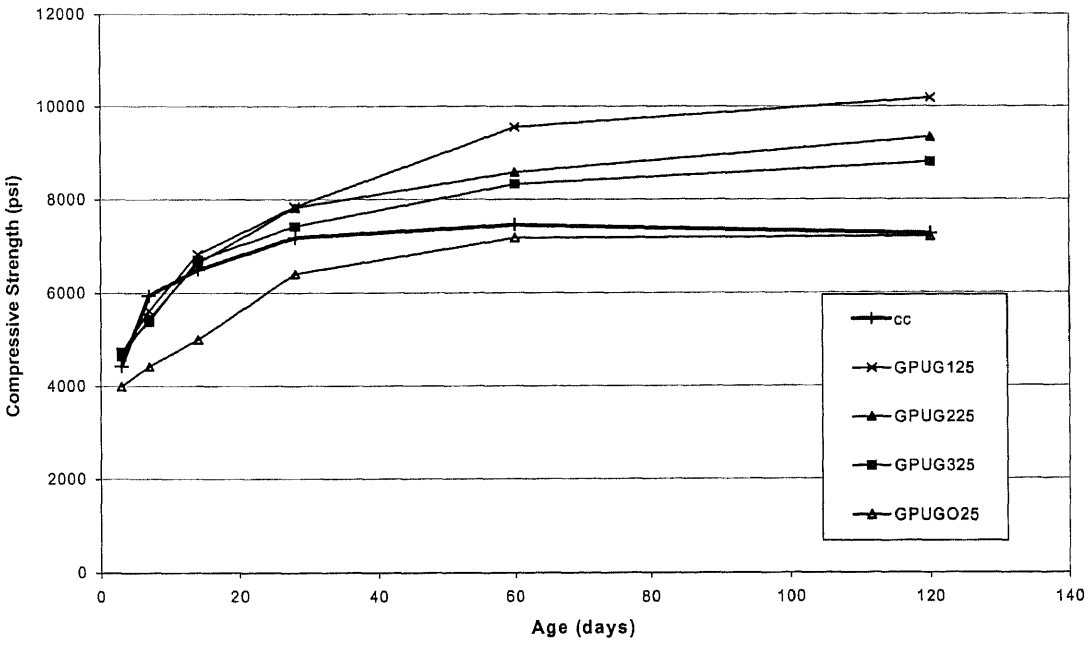

Figure 5.106 Relationship between Compressive Strength of the Ground Low NO_x Fly Ash Mortar (GPUG) and Age with 25% Replacement of Fly Ash

5.8.2.2 35% Cement Replacement: The relationship between the compressive strength of the ground low NO_x fly ash mortar with 35% replacement of cement and its corresponding age is shown in Figure 5.107. The results of this test are the same as for 25% replacement by ground low NO_x fly ash except that the strengths are lower. Most of the early strengths of ground low NO_x fly ash mortar are lower than that of control up to 28 days. Only the mortar containing the finest fly ash could reach the same strength as

the control mortar at an age of 14 days. The results show that the strength of ground low NO_x fly ash mortar depends not only on the fineness of the fly ash but also on the percentage of fly ash used. The greater the percentage of fly ash used in the mortar, the lower is the strength of that mortar.

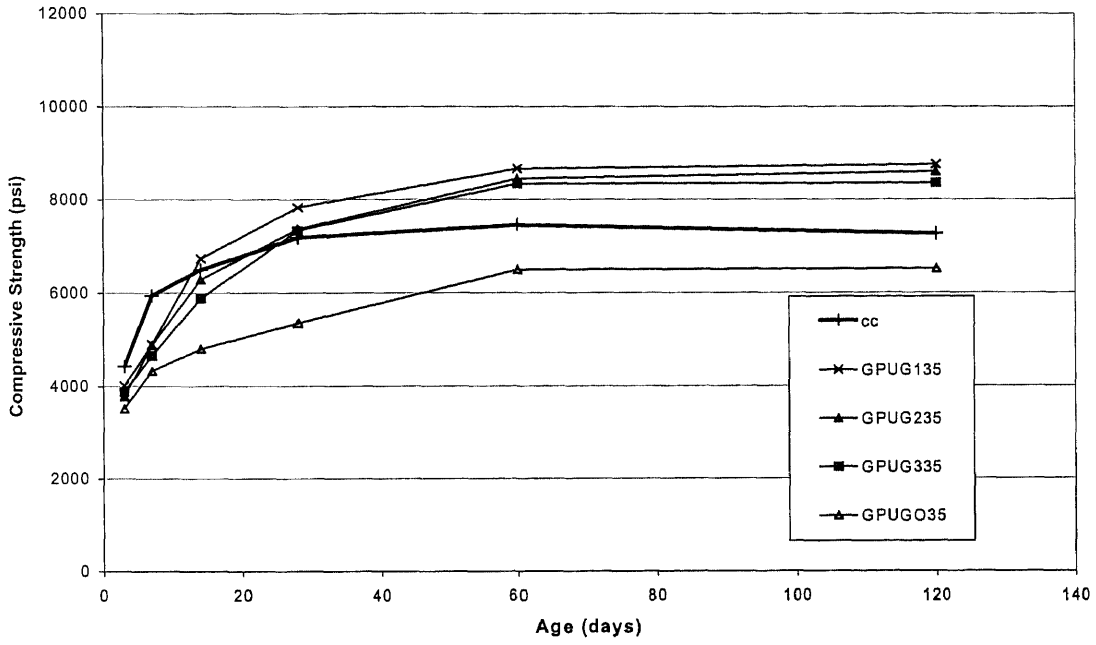

Figure 5.107 Relationship between Compressive Strength of the Ground Low NO_x Fly Ash Mortar (GPUG) and Age with 35% Replacement of Fly Ash

5.8.3 Strength Development of Ground Dry Bottom Fly Ash Mortar

The strength development of ground dry bottom fly ash mortar was examined with respect to time. The effect of cement replacement percentage and the fineness of the fly ash on compressive strength were studied. The dry bottom fly ash, which was treated with STI process, was ground into three size ranges: BTG1, BTG2, and BTG3. Two cement replacement percentages were used: 25% and 35%.

5.8.3.1 25% Cement Replacement: The relationship between the compressive strength of ground dry bottom fly ash mortar and age is shown in Figure 5.108. The compressive strength of raw dry bottom fly ash mortar with 25% replacement is somewhat lower than that of the control mortar at all ages. This is as expected, since the fly ash was not modified. Comparing the three raw fly ash mortars, the raw BOT fly ash mortar gives the lowest strength at later ages, while its early strength was in the same range as that of GPU2O. Since the strengths at later age is governed by the pozzolanic effect of fly ash, it is presumed that the lower late strength of BOT fly ash mortar is due to its lower pozzolanic activity. Results have shown that the pozzolanic activity is related to the percentage of amorphous phase. From Table 5.10 in Chapter 5.3, the percentage of amorphous phase of the BOT fly ash is higher than that of GPU2O fly ash. However, the coarse particle fraction in GPU2O has a higher percentage of amorphous phase, whereas, the coarse particles in BOT fly ash has lower percentage in the amorphous phase. Thus, the coarse particle in GPU2O, which is about 12% of the total could provide more pozzolanic action to the matrix than that in BOT.

As expected, the strengths of ground dry bottom fly ash mortars were higher than that of raw fly ash mortar and control mortar. This phenomenon is the same as that for other ground fly ash mortars. Because the coarser ground fly ash is present, this mortar's early strengths were less than those mortars with finer ground fly ash. The compressive strength of this ground fly ash mortar surpassed that of control after 14 days and gradually increased with age. It is also noted that for less than 14 days the strength of these ground fly ash mortars were very close, regardless of their fineness. One reason for this could be that within this range of fineness, the effect of dispersion and nucleation of

fly ash are about the same. Another explanation is that the percentage of fly ash is not enough to show the difference in their effects. However, the strengths of these ground BOT fly ash mortars were much different after the age of 14 days. The finer the particle size of the fly ash, the greater the rate of pozzolanic activity resulting in the faster rate of the strength development at later ages.

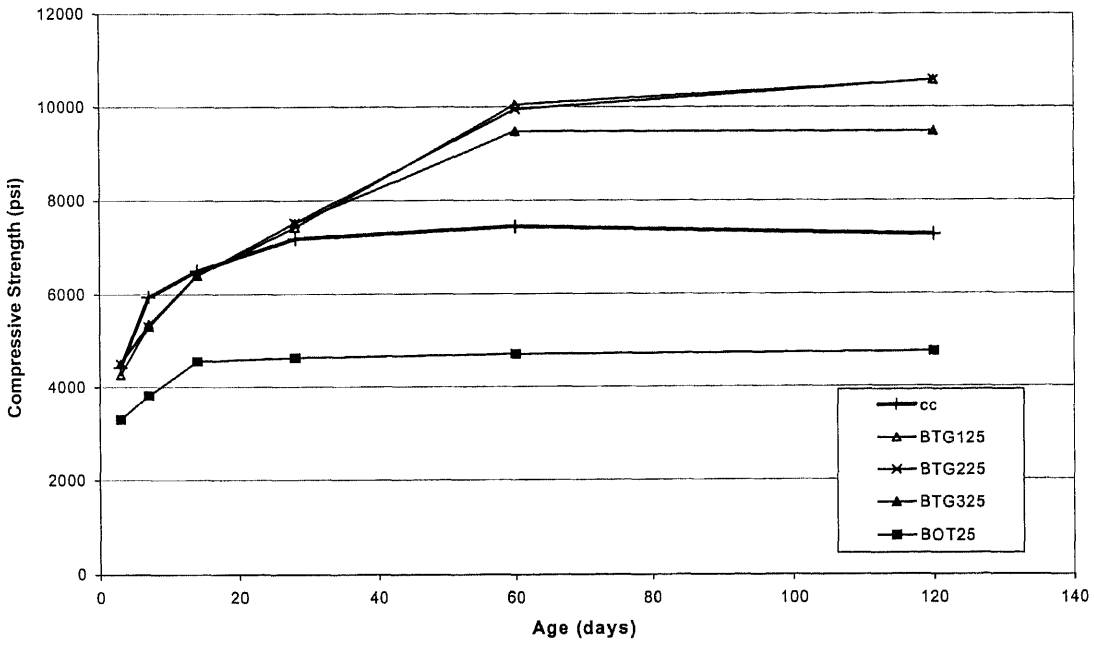

Figure 5.108 Relationship between Compressive Strength of the Ground BOT Fly Ash Mortar and Age with 25 % Replacement of Fly Ash

5.8.3.2 35% Cement Replacement: Figure 5.109 is the relationship between the compressive strength of the ground BOT fly ash mortar and age. With a higher percentage of fly ash in the mix, the early strengths of fly ash mortars were low. The difference between the early strengths of these mortars can be seen more clearly in this high-percent cement replacement. It is believed that the dispersion and nucleation effects of fly ash would increase more when more fly ash is used. The strengths of BTG135,

BTG235 and BTG335 fly ash mortars reached that of control mortar at ages of 14 days, 15 days, and 28 days, respectively. Their strengths increased at about the same rate until 60 days. After 60 days of curing, all fly ash mortars showed little gain in strength. This is contrary to observation by Hensen (1990) that the pozzolanic activity of fly ash proceeds and increases the strength of mortar until 3 years after the casting date. The strengths in this period were about the same as that of mortar with 25% replacement. Regarding the percentage of fly ash, which is source of pozzolanic action, the higher the percentage of fly ash, the more pozzolanic action its mortar should have. Because the pozzolanic activity between fly ash and $Ca(OH)_2$ depends on the percentage of both fly ash and $Ca(OH)_2$ in the paste, the sample with 35% may not have enough $Ca(OH)_2$ content to react with the fly ash.

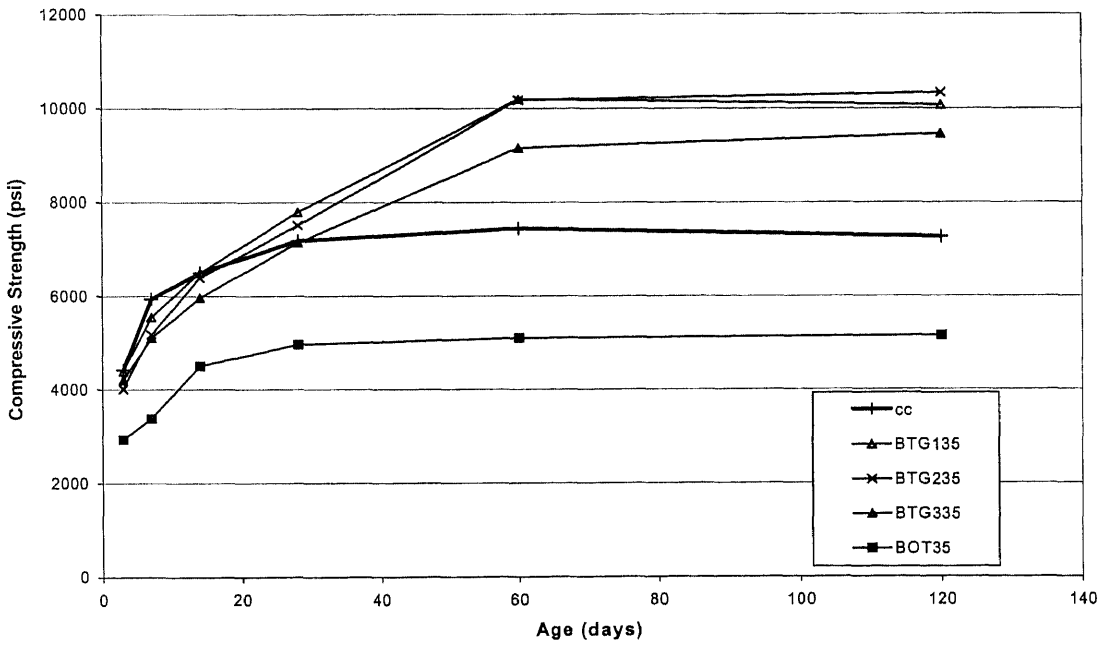

Figure 5.109 Relationship between Compressive Strength of the Ground BOT Fly Ash Mortar and Age with 35%Replacement of Fly Ash

In summary, the results show that at any age the strength of ground fly ash mortar increases with the decrease in the particle size of the fly ash that is incorporated with it. At all ages, the highest strength occurs in the samples with the finest particles of fly ash and the lowest strength occurs in the samples with the coarsest particles of fly ash. The ground fly ash mortar shows higher strength than the raw fly ash mortar.

The strength development of fly ash mortar can be separated into three stages: initial stage, intermediate stage, and final stage. In the initial stage, fly ash contributes strength to mortar by cement dispersion, which enhances the rate of hydration of the cement. The slope of strength development at this stage is high due to the increasing surface area of the cement particles. In the intermediate stage, ground fly ash increases the strength of mortar by its pozzolanic activity, whereby, the pH of the pore solution is high enough to leach out chemical compound, from the fly ash surface. These compounds react with $Ca(OH)_2$ in pore solution and form the C-S-H compound that gives strength to the matrix. The rate of strength development at this stage is low because it depends on the diffusion rate. In the final stage, the pozzolanic activity of fly ash continues to give strength to the matrix but the rate of strength development becomes less. This is because there is less $Ca(OH)_2$ in pore solution to react with, and because of the obstruction from the reaction product that precipitates on the fly ash surface. It is believed that both particle size distribution and the chemical composition of fly ash affect the rate of strength development. The optimum percentage of fly ash incorporated in the mortar follows the same order as the fineness of the fly ash. The finer the fly ash is, the greater the percent replacement of fly ash that can be used in mortar. It can be concluded that the fineness of fly ash has an effect on the optimum percentage of its use.

5.9 Characteristics of Ground Fly Ashes from Raw Feed and from Coarse Portion of Wet Bottom Fly Ash

Fly ashes in the market are heterogeneous in nature from the macro-through the micro-structural level. They have different densities, mineralogy, chemical compositions, and particle size distributions depending on the type of coal, grinding procedure, combustion procedures, type of furnace, and method of precipitation. The variations in the characteristics of fly ash make it difficult to be used as cement replacement. The grinding process can minimize the variations in particle size by breaking it into small particles that have a narrow range of distribution. Yet the differences in other characteristics still exist. This study will investigate the effects of other characteristics besides the particle size distribution on the strength of fly ash mortar. If their influences have fewer effects and the particle size plays an important role, the behavior of fly ash in concrete can be controlled via this grinding method.

When used as cement replacement, it is known that fly ash with a size below 10 microns gives better strength than normal cement. When fractionating is performed, only a small portion of the fly ash can be used, since the fine portion in raw fly ash is normally lower than 30%. The large portion of coarse fly ash left from the fractionating process has less value because it gives lower strength than normal cement. By using the grinding method, the total amount of fly ash can be used efficiently. It has been questioned in term of economic which fly ash is suitable for grinding. If raw fly ash is ground, part of the energy will be wasted in grinding the 30% by volume of fly ash that is already small and reactive. However if coarse fly ash is selected, fractionating is needed and more power is needed to grind coarse fly ash. This study has been conducted to investigate the property of mortar incorporating ground fly ash from both the raw and the coarse portion.

Fly ash generated by a wet bottom burner (MO) was classified into two categories: fine fly ash (M18F) and coarse fly ash (M18C). The size that separates these two fly ashes is 12 μm. Particle that is finer than this size is known to be reactive and is ready to be used. The coarse portion and the raw feed fly ash were then ground. M8CG and MOG1 are the ground coarse fly ash and the ground raw fly ash, respectively. Particle size distributions of these fly ashes including raw feed fly ash were measured by using the optical method. They are shown in chapter 5.2.

In order to obtain the same size as that of MOG1, coarse fly ash (M18C) was ground using two feed rates: 150 and 440 lb/hr. When the higher feed rate (440lb/hr) was used, the mean diameter of the ground fly ash, M8CG2, was bigger than that of MOG1. The bimodal curve of particle size distribution for M8CG2 shows that it still contains a certain amount of large particles. When the lower rate (150 lb/hr) was used, the mean diameter of M8CG1 was smaller than that of MOG1. Thus, the feed rate that yields fly ash having the same particle size as MOG1 must fall between 150 and 440 lb/hr. From this information it can be concluded that coarse fly ash can be ground to the same size as the grinding product of raw fly ash.

Table 5.14 Condition of Grinding Process Received from Union Process

Fly Ash	Feed Rate lb/hr	Original Particle Size				Final Particle Size				
		MV	90%	50%	SD	MV	90%	50%	SD	>10μm %
MOG1	330	21.15	54.22	11.83	19.19	6.32	12.22	3.42	3.42	13.51
M8CG1	150	35.94	79.83	21.92	17.63	5.78	8.72	2.94	2.08	8.16
M8CG2	440	35.94	79.83	21.92	17.63	6.26	12.57	4.58	3.97	16.94

The particle size distributions of the types of fly ash are compared based on their mean diameter (MV) and the standard deviation (SD). The MV value is selected because it is weighed by the presence of coarse particles that are not completely ground. The SD value provides the homogeneity of the particle size of fly ash. In term of MV, the ranking of fly ashes from fine to coarse particle is as follows: M8CG1<M8CG2<MOG1. Comparing the percentages of coarse fly ash bigger than 10 μm, the ranking of fly ash from fine to coarse is: M8CG1<MOG1<M8CG2.

The pozzolanic activity of each fly ash is determined by using the XRD technique. The amount of glassy phase on the surface of fly ash governs its pozzolanic activity since it dissolves at high pH value and gives silicate hydrate to form CSH in concrete. The total amount of the glassy phase of fly ash was calculated from the area under the amorphous curve in the diffraction graph, which is given in Table 5.15. When comparing the ground original fly ash (MOG1) and the fractionated fly ash (M13F), the amount of glassy phase of M13F is higher than that in MOG1. This result agrees with the studies by Fraay (1989) that fine particle has higher amount of glassy phase than coarse fly ash. MOG1 fly ash has a low amount of fine fly ash (30%) in its primary fly ash (MO), therefore it has lower amount of glassy phase than M13F fly ash. When comparing the ground original fly ash (MOG1) and ground coarse fly ash (M8CG1, M8CG2), the amount of glassy phase of the former is higher. This may be because MOG has a large amount of fine particles, which have a high amount of the glassy phase.

Table 5.15 Phase Percentage of Fly Ashes Measuring by XRD

Type of Fly Ash	Amorphous Phase (%)	Crystalline Phase (%)
MO	51.62	48.38
M13F	54.89	45.11
M18C	48.33	51.77
MOG1	50.27	49.73
M8CG1	45.04	54.96
M8CG2	46.04	53.96

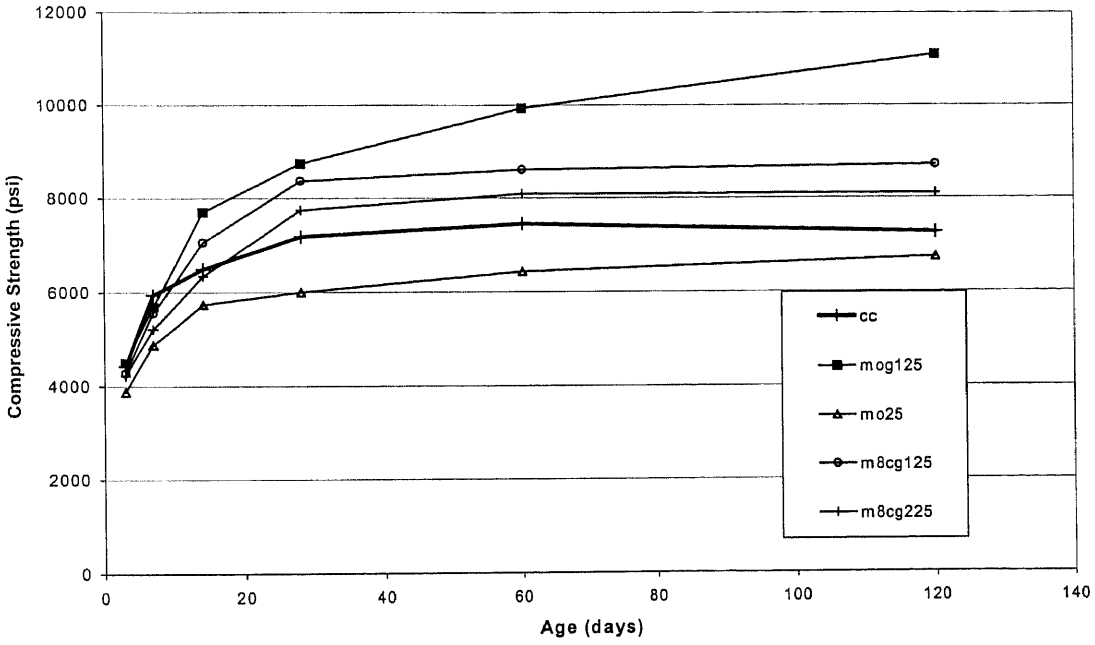

Figure 5.110 Compressive Strength of Ground Wet Bottom Fly Ash Mortar with 25% Cement Replacement

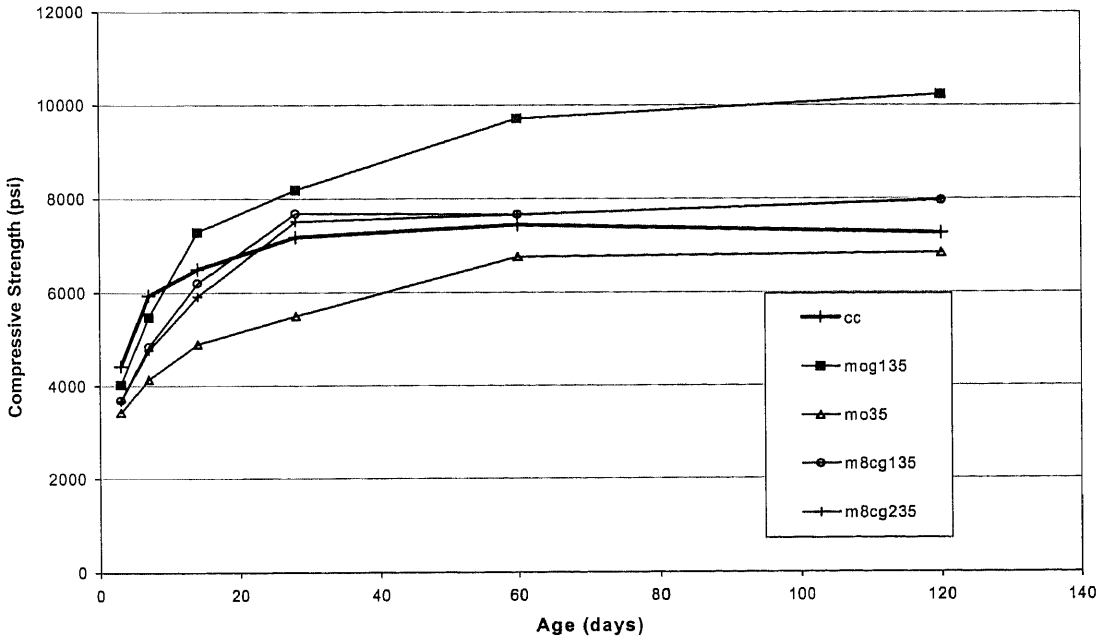

Figure 5.111 Compressive Strength of Ground Wet Bottom Fly Ash Mortar with 35% Cement Replacement

Figure 5.110 and Figure 5.111 shows the compressive strength of ground fly ash mortar with 25% and 35% cement replacement respectively. It can be seen from Figure 5.110 that M8CG1 and MOG1 mortars with 25% replacement develop strength at the same rate as normal cement mortar in the beginning period. As explained in the chapter 5.8 that the strength gain in the first period is due to the nucleation effect with the finer particle size giving higher strength than the coarser particle size. However when 35% replacement is used, its strength is not as high as that of normal cement in this early stage. Unlike M8CG1 mortar, the rate of strength gain of M8CG2 mortar for both 25% and 35% replacement is lower than for the normal cement mortar at the beginning period even if its MV is below 10 μm. This may be because it has a high percentage of particles bigger than 10 μm. Thus, fly ash should be ground to a certain size so it can have a

strength as high as normal cement at early ages. In addition to particle size, irregular shape of ground fly ash may add the strength to the mortar.

In later ages, the rates of strength gain increase significantly. For mortar with 25% replacement, the strength of M8CG1, and MOG1 mortar can surpass that of cement mortar at 10 days, and the strength of M8CG2 mortar can surpass that of cement mortar at 15 days. For mortar with 35% replacement, the strength of fly ash mortars surpass the strength of cement mortar at later ages than that of 25%, but their rates of strength gains are higher. The strength gain at later ages could be a result of pozzolanic activity, which depends on amount of glassy phase of fly ash. However it can be seen that the gaining strength rate caused by pozzolanic activity for these fly ashes are not much different, even though their amounts of glassy phase are different. Therefore, it can be concluded that the particle size distribution has more influence on the strengthening property than the mineralogy of fly ash. Hence, the ground fly ash from the coarse portion can exhibit the same strength as the ground fly ash from raw feed, if they are ground to the same particle size and used at the same mix proportion in the mortar.

5.10 Effect of Carbon in Fly ash on Fresh and Hardened Mortar

5.10.1 The Interaction of Carbon in Fly Ash with Air Entraining Admixture by Using ASTM 311

Comparison between adsorption of fly ash with high carbon and that of cement was examined. The LOI content is used to represent the amount of carbon in fly ash. The LOI of GPU1, GPU2, and M13F are 5%, 12%, and 2.7%, respectively. Loss of air content with time was observed. Figure 5.112, 5.113, and 5.114 demonstrate a tendency for the air content of GPU1, GPU2, and M13F fly ash mortar. The amount of AEA was measured at initial time, 45 min., and 2 hr. after mixing. The 2-hour time is the maximum because after this period the paste becomes solid. It can be seen that the air content decreases with time, which means that the fly ash continues to adsorb AEA.

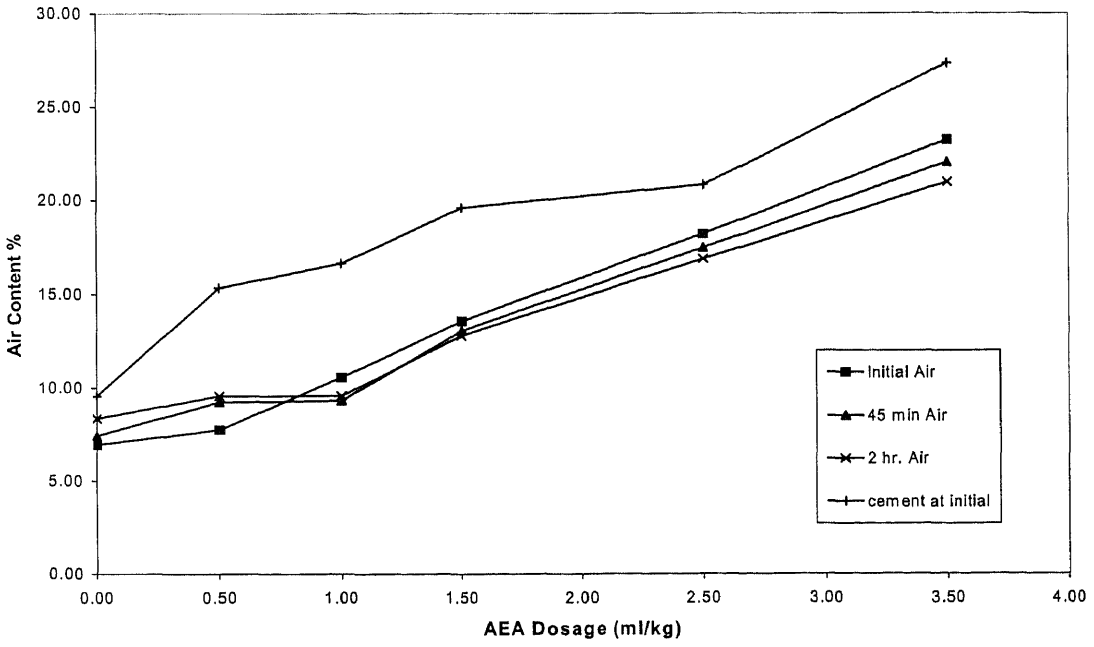

Figure 5.112 AEA Dosage versus Air Content in Low NO_x Fly Ash Plant I (GPU1) with 5% LOI

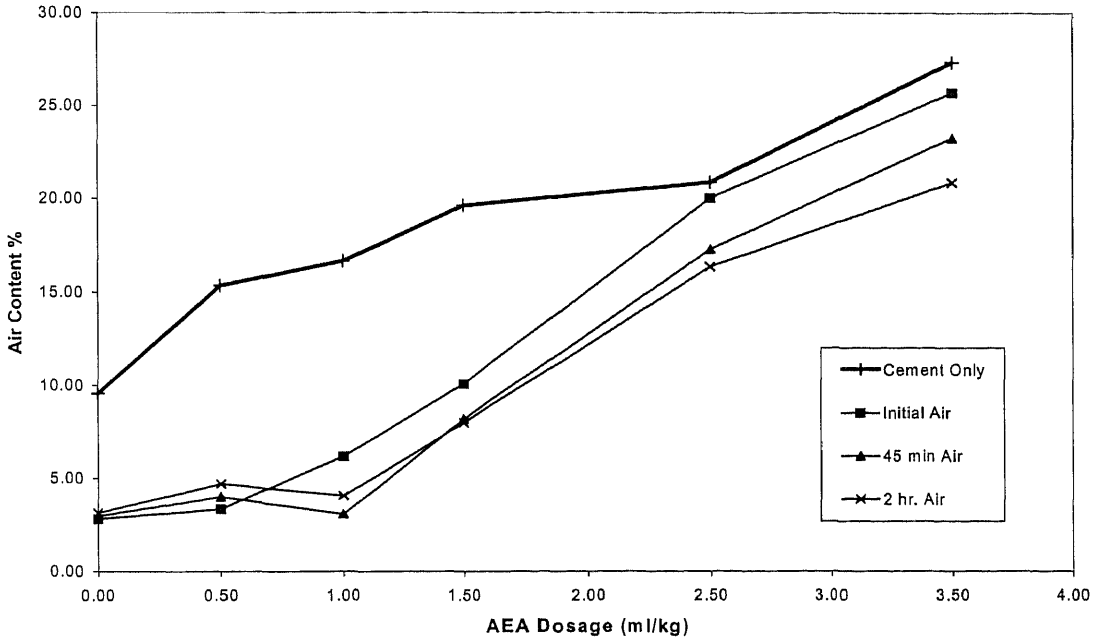

Figure 5.113 AEA Dosage versus Air Content in Low NO_x Fly Ash II Mortar (GPU2) with 12% LOI

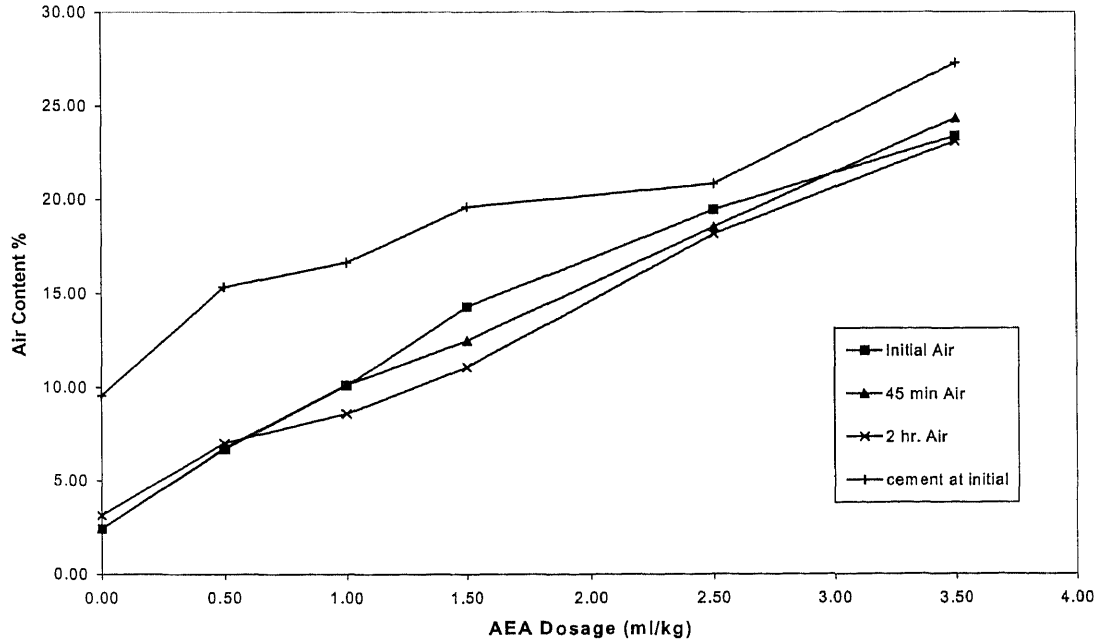

Figure 5.114 AEA Dosage versus Air Content in Fractionated Fly Ash Mortar (M13F) with 2.7% LOI

It can be seen from Figure 5.112- 5.114 that without additional of AEA the air content of fly ash paste has lower percentage than that of cement paste. This can be explained that fly ash liberates throughout the paste and fills most of the air void, which is calculated as an air content. As a result, there is less air content in the fly ash paste than cement paste.

When AEA was introduced to the paste at the dosage recommended by manufacturer to add in cement, air content of GPU2 fly ash paste does not increase much and it is still lower than normal cement paste. It can be seen that the air content of GPU1 GPU2 paste is flat until it reaches 1 ml./kg. Then their air contents of paste with AEA dosage from 1 to 2.5 ml./kg increase in the same rate as that of cement paste with AEA dosage from 0 to 1.5 ml./kg. This may be because at the low dosage, fly ash or its carbon adsorbs AEA until it reaches the maximum limit that it can no longer absorb AEA. Therefore the AEA does not help increasing the air content in the mix during this range. Another note is that the difference between the initial air content and the 45-min air content is quite small at this range. This can be because the AEA was not liberated from carbon or fly ash. The AEA dosage additional to 1 ml./kg can be considered as an effective AEA that is used to trap the air in the paste for GPU2 fly ash.

The effect of carbon content in fly ash on air content can be seen clearly by comparing air content of GPU1 and GPU2 fly ash mortar. The air content of GPU1 begins to increase at smaller dosage of AEA than that of GPU2. This is as expected since the GPU1 contains less carbon to adsorb AEA than GPU2. Thus, it lets the AEA do its work at lower dosage. It can be concluded that to achieve the equal air content the fly

ash with high carbon content needs more AEA dosage than the one with low carbon content.

Another media that may adsorb AEA is fly ash itself. In general, fly ash is spherical and solid particle that does not have pore. Only small percentage of fly ash is cenosphere that is filled with small sphere inside it. After it was ground, it posses angular shape. Therefore it is not likely that fly ash can adsorb the AEA. Figure 5.114 shows the air content versus AEA of M13F mortar. This fly ash is used since it has very low carbon content, so, the loss of air content is the effect of this fly ash. As seen from Figure 5.114, the air content of mixture is lower than that of cement. This can be explained as earlier that the fine particle of fly ash lowers air content by filling the air void. After adding more AEA, the air content increase in the same rate as that of cement. The slope is not flat as the air content of high carbon fly ash. This result suggests that the individual ground fly ash does not adsorb AEA but the carbon that mixed with fly ash does.

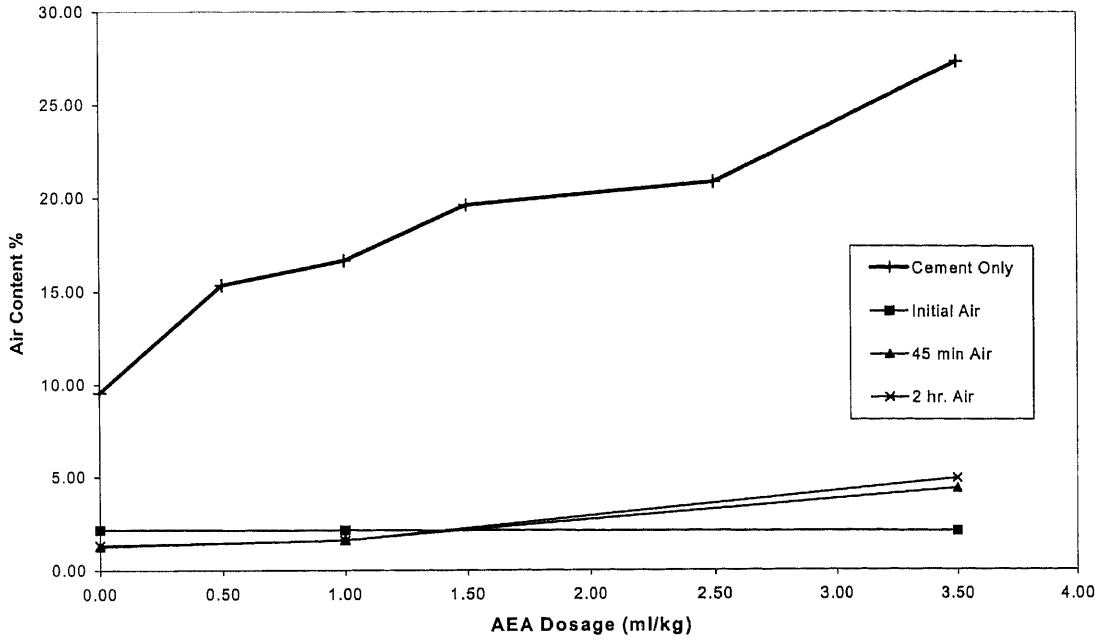

Figure 5.115 AEA Dosage versus Air Content in Ground Low NO_x Fly Ash II Mortar (GPU2G) with 12% LOI

Besides the amount of carbon, the size of carbon also has an influence on adsorption of AEA. The study was done by comparing air content of GPU2 and GPU2G. The GPU2G was prepared by grinding GPU2 down below 10 microns. This ground fly ash has about 4 times higher surface area than the raw fly ash. The air contents of GPU2 fly ash mortar versus AEA dosage is shown in Figure 5.115. It can be seen that the air content of GPU2G hardly changes even when higher dosage of AEA is used. The contents never pass 5%. As seen from micrograph of GPU2G in morphology section, the carbon in GPU2G is very porous. Therefore when they are crushed to fine particle, they will have larger surface area and disperses more evenly in the mixture. Since adsorption process depends on the contact area, therefore the ground fly ash, which has high specific surface than raw fly ash, can adsorb more AEA than raw fly ash. Not only that, the very

fine particle of fly ash may not promote the work of AEA. Therefore, as high dosage of AEA as 3.5 %, there is only slight increase in air content.

5.10.2 Effect of Carbon on Compressive Strength of Fly Ash Mortar Using Thermal Process for Reducing Carbon

The strength comparison of low and high carbon fly ash mortars were made between unground samples and ground samples. Three fly ashes with different carbon content were used: 0% (GPU2O, GPU2G), 6% (GPU2M, GPU2MG), and 12% (GPU2I, GPUIG). Non-carbon fly ash was prepared by burning at 750 °C. Fly ash with 6% carbon was obtained by mixing high carbon fly ash with non-carbon fly ash in equivalent weight.

Table 5.16 Specific Gravity and LOI of Material

Type	Specific Gravity	LOI %
Sand	2.66	0
Cement	3.15	0.73
GPU1	2.35	5.65
GPU2	2.31	12.18
GPU2G	2.62	11.58
M13F	2.75	2.67

Table 5.17 Air Content of Fly Ash and Mortar Paste with Different Dosage of AEA

AEA ml/kg	Air Content (%)												
	Cement	GPU1			GPU2			GPU2G			M13F		
	Initial	Initial	45min.	2 hr.	Initial	45min.	2 hr.	Initial	45min.	2 hr.	Initial	45min.	2 hr.
0	9.55	6.94	7.43	8.35	2.72	2.99	3.16	1.24	1.26	1.26	2.42	2.42	3.13
0.5	15.33	7.77	9.23	9.56	3.18	3.44	4.12	N/A	N/A	N/A	6.68	6.74	7.01
1.0	16.65	10.56	9.32	9.58	5.89	3.04	4.43	1.10	1.31	1.70	10.09	10.13	8.58
1.50	19.62	13.56	13.05	12.77	9.63	7.73	7.58	N/A	N/A	N/A	14.28	12.50	11.08
2.50	20.85	18.23	17.49	16.89	19.44	17.92	15.92	N/A	N/A	N/A	19.48	18.55	18.18
3.50	27.35	23.24	22.05	21.00	25.15	22.49	21.35	4.51	3.93	4.30	23.40	24.37	23.13

5.10.2.1. Distribution of Unburned Coal in Low NO_x Fly Ash: The distributions of fly ash and its carbon content were determined by sieving method. Raw feed fly ash was sieved into different size: #40, 50, 60, 80, 100, 140, 200, 230, 325, and 500. Particle size distribution of fly ash measuring by dry sieving method was conducted by calculating the weight percentage of fly ash retained on the sieve. Size distribution of carbon was conducted by calculating the weight percentage of carbon burnt out at 750 °C of each sieve. The results are shown in the following table.

Table 5.18 Particle Size Distribution of Raw Feed Fly Ash and Carbon by Using Sieving Method

U.S.	Microns	Wt. Of fly ash On Sieve (%)	Cumulative Wt. Of Fly Ash (%)	Wt. Of Carbon on Sieve (%)	Cumulative Wt.of Carbon (%)
Pan	0-31.11	2.18	2.18	0.083	0.133
500	104.7-148	2.08	4.26	0.122	0.327
325	148-176	75.04	79.3	5.617	0.585
230	176-248.9	3.34	82.64	0.760	1.508
200	248.9-296	5.82	88.46	1.651	2.643
140	296-418.6	3.12	91.58	0.945	3.679
100	31.11-44	1.83	93.41	0.521	4.986
80	418.6-704	3.53	96.94	1.363	6.041
60	44-62.3	1.27	98.21	0.639	7.941
50	497.8-592	1.20	99.41	0.529	9.460
40	592-704	0.59	100	0.293	0.293

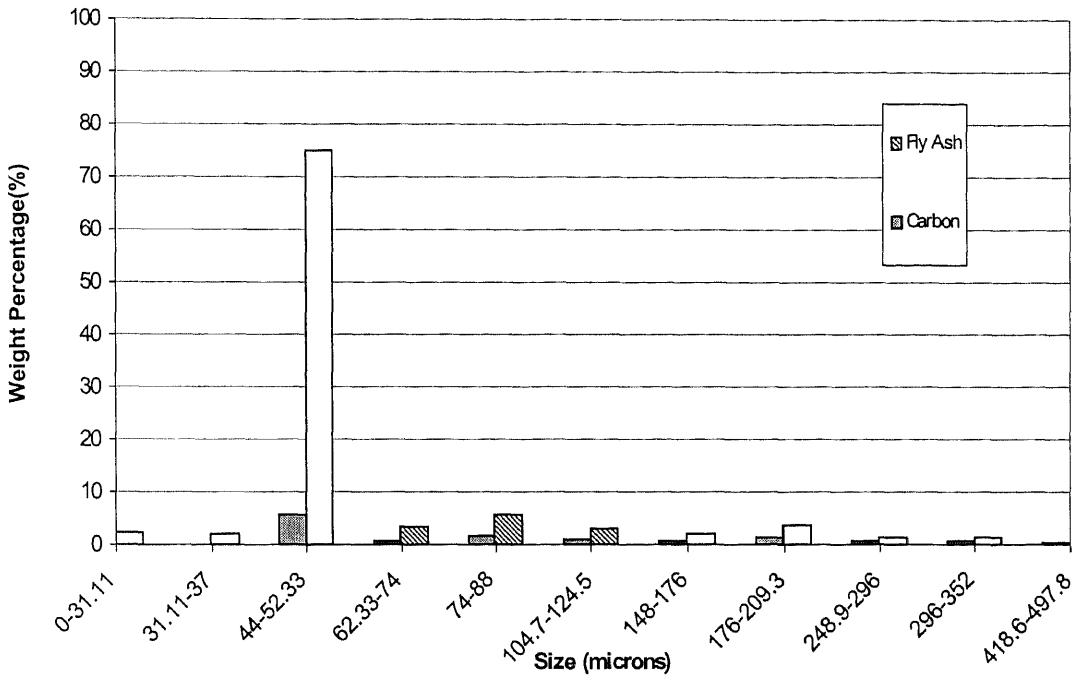

Figure 5.116 Distribution of Fly Ash and Carbon (LOI) in Raw Low NO_x Fly Ash (GPU2O)

By using sieving method, 80 % of fly ash is finer than 50 microns. It can be seen that coarse fly ash contains higher percentage of carbon than fine fly ash. However fine fly ash still contains a significant amount of carbon, 5.6% out of 12.5% of total carbon in fly ash. If fly ash that has size bigger than 53 microns is sieved out, only 6.9% of 12.5% of total carbon is removed. It also removed 20% of fly ash, which is coarse fly ash. 80% of fly ash, which has 5.6% carbon, is recovered. After grinding GPU2O, all particles are smaller than 10 microns.

5.10.2.2 Unground Fly Ash Mortar: The strength of unground Low NO_x fly ash mortars with and without carbon-treated are shown in Figure 5.117 and 5.118. As expected, the compressive strengths of the fly ash mortar samples were lower than that of

normal cement mortar specimens in early age. After 25 days the strength of fly ash mortar is higher than normal mortar. This increasing strength can be related to its pozzolanic activity. For unground fly ash series, It can be seen that strength of non-carbon fly ash mortar is higher than the strength of high carbon specimen at early age. The differences decrease with time. At later age their strengths are about the same. However, it cannot be concluded from this result that the strength of the specimen with low carbon content performs better than that high content. This is because the other characteristics such as particle size distribution and mineralogy of these fly ashes were not comparable. The order of fineness from fine to coarse of unground fly ashes is GPU2I, GPU2M, and GPU2O. The GPU2I is finer than GPU2O because most of the big particle, which is carbon, was removed by thermal process. Therefore, the higher strength of GPU2I may be a result of its finer distribution.

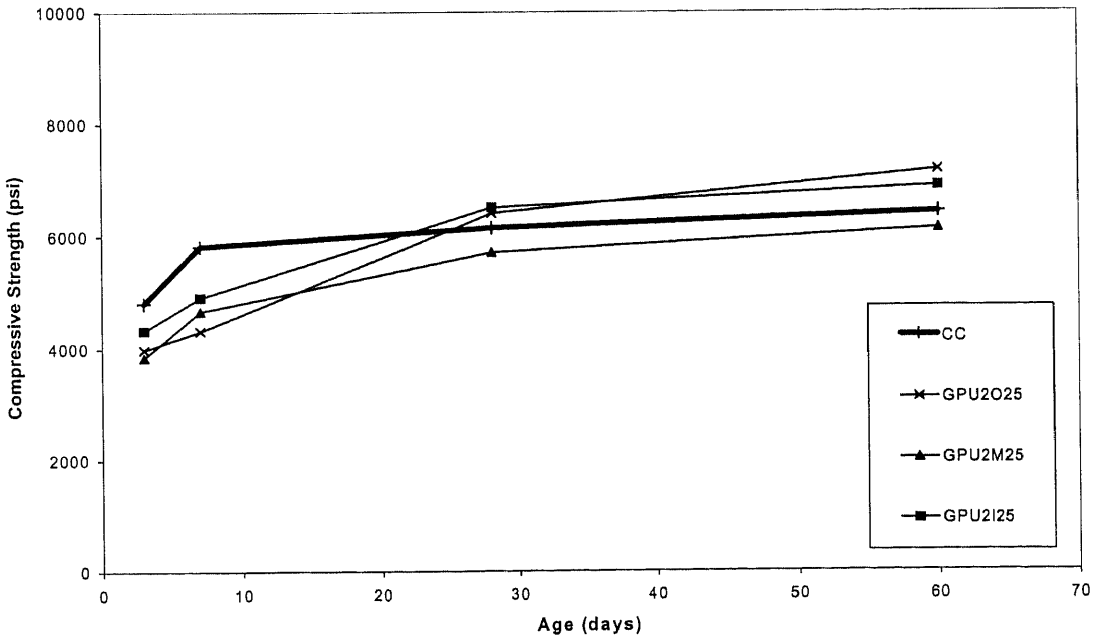

Figure 5.117 Effect of Carbon Content on Compressive Strength of Raw Low NO_x Fly Ash Mortar (25% Cement Replacement)

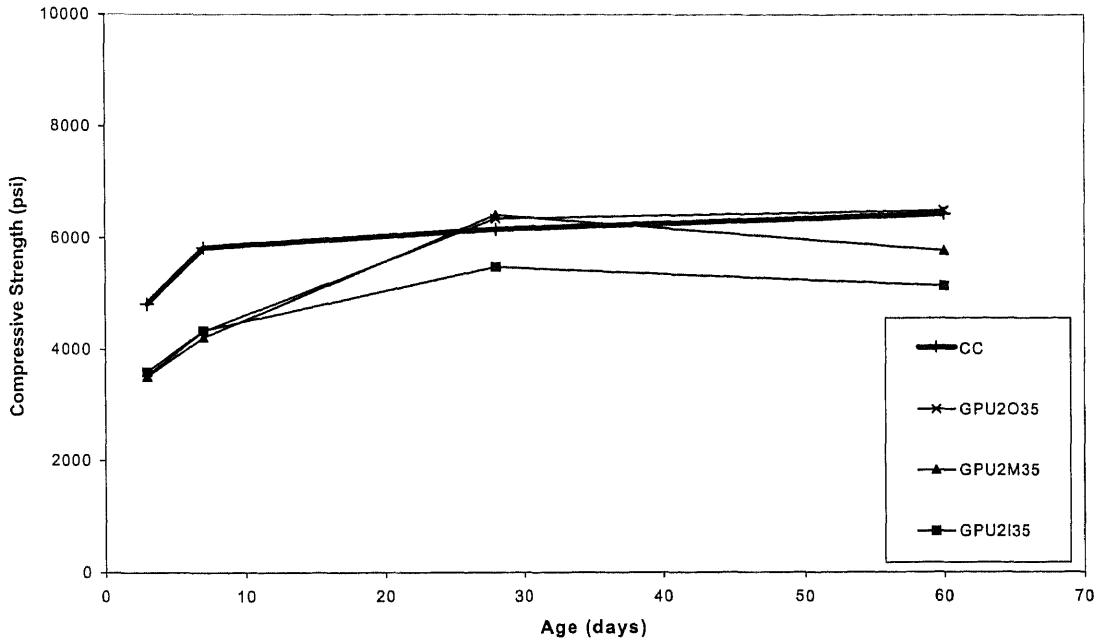

Figure 5.118 Effect of Carbon Content on Compressive Strength of Raw Low NO_x Fly Ash Mortar (35% Cement Replacement)

5.10.2.3 Ground Fly Ash Mortar: To see the effect from carbon content only, the fineness of their fly ashes was controlled by grinding it to the same size distribution. The particle size distribution of GPU2G, GPU2MG, and GPU2IG are shown in Figure 5.119. It can be seen that the PSD of GPU2G is below 10 microns while those of GPU2MG and GPU2IG have some particle bigger than 10 microns. From the grinding experiment, even though it was finer at the beginning, the ignited fly ash or non-carbon fly ash cannot be ground to finer particle size than this distribution. It may be because it became harder after it was burned at 750 C. Since the particle size distributions of these fly ashes are not the same, therefore both particle size and carbon content govern the strength of fly ash mortar.

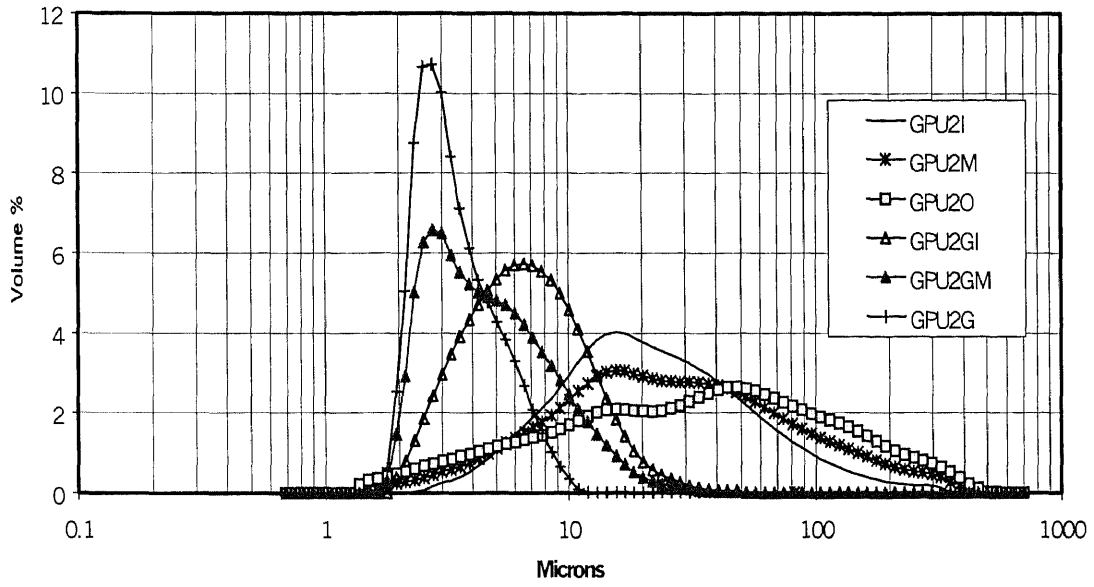

Figure 5.119 Particle Size Distribution of Fly Ashes with Different Carbon Content

Figure 5.120 and 5.121 demonstrate the comparison between strength development of ground fly ash mortar with different carbon content using 25% and 35% replacement respectively. The strengths of ground fly ashes are higher than those of unground fly ashes mortars as expected. Comparing between the strength of ground fly ash mortar, it can be noticed that the strength of GPU2G mortar is higher than GPU2IG mortar even though it has 12% higher in carbon content. Also, the strengths of GPU2G25 and GPU2G35 mortars surpass that of normal cement mortar at early age as 12-14 days. This result shows that coal when ground contributes the strength to the matrix. It is believed that coal has adverse effect on strength of fly ash mortar because it is porous and brittle. However after it is ground, it becomes angular solid particle, which can contribute strength through its chemical compound as well as fly ash. To prove this

hypothesis, the mineralogy of unburned coal in this fly ash was analyzed. It can be seen from Figure 5.122 that the intensity and angle of peaks of unburned coal (GPUC) match that of fly ash. By identifying phase, they have the same phase such as Anhydrite, Calcium Oxide, Hematite, Magnetite, Mullite, and Quartz. The unburned coal also has hump that represents the amorphous phase and may be more reactive than normal fly ash.

However, the strength of GPU2MG fly ash mortars, which has 6% carbon, is lower than that of GPU2IG in both 25% and 35% replacement even its size distribution is finer. This result does not follow with the above assumption that strength of fly ash mortar is the function of fineness. The mineralogy of ignited fly ash, GPU2I, is identical to that of GPU2O, meaning that the mineralogy of fly ash did not change during the thermal process. Therefore, this unexpected result would not be an affect of mineralogy.

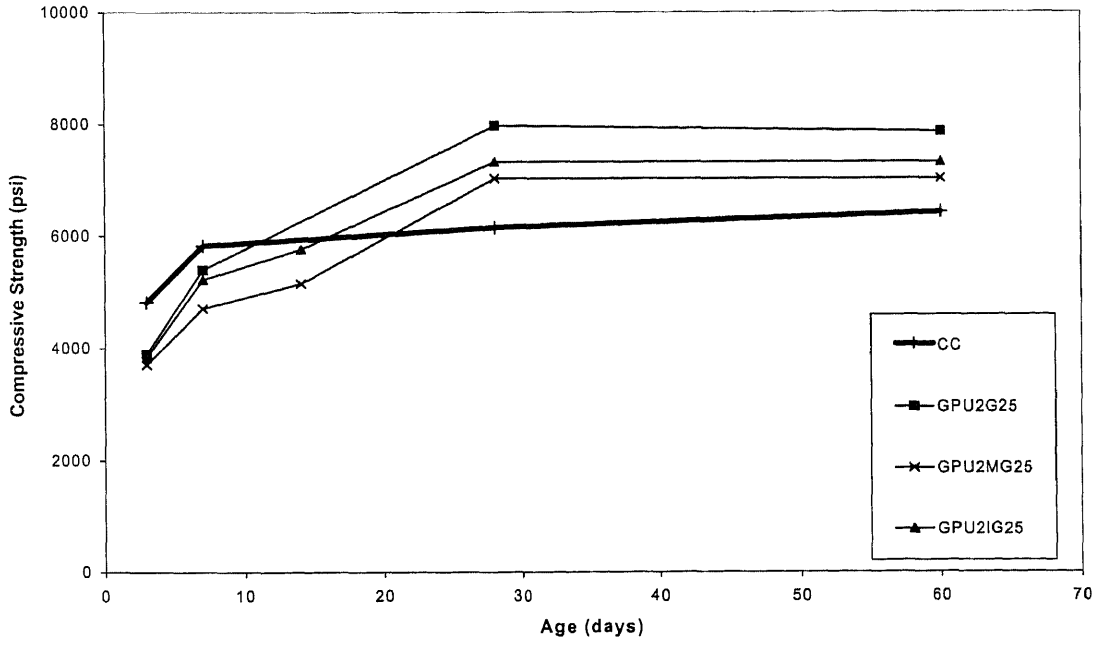

Figure 5.120 Effect of Carbon Content on Compressive Strength of Ground Low NO_x Fly Ash Mortar (25% Cement Replacement)

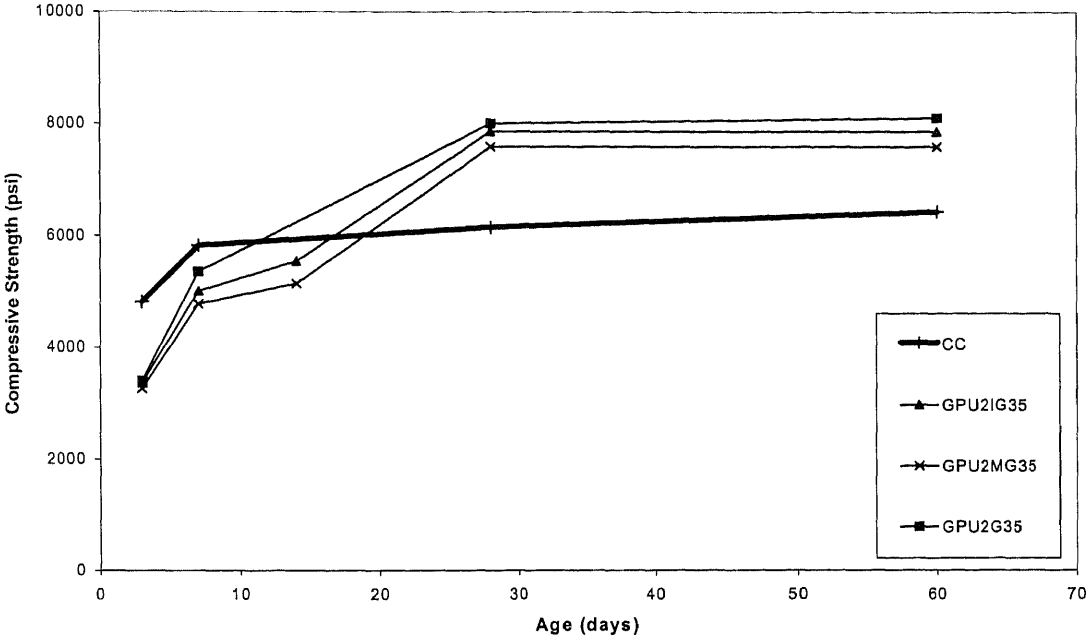

Figure 5.121 Effect of Carbon Content on Compressive Strength of Ground Low NO_x Fly Ash Mortar (35% Cement Replacement)

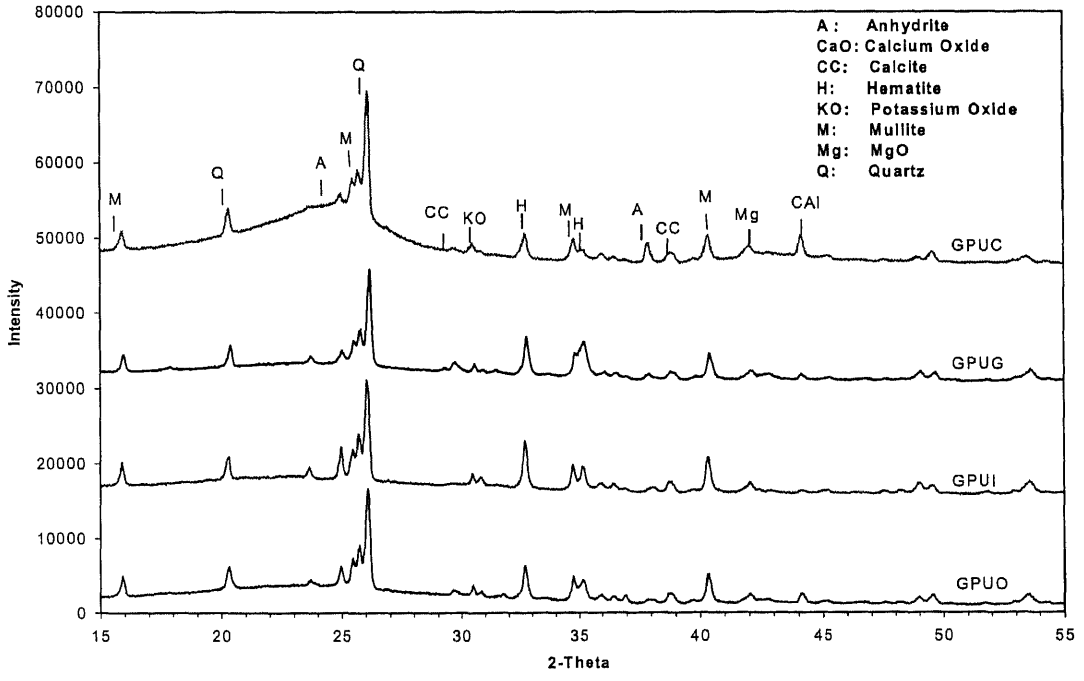

Figure 5.122 Mineralogy of Raw and Ignited Low NO_x Fly Ash

Another subject that was investigated is the microstructure of unburned coal particle. It is believed that the coal particle may have an effect on strength of ground fly ash mortar. After grinding, some of unburned coal may still be in porous form. This porous and brittle particle can be the weakest matrix of the mortar. It can be seen from micrograph of GPU2O fly ash in morphology section that it can be distinguished into several categories which are smooth spheres, spheres with irregular surface, unburnt coal, plerospheres, irregular particle, fused particles, conglomerates. Raw feed fly ash consists of spherical particles but there are some irregular porous materials in the sample. This porous particle is believed to lower the strength of raw low NO_x fly ash mortar.

After it was ground, there is no porous particle in GPU2G as seen from micrograph of GPU2G in morphology section. All unburned coals were ground to fine pieces which are angular. The ground fly ash has two types of general morphologies: a large proportion of spherical fly ash particles remained unchanged and broken fragment. All of spherical particles are fine as if they were not crushed during the process. The broken fragments can be distinguished into different morphologies: shell shaped fragments originated from cracking of cenospheres and plerospheres and solid fragments originated from solid particles.

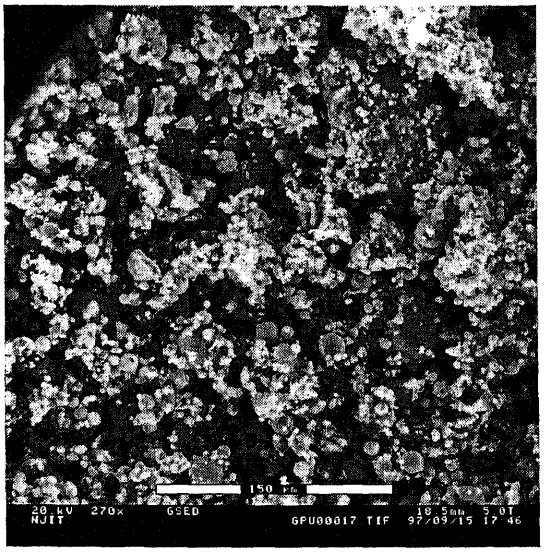

(a) GPU2O, 270x

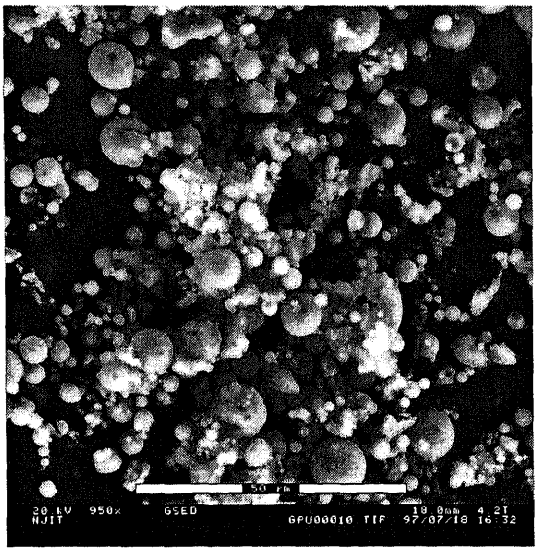

(b) GPU2I, 950x

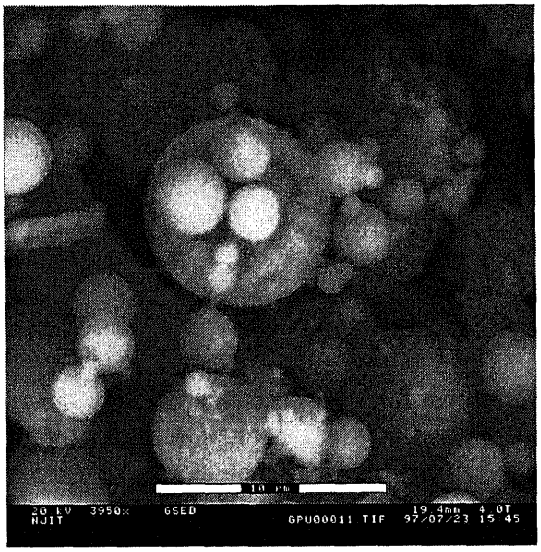

(c) GPU2I, 3950x

Figure 5.123 Micrograph of Low NO_X Fly Ash: (a) GPU2O, 270x; (b) GPU2I, 950x; (c)GPU2I, 3950x

Figure 5.123(b) and 5.123(c) show the micrograph of GPU2I, the ignited fly ash. Porous particle no longer exists in GPU2I and all the coal particles were burned out. In addition to that, some clusters of particles were attached together. This sintering may

occur during the thermal process in this study or during the combustion process in power plant which cannot be distinguished from this study. If it is the result of the thermal process, this sintering can increase the hardness of fly ash and make it difficult to grind.

It can be concluded from the result that the fineness of unburned coal in fly ash affects the strength of high carbon fly ash mortar. It can contribute strength to the matrix, if it is in finely divided form, possibly by its pozzolanic-like compounds. When it is ground, the strength of mortar using this fly ash can surpass that of normal cement mortar and ignited low NO_x fly ash mortar. Thus instead of using costly burning process to remove coal, the grinding process can be used to improve the quality of Low NO_x fly ash. The effect of percentage of unburned coal in fly ash cannot be confirmed clearly by using Thermal Process to vary the carbon content.

5.10.3 Effect of Carbon on Compressive Strength of Fly Ash Mortar Using STI Process for Reducing Carbon

In this study, unburned coal was removed by using Electrostatic technique, so called STI process. This process does not change the mineralogy of the fly ash, hence only the fineness and carbon content are the factors that cause the difference between them. The LOI of BO and BOT fly ashes are 4.5% and 1.47%. The particle size distribution of BO and BOT are shown in Figure 5.124. The compressive strengths of these fly ash mortars with 25%, 35%, and 50% replacement are shown in Figure 5.125, 5.126 and 5.127 respectively.

Table 5.19 Percentage of Carbon in Each Sieve Size

Fly Ash	<300 μm	300-600 μm	600-850 μm	>850 μm
BO	2.386468	12.96045	36.40382	48.24926
BOT	0.424193	9.359586	54.62594	34.73261

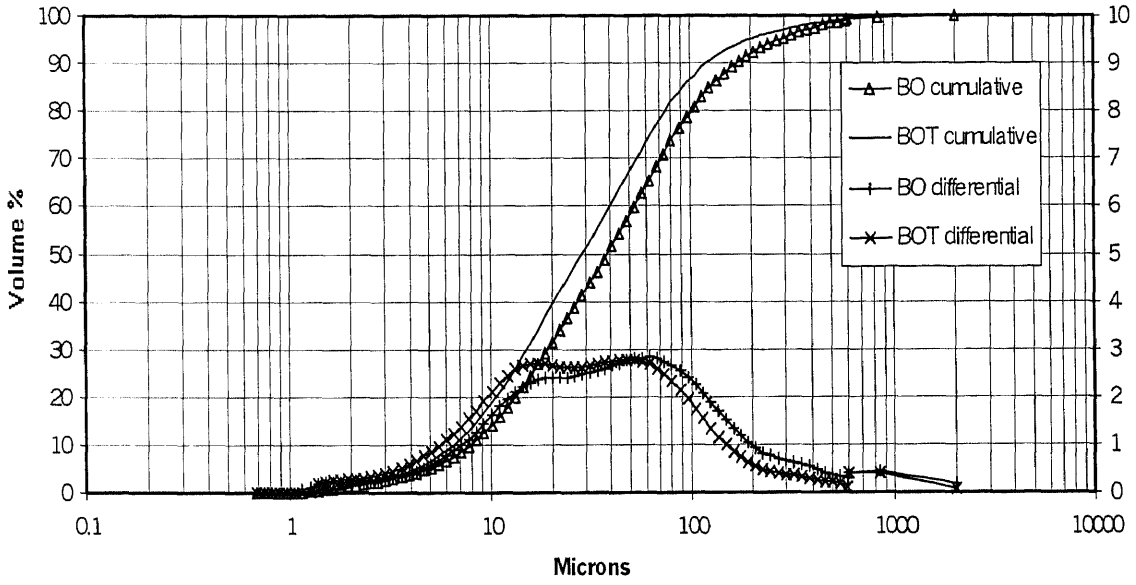

Figure 5.124 Particle Size Distribution of BO and BOT Fly Ashes

It can be seen from Figure 5.124 that the size distributions of BO and BOT are very close to each other. The BOT fly ash has less coarse particles than that of BO fly ash. By consulting with Table 5.19, it can be seen that the percentage of carbon in the coarse size range of BO fly ash was reduced when it was processed. Therefore, the size distribution of BOT is finer since some of its carbon was removed. However the difference in their PSD is considered negligible, thus, the difference in strength would be

a function of the carbon content only. It can be seen that the strengths of these fly ash mortars are much lower than that of control. This is because most of their particles are coarse. About 10-15% of their particles is valuable. Comparing the strengths of high and low carbon fly ash mortar, those of the latter are higher. This result replicates on all percentage of cement replacement. It can be concluded that if raw fly ash has higher carbon content, it reduces the strength of mortar that it incorporating with.

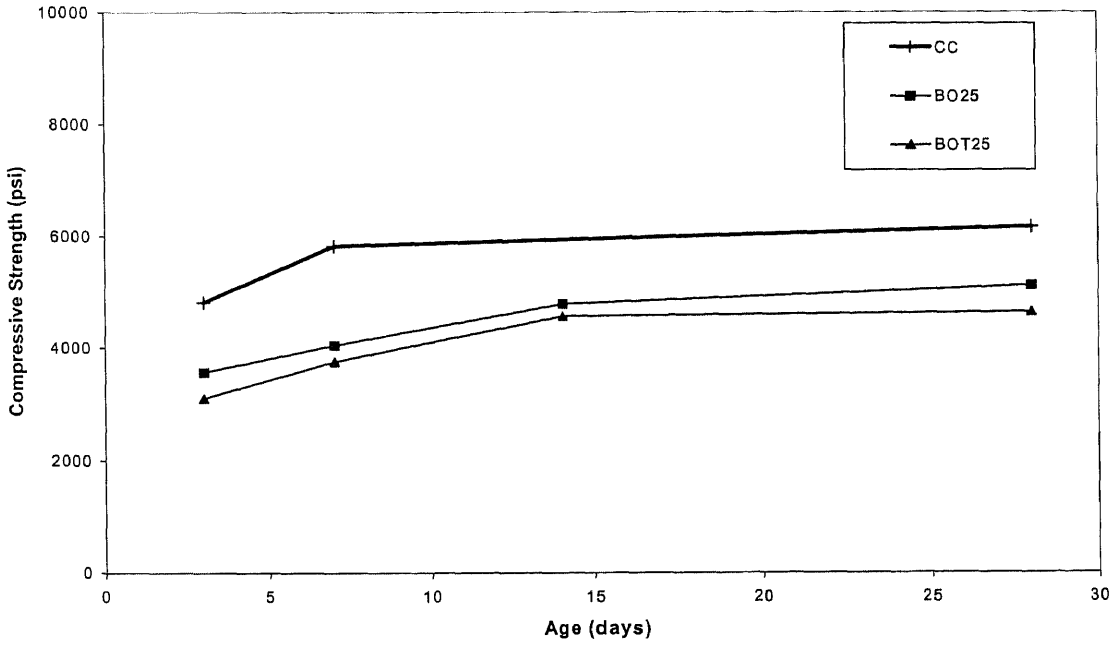

Figure 5.125 Effect of Carbon Content on Compressive Strength of BO Fly Ash Mortar (25% Cement Replacement)

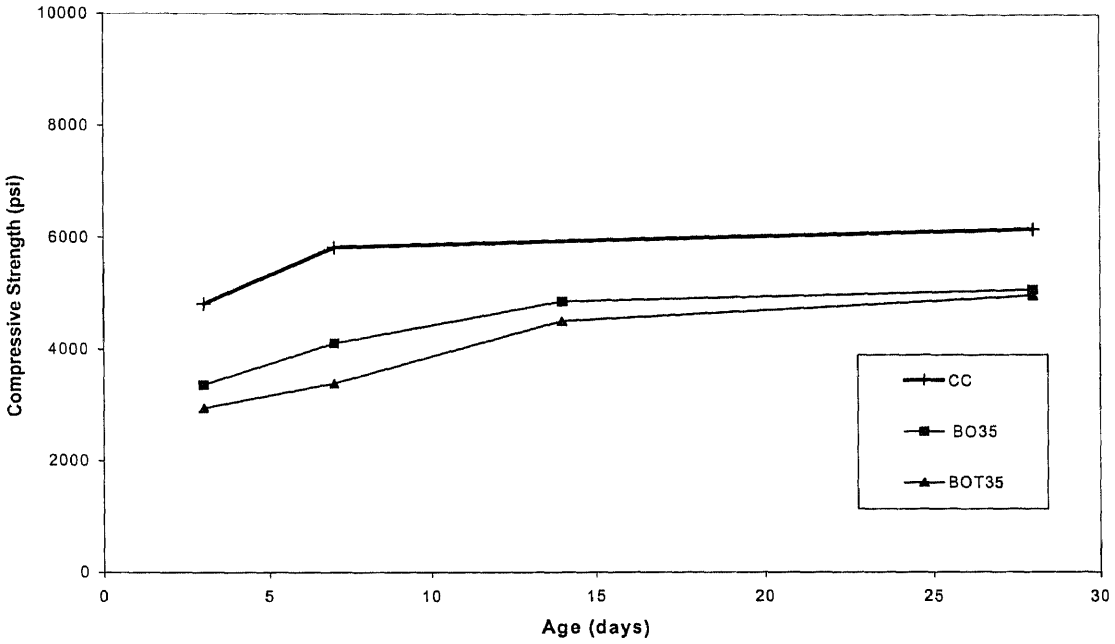

Figure 5.126 Effect of Carbon Content on Compressive Strength of BO Fly Ash Mortar (35% Cement Replacement)

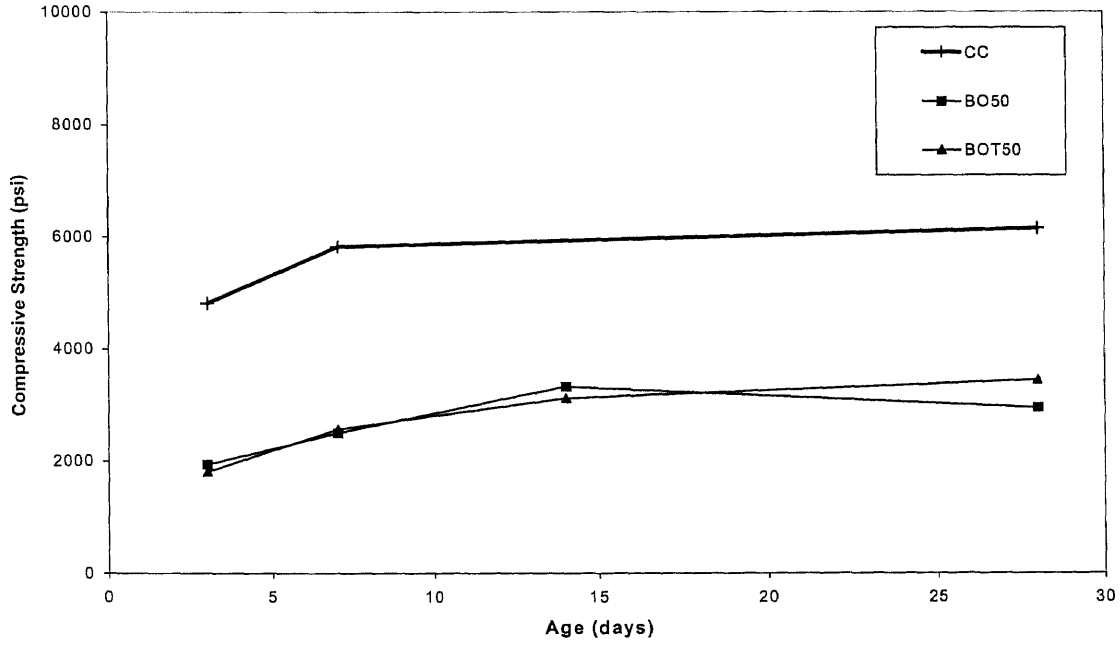

Figure 5.127 Effect of Carbon Content on Compressive Strength of BO Fly Ash Mortar (50% Cement Replacement)

CHAPTER 6

CONCLUSIONS AND SUGGESTIONS

The grinding method is an effective means to process raw wet bottom, dry bottom, and low NO_x fly ash into beneficial products. The quality of fly ash increases significantly after grinding. With cement replacement percent up to 42%, the strength of ground fly ash mortar performed as well as or better than plain cement mortar after 14 days. It was proved that the ground fly ash increases the strength properties of mortar because its fineness enhances the three mechanisms operating for strength gain: dispersion, nucleation, and pozzolanic activity. The conclusions that can be drawn from this study are shown as section by section basis as follows:

6.1 Grinding Process

1. To reduce the effect of iron, which is contaminant from using steel balls as a media, the zirconium beads were used throughout the study. Hence, the change in properties of ground fly ash mortar would be caused by the properties of fly ash itself.
2. The size distribution of fly ash becomes smaller with the longer grinding time. However, after a certain amount of grinding, the size of fly ash was not significantly reduced. Thus, there is a practical limit for size reduction for a given grinding condition.
3. The type of fly ash has a significant effect on grinding efficiency. Using the same grinding condition, the low NO_x fly ash, which was originally coarser, was ground to smaller size than the dry bottom fly ashes.

4. The optimum media-to-fly ash ratio, at constant volume are as follows: 2.5:1 for wet bottom fly ash, 2:1 for dry bottom fly ash, and 2:1 for low NO_x fly ash.

6.2 Chemical Composition and Mineralogy of Processed Fly Ashes

1. The chemical composition of ground fly ash varies slightly from its primary fly ash. The increased iron content comes from the wear of the arms and bowl of grinder.
2. The LOI content of the raw low NO_x fly ash was higher than that of wet bottom and dry bottom fly ash and higher than the acceptable value 4% under ASTM. However, this unburned coal chemically contributes strength to mortar since it is also composed of silica and alumina oxides which can react to form pozzolanic byproducts.
3. The percentages of silica and aluminum oxides can not be used to determine the potential pozzolanic activity of fly ash because much of it is in crystal phases, which could not be dissociated from the fly ash.
4. The percentage of fly ash in the amorphous phase, calculated from the area under the halo of X-ray diffractogram of fly ash, was used to determine the potential pozzolanic activity of fine or ground fly ash. It cannot be used to analyze the potential pozzolanic activity of raw fly ash since much of the amorphous phase is embedded within the coarse particle of fly ash.
5. The fineness of the fractionated fly ash has an effect on the percentage of amorphous phase of fly ash, the finer the fractionated fly ash the larger percentage in the amorphous phase.

6. The ground fly ash has slightly lower percentage of amorphous phase than its original fly ash. This is because grinding process introduces metal, crystalline phase, to the ground fly ash.
7. Using the percentage of amorphous phase as a measure of potential pozzolanic activity, the ground wet bottom fly ash provides the highest potential pozzolanic activity among the fly ashes tested.

6.3 Morphology and Elemental Analysis of Fly Ashes

1. The particle size of fly ash observed from the micrograph was in agreement with the particle size measured by optical method.
2. The raw wet bottom fly ash consists mostly of fine spherical particles. Its ground fly ash contains the angular particles and fine spherical particles. The raw low NO_x fly ash has also a large percentage of porous particles, which are unburned coal. The raw dry bottom fly ash was predominantly clusters of fused particles and some of fine particles.
3. The ground fly ashes contain mostly angular particles, broken clusters and fine spherical particles.

6.4 Effect of Ground Fly Ash on Hydration Process

1. For ages up to 24 hours, the fly ash paste has fewer cement hydration products, as measured by calcium hydroxide, than that of cement paste due to the dilution effect.

2. Pastes containing fine fly ash generate more hydration products than the paste containing coarse fly ash. This is because the fly ash disperses the cement grains more evenly throughout the paste, exposing more cement for hydration.
3. Since pozzolanic products cannot be observed by XRD, the consumption of calcium hydroxide in fly ash paste can be used as an indicator of potential pozzolanic activity of fly ash.
4. It was found that the pozzolanic action of all fly ash pastes, including raw, began at an early age.

6.5 Microstructure Study of Pastes Containing Processed Fly Ash

1. During the mixing period, the fly ash particles disperse the cement grains to smaller grains. The finer the fly ash, the smaller the cement grains.
2. The fly ash particle acts as a nucleation site for growth of hydration product starting at an early age. The finer the particles, the larger the numbers of nucleation sites for the hydration process.
3. At later ages, the pozzolanic action on some fly ash particle is discernable from the deterioration of the surface of fly ash particle.

6.6 Pore Size Distribution of Fly Ash Cement Paste

1. The finer the pore size of the fly ash paste, the higher the compressive strength of the mortar.
2. Additional to the dispersion mechanism of fly ash that reduces the pore size during the mixing, the pore size of all fly ash pastes continues to decrease with curing time

by the nucleation and pozzolanic action which fill the voids between grains with their products. The interconnection of these layers between particles is the major effect that strengthens the matrix bond at early ages.

3. The fineness of fly ash enhances dispersion, nucleation, and pozzolanic activity. Pastes containing finer fly ash yield a finer average pore size than the pastes containing coarse fly ash.
4. The dispersion function of fly ash was observed from the pore size distribution of the 5-minute paste. When fly ash was present, the cement grains were more dispersed, resulting in a finer pore size distribution. This function was enhanced when finer fly ash was used.
5. Between the 3rd and 7th day of hydration, the pore size of fly ash paste was reduced due to the nucleation effect. The decrease in pore size in finer fly ash pastes results from the presence of more particles acting as nucleation centers for hydration products.
6. The pore size reduction at age of 28 days could be a result of both nucleation and pozzolanic action. The evidence of nucleation is the thicker hydration products on fly ash particles and the evidence of pozzolanic action are the deterioration in some fly ash particles as well as the depletion of calcium hydroxide content.

6.7 Strength Development of Ground Fly Ash Mortar

1. Using ground fly ash can increase the rate of strength gain of mortar. The strength of ground fly ash mortar can surpass that of control mortar within 7 to 10 days which is much quicker than the 120 days needed for raw fly ash mortar.

2. The finer the fly ash, the higher the percent of possible cement replacement. The optimum cement replacement percentage, meaning the same strength as control at 14 days, for MOG1, MOG2, MOG3, and M8CG1 fly ash mortars was 42%, 40%, 25%, and 32%, respectively.
3. The strength at any age of ground fly ash mortar, even the low NO_x fly ash, increases with decreasing in fly ash particle size.
4. The fineness of fly ash plays more important role in the early strength while the mineralogy of fly ash does in the later strength.

6.8 Characteristic of Ground Fly Ashes from Raw Feed and from Coarse Portion of Wet Bottom Fly Ash

The type of primary fly ash does not have a significant affect on the strength development of ground fly ash mortar. When incorporating in mortar, the M8CG1 fly ash provided strength similar to the MOG1 fly ash even though their mineralogy is different.

6.9 Effect of Carbon in Fly Ash on Fresh and Hardened Mortar

1. It is found that only the unburned carbon, not the spherical particle in fly ash, adsorbs the AEA. Fly ash with high carbon content adsorbs a larger amount of AEA than the fly ash with low LOI.
2. The size of carbon also has an influence on the adsorption of AEA. The fine carbon in ground fly ash adsorbs more AEA than the carbon in raw fly ash. The finer the carbon, the higher surface area is to adsorb AEA.

3. To achieve equal air content, fly ash paste requires a larger amount of AEA than the normal cement paste.
4. The ground fly ash mortar with high carbon content performs better than that of normal mortar and the ground fly ash mortar without carbon. This is because unburned coal contributes strength through its fine fineness and pozzolanic activity.

6.10 Suggestions for Future Research

1. Study the freeze-thaw behavior of ground fly ash mortar containing high carbon content.
2. Study the mechanical properties such as flexural strength, tensile strength and modulus of elasticity of ground fly ash concrete .

APPENDIX A

COMPRESSIVE STRENGTH OF GROUND FLY ASH MORTAR

Table A 1 Compressive Strength of the Ground Fly Ash (Originating from Coarse and Raw Wet Bottom Fly Ashes) Mortar with 15% Replacement

Sample No.	Compressive Strength (psi)					
	3-d	7-d	14-d	28-d	60-d	120-d
CC	4425	5937	6498	7188	7451	7268
MO15	4009	5500	5869	6744	6830	7033
MOG115	4873	5770	7150	8182	9183	9152
MOG215	4840	5664	6550	7820	8053	8508
MOG315	4450	5628	6588	7004	7093	7539
M8CG115	4790	5720	6293	6946	7542	9091
M8CG215	4500	5803	6208	6644	6928	8238

Table A 2 Percentage Compressive Strength of the Ground Fly Ash (Originating from Coarse and Raw Wet Bottom Fly Ashes) Mortar with 15% Replacement

Sample No.	Percentage Compressive Strength (%)					
	3-d	7-d	14-d	28-d	60-d	120-d
CC	100	100	100	100	100	100
MO15	91	93	90	94	92	97
MOG115	110	97	110	114	123	126
MOG215	109	95	101	109	108	117
MOG315	101	95	101	97	95	104
M8CG115	108	96	97	97	101	125
M8CG215	102	98	96	92	93	113

Table A 3 Compressive Strength of the Ground Fly Ash (Originated from Coarse and Raw Wet Bottom) Mortar with 25% Replacement

Sample No.	Compressive Strength (psi)					
	3-d	7-d	14-d	28-d	60-d	120-d
CC	4425	5937	6498	7188	7451	7268
MO25	3873	4885	5738	6000	6428	6735
MOG125	4498	5684	7711	8737	9934	11095
MOG225	4226	5130	7300	8521	9505	10777
MOG325	3900	4759	6509	7629	8731	9349
M8CG125	4276	5553	7058	8373	8606	8714
M8CG225	4224	5206	6342	7750	8089	8100

Table A 4 Percentage Compressive Strength of the Ground Fly Ash (Originating from Coarse and Raw Wet Bottom) Mortar with 25% Replacement

Sample No.	Percentage Compressive Strength (%)					
	3-d	7-d	14-d	28-d	60-d	120-d
CC	100	100	100	100	100	100
MO25	88	82	88	83	86	93
MOG125	102	96	119	122	133	153
MOG225	96	86	112	119	128	148
MOG325	88	80	100	106	117	129
M8CG125	97	94	109	116	115	120
M8CG225	95	88	98	108	109	111

Table A 5 Compressive Strength of the Ground Fly Ash (Originating from Coarse and Raw Wet Bottom Fly Ashes) Mortar with 35% Replacement

Sample No.	Compressive Strength (psi)					
	3-d	7-d	14-d	28-d	60-d	120-d
CC	4425	5937	6498	7188	7451	7268
MO35	3429	4136	4892	5500	6759	6845
MOG135	4033	5470	7295	8192	9713	10226
MOG235	3970	5051	7290	8271	8933	9000
MOG335	3933	4641	6209	7403	8300	8384
M8CG135	3689	4839	6200	7684	7669	7958
M8CG235	3668	4764	5911	7516	7660	7979

Table A 6 Percentage Compressive Strength of the Ground Fly Ash (Originating from Coarse and Raw Wet Bottom Fly Ashes) Mortar with 35% Replacement

Sample No.	Percentage Compressive Strength (%)					
	3-d	7-d	14-d	28-d	60-d	120-d
CC	100	100	100	100	100	100
MO35	77	70	75	77	91	94
MOG135	91	92	112	114	130	141
MOG235	90	85	112	115	120	124
MOG335	89	78	96	103	111	115
M8CG135	83	82	95	107	103	109
M8CG235	83	80	91	105	103	110

Table A 7 Compressive Strength of the Ground Fly Ash (Originating from Coarse and Raw Wet Bottom Fly Ashes) Mortar with 50% Replacement

Sample No.	Compressive Strength (psi)					
	3-d	7-d	14-d	28-d	60-d	120-d
CC	4425	5937	6498	7188	7451	7268
MO50	2175	2784	3619	4797	5758	6548
MOG150	2499	4239	5500	6534	7143	7366
MOG250	2175	3973	4696	5868	6820	7294
MOG350	2100	3697	4768	5827	6850	7123
M8CG150	2700	3300	4100	4800	5600	7000
M8CG250	2551	3148	3936	4670	5508	7281

Table A 8 Percentage Compressive Strength of the Ground Fly Ash (Originating from Coarse and Raw Wet Bottom Fly Ashes) Mortar with 50% Replacement

Sample No.	Percentage Compressive Strength (%)					
	3-d	7-d	14-d	28-d	60-d	120-d
CC	100	100	100	100	100	100
MO50	49	47	56	67	77	90
MOG150	56	71	85	91	96	101
MOG250	49	67	72	82	92	100
MOG350	47	62	73	81	92	98
M8CG150	61	56	63	67	75	96
M8CG250	58	53	61	65	74	100

Table A 9 Compressive Strength of the Ground Low NO_x Fly Ash Mortar with 25% Replacement

Sample No.	Compressive Strength (psi)					
	3-d	7-d	14-d	28-d	60-d	120-d
CC	4425	5937	6498	7188	7451	7268
GPU2G125	4723	5382	6700	7425	8328	8806
GPU2G225	4640	5443	6636	7824	8582	9338
GPU2G325	4708	5623	6824	7844	9547	10181
GPU2O25	3985	4415	5000	6409	7173	7200

Table A 10 Percentage Compressive Strength of the Ground Low NO_x Fly Mortar with 25% Replacement

Sample No.	Percentage Compressive Strength (%)					
	3-d	7-d	14-d	28-d	60-d	120-d
CC	100	100	100	100	100	100
GPU2G125	107	91	103	103	112	121
GPU2G225	105	92	102	109	115	128
GPU2G325	106	95	105	109	128	140
GPU2O25	90	74	77	89	96	99

Table A 11 Compressive Strength of the Ground Low NO_x Fly Ash Mortar with 35% Replacement

Sample No.	Compressive Strength (psi)					
	3-d	7-d	14-d	28-d	60-d	120-d
CC	4425	5937	6498	7188	7451	7268
GPU2G135	3871	4655	5880	7333	8335	8356
GPU2G235	3776	4883	6280	7369	8453	8600
GPU2G335	4014	4902	6734	7828	8666	8760
GPU2O35	3518	4329	4800	5350	6493	6510

Table A 12 Percentage Compressive Strength of the Ground Low NO_x Fly Mortar with 35% Replacement

Sample No.	Percentage Compressive Strength (%)					
	3-d	7-d	14-d	28-d	60-d	120-d
CC	100	100	100	100	100	100
GPU2G135	87	78	90	102	112	115
GPU2G235	85	82	97	103	113	118
GPU2G335	91	83	104	109	116	121
GPU2O35	79	73	74	74	87	90

Table A 13 Compressive Strength of the Ground Dry Bottom Fly Ash Mortar with 25% Replacement

Sample No.	Compressive Strength (psi)					
	3-d	7-d	14-d	28-d	60-d	90-d
CC	4425	5937	6498	7188	7451	7268
BTG125	4500	5350	6414	7520	9482	9482
BTG225	4500	5300	6384	7530	9943	10580
BTG325	4260	5298	6393	7427	10050	10570
BOT25	3300	3820	4554	4623	4700	4750

Table A 14 Percentage Compressive Strength of the Ground Dry Bottom Fly Mortar with 25% Replacement

Sample No.	Percentage Compressive Strength (%)					
	3-d	7-d	14-d	28-d	60-d	90-d
CC	100	100	100	100	100	100
BTG125	102	90	99	105	127	130
BTG225	102	89	98	105	133	146
BTG325	96	89	98	103	135	145
BOT25	75	64	70	64	63	65

Table A 15 Compressive Strength of the Ground Dry Bottom Fly Ash Mortar with 35% Replacement

Sample No.	Compressive Strength (psi)					
	3-d	7-d	14-d	28-d	60-d	90-d
CC	4425	5937	6498	7188	7451	7268
BTG135	4200	5100	5967	7150	9160	9462
BTG235	4008	5168	6388	7516	10184	10339
BTG335	4379	5549	6499	7798	10196	10073
BOT35	2940	3388	4504	4963	5100	5150

Table A 16 Percentage Compressive Strength of the Ground Dry Bottom Fly Mortar with 35% Replacement

Sample No.	Percentage Compressive Strength (%)					
	3-d	7-d	14-d	28-d	60-d	90-d
CC	100	100	100	100	100	100
BTG135	95	86	92	99	123	130
BTG235	91	87	98	105	137	142
BTG335	99	93	100	108	137	139
BOT35	66	57	69	69	68	71

REFERENCES

ACI Committee 226, 1987, "Use of Fly Ash in Concrete," ACI 226.3R-87, *ACI J.*, Proceedings Vol. 84, No.5, Sep.-Oct., pp. 381-409.

ASTM C 138, 1989, "Standard Test Method for Unit Weight, Yield, and Air Content (Gravimetric) of Concrete," *ASTM C-138-81, Annual Book of ASTM Standards*, Vol. 04.02.

ASTM C 618, 1989, "Specification of Fly Ash and Raw or Calcined Natural Pozzolan for Use as a Mineral Admixture in Portland Cement Concrete," *ASTM C 618-89, Annual Book of ASTM Standards*, Vol. 04.02.

Aimin, X., 1991, "Microstructural Study of Gypsum Activated Fly Ash Hydration in Cement Paste," *Cement and Concrete Research*, Vol. 21, No. 6, pp. 1137-1147.

Aimin, X. and Sarkar, S.L., 1994, "Microstructural Development in High-Volume Fly Ash Cement System," *Journal of Materials in Civil Engineering,* Vol. 6, No. 1, Feb., pp. 117-136.

Aiqin, W. and Chengzhi, Z., 1997, "Study of the Influence of the Particle Size Distribution on the Properties of Cement," *Cement and Concrete Research*, Vol. 27, No. 5, pp. 685-697

Banfill, P.G.F., 1982, *Proceedings international Symposium Use of PFA in Concrete, Leeds*, Vol. 1, No. 141.

Berry E.E., and Maholtra, V.M., 1980, "Fly Ash for Use in Concrete-A Critical Review," *ACI Journal*, Mar.-Apr., pp. 59-73.

Berube, M.A., Carles-Gibergues, A., Duchesne, J., and Naproux, P., 1995, Influence of Particle Size Distribution on the Effectiveness of Type-F Fly Ash in Suppressing Expansion Due to Alkali-Silica Reactivity," *International Conference on the Use of Fly Ash, Silica Fume, Slag, and Natural Pozzolans in Concrete 4th, SP 153-10*, American Concrete Institute, pp. 177-193.

Brunauer, S., and Greenberg, S.A., 1960. "The Hydration of Tricalcium Silicate and β–dicalcium Silicate at Room Temperature," *Proc. 4th Int. Symp. Chem. Cem., Washinton, D.C.*, I, pp. 135-165.

Butler, W.B. and Mearing, M.A., 1986, "Fly Ash Beneficiation and Utilization in Theory and in Practice," *Symposium Proceedings, Fly Ash and Coal Conversion By-Products: Charaterization, Utilization and Disposal II*, Material Research Society, Vol. 65, pp. 11-17.

Cabrera, J.G. and Plowman, C., 1980, *Proceedings,* International Conference Chemical, Paris III, Vol. 84, pp.26-45.

Cornelissen, H.A.W., Gast, C.H., 1992, "Upgrading of PFA for Utilization in Concrete," *International Conference on the Use of Fly Ash, Silica Fume, Slag, and Natural Pozzolans in Concrete 4th, SP 132-26,* Istunbul, Turkey, American Concrete Institute, pp. 457-470.

Cao, H.T., Ho, D.W.S., and Guirguis, S., 1990, "Hydration Characteristics of Cements Containing Fly Ash," *Concrete for the Nineties, International Conference on the Use of Fly Ash, Slag, Silica Fume and Other Silicious Materials in Concrete,* Australia.

De Larrard, F., and Sedran, T., 1994, "Optimization of Ultra-High-Performance Concrete by the Use of a Packing Model", *Cement and Concrete Research*, Vol. 24, No. 6, pp. 997-1009.

Dhir, R.K., Hubbard, F.H., Isles, M.K. and Sangha, C.M., 1982, *Research Mechanica*, Vol. 5, No. 183, pp. 277-289.

Diamond, S., ed., 1981, "Effect of Fly Ash Incorporation in Cement and Concrete", *Materials Science Society, Proceedings Symposium N, Boston*, Nov. 16-18, pp. 1-52.

Diamond, S. and Leeman M.E., 1995, "Pore Size Distributions in Hardened Cement Paste by SEM Image Analysis," *Material Research Society Symposium Proceedings*, Materials Research Society, Vol. 370, pp. 217-226.

Fajun Wei, Grutzack, M.W. and Roy D.M., 1985, "Microstructural Alterations in Fly Ash", *Cement and Concrete Research*, Vol. 15, pp.174-184.

Fraay, A.L.A., Bijen, J.M., and de Haan, Y.M., 1989, "The Reaction of Fly Ash in Concrete-A Critical Examination," *Cement and Concrete Research*, Vol. 19, No. 2, pp. 235-246.

Freeman, E., Gao, Y.M., Hurt, R, and Suuberg, E., 1997, "Interaction of Carbon-containing Fly Ash with Commercial Air-Entraining Admixtures for Concrete," Fuel, June, pp. 16-30.

Frias, M. and Sanchez de Rojas, M.I., 1996, "Microstructural Alterations in Fly Ash Mortars: Study on Phenomena Affecting Particle and Pore Size," Cement and Concrete Research, Vol. 27, No. 4, pp. 619-629.

Gao, Y.M., Freeman E., Hurt R., and Suuberg E., 1996, "Interaction of Carbon-Containing Fly Ash with Commercial Air-Entraining Admixtures for Concrete," *Proceedings*, Second Conference on Unburned Carbonaceous Material on Utility

Fly Ash, Pittsburgh Energy Technology Center, U.S. Department of Energy, pp. 27-36.

Giergiczny and Werynska A., 1989, "Influence of Fineness of Fly Ashes on Their Hydraulic Activity," Fly Ash Silica Fume, Slag, and Natural Pozzolans in Concrete, *SP-114*, American Concrete Institute, Detroit, pp. 97-115.

Glavind, M. and Stang, H., 1992, "A Geometrical Packing Model as a Basis for Composing Cement Paste Containing Clay for High Strength Concrete," *Concrete International,* pp.508-530.

Gopalan, M.K., 1993, "Nucleation and Pozzolanic Factors in Strength Development of Class F Fly Ash Concrete," *ACI Material Journal*, Vol. 90, No. 2, Mar.-Apr., pp.117-121.

Harris, H.A., Thompson, J.L., and Murphy, T.E., 1987, "Factor Affecting the Reactivity of Fly Ash from Western Coals," Cement, Concrete, and Aggregates, Vol. 9, No. 1, pp. 34-37.

He Jun-Yuan, Scheetz, B.E., and Roy, D.M., 1984, "Hydration of Fly Ash-Portland Cements," *Cement and Concrete Research*, Vol. 14, No. 4, pp. 505-511.

Hemming, R.T. and Berry, E.E., 1986, "Specification in Size and Density Fractionated Fly Ash," *Symposium Proceedings, Fly Ash and Coal Conversion By-Products: Characterization, Utilization and Disposal II*, Material Research Society, Vol. 65, pp. 91-103.

Hill, Russell, Shondeep L. Sarkar, Robert F. Rathbone, and James C. Hower, 1997, "An Examination of Fly Ash Carbon and its Interaction with Air Entraining Agent," *Cement and Concrete Research*, Vol. 27, No. 2, pp. 193-204.

Hobbs, D.W., 1980, "The Effect of Pulverized-Fuel Ash Upon the Workability of Cement Paste and Concrete," *Magazine of Concrete Research*, Vol. 32, No. 219, pp. 219-226.

Hornain, H., Miersman, F, and Marchand, J., 1992, "Influence of Residual Carbon in Fly Ash on Microstructure and Strength Development of Mortars and Concretes," *International Conference on the Use of Fly Ash, Silica Fume, Slag, and Natural Pozzolans in Concrete 4th, SP 132*, Istunbul, Turkey, American Concrete Institute, pp. 21-37.

Hubbard, F.H. and Dhir, R.K., 1985, "A Compositional Index of the Pozzolanic Potential of Pulverized-fuel Ash," *Journal of Materials Science Letters*, Vol. 3, pp. 958-960.

Huges, B.P., 1989, "PFA Fineness and Its Use in Concrete," *Magazine of Concrete Research*, Vol. 41, No.147, pp. 99-105.

Jaturapitakkul, C., 1992, "Utilization of Fly Ash in Concrete," Doctoral Dissertation, Department of Civil and Environmental Engineering, New Jersey Institute of Technology, Newark, New Jersey.

James, J., Rao, R.J., 1986, "Reactivity of Rice Husk Ash", *Cement and Concrete Research*, Vol.16, pp. 296-302.

Kautz, K., 1984, "Mineralogical Aspects of the Combustion of Hard Coal in Powerplants, From Coal to Fly Ash," *Fortschr. Mineralogy*, Vol. 62, No. 1, August, pp. 51-72.

Lagrand, C. Wirquin, E., 1994, "Study the Strength of Very Young Concrete as a Function of the Amount of Hydrates Formed-Influence of Superplasticizer," *Materials and Structure*, Vol. 27, No. 167, pp.135-137.

Lane, S.D., 1991, "Testing Fly Ash in Mortars for Air Entrainment Characteristics," *Cement, Concrete, and Aggregrates*, Vol.13, No.1, pp. 25-31.

Lea, F.M., 1971, *The Chemistry of Cement and Concrete*, Chemical Publishing Co., Inc., New York.

Levy, E.K., Salmento, J., Masaki, T., and Ayalon, A., 1996, "Removal of Carbon from Fly Ash Using a Bubbling Fluidized," *Second Conference on Unburned Carbonaceous Material on Utility Fly Ash, Proceedings*, Pittsburgh Energy Technology Center, U.S. Department of Energy, Pittsburgh, Pennsylvania, pp.155-158.

Likov, V., Dimitrova E., Petrov, O.E., 1997, "Hydration Process on Cement Containing Fly Ash and Silica Fume: The First 24 Hours," *Cement and Concrete Research*, Vol. 27, No. 4, pp. 577-588

McCarter, W.J., Afshar, A.B., 1988, "Monitoring the Early Hydration Mechanisms of Hydraulic Cement," *Journal of Material Science*, Vol.1, pp. 488-496.

Malholtra V.M., and Mehta, P.K., 1996, *Pozzolanic and Cementitious materials*, Gordon and Breach Publishers, Pennsylvania.

Malhotra, V.M., 1995, "CANMET Investigation Dealing with High Volume Fly Ash Concrete," *Advances in Concrete Technology*, Natural Resources, Ottawa, Canada, Editor:V.M. Malhotra, pp. 531-542.

Malhotra V.M. and Painter K.E., 1989, "Early-age strength properties, and freezing and thawing resistance of concrete incorporating high volumes of ASTM class F Fly

Ash," *The international journal of cement composites and lightweight concrete*, Vol. 11, No. 1, pp. 38-46.

Mantz, O.E., 1986, "Proposed Revisions to Specifications and Test Methods for Use of Fly Ash in Portland Cement Concrete," *Fly Ash, Silica Fume, Slag and Natural Pozzolans in Concrete, SP-91*, American Concrete Institute, Detroit, pp. 659-680.

Mehta, P.K., 1981, "Studies on Blended Portland Cements Containing Satorin Earth," *Cement and Concrete Research*, Vol. 11, pp. 507-518.

Mehta, P.K., 1982, "Properties of Portland Cement Concrete Containing Fly Ash and Condensed Silica-Fume," *Cement and Concrete Research*, Vol. 12, pp. 587-595.

Mindess, S. and Young, J.F., 1981, *Concrete*, Prentice-Hall, Englewood Cliffs, New Jersey, pp. 95-99 and 566-567.

Minnick, L.J., 1979, "The Role of Fly Ash in Structural Types of Stabilized Application," *Proceedings Fifth International Ash Utilization Symposium*, Department of Energy, Morgantown Energy Technical Centre, Morgantown, West Virginia, Feb. pp. 344-356.

Monzo, J., Paya, J., Peris-Mora, E., Borrachero, M.V., 1995, "Mechanical Treatment of Fly Ashes: Strength Development and Workability of Mortars Containing Ground Fly Ashes," *International Conference on the Use of Fly Ash, Silica Fume, Slag, and Natural Pozzolans in Concrete 4th, SP 153-19,* Istunbul, Turkey, American Concrete Institute, pp. 339-353.

Nagamura, N. and Sakai, R.N., 1992, "Effect of Slag Fineness on the development of concrete Strength and Microstructure," *International Conference on the Use of Fly Ash, Silica Fume, Slag, and Natural Pozzolans in Concrete 4th*,: Istunbul, Turkey, *SP 132-72*, pp. 1343-1366.

Nagataki, S. et. al., 1984, "The Fluidity of Fly Ash Cement Paste with Superplasticizers," *Cement and Concrete Research*, Vol.14, pp. 631-638.

Nagele, E. and Schneider, U., 1989, "The Zeta-Potential of Blast Furnace Slag and Fly Ash," *Cement and Concrete Research*, Vol. 19, No. 5, pp. 811-820.

Naik, T.R., Ramme, B.W., 1989, High-Strength Concrete Containing Large Quantities of Fly Ash, *ACI Material Journal*, Mar.-Apr., pp. 111-116.

Raask, E. and Bhaskar M.C., 1975, "Pozzolanic Activity of Pulverized Fuel Ash," *Cement and Concrete Research*, Vol. 5, pp. 363-376.

Ranganath, R.V., Sharma R.C., and Krishnamoorthy, S. 1995, "Influence of Fineness and Soluble Silica Content of Fly Ashes on Their Strength Development with Respect

to Age," *International Conference on the Use of Fly Ash, Silica Fume, Slag, and Natural Pozzolans in Concrete 4th, SP 153-20*, Istunbul, Turkey, American Concrete Institute, pp. 355-366.

Ravina, D., 1980, "Optimized Determination of PFA (Fly Ash) Fineness with Reference to Pozzolanic Activity," *Cement and Concrete Research*, Vol. 10, pp. 573-580.

Ravindrarajah, R.S. and Tam, C.T., 1989, "Properties of Concrete Containing Low-Calcium Fly Ash Under Hot and Humid Climate," *Fly Ash Silica Fume, Slag, and Natural Pozzolans in Concrete, SP-114*, American Concrete Institute, Detroit, pp.139-155.

Paya J., Monzo, J., Borrachero, M.V., Peris-Mora, E. and Gonzallez-Lopez, E., 1997, "Mechanical Treatments of Fly Ashes. Part III: Studied on Strength Development of Ground Fly Ashes (GFA)-Cement Mortars," *Cement and Concrete Research*, Vol. 27, No. 9, pp. 1365-1377.

Plowman, C., and Cabrera, J.G., 1991, "The Use of Fly Ash to Improve the Sulphate Resistance of Concrete", *Cement and Concrete Research*, Vol.21, No.5, pp.145-149.

Plowman, C., 1984, "The Chemistry of PFA in Concrete-A Review of Current Knowledge," *Proceedings 2nd International Conference on Ash Technology and Marketting*, London, pp. 437-443.

Power, T.C. and Brownyard, T.L., 1947 "Studies of the Physical Properties of Hardened Portland Cement Paste," *Research and Development Bulletin 22*, Portland Cement Association, reprinted from Journal, American Concrete Institute, Proceedings, Vol. 43.

Santhanam, C. and Khoury, D. et al., 1981, "Flue Gas Cleaning Wastes, Part III: Utilization, pp. 546-636.

Slanicka S., Lamacska, 1991, "The Influence of Fly Ash Fineness on the Strength of Concrete," *Cement and Concrete Research,* Vol. 21, No.2, pp.285-296.

Stencel, J.M., Ban, H., Li, I.X., Neathery, J.K., and Schaefer, J.L., 1996, "Dry, Electrostatic Separation of Carbon from Coal Fly Ash," *Proceedings, Second Conference on Unburned Carbonaceous Material on Utility Fly Ash*, Pittsburgh Engergy Technology Center, U.S. Department of Energy, Mar., pp. 159-174.

Stoltenberg-Hanson, E., 1988, "Fly Ashes Used for Blended Portland Cement: Effect of Grinding on Cement Quality," *Symposium Proceedings of the Materials Research Society*, Vol. 136, pp. 175-184.

Suprenant and Bruce A., 1992, "Thermal Processor Burns off Carbon to Reduce Fly Ash Variability," *Concrete Construction*, February, pp. 114-118.

Tazawa, E., Yonekura, A., Kawai, K., Kohata, H., Teramoto, H., 1992, "Properties of Mortar Containing Ultra-Fine Fly Ash Particles," *International Conference on the Use of Fly Ash, Silica Fume, Slag, and Natural Pozzolans in Concrete 4th*,: Istunbul, Turkey, *SP 132-6*, American Concrete Institute, pp. 79-95.

Tondu E., Thompson, W.G., Whitlock, D.R., Bittner, J.D., and Vasiliauskas, A., 1996, "Commercial Separation of Unburned Carbon from Fly Ash," *Mining Engineering*, June, pp. 47-50.

Tokyay, M., and Hubbard, F.H., 1992, "Mineralogical Investigations of High-Lime Fly Ashes,", *International Conference on the Use of Fly Ash, Silica Fume, Slag, and Natural Pozzolans in Concrete 4th, 1992: Istunbul, Turkey, SP 132-2,* American Concrete Institute.

Uchikawa, H., Uchida, S., 1980, "Influence of Pozzolana on the Hydration of C_3A", *7th Int. Congress on the Chemistry of Cement, Vol. III theme IV., Structure of Pozzolana and the Hydration of Pozzolanic and Fly Ash Cements,* Paris, pp. IV 24 – IV 29.

Ukita, K., Ishii, M., Yamamoto, K., Azuma, K., and Kohno, K., 1992, "Proporties of High Strength Concrete Using "Classified Fly Ash"," *International Conference on the Use of Fly Ash, Silica Fume, Slag, and Natural Pozzolans in Concrete 4th*,: *Istunbul, Turkey, SP 132-3*, American Concrete Institute, pp. 37-52.

Urhan S., 1987, "Alkali Silica and Pozzolanic Reactions in Concrete Part 1: Interpretation of Published Results and Hypothesis Concerning the Mechanism," *Cement and Concrete Research*, Vol. 17, No. 1., pp.141-152.

Van Roode, M., Douglas, E., Hemmings, R.T, 1987, "X-ray Diffraction Measurement of Glass Content in Fly Ashes and Slags," *Cement and Concrete Research*, Vol.17, pp. 183-187.

Watt, J.D. and Thorne D.J., 1966, The Composition and Pozzolanic Properties of Fly Ashes, Part III. *Journal of Applied Chemistry*, Vol.16, Feb., pp.33-39.

Yuan, R.J., Jin, S.X. and Qiam, J.C., 1982 "Effects of Fly Ash on the Rheology of Fresh Cement," Skanly, J.P., Ed., Effect of Surface and Colloid Phenomena on Properties of Fresh Concrete, *Proc. Symp. Mater. Res. Soc., Annual Meeting, Univ. Park, Pennsylvania*, Nov., pp. 182-191.